Fakultät für Maschinenwesen

Lehrstuhl für Energiesysteme

Optimization for Building Control Systems of a School Building in Passive House Standard

Yang Wang

Vollständiger Abdruck der von der Fakultät für Maschinenwesen der Technischen Universität München zur Erlangung des akademischen Grades eines

Doktor-Ingenieurs

genehmigten Dissertation.

Vorsitzender:	Univ. -Prof. Dr.-Ing. M. Hajek
Prüfer der Dissertation:	1. Univ.-Prof. Dr.-Ing. habil. H. Spliethoff
	2. Univ.-Prof. Dr.-Ing. W. Lang

Die Dissertation wurde am 18.05.2015 bei der Technischen Universität München eingereicht und durch die Fakultät für Maschinenwesen am 22.10.2015 angenommen.

Eidesstattliche Erklärung

Hiermit versichere ich, die vorliegende Arbeit selbständig und ohne Hilfe Dritter angefertigt zu haben. Gedanken und Zitate, die ich aus fremden Quellen direkt oder indirekt übernommen habe sind als solche kenntlich gemacht. Diese Arbeit hat in gleicher oder ähnlicher Form noch keiner Prüfungsbehörde vorgelegen und wurde bisher nicht veröffentlicht.
Ich erkläre mich damit einverstanden, dass die Arbeit durch den Lehrstuhl für Energiesysteme der Öffentlichkeit zugänglich gemacht werden kann.

_____, den _____ _____

Unterschrift

Acknowledgements

I really appreciate my mentors Dr. J. M. Kuckelkorn, Prof. Dr.-Ing H. Spliethoff and Prof. Dr.-Ing W. Lang for giving me an opportunity as their student and for their kindness and guidance as well as supports. They have guided me in the region of building energy investigation and have introduced me from an outsider of building energy to be a building energy researcher. Their deep insights into the relationship between theory and practice impressed me. I am also deeply indebted to Prof. Fu-Yun Zhao for all his help and encouragements on my study and work, particularly the fields of mathematical methodologies and modelling etc. I also really would like to thank Prof. Dr. C. Kargel for his great guidance on how to study and work scientifically and valuably.

I wish to thank all my current and past colleagues in Division of Technology for Energy Systems and Renewable Energy, Bavarian Center for Applied Energy Research (ZAE Bayern, Garching), Institute for Energy Systems (Faculty of Mechanical Engineering, TUM) and Division of Sensor Technology and Measurement Systems (UniBw), especially Dr. A. Hauer, Mr. A. Kirschbaum, Mr. C. Brandt, Mr. N. Schueler, Ms. G. Streib, Mr. F. Volz, Mr. F. Fischer, Mr. D. Niederlechner, Mr. C. Müller, Mr. C. Hilgers, Mr. M. Adeili, Mr. A. Robrecht, Mr. R. Kunde, Mr. H. Fink, Ms. L. Meyering, Dr. A. Pugachev, Mr. W. Liu, Prof. Dr. M. Horn, Dr. V. Rengaraju, Dr. K. Spasokukotskiy, Dr. D. Zhelondz, Dr. H. Ruser, Mr. S. Brunner, Dr. A. Eder, Mr. P. Fomin, Mr. K. Wenzl and Mr. Y. Shao. They offered heartfelt help and showed enough patience when I discussed with them. I will miss the seminar every Wednesday. I like that kind of discussion environment.

I gratefully acknowledge the China Scholarship Council (CSC), Ministry of Education of the P. R. China (Grant No. 2009837130) for giving me the opportunity to study in Munich, Germany and the financial support. This project has been supported by the German Federal Environmental Foundation (Deutsche Bundesstiftung Umwelt, DBU AZ 26170/02-25), administrative district of Erding (Landkreis Erding) and the school building of the FOS/BOS Erding.

My time in Munich would not have been rich and colourful without my dear friends and their help and supports, especially Dr. Ya-Zhou Zou, Ms. Dong-Hui Yang, Mr. Ji-Qiang Dai, Dr. Jun-Lan Qian, Ms. Zhao-Fen Huang, Dr. Chang-Song Xie, Ms. Li Li, Ms. Xue-Mei Yang, Ms. Yan Du, Dr. Da-Guang Han, Ms. Chun-Li Ying, Dr. Mou-Zhi Ge, Ms. Jin Yu, Dr. Qiang Yu, Dr. A. Estes, Dr. Chang-Xia Ke, Dr. Mulan Mu, Dr. Jian-Bo Gao, Dr. Li-Qun Liu, Dr. Kai Zhao, Dr. Lian-Fei Kuang, Ms. Ying Xiong, Mr. Wei Xie, Ms. Xiao-Can Wang, Dr. Jun-Sheng

Wei, Ms. Yin-Yin Yang, Ms. Yin Zhang, Dr. Guo-Yin Yin, Dr. Hou-De Dai, Dr. Feng-Xiang Wang, Dr. Zhi-Xun Ma, Mr. Zhe Chen, Mr. Zhen-Bin Zhang, Ms. Xue-Zhu Mei, Mr. Zi-Xing Zhang, Mr. Jian Zheng, Dr. Ling-Xiang-Yu Li, Dr. Zhen-Lan Xu, Dr. Yu-Chen Xia, Ms. Xiao-Ming Cheng, Dr. Ming-Xia Su, Dr. Zhen-Li Chen, Mr. Bo-Yu Liu, Mr. Kai Wang, Dr. Hao-Jin Ba, Dr. Yi-Jun Yan, Ms. Ying Tian, Ms. Ge-Fei Fu, Mr. J. Vinke, Mr. F. Will, Mr. J. Kettenberger, Ms. M. Kettenberger, Mr. C. Metz, Ms. A. Heide, Ms. Lan-Fei Wang, Mr. Jun Wu, Mr. Ke Gong, Dr. Rui Ding, Mr. Ge Zhu, Dr. Jun-Wei Yuan and every member of our Badminton association. There are also many other friends I met when I have been living in Munich, whom I will never forget and will remember their supports and friendship forever.

The author is also very grateful to the referees who provided valuable and positive comments.

Finally, and most importantly, I would like to thank my family for their everlasting support and love all these years, particularly my mother – Ms. Xiu-Qin Cao. She has always supported and encouraged incredibly what I did and thought. In one word, I have got here in my life just due to her. I love you very much forever.

Abstract

Passive houses or the ultra-low energy buildings have been introduced into the practical operations, and these buildings require very little energy for space heating and cooling. With the time past, there were many researches and experience on the passive residential and office buildings but almost few have been done in the school buildings.

One school building with Passive House standard of the FOS/BOS Erding implemented with HVAC control systems was recently built up, which has adopted a novel heat recovery air conditioning system particularly operating in cold winter and hot summer. School building energy conservation performance and classroom air environment quality enhancement was simultaneously investigated in the present work. Heat recovery efficiency of the heat recovery facility and energy conservation ratio of the air conditioning unit were analytically modelled, taking the classroom ventilation network into account. Following that, classroom displacement ventilation and its thermal stratification have been investigated concerning the effects of delivering ventilation flow rate and supplying air temperature. Representative thermal comfort parameters, the percentage of dissatisfied, temperature difference between ankle and head, and draft dissatisfaction have been evaluated. Indoor air quality indicated by the CO_2 concentration was also investigated in terms of different levels of ventilation flow rate. Classroom energy demands for ventilation and winter heating/summer cooling have shown that they decrease with the promotion of heat recovery efficiency of the ventilation facility, and the energy conservation ratio of the air conditioning unit increases/decreases with the promoting temperature of supplying fresh air in winter/summer. Detailed fitting correlations of heat recovery ventilation and air conditioning energy conservation have been presented. Numerical results indicated that the promotion of mechanical ventilation could simultaneously boost the dilution of indoor air pollutants and the non-uniformity of indoor thermal and pollutant distributions. The research illuminated that enhancement of classroom air quality and reduction of school building energy consumption could be simultaneously achieved with the appropriate operation of heat recovery air conditioning and ventilation system.

In the transitional seasons, natural ventilation is an effective method to improve indoor air quality and reduce energy consumption in buildings, especially when the indoor temperature approaches closely to ambient level. Heat losses due to the opened windows and ventilation effectiveness ratio are analytically modelled. After air flow models were set up,

the effects of thermal buoyancy on the classroom airflow and thermal stratification comfort as well as the contaminant dispersion are numerically investigated and discussed. Natural ventilation of a classroom and its thermal stratification as well as indoor air quality indicated by the CO_2 concentration have been investigated concerning the effects of supplying fresh air temperature and delivering natural ventilation flow velocity. Subsequent energy efficiency analysis illuminates that classroom energy demands for natural ventilation could decrease with the promotion of the ventilation effectiveness ratio for heat distribution when the natural ventilation rate maintains a constant, and with the shrinking of the ventilation effectiveness ratio for heat distribution when the supplying air temperature is not changeable. Following that, detailed correlations of heat loss resulted from opened window and ventilation effectiveness of natural ventilation inside the classroom have been presented.

Building energy performance analysis based on the network model could dynamically identify the important parameters of building energy consumption and thermal environment such as HVAC energy demands, room air temperature and facade temperature, to name just a few. A sample test classroom and the whole passive school building, whose heating/cooling and ventilation parameters were accurately known as prior, are analytically modelled. In order to fully investigate the energy performance of the sample test classroom and the whole building, six different classroom design points and three building scenarios have been representatively simulated respectively, depending on practical operational situations in this school building implemented with HVAC control systems. Heating/cooling and ventilation energy demands of the sample test classroom and the whole building and thermal comfort inside the sample classroom have been evaluated regarding the effects of different indoor set-point temperatures in winter/summer, pre-ventilation in winter, the air exchange rates of night ventilation in summer, solar shading system, and the efficiency of the heat recovery facility. The subsequent analysis results indicate that the set-point combination 21.5/26 °C could be selected as a suitable set-point indoor temperature combination in winter/summer, which could not only meet the requirement of human thermal comfort, but also effectively reduce energy consumption. Moreover, the annual wall heating and pre-heating as well as active cooling demands are expectedly few. In addition, night ventilation in summer could effectively result in cooling energy storage, which could provide more appropriate living conditions for the following day, and meanwhile it could greatly reduce energy costs for cooling at daytime. The optimized control systems for HVAC and sun-shading show an expectedly energy efficient performance.

Kurzfassung

Passivhäuser und Ultra-Niedrigenergiehäuser sind heute bereits Stand der Technik und in der Baupraxis etabliert. Diese Gebäude benötigen sehr wenig Energie für Raumheizung und -kühlung. Mittlerweile wurden viele Untersuchungen zu Wohn- und Bürogebäuden mit Passivhausstandard durchgeführt und es existiert umfangreiche Erfahrung. Allerdings wurden dabei nur sehr wenige Schulgebäude untersucht.

Für die FOS / BOS Erding wurde ein Schulgebäude in Passivhaus-Standard neu errichtet, dessen Heizungs-, Lüftungs- und Klimatisierungssysteme mit energieeffizienten Wärme- /Kälterückgewinnungsanlagen ausgestattet wurden. In der vorliegenden Arbeit wurde die Energieeffizienz des Schulgebäudes in Zusammenhang mit der Steigerung der Luftqualität und der thermischen Behaglichkeit in den Klassenräumen untersucht. Die Rückwärmzahl und ein neu definiertes Energieeinspar-Verhältnis der raumlufttechnischen Anlagen wurden analytisch modelliert, wobei der Luftverbund aller Klassenräume betrachtet wurde. Anschließend wurden der Luftwechsel und die Temperaturschichtung im Klassenraum in Abhängigkeit des Zuluftvolumenstroms und dessen Temperatur untersucht. Dabei wurden repräsentative Parameter für die thermische Behaglichkeit, der Anteil Unzufriedener, die Temperaturdifferenzen zwischen Fuß- und Kopfhöhe sowie für das Auftreten von Zuglufterscheinungen evaluiert. Die Innenraumluftqualität wurde über die CO_2-Konzentrationen betrachtet und im Hinblick auf verschiedene Luftwechselraten untersucht. Der Energiebedarf der Klassenräume für Zuluftkonditionierung und Heizung im Winter bzw. Kühlung im Sommer sinkt mit steigender Rückwärmzahl und das Energieeinspar-Verhältnis der raumlufttechnischen Anlagen steigt mit zunehmender Zulufttemperatur im Winter bzw. sinkt im Sommer. Detaillierte Korrelationskurven hierzu werden vorgestellt. Ergebnisse aus numerischen Simulationen zeigen, dass die Erhöhung der über die Lüftungsanlage zugeführten Luftmenge zu einer höheren Verdünnung der Luftschadstoffe, aber gleichzeitig auch zu einem höheren Ungleichförmigkeitsgrad der Temperatur- und Schadstoffverteilung im Raum führt. Die Untersuchungen zeigen weiterhin, dass durch eine geeignete Leittechnik gleichzeitig eine Verbesserung der Luftqualität in den Klassenräumen und eine Senkung des Energieverbrauchs des Schulgebäudes erreicht werden kann.

In der Übergangszeit ist eine natürliche Belüftung eine wirksame Methode, um die Raumluftqualität zu verbessern und den Energieverbrauch im Gebäude zu reduzieren, vor allem wenn die Außentemperatur im Bereich der Innentemperatur liegt. In der Arbeit werden die Wärmeverluste aufgrund geöffneter Fenster sowie die Lüftungseffektivitätsrate analytisch modelliert. Mit numerischen Strömungsmodellen wurden die Effekte des thermischen Auftriebs der Luftströmung auf die Temperaturschichtung sowie die Schadstoffdispersion in

einem Klassenraum untersucht und diskutiert. Die natürliche Lüftung eines Klassenraums und die sich dabei einstellende Temperaturschichtung sowie die Innenraumluftqualität, betrachtet über die CO_2-Konzentration, wurden hinsichtlich des Einflusses der Zulufttemperatur und der Strömungsgeschwindigkeit bei natürlicher Belüftung untersucht. Eine anschließende Effizienzanalyse zeigte, dass der Energiebedarf eines Klassenraums bei natürlicher Belüftung und konstanter Luftwechselrate mit zunehmender Lüftungseffektivitätsrate für Temperaturverteilung sinkt. Ebenfalls sinkt der Energiebedarf, wenn bei konstanter Zulufttemperatur die Lüftungseffektivitätsrate für Temperaturverteilung abnimmt. Weiterhin konnten detaillierte Korrelationen zwischen dem Wärmeverlust durch geöffnete Fenster im Klassenraum und der Lüftungseffektivität der natürlichen Lüftung untersucht werden.

Mit dynamischen, numerischen Gebäudesimulationen konnten die wichtigsten Parameter zum Energiebedarf des Gebäudes und seiner thermischen Randbedingungen, wie zum Beispiel der Heizungs-, Lüftungs- und Klimatisierungsenergiebedarf, die Raumlufttemperaturen und die Fassadentemperaturen, identifiziert werden. Zunächst wurden die Heizungs-/Kühlungs- und Lüftungsparameter, die aus dem Gebäudebetrieb bekannt waren, analytisch für einen Referenzklassenraum sowie für das gesamte Passivhaus-Schulgebäude betrachtet. Um die Energieeffizienz des Referenzklassenraums näher zu untersuchen, wurden sechs verschiedene Auslegungsszenarien dynamisch simuliert. Ebenso wurde das gesamte Gebäude mit drei verschiedenen Betriebsszenarien modelliert. Die untersuchten Auslegungsszenarien wurden jeweils auf Basis realer Betriebssituationen in dem Schulgebäude und anhand von Messdaten eines Gebäudemonitorings abgeleitet. Für diese Szenarien wurden der Energiebedarf sowie die thermische Behaglichkeit im Hinblick auf die Auswirkungen verschiedener Aspekte, wie die Variation der Innensolltemperaturen im Winter und Sommer, ein Vorlüftungsbetrieb im Winter, die Variation von Luftwechselraten bei Nachtlüftung im Sommer, der Einfluss einer Verschattungsanlage und die Effizienz der Wärmerückgewinnungsanlagen ausgewertet. Die Ergebnisse zeigen, dass die Anforderungen an den thermischen Raumkomfort und gleichzeitig die hohen Anforderungen an die Energieeffizienz mit Raumlufttemperatur-Sollwerten von 21,5 °C im Winter und 26 °C im Sommer erfüllt werden können. Insgesamt ist der Jahresenergiebedarf für Wandheizung und Luftvorwärmung sowie die aktive Kühlung erwartungsgemäß niedrig. Weiterhin konnte mit der Nachtlüftung Kühlenergie im Sommer effektiv gespeichert werden, um jeweils am nächsten Tag einen ausreichenden Raumkomfort sicherzustellen. Dadurch können die Energiekosten für die Kühlung erheblich gesenkt werden. Optimierte Regelungen für den Betrieb der Klimatechnik und der Verschattungsanlagen zeigen eine erwartet hohe Energieeffizienz.

Contents

List of Figures

List of Tables

Acronyms

ACH Air Change per Hour

BES Building Energy Simulation

CEPHEUS Cost Efficient Passive Houses as European Standards

CFD Computional Fluid Dynamics

DCV Demand Controlled Ventilation

EnEV Energieeinsparverordnung (Energy saving regulation)

EPA Environmental Protection Agency

FOS/BOS Fachoberschule/Berufsoberschule (Specialized secondary school/Vocational high school)

HEPA High Efficiency Particulate Air

HVAC Heating, Ventilation and Air-Conditioning

IAQ Indoor Air Quality

NIOSH National Institute for Occupational Safety and Health

NO_x Nitride

OLED Organic Light-Emission Diodes

OSHA Occupational Safety and Health Administration

PD Percentage Dissatisfied

PHPP Passive House Planning Package

PLED Polymer Light-Emission Diodes

PMV Predicted Mean Votes

PPD Predicted Percentage of Dissatisfied

PV Photovoltaik

RLT Raum Luft Technik (Room ventilation technique)

RMS Root Mean Square

SO_x Sulfide

STD Standard Deviation

TMY Typical Meteorological Year

VOCs Volatile Organic Compounds

WoFlVO Wohnflaechenverordnung (Residential area regulation)

WSVO Waermeschutzverordnung (Thermal protection regulation)

ZAE Bayern Bayerisches Zentrum für Angewandte Energieforschung (Bavarian Center for Applied Energy Research)

Nomenclature

Roman Symbols

A area of cross section

a coefficients

b coefficients

C tracer gas mass concentration, specific heat capacity of air

c coefficients

D dimension

d coefficients

f the ratio of the surface area

h heat transfer coefficient

I thermal resistance, injection rate of the tracer gas

k the difference of initial and final temperature in balance, turbulent kinetic energy

M human activity, mass of air, air flow rates

m mass of tracer gas

N natural ventilation rate

P pressure

Q airflow rate, thermal energy, total convective heat flux

q heat removal, heat loss, conduction heat flux

R regression

RH relative humidity in percent

S source term

T temperature

t time

U heat transfer coefficient

u momentum

v velocity

V volume, volume flow rate, air velocity

Greek Symbols

Δ difference

τ thermal time constant

ρ density

η heat recovery efficiency

φ energy conservation ratio, generic variable

Γ digression coefficient

ε ventilation effectiveness ratio

Subscripts

a, out monthly mean outdoor air

ac air conditioning

a,v difference between ankle and head

building tested building

C contaminant removal

c convective

cl clothing

comf comfort

cool set-point indoor air temperature in summer

coolingrec cooling recovery system

cplg coupling gains

CO_2 carbon dioxide

exhaust exhausting port of the classroom

fresh exterior surrounding fresh air

g gains

heat set-point indoor air temperature in winter

heatrecovery heat recovery system

i indoor air, internal environment, air node, inside surfaces

in entraining into the air conditioning unit

inf infiltration

k term in the time series

k-p Kronvall and Persily model

long long wave radiation exchange

Max maximal value

Min minimum value

mrt mean radiant temperature

o external environment

out exhaust from the heat recovery unit

r heat recovery unit, radiative gains

s saturated vapour, time series

sol solar gains

t heat distribution

sqr square root

supply supplying port of the classroom

v vapour

vent ventilation

w wall

0 in balance

50 50 Pascal

Other Symbols

< > mean value

¯ volume averaged value

* simulation results of the second year

1 Introduction

1.1 Background and motivation

In today's world, the global energy crisis and carbon emission have placed heavy pressure on the building energy reductions, particularly on high energy consumption buildings (Chwieduk 2003, Beusker et al. 2012, Katunsky et al. 2013). In Germany, the building sector accounts for approximately 40% of total final energy consumption and for about one third of CO_2 emissions into the atmosphere, which can result in global warming and climate changes. Furthermore, over 70% of the building energy consumption in Germany is expended on indoor space heating. Similar statistics also appear in other most countries, where about 40% of the total annual energy consumption is due to buildings (Liu et al. 2010). The increasing trend towards building energy consumption will persist in the coming years due to the extension of built regions and related energy demands (Perez-Lombard et al. 2008).

The energy requirements for building in Germany are based mostly on the building area or the heated living space according to the Wohnflächenverordnung (Living Space Ordinance - WoFlVO). The usual measurement value for energy demand is "kilowatt hours per square meter per year" i.e. kWh/(m^2a).

Table 1.1 shows the common and generally accepted basic standards for building energy requirements in Germany. In the table, WSVO stands for Wärmeschutzverordnung (Thermal Insulation Regulations), EnEV represents Energieeinsparverordnung (Energy Conservation Regulations), KfW means Kreditanstalt für Wiederaufbau (Reconstruction Credit Institute) and PHPP stands for Passivhaus Planning Package (Johannes Volland 2014, Beecken et al. 2011, Drinkuth 2010, Feist et al. 2005). As can be seen from this table, people are becoming increasingly conscious of the importance of energy conservation for the building sector.

Table 1.1: Basic standards for building energy requirements in Germany

Standard	Space heating demand Q_h, kWh/(m²a)	Primary energy demand Q_p kWh/(m²a)
Non-renovated house, built in the years: 1960…1980	300	
German average value in 2002	160	
Insulation regulation (WSVO 1977)	≤ 250	
Insulation regulation (WSVO 1982)	≤ 150	
Insulation regulation (WSVO 1995)	≤ 100	≤ 160
Low-energy house (EnEV 2002)	≤ 70	
KfW-Efficient house 85 (EnEV 2009)	≤ 55	≤ 60
KfW-Efficient house 70 (EnEV 2009)	≤ 45	≤ 50
KfW-Efficient house 55 (EnEV 2009)	≤ 35	≤ 40
KfW-Efficient house 40 (EnEV 2009)	≤ 25	≤ 30
Passive house (PHPP)	≤ 15	≤ 120

Three decades ago, passive houses or the ultra-low energy buildings were gradually introduced into the practical operations in Germany, meaning that the buildings consume little energy for space heating (Table 1.1). In the past, there has been much research carried out and experience gained on passive residential and office buildings, but almost nothing has been done on school buildings (Badescu et al. 2003, Feist et al. 2005, Chel et al. 2009, Eicker 2010). This is mainly due to the fact that administrators and taxpayers generally are of the opinion that energy costs in school buildings are not comparable in importance to the learning performance and safety of students crowded within the school buildings.

Recently, passive school buildings were initiated, in which high level thermal insulation, energy efficient windows, extremely airtight building envelopes, and a heat recovery mechanical ventilation system are simultaneously applied. Additionally, in order to promote the potentials presented by the heat recovery mechanical ventilation system and extremely airtight building envelopes, windows in classrooms are normally shut in order to avoid indoor heating energy losses (Johansson et al. 2001, Chowdhury et al. 2008, Liu et al. 2010).

Consequently, special attentions should be paid to the classroom air environment governed by such ventilation systems, as hygienically healthy and comfortable indoor air climate conditions are essential to any type of built environment. In particular, classroom environment and thermal comfort play an important role in teaching and learning, as they help students to engage in activities that promote their performances, such as an understanding of concepts, problem solving abilities and attitudes towards learning etc. (Puteh et al. 2012). Due to the crowded living and learning environment in schools, recent research has found,

after extensive surveys conducted on traditional school buildings, that more than half of school children have some kinds of allergy and asthma (Karimipanah et al. 2007). Thermal comfort and indoor air quality in particular should be investigated in the newly-built low energy school buildings with an aforementioned heat recovery ventilation system in order to answer common doubts on classroom air quality due to the closed windows and airtight building envelopes as well as the large numbers of students in each room.

It is necessary to create a comfortable thermal environment with a suitable combination of comfort variables, which include personal factors, for example the metabolic rate and clothing insulation and activity level; environmental factors such as air velocity, air temperature, mean radiant temperature, relative humidity, draft rate, and vertical air temperature differences based on ASHRAE Standard 55 (ANSI/ASHRAE Standard 55 2004, 2010) and EN 15251(CEN EN 15251 2007) as well as ISO EN 7730 (ISO EN 7730 2005), to name just a few. There are a number of thermal comfort models available in the research fields, which mainly include two different models: the static model and the adaptive model (La Roche 2011), and the parameters of percentage dissatisfied (*PD*) and temperature difference between ankle and head ($\Delta T_{a,v}$) as well as draught dissatisfaction will be used in this study as thermal comfort criteria.

The static comfort model accords with the physiological approach, based on which the comfort zone can be identical for all occupants, disregarding location and adaptation to the thermal environment (La Roche 2011). Basically, it declares that the indoor temperature should not alter with the changing of the seasons. Furthermore, there should be one fixed temperature all year around. In other words, this model takes the more passive stance that occupants do not have to acclimatize to different temperatures due to the fact that it will always remain invariable (Ye et al. 2006, Khodakarami et al. 2008).

In addition, this static model is based on the Predicted Mean Votes (PMV)/Predicted Percentage of Dissatisfied (PPD) model, which employs the PMV formula (see Eqs. 1.1-1.4) by P. O. Fanger (Fanger 1970). The PMV is the average comfort vote, utilizing a seven-point thermal sensation scale from cold (-3) to hot (+3), prophesied by a theoretical index for a large number of subjects when subjected to special environmental conditions (Fanger 1970). Zero is an ideal value, which represents thermal neutrality. This model was originally derived by gathering data from a large group of surveys on occupants exposed to dissimilar conditions within a climate chamber. This data was then employed to develop a mathematical model of the relationship between all the physiological and environmental factors involved (La Roche 2011).

$$PMV = (0.325e^{-0.042M} + 0.032)[M - 0.35(43 - 0.061M - P_v) - 0.42(M - 50) - 0.0023M(44 - P_v) - 0.0014M(34-T_i) - 3.4 \times 10^{-8} f_{cl}((T_{cl} + 273)^4 - (T_{mrt} + 273)^4) - f_{cl}h_c(T_{cl} - T_i)] \quad (1.1)$$

with

$$T_{cl} = 35.7 - 0.032M - 0.18I_{cl}[3.4 \times 10^{-8} f_{cl}((T_{cl} + 273)^4 - (T_{mrt} + 273)^4 - f_{cl}h_c(T_{cl} + T_i)] \quad (1.2)$$

$$h_c = \begin{cases} 2.05(T_{cl} - T_i)^{0.25} & for \quad 2.38(T_{cl} - T_i)^{0.25} > 10.4\sqrt{v} \\ 10.4\sqrt{v} & for \quad 2.38(T_{cl} - T_i)^{0.25} < 10.4\sqrt{v} \end{cases} \quad (1.3)$$

$$P_v = P_s RH/100 \quad (1.4)$$

Whereas M is the human activity (kcal/hm^2), P_v is the vapour pressure in the air (mmHg), T_i is the indoor air temperature (°C), f_{cl} is the ratio of the surface area of the clothed body to the surface area of the nude body, T_{cl} is the outer surface temperature of the clothing (°C), T_{mrt} is the mean radiant temperature (°C), h_c is the convective heat transfer coefficient (kcal/m^{2}h°C), I_{cl} is the thermal resistance of clothing (m^{2}h°C/cal), v is the relative air velocity (m/s), P_s is the saturated vapour pressure at a specific temperature and RH is the relative humidity in percent.

The comfort zone (see Fig. 1.1) is determined by the combinations of the six key parameters for thermal comfort, which include the air temperature and mean radiant temperature in question along with the applicable metabolic rate, clothing insulation, air speed, and relative humidity and for which the PMV should lie within the suggested limits (-0.5<PMV<+0.5) (Fanger 1970, ANSI/ASHRAE Standard 55 2004, 2010), which stands for that a comfort zone lies approximately between 18 °C and 24 °C temperature and between 30% and 70% relative humidity (Leusden et al. 1951, Frank 1975, Pistohl 2009). If the resulting PMV value produced by the model lies within the recommended range, the conditions are regarded as being within the comfort zone. In addition, recommended thermal comfort range for new building and renovations is 20 °C to 24 °C for heating with 1.0 clo, and 23 °C to 26 °C for cooling with 0.5 clo (CEN EN 15251 2007, Spasokukotskiy 2005).

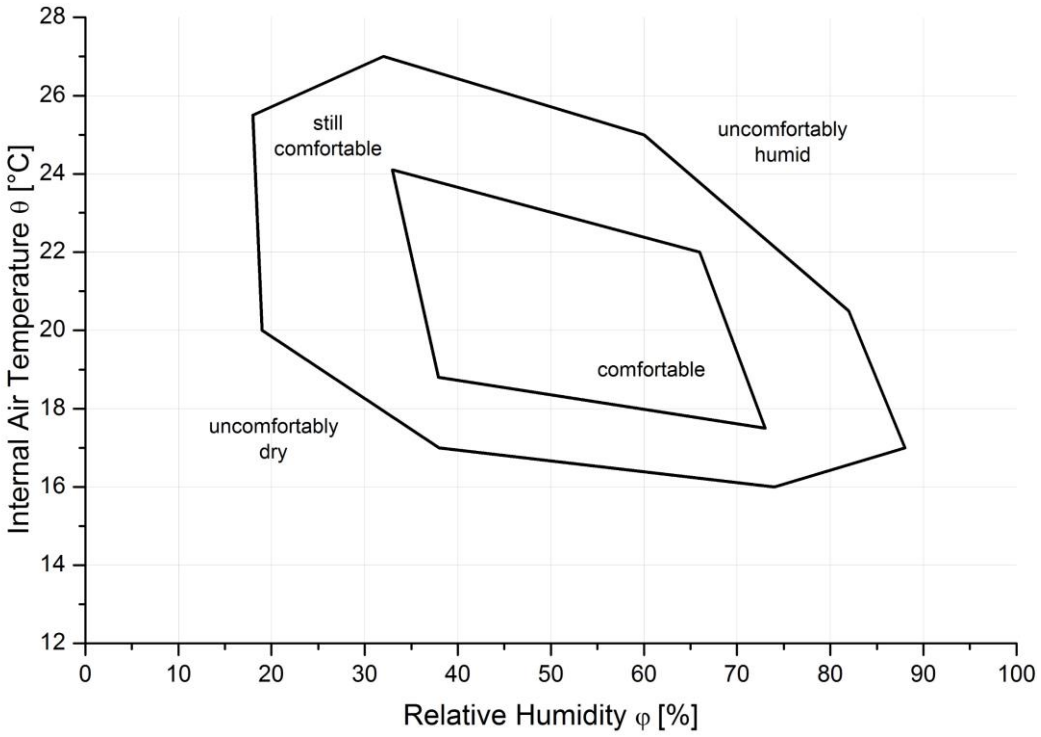

Figure 1.1: Comfort zone. (Leusden et al. 1951, Frank 1975, Pistohl 2009)

ANSI/ASHRAE Standard 55-2010 defines an acceptable range of conditions, which must be conformed with in order to utilize this approach and define the comfort zone: occupants' metabolic rates between 1.0 and 1.3 met, and clothing insulation between 0.5 and 1.0 clo as well as air speeds under 0.2 m/s, where 1 met is equal to the energy generated per unit surface area of an averaged person seated at rest; and where 1 clo equals the standard amount of insulation required to keep a resting occupant warm in a windless room at 21.1 °C (ANSI/ASHRAE Standard 55 2010).

In fact, the PMV model was derived from a thermal balance approach under steady state condition in a controlled climate chamber. However, in our era of increasingly expensive fuel and limitations on thermal comfort prophecies in naturally ventilated buildings, and due to the theoretical complexity of the heat balance method, many researchers have been stimulated to go beyond the thermal balance approach to foresee occupants' thermal comfort by employing a statistical approach known from adaptive models (Djamila et al. 2012, Halawa et al. 2012). The adaptive model is based on the notion that a strong relationship between indoor thermal comfort and exterior climate could be set up, taking into account

that occupants can acclimatize and tolerate different temperatures within different periods of the year.

Based on the adaptive hypothesis, contextual factors and past thermal history modify building occupants' thermal expectations and preferences (de Dear et al. 1997 and 1998, Halawa et al. 2012). Humans in warm climate regions should prefer higher indoor temperatures than humans living in cold climate regions, which is in contrast to the assumptions underlying comfort standards according to the PMV model (de Dear et al. 1997 and 1998, Halawa et al. 2012).

The adaptive model is utilized particularly in natural conditioned and occupant-controlled areas, where the exterior climate will indeed influences indoor environments and the comfort zone (de Dear et al. 1997 and 1998). In fact, investigations by de Dear and Brager (de Dear et al. 1997 and 1998) indicated that occupants in naturally ventilated buildings could experience a wider temperature range. This is mainly due to the fact that occupants could adapt to temperature changes through different kinds of behavioural and physiological adjustments (La Roche 2011). According to ASHRAE Standard 55-2010, differences in changing of clothing, current thermal experiences and the availability of control options and shifts in occupant expectations could alter humans' thermal responses (ANSI/ASHRAE Standard 55 2010). Thermal adaptation basically consists of three types, i.e. physiological, psychological and behavioural adjustment. The latter, which relates to a changed thermal action and perceptions based on past expectations and experiences, is the key parameter to explaining the difference between PMV predictions according to the thermal static model and field observations in naturally ventilated buildings.

There is a significant expression of indoor comfort temperature as a function of outdoor temperature for the adaptive model (Nicol et al. 1998, Saman et al. 2008, Halawa et al. 2012):

$$T_{comf} = A * T_{a,out} + B \tag{1.5}$$

where T_{comf} = comfort temperature (°C); $T_{a,out}$ = monthly mean outdoor air temperature (°C); A, B = constants.

Table 1.2 shows a summary of the available, aforementioned equations derived from some researchers of the adaptive model (Djamila et al. 2012).

Table 1.2: Indoor comfort temperature predictions using the adaptive model

Equation	Researcher
$T_{comf} = 0.534 * T_{a,out} + 11.9$	Humphreys 1976
$T_{comf} = 0.31 * T_{a,out} + 17.6$	Auliciems and de Dear 1986
$T_{comf} = 0.38 * T_{a,out} + 17$	Nicol and Roaf 1996
$T_{comf} = 0.31 * T_{a,out} + 17.8$	Brager and de Dear 2001

A comparison of observed indoor comfort temperatures using the adaptive model with those predicted by the PMV model has been illustrated in Fig. 1.2 (de Dear et al. 1997 and 1998). As seen in Fig. 1.2, in the case of buildings with centralized Heating, Ventilation and Air-Conditioning system (HVAC) (Fig. 1.2(a)), the results observed in the database of ASHRAE RP-884 (de Dear et al. 1998) building field experiments with the adaptive comfort model almost agree with the predicted static model i.e. PMV model. Therefore, this illustrates that PMV model can successfully predict indoor comfort temperatures in the HVAC buildings. However, in the case of buildings with natural ventilation (Fig. 1.2(b)), the obvious discrepancy between the adaptive model and the PMV model can be seen. It also explains why occupants who experience a wider temperature range through different kinds of behavioural and physiological adjustments could adapt to a broader range of conditions with natural ventilation based on the adaptive model than has been predicted by the PMV model.

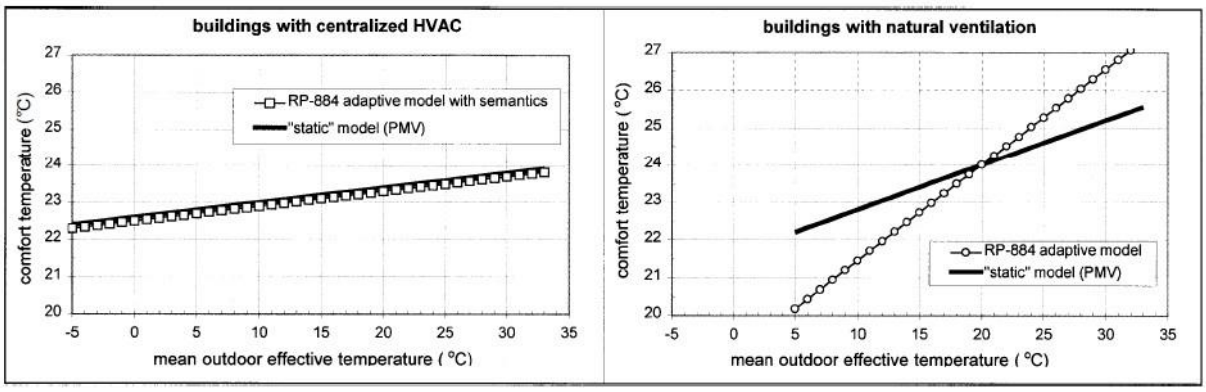

(a) (b)

Figure 1.2: Comparison of indoor comfort temperatures. Observed by the adaptive model with those predicted by the PMV model for both centralized HVAC (a) and naturally ventilated (b) buildings as the function of mean outdoor effective air temperatures (de Dear et al. 1998).

More advanced investigations and research on thermal comfort consider the thermal balance of the human body, and also calculate comfort and sensation for local body parts (Zhang et al. 2009 a, b, c).

On the other hand, indoor air quality (IAQ) is also an important factor for evaluating the performance of the ventilated buildings/rooms, which relates to the air quality within and around buildings/rooms with potential effects on the health of occupants. The topic of IAQ has recently become more and more popular, since people are gradually becoming aware of health problems resulting from high levels of CO_2 concentrations and mold, which can trigger asthma and allergies.

Many gaseous materials, such as volatile organic compounds (VOCs), formaldehyde, NO_x, SO_x, Ozone, CO_2, CO and particulate matters, have frequently been adopted as indicators for IAQ (Liu et al. 2012). The indoor concentrations of VOCs and formaldehyde are mainly influenced by the building materials used (Johansson 1978, Berglund et al. 1982, Ashmore et al. 2009). VOCs and formaldehyde levels are strongly connected with painting activities, cleaning products, decorating and installation of new furniture as well as smoking activities (Berry et al 1996, Brown et al 1996, Ashmore et al. 2009). The emission rates for VOCs and formaldehyde will not be considered in the present work due to the strict limitation through standards in this school building project for the building materials and new furniture as well as regulations for no smoking. In particular, indoor concentrations of these gaseous contaminants - except CO_2 - have been measured as low in classrooms, and the classroom CO_2 concentration was generally measured higher due to the airtightness of materials and the low ventilation rates of low energy buildings as well as the respiration of students crowded into rooms (Wang et al. 2014 a, b, c). CO_2 concentrations at high levels inside rooms may cause occupants to get headaches, become drowsy and work more inefficiently at lower activity levels, and may result in bad sleep, eye and throat irritation, fatigue, etc. Therefore, indoor CO_2 concentrations will be used as an important indicator of IAQ in the present investigation. On the other hand, many researchers over the last three decades also emphasized that indoor CO_2 concentration is a significant index for evaluating IAQ or indoor ventilation levels, for example Sterling et al. employed CO_2 concentrations as an indicator of whole ventilation sufficiency (Sterling et al. 1987). Persily indicated that indoor CO_2 concentrations could be valuable for understanding ventilation and IAQ, and furthermore that CO_2 could also be employed to evaluate building/room air change rates (Persily 1997). Stonier pointed out that the most significant parameter measured for the evaluation of IAQ is indoor CO_2 concentration (Stonier 1995). Through numerous investigations of on-site measurements and actual working experience, Wang et al. also found that indoor CO_2 concentrations are indeed an important indicator of IAQ, particularly for the very densely populated places such as school buildings etc. (Wang et al. 2014 a, b, c).

Currently, the global average CO_2 volume concentration in the atmosphere is approximately 390 ppm, but people can produce 4% volume concentration CO_2 through breathing. Normally, one can consider a CO_2 volume concentration of 1000 ppm as the indoor air quality standard in accordance with the Pettenkofer limit (Pettenkofer 1858). The same suggestion has been made by the National Institute for Occupational Safety and Health (NIOSH), which also recommends that indoor air concentrations of CO_2 that exceed 1000 ppm are a marker indicating inadequate ventilation (NIOSH 2008). ASHRAE suggests that CO_2 levels should not exceed 700 ppm above outdoor ambient levels (NIOSH 2008). The UK standards in public schools are that CO_2 in all teaching and learning regions, measured at seated head height and averaged over the total day, should not surpass 1500 ppm. The total day relates to common school hours (i.e. 9 am to 3:30 pm) and includes unoccupied time, for example lunch breaks etc., European standards limit CO_2 to 3500 ppm. The occupational Safety and Health Administration (OSHA) limits CO_2 concentration in the workplace to 5000 ppm for extended durations, and 35000 ppm for 15 minutes (NIOSH 2008).

Contaminant distribution and transportation generally depend on the building/room size and geometry, ventilation system, heat and contaminant source characteristics, and fluid/thermal boundary conditions, for example supply airflow rates and temperatures of ventilation, positions of supply inlets and exhaust outlets and supply diffuser attributes (Lin et al. 2005). As the ventilation rate increases, the IAQ could be enhanced correspondingly. At the same time, the results of increasing ventilation rates will cause much higher energy consumption and ventilation apparatus costs etc. (Lin et al. 2005). One key technique, which can reduce energy consumption as much as possible whilst maintaining an adequate indoor air quality, is Demand Controlled Ventilation (DCV) (Wang et al. 2012). Instead of a constant air exchange rate, CO_2 sensors installed inside the room/building could be used to control the air exchange rate dynamically according to the CO_2 emissions of actual room/building occupants.

For the past decade, many indoor air quality experts and researchers have debated about a suitable definition for indoor air quality, and particularly what an “acceptable” indoor air quality might be. These debates still persist today. At the same time, the investigations and researches on ways to improve indoor air quality have also been developed continuously. One method of quantitatively ensuring the health of indoor air is through frequently effective air exchange using fresh outdoor air instead of interior stale air. In the UK, for instance, 2.5 outdoor air exchanges per hour are required for classrooms. The ventilation should be ad-

equate to limit CO_2 volume concentration to 1500 ppm in halls, dining halls, gym, and physiotherapy spaces. In the USA, and based on the ASHRAE Standards, ventilation in classrooms is specified according to the amount of exterior air per occupant plus the amount of exterior air per unit of floor area, not according to the number of air exchanges per hour. This is due to the fact that the level of CO_2 indoors derives from occupants' respiration and outdoor air, and the sufficiency of ventilation per occupant is indicated by the indoor concentration minus the outdoor concentration. The value of 610 ppm above the concentration outdoors indicates approximately 15 cubic feet per minute of outdoor air per adult occupant doing sedentary work in places where the outdoor air concentration is about 390 ppm, the current global average atmospheric CO_2 volume concentration. According to the requirements of the ASHRAE Standards 62.1 (ASHRAE Standards 62), ventilation in classrooms for acceptable indoor air quality should be approximately 3 air changes per hour based on the occupant density. Of course, the occupants are not the only source of contaminants, meaning that air ventilation might be needed more if strong and unusual sources of contaminant exist inside the room (Liu et al. 2012). For classrooms in Germany, it is necessary to meet the air volume requirement of each occupant; 15 to 20 m^3/h (Wang et al. 2014) during the period of use.

In addition, the use of air filters can purify air and trap some of air contaminants (ASHRAE 52.2, 1999). Air filters, which are installed for example in a ventilation network, are employed to lower the amount of dust etc. in order to improve indoor air quality (Wang et al. 2014). Abadie et al. have investigated the particle pollution using a one-zone model and experiments. The results clearly indicated that the indoor air quality could be enhanced by a high-efficiency filter (Abadie et al. 2001, 2004).

1.2 Passive House

1.2.1 Background and concept for the Passive House

The Passive House standard originated from a dialogue in May 1988 between Professor Bo Adamson of Lund University in Sweden and Professor Wolfgang Feist of the Institute for Housing and the Environment in Germany (Feist et al. 2005). The Passive House concept was developed through a large number of research projects, which were supported by financial assistance from the State of Hessen in Germany (Feist et al. 2005). The first Passive House dwellings were built in Darmstadt, Germany in 1990. The Passive House Insti-

tute was then founded in September 1996 also in Darmstadt, in order to promote and develop the Passive House standards. It is estimated that approximately more than 25000 Passive House structures have been built around the world up to now. Most of those Passive Houses were located in German-speaking countries or in Scandinavia; for example Germany, Austria and Sweden etc.

Once the Passive House concept had been validated in Darmstadt, with space heating totally about 80% less than requested for a conventional new building standard (Feist et al. 2005), the Economical Passive Houses Working Group was then founded in 1996. This group has developed the planning package and initiated production of the innovative components which had been already employed by users, specifically the energy efficient windows and the high efficient ventilation systems etc. The products based on the Passive House standard have been further commercialized within and according to the European Union-sponsored Cost Efficient Passive Houses as European Standards (CEPHEUS) project, which verified the concept in five European countries during the winter of 2000 to 2001 (Feist et al. 2005).

In fact, as mentioned before, Passive House is a standard for building energy requirements (Table 1.1; Dodoo et al. 2011), where the passive heat input-delivered exteriorly by solar irradiation through the glazing of windows and provided internally by the heat emission of electrical appliances and occupants is essentially enough to keep the building/room at thermally comfortable indoor air temperature throughout the heating period (Badescu et al. 2003). Many technologies have been developed especially for the Passive House standard, for example the passive solar building concept and super insulation etc. In fact, previous standards had already been set up for low energy buildings such as, notably, the German low energy house standard (Table 1.1), and the buildings in Sweden and Denmark, which were constructed according to demanding energy codes.

In the past three decades, there has been already much research carried out and experience gained on passive residential and office buildings (Badescu et al. 2003, Feist et al. 2005, Schnieders et al. 2006, Chel et al. 2009, Eicker 2010, Firlag et al. 2013). (Badescu et al. 2003) proposes a model to investigate and calculate as well as evaluate the contribution of renewable energy sources to meet the heating demand of a three-zone passive house for a standard German family with two adults and two children in Rhineland Palatinate, Germany. It also described the time-dependent models, which take into account properly the thermal inertia of the rather thick walls of passive house's envelope, employed

to evaluate the thermal heat requirement and the operation of the ventilation-heating system. In addition, internal heat sources and their detailed time schedules in this three-zone passive house were precisely represented. However, the effect of all those internal heat sources on energy consumption and indoor parameters was not investigated and analysed.

(Firlag et al. 2013) studies the example of a single-family passive house of "JDL: Jangster de Lux" type located in a passive housing estate in Hannover-Kronsberg (Germany). A detailed twelve-zone TRNSYS (Transient Simulation Programme) model of a house with HVAC system was employed as its simulation environment. It investigated how various models of the internal heat and moisture gains, as well as natural airflows between building zones, affect the accuracy of the calculation of the energy performance, indoor temperatures and absolute humidity in that single-family passive house. The most effects were observed on the values of the relative air humidity and energy demand for space heating due to internal heat and moisture gains as well as airflows between the building zones. The difference in absolute humidity of the exhausted air for the investigated passive house was 35.7% (for the studied models with and without moisture gains, respectively). The discrepancy in energy demand for heating computed using precise and simplified methods of internal heat gains determination was 30.1%. In addition, heating demand for the simulation case with closed doors between rooms was 25.5% lower than the case of opened doors (with natural airflows). This article also revealed whether the designed building qualified as "nearly zero" energy building (or passive building) depends rather heavily on the accurate method of numerical calculation.

(Schnieders et al. 2006) presents the detailed measurement and occupant-satisfaction results for eleven Passive House projects with more than 100 dwelling units from European Union-sponsored demonstration project CEPHEUS. Compared with conventional new buildings, all new buildings with Passive House standard of CEPHEUS project may reduce 80% space heat consumption. Meanwhile, total primary energy consumption can decrease approximately 50%. In addition, all those buildings with Passive House standard can also provide thermally comfortable indoor conditions and favourable indoor air quality in summer and winter based on the measurement data and the satisfaction-questionnaire results of occupants. Finally, it concluded that the building with Passive House standard can fulfil the sustainable conditions from the social, ecological and economic points of view and should thus be disseminated on a large scale. Schnieders et al. also recommended that there are political possibilities to push Passive House into the market and to stimulate a powerful market-influence for this thermally comfortable and high energy efficient building type.

(Eicker 2010) analyses the summer comfort and energy performance of a highly insulated Passive House standard office building with mechanical night ventilation, ground heat exchange facility and PCM (Phase Change Materials) storage. In this study, the average COP (Coefficient of Performance) for night ventilation is 4.0, with a maximum value of 7.8. The utilization of PCM in the gypsum boards of the top floor ceiling and walls did not effectively control the indoor temperature level. The melting point of PCM is very high up to 26 °C to 28 °C and the latent heat capacity limited to approximately 80 Wh/m^2. The major problem was however the low heat flux for discharging PCM boards during the night with the limited air exchange rates. The mean nightly heat flux of the ceiling is less than 2 W/m^2, corresponding to the total energy removed of 30 Wh/m^2. Because of rather low insulation thickness of the floor with U-value of 0.39 W/m^{2}K, the ground floor contributes obviously to the heat removal. The measured heat flux via the ground floor into the earth was from 2 W/m^2 to 3 W/m^2 on average, which is the same value as the measured heat flux removed from the ceiling during night ventilation i.e. 2.7 W/m^2 on average. In addition, the summer comfort in this office building is generally acceptable, although the limitations in heat removal through mechanical night ventilation. There were 220 hours in summer of 2005, whose ambient temperatures were higher than 25 °C. However, all rooms in the office building had very favourable room air conditions, only with 4.2% of all office hours above 26 °C. In summer of 2006, 10.6% of all office hours had room air temperatures larger than 26 °C, although the average ambient temperatures in July were higher than average ambient temperatures up to 4 K.

(Audenaert et al. 2008) investigates three building types i.e. the standard house (3), the low-energy house (3) and the passive house (5) based on 11 different houses from an economic investment point of view. Firstly, the specific additional costs of each type have been studied and compared with each other. After analysis, it was concluded that the extra cost of the low-energy house is 4% and of the passive house is 16% in comparison with the standard house. The additional costs for isolation and ventilation result in the largest surplus cost for the passive house i.e. 64% and 27% of total costs, respectively. Secondly, a break-even time has been calculated compared with the three types of houses. The analysis results show that the break-even time is always shorter for the low-energy house than for the passive house. Meanwhile, it is rather dependent on the growth of the energy prices. However, the annual growth of the energy price would be minimally 25% when a maximum time of regain for the passive house is imposed. In addition, the return time is 20 years for an annual growth of 9%. Thirdly, the cash flow analysis has been also performed in order to

calculate the effect of housing type on annual family budget. The analysis results demonstrate the low-energy house is the safest choice with a minimal effect on the family budget with constant energy prices. After 20 years both passive and low-energy houses have a positive impact on annual family budget, due to the neglected mortgage and the remaining measures for energy saving. The positive influence of the passive house reaches up to 26450 € after 20 years in the case of that the energy costs improve with 15% annually. The impact of passive house is heavily dependent on the change of the energy prices. If the energy prices increased with 5%, 10% and 15% annually, respectively, the impacts on family budget are completely different i.e. -15229 € (over a 20-year timeframe), 1106 € (total gain after 20 years), and 30599 € (total gain after 20 years), respectively.

(Dodoo et al. 2011) analyses the impact of the passive house standard or Swedish building codes on the life cycle primary energy use of residential buildings. The results demonstrate the importance of a life cycle primary energy perspective and the choice of heating system in shrinking primary energy use in built environment. The Passive House building with district heating achieves 30% lower life cycle primary energy use than that with electric heating, emphasizing the importance of heat supply system. It suggests that efficient energy supply system is very significant for a low energy building and should be an integral part of the effort to create a low energy built environment. The primary energy of production, excluding the energy obtained from biomass residues, for the Passive House buildings with wood-frame are 19% and 30% of primary energy for production and space heating and ventilation during 50 years for electric and district heating, respectively. With a concrete-frame the corresponding values are 22% and 36%. With BBR 2009 (energy-efficiency standard of current Swedish building codes) and wood-frame the corresponding range is 14% and 17%. As building energy-efficiency standards continue to improve, strategies of reducing production primary energy use will become much more important. The analysis illuminates that the production phase primary energy balance is approximately twice as much when the buildings are constructed with concrete instead of with wood frames. The recovery of biomass residues during the production and end-of-life phases completely compensates the primary energy used for production for the buildings. Significant quantities of biomass residues are produced because of the use of wood-frame material. The life cycle primary energy mostly determines natural resources efficiency and environmental effect of buildings. If minimizing primary energy use was an aim for constructing passive houses, district heating should be encouraged in passive houses when possible and electric heating should be avoided.

(Gustafsson et al. 2014) investigates and compares energy performance of three innovative HVAC systems for a renovated single family house with Passive House standard through two dynamic simulation tools: TRNSYS 17 and Matlab/Simulink, respectively. All HVAC systems have been tested with a model for different U-values, climates, infiltration and ventilation rates. The difference in energy consumption of the reference system is less than 2 kWh/(m^2a) between Matlab/Simulink and TRNSYS. It can be possibly explained by different ways of handling solar gains, in addition, by the fact that TRNSYS systems can supply slightly more than the ideal heating demand. It suggests that for retrofitted buildings the use of domestic hot water will make up a larger part of total energy consumption when space heating demand is reduced through the building envelope renovation. Meanwhile, cooling demand should also be considered in warm climates.

(Ridley et al. 2014) reports on the energy and thermal performance of two detached Welsh Passive Houses side by side, which have been monitored over 2 years. The two residential houses provide a valuable insight into different methods to achieve low and near zero low carbon performance based on different glazed area, the use of thermal storages, area of installed PV (Photovoltaic) and occupant behaviour. In particular, the impact of different glazing areas on the risk of summer time overheating in the residential buildings has been analysed and investigated in depth. It also illuminates that occupant electricity consumption behaviour and occupant appliance choices have a large impact on energy performance of the residential passive houses. Under current carbon intensities electricity consumption in UK, the passive houses requires to be limited to about 30% of current UK average household if primary energy and zero energy targets needed to be obtained, meanwhile, PV size needs to be below 5 kW peak.

(Flaga-Maryanczyk et al. 2014) analyses experimental measurements and CFD numerical simulations of a ground source heat exchanger implementing at a cold climate for a passive house ventilation system. In this work, the ground source heat exchanger implementing for the passive house ventilation system at cold climate capacitated to employ the heat capacity of the ground for heating, successfully restraining the large fluctuations of external air temperature, in particular during severe frost in early February. The ground source heat exchanger can provide 24% of thermal energy for heating the ventilation air in February on average. However, its average level is approximately 15% for heating the ventilation air during the months from December to April. Based on measurement data and CFD simulations, which have been performed for the ground source heat exchanger operated by passive house ventilation system on February, showed very good correlation with

the measured results. The calculated RMS (Root Mean Square) error is only 0.62%, which demonstrates that the difference between CFD simulation results and measurement data is just 1.7 °C on average. This shows that using CFD tool is very suitable for simulations of the ground source heat exchanger at a cold climate for a passive house ventilation system. In addition, CFD simulation results can physically and accurately predict the trend of indoor thermal environment.

(Mahdavi et al. 2010) compares one passive house apartment with one low-energy apartment in Vienna based on monitored indoor environmental conditions (including indoor air temperature, relative humidity and CO_2 concentration), metered energy use, calculated embodied energy, CO_2 emissions, user evaluation, and construction costs data over a period of 5 months. Meanwhile, both of two apartments were constructed simultaneously in the same location and using comparable building construction properties and floor plan. However, the major difference between them is their ventilation systems: Passive building employs controlled mechanical ventilation, whereas low-energy building applies mostly user manual natural ventilation – open/close the windows. The results demonstrate that both passive and low-energy buildings operated very well from the points of view of thermal conditions and indoor air quality etc., although the passive building performance was slightly better. It also shows that passive building consumed about 65% less heating energy and 35% less electrical energy as compared with low-energy building. In addition, CO_2 emissions of passive building were about 25% to 40% less than low-energy building. But, the initial costs penalty combined with the construction of passive building, which can be resulting in an estimated payback period of 8-18 years, was 5% compared to low-energy building.

(Georges et al. 2014) investigates and analyses the air heating (AH) applied as space heating (SH) for passive houses (PH) in cold climates. It presents the feasibility of the AH concept in PH along with its challenges from the thermal dynamics point of view: the temperature difference between different rooms, the magnitude of the AH temperature required, the effect of thermal losses from ventilation ducts and AH control, and the impact of internal gains. It has been performed using detailed dynamic simulations i.e. TRNSYS on a typical detached house typology. Four different cold climate zones have been practically simulated as well as different construction materials and insulation levels. The performance of AH has been analysed for standard design conditions (STD), which are defined as an SH design outdoor temperature and without solar gains, and using a Typical Meteorological Year (TMY). The simulation results demonstrate that the limitation related to a centralized AH and provide design guidelines for a consistent AH in cold climates. Furthermore, a simple

analytical method employed for the German PH design has been tested and proved that it is enough accurate to estimate maximal AH temperature during the heating season.

(Kuzman et al. 2013) compares different construction types for the passive houses including solid wood, wood-frame aerated concrete, and brick etc. so as to demonstrate the advantages and disadvantages of those common construction materials. The analytic hierarchy process (AHP) method, which is widely applied for analysing the different decision criteria, has been employed to quantify the above comparison. The model analysis illuminates that the highest ranking criteria in decision-making are well-being, the psychological aspect, functionality and end-of-life disposal, emissions, and aesthetics, apart from fire safety, load capacity and energy efficiency. In addition, the analysis results also show that the wood, which is a renewable raw material, is one of the most suitable choices for energy-efficient construction since it is also a good thermal insulator, meanwhile, it has good mechanical characteristics, and it can provide a comfortable indoor climate. Furthermore, the AHP analysis method is very useful for professionals and future dwellers to determine a reasonable choice on further developing and optimizing a special aspect of building process through providing them the possibility of comparing different selections on a common and comprehensive basis. According to the growing importance of energy-efficient building methods, wood construction will play an increasingly significant role in the future.

(Koci et al. 2014) presents the computational analysis of thermal performance for a passive family house built of hollow clay bricks from the architectural, constructional, and material solution points of view. The results demonstrate that the thickness of thermal insulation layer could be decreased several times if up-to-date hollow bricks with lightened brick body and its sophisticated systems of interior cavities were employed, instead of old-fashioned hollow bricks or traditional bricks with only several large cavities. From a building envelope thickness point of view, the designed brick-built passive house can therefore nearly identical with timber-based houses. Furthermore, it retains some very important advantages and characteristics for common brick structures e.g. good thermal accumulation properties, fast water vapour transport through the walls, and fire resistance, or a low risk of biological degradation. The up-to-date hollow brick block can thus be considered a proper construction material for passive house design.

(Rohdin et al. 2014) investigates indoor thermal and energy performance of 9 passive houses built in Sweden with a combination of a post-occupancy survey, measurements and validated building energy simulation (IDA Indoor Climate and Energy). The performance of

passive houses has been analysed based on energy use, thermal comfort, and local comfort including cold floor temperatures and draught risk. Furthermore, indoor thermal environment of all those studied passive houses has been also compared with 30 conventional houses built at the same time and located in the same region based on a post-occupancy survey. The methodology of this work is on the basis of on-site measurements and two different types of simulations i.e. CFD and BES (Building Energy Simulation). It shows some interesting findings related to local comfort such as cold floors, which are found in the post-occupancy evaluation as well as in the predictions. In addition, a higher degree of complaints also appears in the post-occupancy evaluation during summer in passive houses. The possible reasons are due to the facts that the buildings did not install external shadings, and the passive houses are much more well-insulated and airtight than conventional buildings. The study also demonstrates that the energy use in all those buildings agrees well with the predictions, and it depends heavily on the set points. For example, for the set point 20 °C, the specific annual energy demand for space heating is around 21 kWh/m^{2}a, however, it is about 35 kWh/m^{2}a for the set point 24 °C.

(Georges et al. 2012) analyses the environmental and economic performance of heating systems used in new passive and low-energy single-family houses. The evaluation method in this study has employed three European Standards i.e. EN 15316 (2007), EN 15459 (2007) and EN 15603 (2008) using parameter values representative of current Belgian market based on prices and energy carriers, however, the evaluation method did not consider any incentive or maintenance costs. The only two indicators including total primary energy consumption and equivalent CO_2 emissions have been investigated in order to evaluate the environmental impact, meanwhile, the total discounted costs has been analysed so as to rate the economic performance. To analyse the performance of heating systems without considering the architectural measures has been the first objective of this work. In addition, the second objective was in order to analyse the global performance, considering the heating system and energy-savings measures for the envelope, for one representative detached house typology.

(Fux et al. 2014) presents the simulation results of different lumped-parameter using Model Predictive Control (MPC) with an extended Kalman filter (EKF) based on self-adaptive thermal building models for a passive house compared with measurement data. The evaluation demonstrates that thermal building models with simple lumped-parameter can simulate the mean room temperature level of an entire building with an RMS error of approximately 0.5 °C during a simulation period of around two weeks. In addition, this work presents that a method using one resistor and one capacitor (1R1C) model can provide a

demand prediction for the HVAC system. The aforementioned method employs an online identification of the relevant building parameters combined with an estimation of the disturbance heat gain resulted from the presence of occupants inside the building. The EKF approach employed illuminates a robust convergence of the two thermal building model parameters. What's more, the online identification of the disturbance heat gain obviously enhances the prediction accuracy of the model when occupied. According to the predicted system behaviour, an MPC controller can produce optimal inputs for the HVAC system. Furthermore, the self-adapting model ensures an energy-optimal performance of the building services under different operation conditions, the thermal comfort of the occupants is also maintained at the highest acceptable level.

The Passive House standard for central Europe calls for the building to meet the following requirements (Feist et al. 2002, 2005, Schnieders et al. 2006):

1) The annual heating/cooling demand must not exceed 15 kWh/m^2 per year in accordance with the Passive House Planning Package (PHPP), or the building is designed with a peak heat load of 10 W/m^2.
2) The entire primary energy (source energy for electricity and so on) consumption (primary energy for heating, electricity and hot water etc.) must not exceed 120 kWh/m^2 per year.
3) The air infiltration rate of the building must be less than 0.6 per hour at 50 Pa (N/m^2) as tested by a blower door, and less than 0.3 per hour at 50 Pa (N/m^2) is recommended.
4) In addition, the specific heat load for the heating source at set temperature is suggested, but not compulsory, as remaining less than 10 W/m^2.

Most normal building standards are much lower than the aforementioned standards. Fig. 1.3 shows the significant difference between a Passive House building (right) and a traditional building (left). As seen in Fig. 1.3, little heat is escaping from the Passive House building due to the high level of thermal insulation and energy efficient windows as well as the extremely airtight building envelopes etc. in comparison with the common building (Feist et al. 2002). In fact, some European countries such as the partners of the Consortium for the Promotion of European Passive Houses think that the aforementioned Passive House standards should contain a certain amount of flexibility to adapt theses limits based on local conditions.

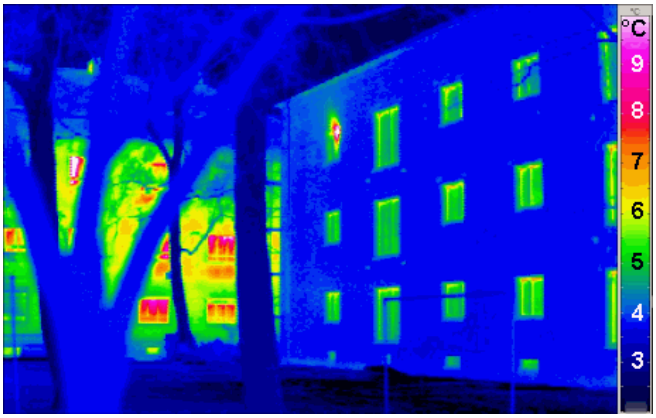

Figure 1.3: Comparison of the thermo gram. Passive House building (right: with high level of thermal insulation) and a traditional building (left: with much more heat losses compared to right Passive House building) (Feist et al. 2002).

1.2.2 Passive House design and construction

A suitable design and construction for the Passive House are definitely necessary to achieve the major decrease in heating energy consumption requested by the Passive House standard. The Passive House design is performed with the aid of the PHPP and specifically designed computer simulations. A large number of technologies are employed in combination in order to fulfil the Passive House standards (Feist et al. 2002, 2005, Schnieders et al. 2006).

1.2.2.1 Super insulation

The Passive House buildings utilize super insulation to decrease the heat transfer through the walls, floor and roof substantially compared with traditional buildings. A large range of thermal insulation materials could be employed to obtain the required low heat transfer coefficients i.e. U-values, which should typically be within the range of 0.10 W/(m^{2}K) to 0.15 W/(m^{2}K). Technically, particular attentions must be paid to exclude thermal/cold bridges (Badescu et al. 2003). In order to avoid thermal/cold bridges, the minimum internal surface temperatures should be not less than 13 °C anywhere (Schnieders et al. 2006).

1.2.2.2 Air tightness

Building envelopes in terms of the Passive House standard are required to be extremely airtight compared with traditional building constructions. In order to achieve the standard, air barriers, careful sealing of each construction joint in the building envelope, and sealing of all penetrations across the envelope are employed together. Air tightness can minimize

the amount of warm/cold air which can transfer through the envelope structure, so as to ensure that the mechanical ventilation system can recover the heat/cooling before exhausting the indoor air outside, and strongly reduce the heat losses by mechanical ventilation and space heating (Badescu et al. 2003).

1.2.2.3 Advanced window technology

In order to fulfil the requirements of the Passive House standard, windows are produced with particularly low U-values, typically in the range of 0.70 W/(m^{2}K) to 0.85 W/(m^{2}K) for the total window including the window frame. This could be realized by combining triple-pane insulated glazing, which has low emissivity, a fine solar heat gain ratio, warm edge insulating glass spacers and sealed krypton or argon gas filled inter-pane voids, with specially developed thermally broken window frames and air sealing (Feist et al. 2002, 2005). In fact, in most of the US and central Europe, the solar heat gains for unhindered Passive House windows with a southern exposure are on average higher than the heat losses, even also in midwinter. In addition, it is also necessary to install the windows correctly in order to avoid thermal bridge loss and increasing overall U-value of windows e.g. the windows should be positioned within the insulation plane of thermal envelope and that insulation overlaps the window frame as far as possible, which can make thermal bridge loss coefficient of installation as zero (Schnieders et al. 2006).

1.2.2.4 Space heating

Passive House buildings make full use of their inherent heat from interior heat sources, for example the waste heat from lighting and electrical appliances, and body heat from the people inside the building/room. This is mainly because the human body is a heat source with an average power of about 100 W (ISO EN 7730 2005). Normally, a well-designed Passive House under the influence of the European climate would not need any additional heat source if the heat load inside the building/room is maintained as lower than 10 W/m^2, even if we do not consider the recovery of the heat by the heat recovery ventilation unit. This is due to the fact that both the heating energy demand and the heating capacity for a Passive House are very low. Air heating components, such as a hot water storage tank, could be heated annually by direct heat energy from the solar and geothermal solar, and by a heat pump, as well as by oil burner or a natural gas.

1.2.2.5 Ventilation system with heat recovery

Normally, in order to enhance the potential of the heat recovery mechanical ventilation system and extremely airtight building envelopes, windows in the building/room are shut in order to avoid indoor heating energy losses. Therefore, the air exchange rate must be strictly controlled and optimized to maintain a sufficient volume of fresh breath air for the occupants inside the building/room. The heat recovery rate should be over 75% at least so as to recover sufficient heat to supply to the building/room (Schnieders et al. 2006), and air filters should be employed in mechanical ventilation networks to maintain the indoor air quality to some extent. Moreover, all ventilation ducts should be well-insulated and sealed against air leakage in order to avoid heating energy losses. Electricity-saving fans and low pressure losses inside the heat recovery ventilation system, which are generally driven by highly efficient direct current motors and consume 0.4 W/(m^3/h) or less on average, are rather essential. In addition, it is suggested but not compulsory to pre-heat/pre-cool the intake air for the ventilation system for the purpose of promoting the heat efficiency; at the same time, the warmed air could also prevent ice/frost formation into the heat exchanger of the heat recovery system in winter. Also, the heat exchanger of the heat recovery system must have a bypass especially design for summer operation (Feist et al. 2002, 2005).

On the other hand, when indoor temperatures lie close to exterior temperatures for example in the transitional seasons, natural ventilation is still an effective method of improving indoor air quality and reducing energy consumption in Passive House buildings. Passive means of natural ventilation include singular or cross ventilation and a simple opening, or are promoted by the stack effect from a smaller ingress to a large outlet window etc**.**

1.2.2.6 Electrical appliances and lighting

Electrical appliance products should fulfil individual energy efficiency verifications and obtain Eco-label license markings in order to lower electrical consumption. Moreover, the carbon emission labels of electrical appliance product manufacturing should be preferred for application in Passive House buildings.

Many passive and active lighting techniques are employed, for example creative sustainable lighting design with low energy sources, solid state lighting using light emission diode-LED lamps, and polymer light emission diodes (PLED) as well as organic light-emission diodes (OLED) etc. for the purpose of minimizing the total primary energy waste. Furthermore, it is extremely necessary to employ motion detection and natural light intensity sensors as well as timers in Passive House buildings so as to save electrical energy. In addition,

according to the requirements of Passive House building's gardens and outdoor, solar powered landscape, security and external circulation lighting with photovoltaic cells for connection with a central solar panel system or individual fixture are available**.**

1.2.3 Traits of Passive House

Based on the aforementioned design and construction, Passive House buildings normally have the following characteristics:

1) The supply air from the diffuser is fresh and quite clean. This is mainly because exterior ambient fresh air is sucked into the ventilation system, and it is then filtered through an air filter, for example a High Efficiency Particulate Air filter (HEPA) etc. A suitable air exchange rate such as 0.3 1/h is set by users according to their demands such as IAQ and thermal comfort, otherwise the indoor air will become stale and polluted, as a result of excess CO_2 generated by the occupants and the flushing of interior air contaminants; as well as becoming excessively dry, for example, less than 40% relative humidity.
2) Due to the extremely low heat transfer coefficients (high resistance to heat flow) of exterior walls and roofs, other walls are not much warmer than the exterior walls and roofs.
3) The indoor temperature for a Passive House is uniform, which means that the indoor temperature of single rooms should be the same as the rest of the house.
4) Even if the ventilation and heating systems are not put into operation, the indoor temperature still varies very slowly. Normally, a Passive House only reduces in temperature by less than 0.5 °C per day in winter. Furthermore, it can stabilize at approximately 15 °C in a Central European climate.
5) The indoor air can very quickly recover to the normal temperature within a Passive House after windows or doors have been opened and then closed again after a short time period. This illustrates that there is only a very tiny effect on indoor temperature for short periods of natural ventilation.
6) Heating could be supplied exclusively by the mechanical ventilation system with heat recovery unit for a Passive House if the space heating demand is sufficiently low.

1.3 Objectives

The objectives set and accomplishments made in this thesis are:

The main goal of this thesis is to investigate energy performance through optimizing the school building control systems for the heating/cooling, pre-heating/pre-cooling (air conditioning), ventilation and sun-shading etc. and to investigate classroom airflow motion, heat transfer and CO_2 emission so as to minimize energy consumption and at the same time improve human thermal comfort and indoor air quality. Also, due to the innovative heat recovery ventilation facility and air heating/cooling system adopted by the Passive House School buildings in winter/summer, the energy performance and built environment of the school buildings should be particularly paid attention.

The heat recovery efficiency of the heat recovery facility and energy conservation ratio of the air conditioning unit were analytically modelled, taking the ventilation network into account. Subsequently, the mathematical modelling of displacement ventilation airflow in the classroom are briefly described (Shao et al. 1995, Chow 2004, Zhao et al. 2008, Chen 2009, Wang et al. 2012, Liu et al. 2012), and the corresponding computational fluid dynamics (CFD) program are validated by the on-site measurements. Following that, classroom displacement ventilation and its thermal stratification were investigated concerning the effects of delivering ventilation flow rate and supply air temperature. Displacement ventilation essentially belongs to an energy efficient air delivery and distribution strategy, where fresh and conditioned air are delivered at floor level and heated or polluted by indoor occupants, and then naturally extracted from upper exhausts. With such advantages, displacement ventilation is well-suited for improving indoor air quality in occupied spaces. On the other hand, displacement ventilation may be a cause of discomfort due to large vertical temperature differences and ventilation drafts (Yuan et al. 1998, Yuan et al. 1999). Therefore, it is essential for us to investigate the thermal comfort of occupants in low energy school buildings with displacement ventilation.

Representative thermal comfort parameters such as percentage dissatisfied, vertical temperature difference between ankle and head, and the normalized standard deviations of horizontal plane averaged temperatures in the classroom as well as draft dissatisfaction have been analyzed and evaluated. The indoor air quality as indicated by the CO_2 concentration was also investigated in terms of the different levels of ventilation flow rate. The effect of ventilation strategies on the classroom volume averaged temperature, vertical thermal gradient and classroom CO_2 concentration reductions are included.

Numerical results indicate that the promotion of a mechanical ventilation rate can simultaneously enhance the dilution of indoor air pollutants and the non-uniformity of indoor thermal and pollutant distributions. Subsequent energy performance analysis illuminates that classroom energy demands for ventilation and summer cooling/winter heating could be decreased with the promotion of heat recovery efficiency of the ventilation facility, and that the energy conservation ratio of the air cooling/heating unit is a decreasing/increasing function of supplying fresh air temperature. Detailed correlations of heat recovery ventilation and cooling/heating energy conservation have been presented.

On the other hand, built environments and energy performance in transitional seasons must also be investigated. This is due to the fact that natural ventilation is an energy efficient air delivery for the reduction of energy consumption, especially when the difference between indoor temperature and exterior surrounding temperature is minor, such as during the transitional seasons (Allocca et al. 2003). Consequently, in recent decades, many researchers have investigated the airflow patterns, the temperature and contaminant distributions, and thermal stratification comfort as well as the effects of thermal buoyancy and wind force for naturally ventilated rooms or buildings (Zhong et al. 2012, Linden et al. 1990 and 1996, Li 2000 and 2001, Jiang et al. 2003, Fitzgerald et al. 2004, Chen 2009). However, most of the aforementioned research and experience focused on the residential and office buildings, but almost nothing was done on school buildings.

In this section of the natural ventilation study, a theoretical analysis of ventilation effectiveness and heat loss due to natural ventilation is presented. Subsequently, displacement natural ventilation air flow motion, thermal transport and indoor CO_2 dispersion with and without thermal buoyancy is fully simulated by the validated numerical codes. The effects of natural ventilation parameters on the classroom volume averaged temperature, vertical thermal gradient as well as classroom CO_2 concentration reductions are also included. Typical thermal comfort parameters are also analyzed. Finally, the heat loss resulting from natural ventilation is correlated with functions of the ventilation effectiveness ratio.

In order to evaluate and optimize the school building control systems with the Passive House Standard, it is essential to investigate the detailed space-averaged and steady state results of factors such as all kinds of energy consumption (or demand) and gains etc. as well as the energy balance of a single classroom and whole building. We employ a single reference classroom 2.28 and the whole school building respectively as our objects of research for those investigations. Furthermore, all the structure including geometry, orientation, size of envelope e.g. walls and windows, building elements, air infiltration, forced and

natural ventilation including pre-day ventilation and day ventilation, night ventilation, sun-shading, internal gains, artificial lighting, schedule, heating/cooling and thermal parameters for the reference rooms and school building can be definitely obtained or measured precisely. Therefore, it is possible for us to build models with the Building Energy Simulation (BES) program which is based on the network model. For the purpose of good evaluation and optimization of the structure planning and designs and control systems for the single reference classroom and whole building through analyzing the energy balance of aforementioned single reference classroom and whole building under all possible and practical operational conditions, the BES results are experimentally validated and compared with measurement results obtained from monitoring database in our ZAE Bayern considering standard weather data sets in Munich.

In addition, in order to further develop and test the school building control systems using the BES tool, separate analyses and evaluations have been carried out for the following completely different cases, i.e. with and/or without a) pre-ventilation in winter, b) night ventilation in summer, c) sun-shading system, d) heating and e) active cooling as well as f) the heat recovery systems etc. for the single room and whole building. Also, comparisons and evaluations have been conducted under different control parameter settings for a single room and the whole building, for example the efficiency of the heat recovery facility, the night ventilation flow rate and the indoor air temperature set-point for heating and cooling etc.

2 School Building Project and Measurements

In this chapter, a project of new school building with Passive House standard of the FOS/BOS Erding has been introduced. It includes building envelope, heating and cooling, mechanical ventilation system with heat recovery unit and its operation mode in winter and summer, and our research platform: reference classroom 2.28 etc. Following that, some important measurements including blower door test, infiltration rate, natural ventilation rate, and thermal time constant etc., which will be used for the simulations, have been presented and analyzed.

2.1 Project introduction

2.1.1 New concept passive school building of the FOS/BOS Erding

Recently, school buildings in Germany have been shown to have high energy demand and often low air quality as well as thermal discomfort. Several pilot projects are started with modern building concepts for energy efficient school buildings. ZAE Bayern (Bavarian Centre for Applied Energy Research) has been monitoring and optimizing the Passive House School Building at the State Technical and Vocational Secondary School (FOS/BOS) Erding (Lat.: 48° 18' 40", Long.: 11° 53' 49") , composed of the south building and north building as well as the atrium as illustrated in Fig. 2.1 and Fig. A.1 (location plan in Appendix A), including about 750 students from March, 2011 (Kuckelkorn 2011).

The control systems of this building include single-room control for heating, cooling, air quality, artificial light, sun-shading systems and mechanical ventilation (including pre-ventilation and day ventilation) as well as the main energy efficient supply units etc. The controlled sensors-data and additional measurement results have been already recorded in a monitoring database (Medview2) in our ZAE Bayern over 3 and half years.

(a) Overview of the school building

(b) Atrium

(c) South facade

(d) North facade

Figure 2.1: New school building with Passive House standard. Overview of the building from west (a): including north building, atrium and south building, the atrium (b): used as a resting area, with high efficient day lighting and exterior sun protection and integrated with ventilation system in buildings for night ventilation in summer, the south façade (c) and north façade (d) of the school building.

2.1.2 Envelope

2.1.2.1 Wall and layer

As such low energy school building, external walls are composed of interior plaster, reinforced concrete, and heat insulation (from indoor to outdoor, respectively), whereas the roof is formed by reinforced concrete and heat insulation. WLG 035 insulation material is applied in the wall insulation layers such that heat transfer coefficients (U-values) of the classroom envelopes are maintained at lower values, i.e. external wall 0.128 W/m^{2}K, roof 0.095 W/m^{2}K, interior walls 4.357 W/m^{2}K and floor 2.450 W/m^{2}K as well as the ground floor 0.176 W/m^{2}K. Thermal bridges are also excluded in whole building structure. Fig. 2.2 shows the infrared (IR) thermograph measurement results in winter. Seen from Fig. 2.2, only very little

heat is escaping from the school building with Passive House standard due to high level thermal insulation, free thermal bridge construction and energy efficient windows.

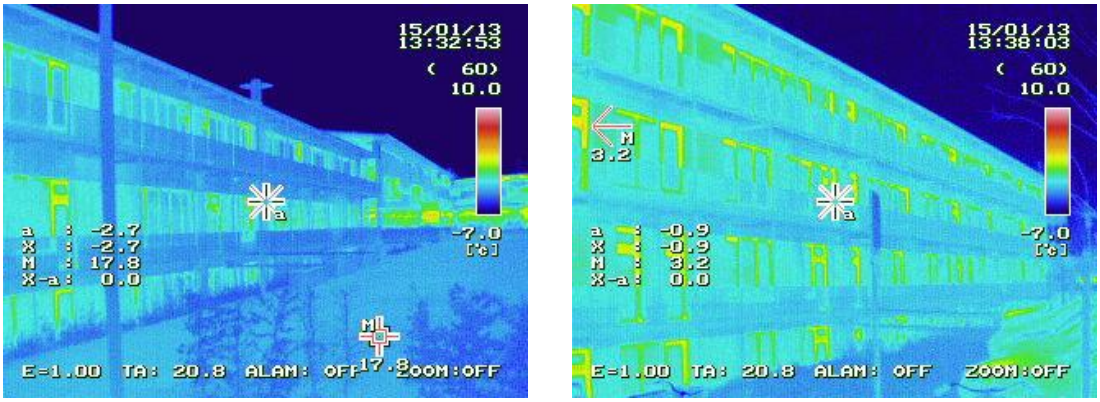

(a) South facade (b) North facade

Figure 2.2: IR temperature measurements. IR temperature measurements for south façade (a) and north façade (b): measurement date is Jan. 15. 2013. Seen from the photos, only very little heat was escaping from the school building with Passive House standard.

2.1.2.2 Window

In order to avoid heat energy consumption, triple glazing (top energy-saving glass from UNIGLAS Corporation) with high performance is adopted for the windows; moreover, the heat transfer coefficient (U-value) of the window including the window frame is 0.870 W/m^{2}K, whereas the heat transfer coefficient (U-value) of the glass is only 0.600 W/m^{2}K. The g-value of the glass is 0.520. Fig. 2.2 also demonstrates that the windows high level thermal insulation glazing and high performance thermal insulation aluminium frames.

2.1.3 Heating and cooling

There is the wall heating, which is supplied by the return of a geothermal district heating, under the windows in each classroom. The specific power of the wall heating is 10.5 W/m^2, and the rated average inlet temperature and outlet temperature of the water flow for the wall heating are approximately 45 °C and 40 °C, respectively. In addition, the supply water flow volume of the south building is 3.5 m^3/h; for the north building it is 6 m^3/h.

Cooling is based on thermal use of the groundwater with average temperature about less than 13 °C in summer, which is employed by a central air conditioner of the whole building to cool the fresh and warm ambient inlet air into suitable inlet air temperature for mechanical

ventilation in each classroom. In other words, the heat transfer from the cooling is realized through mechanical ventilation.

On the other hand, in summer, the large temperature difference between night and day in Munich is made full use, which can provide comfortable indoor temperatures in the daytime of the following day (Blondeau et al. 1997) in primary classrooms (i.e. the classrooms with external walls and windows) of the school building due to the ability of the concrete in the ceiling to store cooling energy. There are four large mechanical exhaust ventilators in the atrium roof as illustrated in Fig. 2.3 which can drive lots of outdoor air with lower temperature e.g. 10 °C at night through the opened windows (i.e. night natural ventilation) of primary classrooms to cool the concrete ceiling of each primary classroom. Cooling and night cooling's detailed introductions will be described in the following section on mechanical ventilation.

Figure 2.3: Four mechanical exhaust ventilators for night ventilation. All of them are placed in the atrium roof of the school building and are operated during summer as the driving force.

2.1.4 Mechanical ventilation system with a heat recovery unit

2.1.4.1 Day ventilation

The ventilation of this school building is facilitated by a heat recovery unit, which is integrated with the mechanical ventilation system. The rotary heat exchanger (AL-KO Therm GMBH), which consists of a circular honeycomb matrix of heat-absorbing material, with heat and humidity recovery is employed to improve energy and humidity efficiency. The minimal air flow requirement of the ventilator is 0.49 Wh/m^3 for the inlet and outlet, which is lower than the reference value 0.69 Wh/m^3 for EnEV 2009. The heat recovery rate is normally equal to or over 76%, although there is a small extra energy requirement for rotating the

wheel, which meets Passive House standards and is higher than the EnEV 2009 reference value of 60%.

When the mechanical ventilation unit was originally put into use, fresh supply air from the diffusers as depicted in Fig. 2.4 of each classroom was usually maintained at variable supply temperatures between 17 °C and 24 °C, supplied into the enclosure, and to meet the minimal average air volume requirement of each occupant 20 m^3/h as the air exchange rate for single rooms in Germany (Wang et al. 2014). After our optimization for mechanical ventilation control system, the supply fresh air temperature is now 19 °C in winter and 19 °C to 21 °C in summer respectively (Wang et al. 2014). The air flow volume regulation for each classroom is actually based on real occupants and indoor air quality requirement.

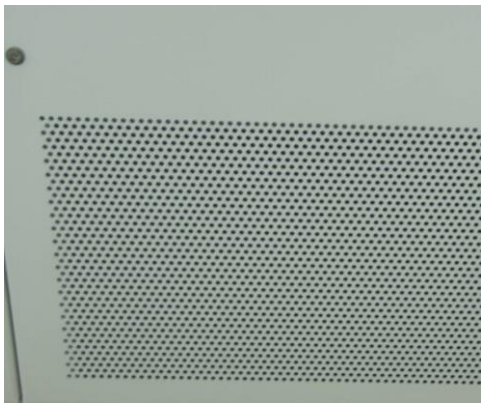

Figure 2.4: Air diffusers. They are installed side by side in the lower part of the wall beneath the window and immediately 0.10 m above the floor and horizontally discharge fresh air into the space in each classroom in the school building.

2.1.4.2 Night ventilation

Night ventilation employs cold night outdoor air to cool down the envelope structure of a building in order that it can absorb the heat flows/gains in the daytime of the following day (Wang et al. 2014). This will then shrink the daytime indoor temperature increase, which can provide more approximate thermal comfort and save lots of energy costs for cooling at the same time (Blondeau et al. 1997). Night ventilation is usually applied to buildings, which are not occupied at night, such as public school building, and where the outdoor temperature difference between day and night is significantly large e.g. more than 10 K or even 20 K in summer in Munich region (Jacob et al. 2008).

2.1.5 Artificial lighting

Artificial lighting can project direct luminaires with high lighting efficiency. Low-energy lighting is located in separate panels as illustrated in Fig. 2.5. Its installed power is 8.0 W/m^2, which is lower than the reference value 11.2 W/m^2 for EnEV 2009. Furthermore, the artificial lighting is dimmed automatically according to the amount of daylight and presence.

Figure 2.5: Artificial lighting in the classroom. Lightings are placed in each classroom with 3 lines and a control system, which can turn on/off and adjust artificial lightings' brightness based on natural light brightness for each line.

2.1.6 Rain water utilization

Rainwater is made full use of to irrigate the school garden and flush the toilets. The rainwater utilization system includes a sedimentation device and three rainwater tanks with a volume of 9 m^3 each as well as an emergency drain-pipe in order to prevent rainwater overflowing from the water tank. Fig. 2.6 depicts a cross section of the system.

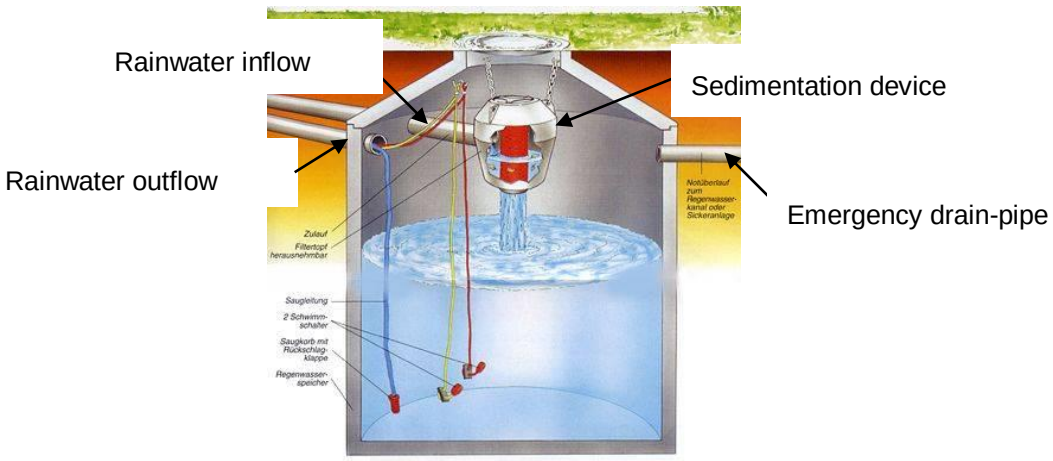

Figure 2.6: Rainwater utilization system. This system can employ rainwater to irrigate school garden and flush the school toilets.

2.1.7 Weather stations

To monitor and optimize the control systems and operation situation of this Passive House school building, it is very important to obtain in-time and reliable weather information e.g. outside temperature, wind situation and solar radiation etc. Three weather stations are installed in the school building as illustrated in Fig. 2.7 whose temporal resolution of data acquisition is one minute.

Global solar radiation is measured by the SP Lite2 silicon pyranometer of Kipp and Zonen. Its directional error (up to 80° with 1000 W/m^2 beam) is less than 5 W/m^2. Wind speed and direction, outdoor air temperature and outdoor relative humidity as well as precipitation and brightness are measured using a Thies CLIMA measurement device with a temporal resolution of one minute. The outside temperature is also measured outside of the building using a Thermokon outdoor temperature sensor (including type AGS43/AGS54/AGS54ext) with an accuracy of ±1% of measuring range at 21 °C. The aforementioned weather conditions including outdoor air temperature, outdoor relative humidity, wind velocity and wind direction and global horizontal radiation etc. will be employed in the following measurements and simulations.

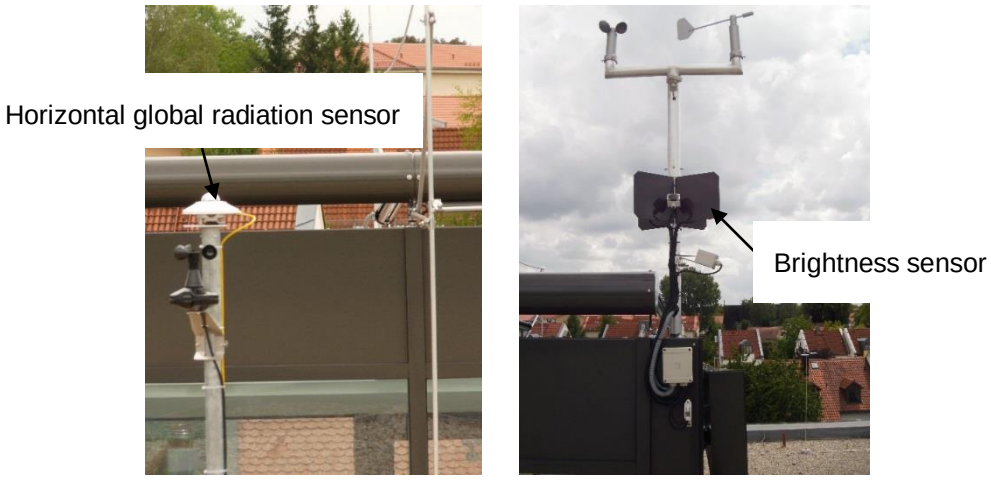

(a) Weather station 1 (b) Weather station 2

Figure 2.7: Weather stations. (a) includes the pyranometer global solar radiation sensor for the building radiation control system, wind speed and temperature and external relative humidity sensors. (b) could measure wind velocity and direction and brightness for the building shading control system.

2.2 Ventilation and heat transfer operation mode in the whole building

2.2.1 Winter case

Fig. 2.8 illustrates the schematics of the winter operation mode for the ventilation and heat transfer in the entire building. In winter, outdoor fresh and cold air firstly passes through mechanical ventilation system with highly efficient heat recovery and pre-heating system (air conditioning) for heating and further heating. Then, the air with 19 °C delivers into primary classrooms through air diffusers in the lower part of room. After displacement ventilation inside the room, air will escape from the exhaust installed in the upper region of the room into the secondary rooms (e.g. teacher offices etc.). Through overflow into the atrium, air with higher temperature will finally return back to the heat recovery unit for the heat exchange with the new fresh and cold air outside.

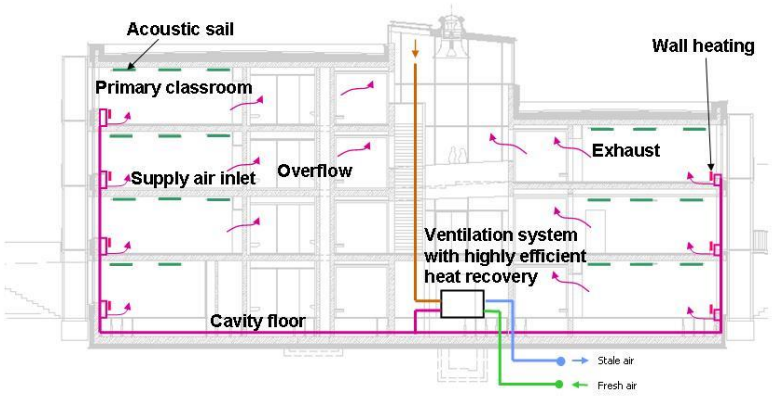

Figure 2.8: Mechanical ventilation and heat transfer operation mode in winter. The school building concept implements a mechanical ventilation system with a highly efficient heat recovery facility and pre-heating unit for heating and further heating. (Background picture: (kplan 2011))

2.2.2 Summer case

Fig. 2.9 depicts day ventilation operation conditions in the entire building in summer. Outdoor fresh and warm air in summer firstly passes through mechanical ventilation system with cooling recovery and pre-cooling system (air conditioning) for cooling and further cooling. Then, the air delivers into primary classrooms through air diffusers in the lower part of room. After displacement ventilation inside the room, air will escape from the exhaust installed in the top side of the room into the secondary rooms. Through overflow into the

atrium, air with lower temperature than outside will finally return back to the cooling recovery unit for the heat exchange with the new fresh and warm air outside.

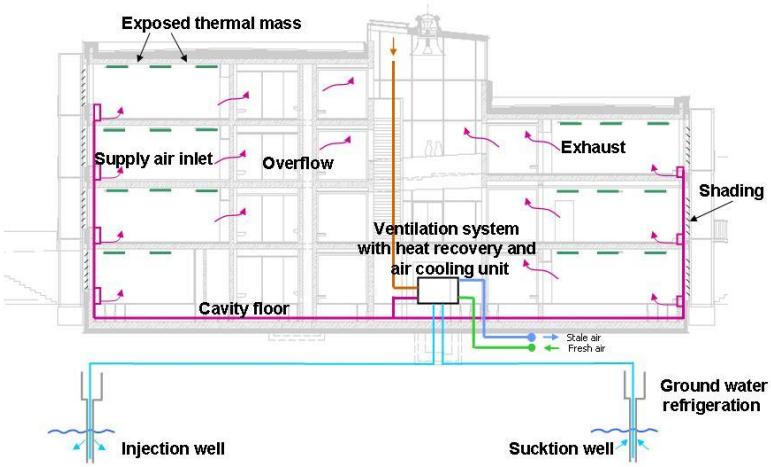

Figure 2.9: Day ventilation and heat transfer operation condition in summer. Similar to winter operation mode, however, there is an air cooling system, whose inlet cooling water with average temperature about 13 °C in summer comes from the groundwater. (Background picture: (kplan 2011))

Fig. 2.10 shows the night ventilation operative situation in summer. The concrete of classroom ceiling with exposed thermal mass can be cooled down by night ventilation. After that, much more cooling energy storage within the concrete of classroom ceiling could be obtained, which can then cool the indoor temperature for the following day i.e. it can provide much more favorable thermal living conditions for occupants and save lots of energy costs for cooling at day.

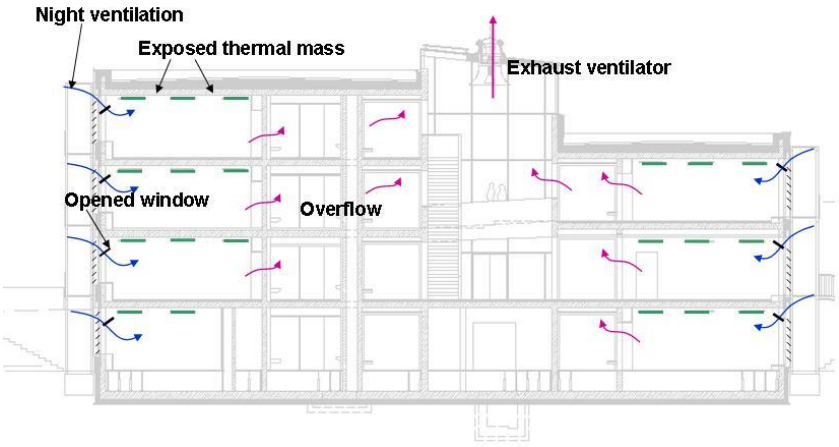

Figure 2.10: Night ventilation and heat transfer operation condition in summer. The concrete of classroom ceiling with exposed thermal mass can be cooled down by night ventilation. (Background picture: (kplan 2011))

2.3 Reference classroom 2.28 – research platform introduction

A representative reference classroom of 9.77 m (length) x 7.25 m (width) x 3.00 m (height) is extracted from the Passive House School building as a research platform, as illustrated in Fig. 2.11, Fig. 2.13 and Fig. 2.14. There are large windows of 5.00 m x 2.10 m in size which are normally closed and a small window which can be opened as natural ventilation and which is a common side-hinged window 1.25 m x 2.10 m in size as well as an entrance door with 1.25 m x 2.85 m. This classroom has all kinds of measurement set-ups such as the sensors etc. installed.

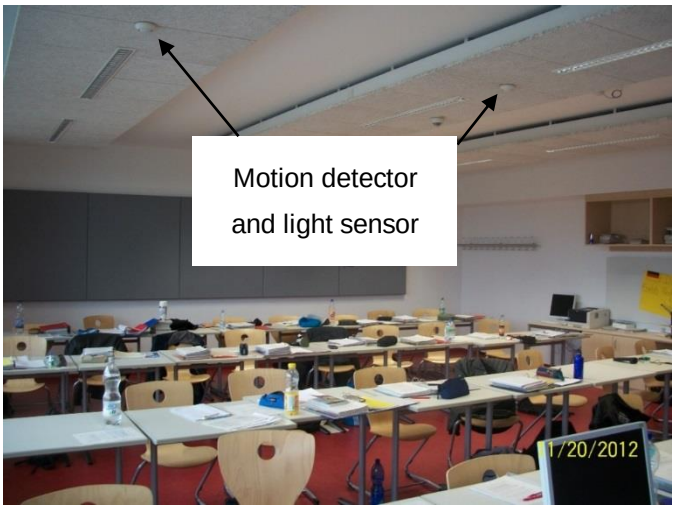

Figure 2.11: Reference classroom 2.28 as the research platform. There are more than 15 different kinds of sensors installed inside this classroom.

2.3.1 Inside surface temperature sensor

Inside surface temperatures of the envelope such as the walls in the reference classroom are measured at the top with a temporal resolution of one minute using a Thermokon cable temperature sensor (TF14/OF14), as indicated in Fig. 2.12, with an accuracy of ±1% of measuring range with the cable of maximal 2 m at 21 °C.

2.3.2 Relative humidity and indoor air temperature sensors

Relative humidity (RH) and indoor air temperature are measured in the top half of the room with a temporal resolution of one minute using a Thermokon surface mounting room sensor for relative humidity and air temperature (LCN-FTW04) as illustrated in Fig. 2.13 with an accuracy of ±3% (25% till 85%) and ±1 °C (5 °C till 45 °C) respectively of the measured values. Meanwhile, both sensors are integrated with the monitoring systems.

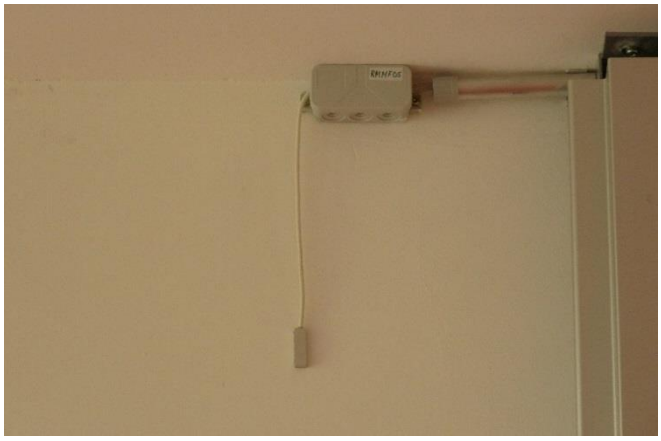

Figure 2.12: Inside surface temperature sensor on the wall in reference room 2.28.

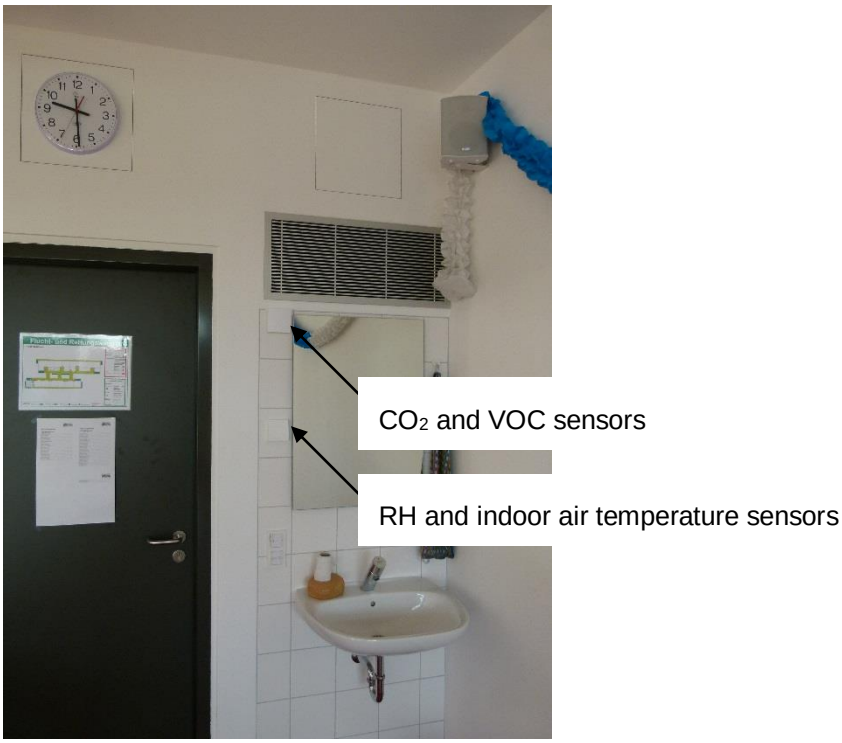

Figure 2.13: Relative humidity, temperature, and CO_2 and VOC sensors. CO_2 sensor is also a regulator for mechanical ventilation system.

2.3.3 Indoor CO_2 sensor

The indoor CO_2 concentration is measured in the top half of the room near the relative humidity and indoor air temperature sensors with a temporal resolution of one minute using an AERASGARD CO_2 sensor, as illustrated also in Fig. 2.13, with an accuracy of ±100 ppm

of the measured values. Meanwhile, it is combined with the control systems, which will determine mechanical ventilation rates based on indoor CO_2 concentration. In addition, there is another more accurate Testo CO_2 sensor for on-site measurements as depicted in Fig. 2.14 with an accuracy of 50 ppm plus 2% of the measured value.

2.3.4 VOC/indoor air quality sensor

VOC is also measured in the top half of the room near the relative humidity and indoor air temperature sensors with a temporal resolution of 1 minute using an AERASGARD VOC sensor as shown also in Fig. 2.13 with an accuracy of ±20% of the measured values.

Figure 2.14: Testo 435 CO_2 sensor. Indoor CO_2 concentration on-site measurement during a class on November 20th, 2012.

2.3.5 Motion detector and light sensor

Light inside the classroom is measured on the ceiling using a Thermokon light sensor (LDF) as illustrated in Fig. 2.15 and Fig. 2.11 with an accuracy of ±5% of measuring range, which is a device in order to detect light and automatically control the brightness level of the artificial lights in the classroom and then supply a more comfortable level for the occupants. Normally, there are three light sensors for each classroom. Additionally, there is also a motion detector/occupancy sensor as shown in Fig. 2.11 which is employed to detect whether or not the classroom is occupied.

Figure 2.15: Light sensor and motion detector. The function combines the light sensor with the motion detector. Light sensor can measure natural light brightness and provide feedback to control system, which then turn on/off artificial lightings and adjust artificial lightings' brightness. Motion detector can monitor whether classroom is occupied or not in order to turn on/off mechanical ventilation system.

2.3.6 Brightness sensor

For the reference classroom, there is an additional brightness sensor mounted on the ceiling shown in Fig. 2.16 which is employed to measure the brightness level and light intensity of indoor ambient sunlight so as to automatically turn on or off the artificial lights inside the room at dark or dawn i.e. it could take advantage of natural daylight.

Figure 2.16: Brightness sensor. It can measure the brightness of natural light in order to determine whether turn on/off artificial lightings inside the classroom.

2.4 Measurements

2.4.1 Blower door testing and air infiltration rate

Air leakage is usually regarded as one of the main causes of building energy loss. For this passive school building, the performance of air tightness has been measured on-site by the use of blower door methodology (Sherman 1995) as illustrated as in Fig. 2.17.

Figure 2.17: Blower door test for the school building. Two measurements have been performed and test results ACH_{50} were known as 0.13 h^{-1} and 0.17 h^{-1}. (Wild 2011)

The blower door is actually a machine deployed to measure the air tightness of small to medium size buildings. There are three primary components to a blower door: a calibrated variable speed fan, a manometer and a mounting system. The air change per hour at a specified building pressure at 50 Pa is defined, i.e.

$$ACH_{50} = \frac{Q_{50}}{V_{building}} \tag{2.1}$$

where ACH_{50} is the air change per hour at 50 Pascal (h^{-1}), Q_{50} is the airflow rate at 50 Pascal (m^3/h), $V_{building}$ is the volume of the tested building (m^3).

This metric indicates the rate which the air in a building or enclosure is replaced with outside air, and as a result, is an important metric in determining indoor air quality (Sherman 1995). While these blower door testing experiments are useful in identifying leakage pathways and in accounting for otherwise inexplicable energy losses, the results could not be used to determine real-time air exchange in buildings under natural ventilation, i.e., air infiltrations which is determined here by the most popular estimation model developed by Kronvall and Persily (Sherman 1987), formulated as follows,

$$ACH_{k-p} \equiv \frac{ACH_{50}}{20} \tag{2.2}$$

where $ACH_{k\text{-}p}$ is the average infiltration rate (h^{-1}). With our tests, ACH_{50} is 0.17 h^{-1} and then $ACH_{k\text{-}p}$ = 0.01 h^{-1} was determined in the present work based on the principles of Standard EN ISO 9972 (ISO EN 9972 2006). ACH_{50} is normally employed as an indicator of air leakage or energy losses for the building/room. The smaller its value is, the less energy is lost due to air leakage from the building/room. It therefore illustrates that the passive school building with a tiny air infiltration rate of 0.01 h^{-1} can obviously reduce energy losses due to air leakage. The aforementioned values are used for the simulations.

2.4.2 Measurement of natural ventilation rate

2.4.2.1 Tracer gas measurements

The tracer gas measurement method is utilized to calculate air exchange rates due to the fact that it is relatively easy to implement and the selected tracer gas carbon dioxide has most favourable characteristics such as non-toxicity, non-reactivity, rather low concentration in surrounding air, high detectability, inexpensiveness and neutral buoyancy (ASHRAE Handbook Fundamentals 2009, Wang et al. 2012). It is in contact with the exterior environment in terms of the mass conservation of the injected tracer gas within the room/building. The temperature dependence of the air density could be neglected with moderate weathers (ASHRAE Handbook Fundamentals 2009, Wang et al. 2012). It is assumed that the interior air is well and uniformly mixed. The total conservation equation is as follows (ASHRAE Handbook Fundamentals 2009):

$$\frac{dm}{dt} = I + C_o Q_{oi} - C_i Q_{io} \tag{2.3}$$

Where m is the mass of tracer gas in the room/building (kg), I is the injection rate of the tracer gas (kg/s), C is the tracer gas mass concentration, Q is the mass airflow rate (for instance, Q_{io} means the airflow rate from inside to outside), i subscript is for the internal environment and o subscript is for the external environment. Furthermore, the conservation of the air mass gives:

$$Q_{oi} = Q_{io} \tag{2.4}$$

The mass of tracer in the room/building is relevant to the mass of air M by:

$$m = C_i M \tag{2.5}$$

Since M is very close to a constant when ignoring the influence of temperature on the air density. In principle, the airflow exchange rate can be directly obtained by substituting Eq. (2.4) and Eq. (2.5) to Eq. (2.3):

$$Q_{io} = \frac{I - M\dfrac{dC_i}{dt}}{\Delta C} \tag{2.6}$$

writing $\Delta C = C_i - C_o$.

The aforementioned method is, however, rather inaccurate, because the concentration may vary very quickly and randomly due to turbulence and non-homogeneities. It is therefore better to take a time average by integrating it for a given period of time:

$$\int_t^{t+\Delta t} Q_{io}\,dt = \int_t^{t+\Delta t} \frac{I}{\Delta C}\,dt - M\int_t^{t+\Delta t} \frac{dC_i}{\Delta C} \tag{2.7}$$

Thus:

$$\int_t^{t+\Delta t} Q_{io}\,dt = \int_t^{t+\Delta t} \frac{I}{\Delta C}\,dt - M\left[\ln(\Delta C(t+\Delta t) - \ln(\Delta C(t))\right] \tag{2.8}$$

Or, dividing all members by Δt, it becomes:

$$\langle Q_{io} \rangle = \left\langle \frac{I}{\Delta C} \right\rangle - \frac{M}{\Delta t}\ln\left(\frac{\Delta C(t+\Delta t)}{\Delta C(t)}\right) \tag{2.9}$$

Where the quantity between the brackets <> is averaged over the time period Δt. This solution can be simplified, depending on the way the tracer is injected.

Normally, tracer gas e.g. CO_2 volume concentration is easier to measure and obtain. The Eq. (2.3) can therefore be expressed as follows:

$$\frac{dC_{CO2}(t)}{dt} = \frac{V_{CO2}(t)}{V} - (C_{CO2}(t) - 390)\frac{V_{air}(t)}{V} \tag{2.10}$$

Where $C_{CO2}(t)$ is CO_2 volume concentration at time instant t (ppm), $V_{CO2}(t)$ is the CO_2 injection volume rate at time t (m^3/h), $V_{air}(t)$ is the airflow rate out of the building/room at time t (m^3/h) and V is the volume of the test building/room (m^3). It should be noted here that the outdoor CO_2 concentration is 390 ppm. On the other hand, $C_{CO2}(t)$ can be given by a simple exponential decay model with t_{CO2} as a time constant based on the aforementioned Eq.

(2.10). Furthermore, the air exchange rate with unit air changes per hour is defined as the inverse of t_{CO2}.

The natural ventilation rate of reference classroom 2.28 was determined from exponential fits to the CO_2 concentrations measured near the exhaust airflow outlet of the room at a height of approximately 1.8 m with a temporal resolution of one minute using an AERASGARD CO_2 sensor with an accuracy of ±100 ppm. The ideal decay equation is obtained as follows:

$$C_{CO2}(t) = -607.1 + 2409e^{-0.27t} \tag{2.11}$$

The measured natural ventilation rate with one opened window is therefore $1/t_{CO2}$ = 1/0.27 h = 3.7 1/h. The aforementioned value will be used for the simulations.

In Fig. 2.18 it can be seen that the measurement and ideal decay results – shown for the natural ventilation case with one opened window – are very close to each other.

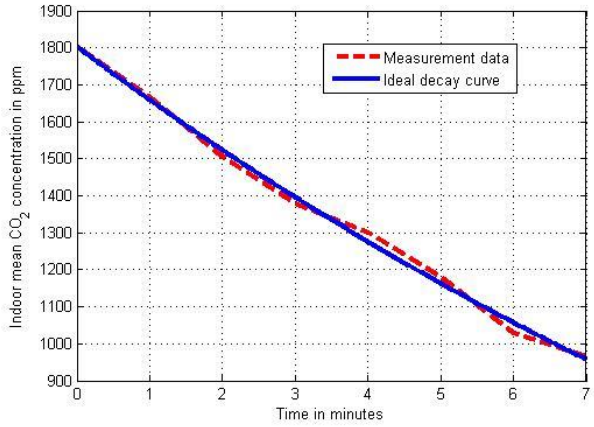

Figure 2.18: CO_2 concentration measurement in reference classroom 2.28. Measurement has been under natural ventilation (one window opened completely): the natural ventilation rate determined from an exponential fit to the measurement data was found to be 3.7 1/h (initial concentration: 1803 ppm, measurement date: Nov. 20, 2012, mean wind speed: 0.45 m/s, mean wind direction: 270.4°, mean outdoor temperature: 4.9 °C).

2.4.3 Measurements of thermal time constant

The thermal time constant is the time required for a thermistance to change 63.2% of the total difference between its initial and final temperature when subjected to a step function change in temperature (Lewis et al. 2004). According to the definition of the thermal time

constant, a simple exponential decay model with τ as thermal time constant is employed as follows.

$$T = T_0 + ke^{\frac{-t}{\tau}} \tag{2.12}$$

where T is the measured indoor temperature (°C), T_0 is indoor temperature in balance (°C), k is the difference of initial and final temperature in balance (°C), t is the time (min), τ is the thermal time constant (min). Based on the measurement data of the reference classroom 2.28 and the aforementioned exponential decay model, the ideal regression decay equations for increasing and decreasing indoor air temperature were respectively determined and then shown in the following.

$$T_{inc.} = 24.15 - 1.391e^{\frac{-t}{157.48}} \text{ } (R_{sqr} \text{ is } 0.972) \tag{2.13}$$

$$T_{dec.} = 22.35 + 1.92e^{\frac{-t}{150.58}} \text{ } (R_{sqr} \text{ is } 0.993) \tag{2.14}$$

where R_{sqr} is a statistical measure of how well a regression line approximates real data points (here, i.e. measurement data). The closer its R_{sqr} value is to one, the greater the ability of that model to predict a trend. Here, both the R_{sqr} values are rather closed to one; this therefore means the aforementioned regression decay equations can be employed in thermal time constant measurements for room/building. Table 2.1 shows the STD errors for all parameters of the above decay model. From the table, it can be seen that both STD errors of two thermal time constants τ are very close to zero. It indicates that the thermal time constants obtained through the aforementioned regression approximate real time constants of the measurement data.

Table 2.1: STD errors. They are for all parameters of the above employed exponential decay model

		STD Error
Increasing temperature	T_0	6.342e-3
	k	1.008e-2
	τ	1.232e-4
Decreasing temperature	T_0	1.255e-2
	k	1.048e-2
	τ	1.137e-4

The corresponding indoor air temperatures of measurement data, which can determine thermal time constants for the reference classroom 2.28, and the ideal decay curve are

depicted in Fig. 2.19. It can be seen that the measurement data and ideal decay curve are very similar, which can also explain why the aforementioned exponential decay model can be well applied in determining thermal time constants. In terms of Eqs. (2.13) and (2.14), the thermal time constant of the reference classroom 2.28 was calculated and known to be 2.62 hours (157.48 min) for increasing indoor air temperatures, and 2.51 hours (150.58 min) for decreasing temperatures. For the measurement data of indoor temperature in Fig. 2.19, the temperature steps are mainly due to the resolution of the digital temperature sensors. In addition, the aforementioned values will be used for the simulations.

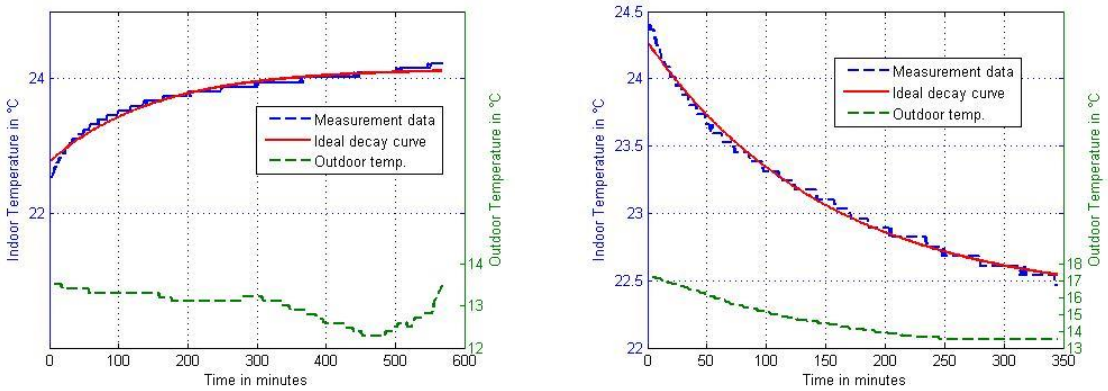

(a) Increasing temperatures (b) Decreasing temperatures

Figure 2.19: Indoor air temperatures of measurement and regression. Both figures are for increasing temperatures (a) and decreasing temperatures (b), respectively, in the reference classroom 2.28 and the corresponding outdoor temperatures

2.4.4 Measurement of noise

Noise pollution, particularly excessive noise, affects both behaviour and health, e.g. it may result in sleep disturbance, hearing impairment, annoyance and aggression, high stress levels, hypertension, ischemic heart disease, tinnitus, and other harmful effects (Rosen et al. 1965, Field 1993). In addition, birth defects and changes of the immune system have resulted from noise exposure (Passchier-Vermeer et al. 2000). However, for the school students, the level of noise could even influence their learning process and performance e.g. reading comprehension, problem-solving abilities, etc. (Ronsse et al. 2010). It is therefore very significant to investigate the noise levels in the Passive House School Building. Normally, indoor noise is mainly caused by building activities, machines and music performance etc. However, the aforementioned conditions will actually be avoided or mini-

mized during daylight, particularly during lessons, due to school regulations and high- quality soundproof materials as well as the normal closing of windows in the classrooms. There is, however, noise pollution caused by four large mechanical exhaust ventilators in the atrium roof for night ventilation at night in summer which should be tested and investigated in the following part as to whether it can affect the surrounding residents' sleep and life around the school building.

Environmental noise regulations generally restrict outdoor noise to a maximum level of 60 to 65 dB. On the other hand, for indoor noise pollution in residential buildings, the American Environmental Protection Agency (EPA) has not constituted any restrictions on limits to the noise level. On the contrary, it has supplied a list of suggested noise levels in its Model Community Noise Control Ordinance, which was issued in 1975. Take an example from the list, the recommended level of noise for the residences inside the building should be less than or equal to 45 dB (Williams et al. 2000, Schmidt et al. 2005, Staples et al. 1996).

In fact, there are many factors such as mechanical facilities or machines (mechanical ventilation systems etc.), building activities and music performance etc., which could result in indoor/outdoor noise pollution. The total noise level will be determined by all the aforementioned factors and could be calculated as (Avsar et al. 2005, Mydlarz et al. 2013),

$$L_{dBsum} = 10\log_{10}(10^{L1/10} + 10^{L2/10} + \ldots + 10^{Ln/10}) \quad (2.15)$$

Where, L_{dBsum} is the total noise level (dBA) and L_1, $L_2 \ldots L_n$ represent the noise levels of different noise sources (dBA). Noise propagation as geometrical spreading could be written as (Cheremisinoff et al. 1975, Avsar et al. 2005),

$$L_{dB} = L_{dB0} - 10\log_{10}(d/d0)^2 \quad (2.16)$$

Where, L_{dB} and L_{dB0} are the noise level at the receiver and at source (dBA) respectively and d and d_0 represent the distance between source and receiver and the distance from the measurement point to source (m) respectively.

Firstly, the unoccupied background noise level was measured in the middle of atrium on the ground floor of the school building at a height of approximately 1.1 m using a Voltcraft 4 in 1 multifunctional environment measuring instrument with an accuracy of 3.5 dB at 94 dB and a measure resolution of 0.1 dB and was known to be 30.8 dB (measuring date, July 16th, 2012), which meets the background noise level recommendation of 35 dB for classrooms (ANSI 2002, Ronsse et al. 2010).

Subsequently, the noise level of all running ventilators with all closed windows in the school building and with classroom windows opened for night ventilation were tested respectively as depicted in Table 2.2 and Table 2.3. As shown in the two tables, both noise levels are very similar for closed and opened windows when running ventilators. For instance, for the 100 % frequency, one is 70 dB, another is 72 dB. It illustrates that there is no large influence in noise level with or without opened windows in buildings when running ventilators in the atrium. In addition, it should be noted here that the maximum outdoor restriction noise level of 65 dB might be exceeded if the ventilator frequency of control signal is larger than 80%, although the measuring point is near the east stairs on the ground floor inside the atrium. It is therefore very necessary to measure/calculate the noise level near local residential buildings with the ventilators running at the frequency of control signal larger than 80%, even maximal frequency 100%.

Meanwhile, the noise level near the ventilator about 1 m from the roof of the school building was tested as depicted in Table 2.4. As can be seen in Table 2.4, the noise level is also similar to both aforementioned cases which were measured inside the building. It illustrates that night ventilation might influence the residents around the school building at night in summer when the ventilator frequency is controlled above or equal to 80% and the measuring point is about 1 m from the ventilator on the roof of the building.

As mentioned before, it is therefore very necessary to determine the noise level near local residential buildings with the ventilators running at maximal frequency of control signal i.e. 100%. The background noise level without running ventilators was measured and known to be 31 dB (the background noise level is 31.0 dB without running ventilators: measuring time: 9:30 am, July 16th, 2012). The measuring point was approximately 50 m away from the building near the border of the residential buildings as seen in Fig. 2.20. Based on the Eqs. 2.15 and 2.16, the outdoor noise level for the same point (50 m away from the school building) was calculated and known to be 41 dB (one ventilator) and 47 dB (4 ventilators), which are similar to measurement results 41.2 dB and 47.6 dB, respectively. That is to say, the maximal noise level i.e. 47 dB resulted from night ventilation of the building in summer does not exceed the maximum outdoor noise level restriction of 65 dB absolutely even if the ventilator frequency control signal is at its maximum i.e. 100% due to the building being enough away from the local residential buildings.

Table 2.2: Indoor noise level measurement 1. This measurement has been under different ventilator control signal frequencies and with all windows in the school building closed (*100% means the rotational maximal velocity of the ventilator motor. The measuring point is near the east stairs on the ground floor inside the atrium).

Ventilator motor control signal at %	Noise level, dB
100*	70
90	68
80	65
70	60
60	55
50	48
40	38

Table 2.3: Indoor noise level measurement 2. This measurement has been at different ventilator control signal frequencies and with the windows in the school building opened for night ventilation (The measuring point is near the east stairs on the ground floor inside the atrium).

Ventilator motor control signal at %	Noise level, dB
100	72
90	68
80	65
70	60
60	55
50	48
40	36

Table 2.4: Outdoor noise level measurement. This measurement has been with a different ventilator control signal frequencies (The measuring point is near the ventilator about 1 m on the roof of the building with one running ventilator)

Ventilator motor control signal at %	Noise level, dB
100	75
90	73
80	64
70	59
60	54
50	45
40	34

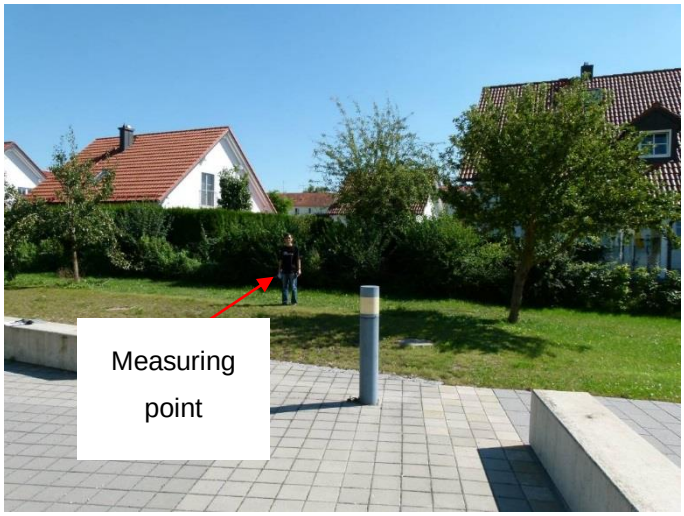

Figure 2.20: Outdoor noise level measuring point. It is approximately 50 m away from the school building. Behind the measuring point, there are residential buildings near the school building.

3 Classroom air environment and school building energy performance

In this chapter, physical model of the investigated reference classroom 2.28 has been firstly introduced. Heat recovery efficiency of the heat recovery facility and energy conservation ratio of the air conditioning unit are then analytically modelled, taking the classroom ventilation network into account. Then, some representative on-site measurements have been implemented to favourably validate present CFD methodology and numerical codes. Following that, classroom displacement ventilation and its thermal stratification in winter and summer, respectively, have been investigated concerning the effects of delivering ventilation flow rate and supplying air temperature. Representative thermal comfort parameters, percentage dissatisfied, temperature difference between ankle and head, and draft dissatisfaction have been evaluated. Indoor air quality indicated by the CO_2 concentration is also investigated in terms of different levels of ventilation flow rate. Detailed fitting correlations of heat recovery ventilation and air conditioning energy conservation have been presented. Heat loss due to opened window in transitional seasons and ventilation effectiveness ratio are analytically modelled. The effects of thermal buoyancy on the steady classroom airflow and thermal stratification comfort as well as the contaminant dispersion are investigated and discussed. Classroom displacement natural ventilation and its thermal stratification as well as indoor air quality indicated by the CO_2 concentration have been investigated concerning the effects of supplying fresh air temperature and delivering natural ventilation flow velocity. Finally, detailed correlations of heat loss resulted from opened window and ventilation effectiveness of natural ventilation inside the classroom have been presented.

3.1 Physical model of the investigated classroom

As the aforementioned Section 2.3 introduced, a representative classroom 2.28 of 9.77 m (length) x 7.25 m (width) x 3.00 m (height) is extracted from one of the Passive House school building as a research platform. This classroom has been fully modelled as a rectangular parallelepiped enclosure, as illustrated in Fig. 3.1. The enclosure space totally accommodates 30 students, who are spatially distributed in 5 lines and 6 rows and 1.20 m in height. In addition, one teacher is 1.70 m in height and standing before the students and 6 slender tables. All occupants are described by the hexagonal shapes in the research model.

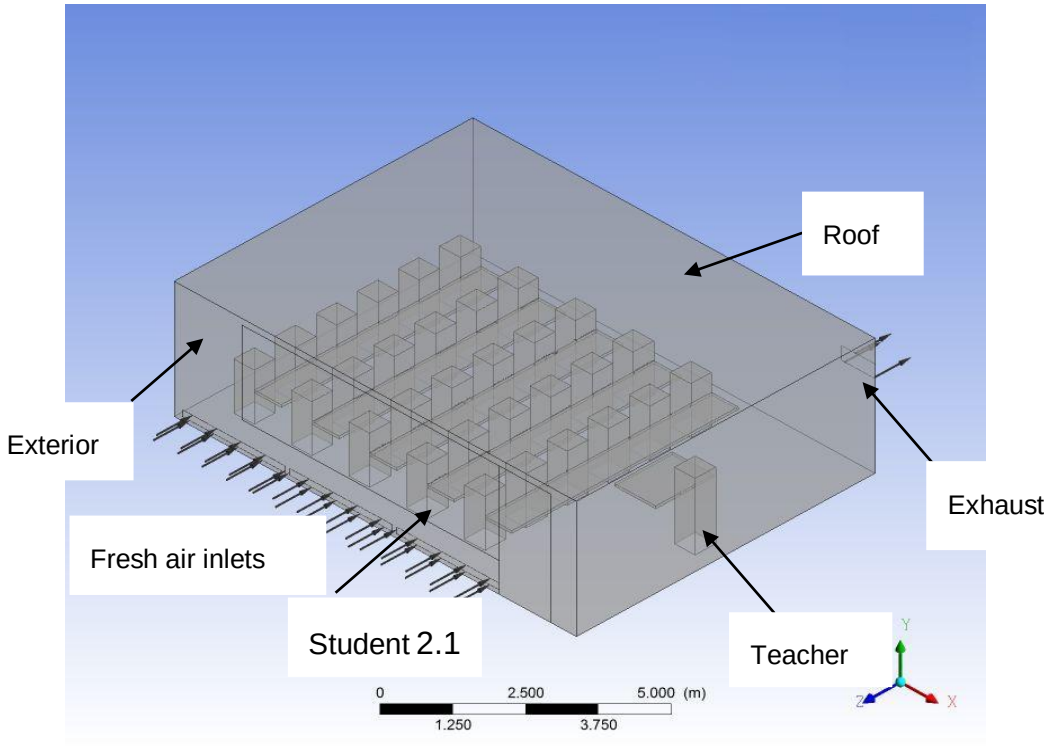

Figure 3.1: Geometry of the modelled classroom. It is extracted from the Passive School Building, where all the occupants (students and teacher) are simplified into cuboids and the symbol Student 2.1 represents that the student sits at Line 2 and Row 1.

The objective classroom is located in the top floor, such that the roof and front wall both expose to the surrounding environment. On the front wall, there is a large window sizing of 6.25 m x 2.10 m (actually, it includes a large window sizing of 5.00 m x 2.10 m, which is normally shut down, and a small window, which can be opened as natural ventilation and is common side-hinged window, with 1.25 m x 2.10 m. Here should be noted that it was modelled one large window due to all of them are closed for winter and summer cases) and an entrance with 1.25 m x 2.85 m.

There are three diffusers of the same size (2.50 m x 0.15 m) which are installed side by side in the lower part of the front wall (beneath the window and immediately 0.10 m above the floor) and they horizontally discharge fresh air into the space. On the backward side opposing to the front wall, the exhausting port sizing of 0.825 m x 0.325 m is positioned in the high altitude and lying just 0.60 m below the ceiling. With such arrangement, displacement ventilation then will be established, i.e., fresh air will be supplied by the diffusers into the classroom and spread along the floors; after being heated and polluted by the indoor occupants, it will become warm and travels upward to the top exhaust.

3.2 Winter case

3.2.1 Heat recovery unit and preliminary exchange analysis

The ventilation of this school building is facilitated by a heat recovery unit, which is integrated with the mechanical ventilation system. With the illustrated ventilation flows shown in Fig. 3.2, where exterior surrounding fresh air of T_{fresh} is firstly cleaned by the primary pollutant filter and then passes through the cold side of heat recovery unit, after absorbing some recovering heat from the hot side of that unit, its temperature increases to T_{in} and then it is entrained into the air conditioning unit (water-resource system adopted in practical situation) for further heating and cleaning, finally being delivered into the school classrooms with temperature T_{supply}. On the other side, stale air of relatively hot temperature $T_{exhaust}$ in the classrooms is firstly bypassing the hot side of the heat recovery unit, after being cooled by the entrained ambient air and its temperature decreased to T_{out}, and then it is exhausted to the ambient air environment. Therefore, energy balance of the heat recovery facility ventilating the fresh air and exhaust air could be described in the following relation,

$$M_{fresh}\times\rho_{fresh}\times C_{fresh}\times(T_{in}-T_{fresh}) = M_{exhaust}\times\rho_{exhaust}\times C_{exhaust}\times(T_{exhaust}-T_{out}) \tag{3.1}$$

Where, M_{fresh} and $M_{exhaust}$ represent the fresh entrained and stale exhausted airflow rates (m^3/h) by the system, respectively. Their specific thermo-physics have been respectively determined by ρ_{fresh}, $\rho_{exhaust}$ (kg/m^3), C_{fresh} and $C_{exhaust}$ ($J/kg\cdot K$). In addition, the volumes of air flow rates across this school building should be maintained balanced, i.e.,

$$M_{fresh} = M_{exhaust} \tag{3.2}$$

Assuming constant heat capacity and density for the air in the range of the studied temperatures, energy balance equation can be further written as,

$$T_{in} - T_{fresh} = T_{exhaust} - T_{out} \tag{3.3}$$

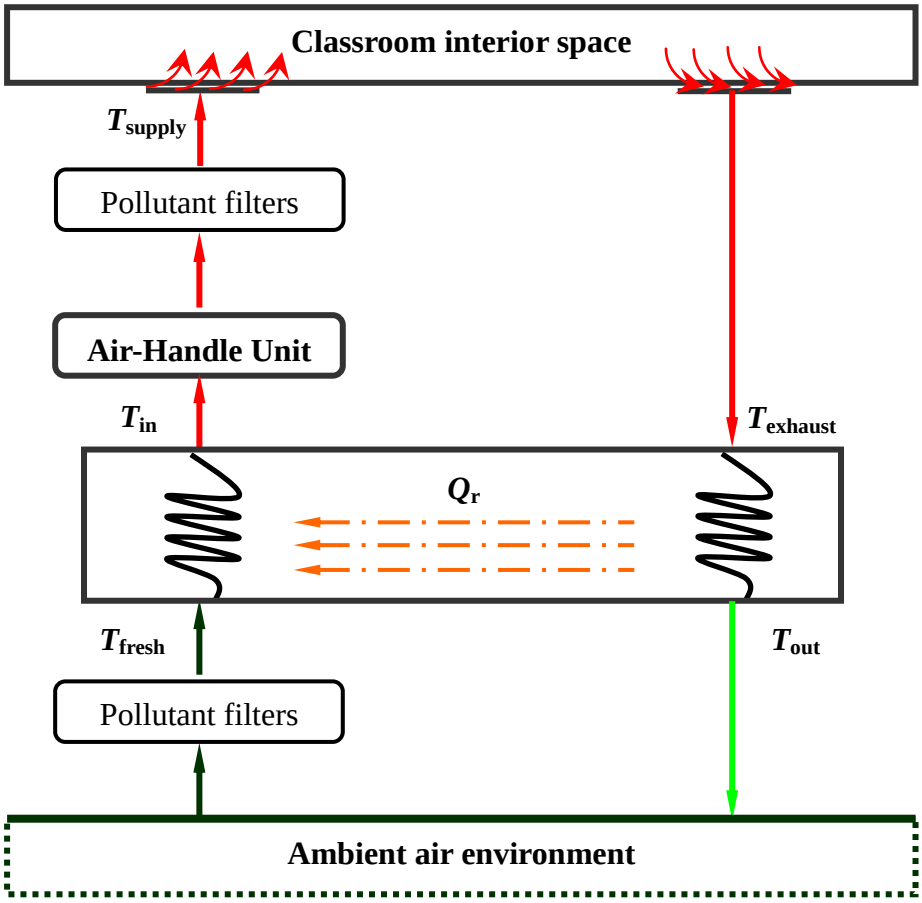

Figure 3.2: Heat recovery unit and ventilation flowing heat exchange for winter case.

As expected, temperature difference of this heat exchanger could be asymptotically approaching to $T_{exhaust} - T_{fresh}$ for the ideal situation. As such, the efficiency of the heat recovery facility ($0 < \eta < 1$) can be defined as,

$$\eta = \frac{T_{in} - T_{fresh}}{T_{exhaust} - T_{fresh}} \times 100\% = \frac{T_{exhaust} - T_{out}}{T_{exhaust} - T_{fresh}} \times 100\% \tag{3.4}$$

One can observe that temperatures of entraining fresh air and exhausting stale air could respectively approach those of room air and outdoor air temperatures, if the heat recovery efficiency achieves unit ($\eta = 1$).

As mentioned before, the stale air exhausted from the classroom is $T_{exhaust}$. The supplying fresh air from the diffusers is maintained at T_{supply}, which could be determined by the operations of the air handle unit. As the heat recovery displacement ventilation system is operated, the efficiency of the air handle unit could be enhanced by reducing the temperature difference between supplying air and entrained fresh air, i.e., $T_{supply} - T_{fresh}$ being replaced by $T_{supply} - T_{in}$. Due to the heat recovery process, original heating load $M_{fresh} \times C_{fresh} \times \rho_{fresh} \times (T_{supply} - T_{fresh})$ could be conserved, such that it reduces to the heating

load $M_{fresh}\times C_{fresh}\times\rho_{fresh}\times(T_{supply}-T_{in})$. With the principle of system energy conservation, the heating load reduction exactly equals the heat recovery thermal energy Q_r, i.e., being written as,

$$M_{\text{fresh}}\times\rho_{\text{fresh}}\times C_{\text{fresh}}\times(T_{\text{supply}}-T_{\text{fresh}}) = M_{\text{fresh}}\times\rho_{\text{fresh}}\times C_{\text{fresh}}\times(T_{\text{supply}}-T_{\text{in}}) + Q_{\text{r}} \quad (3.5)$$

Combining with aforementioned formulations and assumptions, the energy conservation ratio of the air conditioning unit could be defined by,

$$\varphi = \frac{Q_r}{M_{fresh}\rho_{fresh}C_{fresh}(T_{supply}-T_{fresh})} = \frac{T_{in}-T_{fresh}}{T_{supply}-T_{fresh}} = \frac{T_{exhaust}-T_{out}}{T_{supply}-T_{fresh}} \quad (3.6)$$

If the energy conservation ratio could be equivalent to unity, the heat recovery unit even could replace the air conditioning unit completely. In fact, the air conditioning unit could not be replaced by the heat recovery unit due to the heating load provided by the air conditioning unit, occupying the portion of the whole classroom ventilation heating load such that $\varphi<1$. Combining both definitions of η and φ, one can observe,

$$\varphi\times(T_{supply}-T_{fresh}) = \eta\times(T_{exhaust}-T_{fresh}) \quad (3.7)$$

In winter of Munich region, ambient air environment averaged temperature is approximately -4.5 °C (T_{fresh}) (Jacob et al. 2008), while the supplying and exhausting air temperatures T_{supply} and $T_{exhaust}$ are the nominal temperatures of the supplying ports and exhausting ports, respectively. In the present investigation, exhausting air temperatures could be determined by the full Computational Fluid Dynamics (CFD) modelling of classroom airflows upon the supplying air temperatures are given as a priori.

3.2.2 Mathematical modelling and numerical program

The ventilation performance of this classroom, including the air flow, heat and airborne pollutant dispersions, could be simulated using the technique of computational fluid dynamics. Detailed numerical methods and grid dependence will be introduced, before the numerical procedure and code could be validated against a set of experimental data.

3.2.2.1 Numerical methods and modelling

The Computational Fluid Dynamics (CFD) software package ANSYS/CFX is used to simulate air flow, heat transfer and airborne contaminant concentrations and solves the governing flow equations (ANSYS 2012). It can predict the important parameters of building

thermal environment and indoor air quality e.g. air temperature, air velocity and CO_2 concentration etc. with high spatial and temporal resolution. The most popular standard *K-Epsilon* turbulence model (*K-Epsilon*: *K* is turbulent kinetic energy; *Epsilon* is the turbulent dissipation) was adopted to account for the turbulent buoyancy effects and near wall turbulence shear transitions (Chen et al. 2004 and 2009).

The modelling and codes described by the set of differential equations, including momentum, energy, and species equations, which can be found in the recent publications (Zhao et al. 2008, Wang et al. 2012, Liu et al. 2012). The general form of these conservative equations may be expressed as,

$$\frac{\partial}{\partial \tau}(\rho\varphi) = \frac{\partial}{\partial x_j}\left(\Gamma_\varphi \frac{\partial \varphi}{\partial x_j} - \rho u_j \varphi\right) + S_\varphi \tag{3.8}$$

Where φ is a generic variable (unity for the continuity equation, u_j for the momentum equation, T for the energy equation, C for the pollutant species equation and k, ε for the turbulence equations), Γ_φ is the digression coefficient and S_φ is the source term (Patankar 1980).

Finite volume method is applied to discretize the corresponding differential governing equations with the convective terms discretized by the second-order upwind scheme, and SIMPLE algorithm is adopted to couple the momentum and continuity equations. The airflow inside the classroom is turbulent, and the standard *K-Epsilon* turbulence model is adopted to account for the turbulent buoyancy effects and near wall turbulence shear transitions. The logarithmic law of the wall is used in the vicinity of solid walls, i.e., wall functions being adopted to establish the fully turbulent flow and the viscous flow along the walls (Launder et al. 1974).

In order to meet reasonable convergence of the model, the Root Mean Square (RMS) residuals for mass and momentum equations are taken as 0.01%, whereas overall conservation target of energy and species is set to 1% (Zhao et al. 2008, Wang et al. 2012, Zhao et al. 2012). Solution of the mathematical model has allowed for the calculation of the conditions and pattern of the airflow inside the classroom, heat dissipation and pollutant emission from each of the occupant.

Test of grid independence solutions was tried with series of 127551, 293301, 381588, and 452270 nodes inside the enclosure. Volume averaged air temperature was almost un-

changed (22.3 °C) after 381588 nodes were implemented, for the typical steady flow situation with fresh air ventilation rate maintained at 660 m^3/h. Therefore, grid system of 381588 nodes will be adopted in the subsequent researches.

The mesh is implemented in Tetra meshing with Hexa core and Prism layers. Tetra meshing is not efficient for capturing shear or boundary layer physics. Prism mesh efficiently captures these effects near the surface while maintaining the ease and automation of Tetra mesh (ANSYS 2012). Mesh refinement (Finer grid) is employed in those regions where the variables of air flow have much larger gradients e.g. air supply inlet and air exhaust outlet etc. (ANSYS 2012, Liu et al. 2012).

3.2.2.2 Thermal boundary conditions

Based on EN ISO 7730 (ISO EN 7730 2005), a seated student can produce about 75 W heat gains, a standing teacher can generate about 100 W heat gains. Heat generated by the occupants will be removed simultaneously by both thermal radiation and convective modes, according to Chen 2004 (Chen et al. 2004), for the displacement ventilation, the convective and radiative ratio should be assumed by 80/20 for occupants, therefore, it can be calculated that the convective heat gains are 60 W and 80 W, respectively, for a seated student and a standing teacher. The convective heat in this study is assumed to be uniformly distributed on the entire surface of the heated objects (Srebric et al. 2002). Solar radiation from the windows of such school building is almost employed as the floor heating source in winter.

3.2.2.3 Validation of CFD simulations against with measurements

It is necessary to validate the CFD program before it is extensively adopted as the tool of investigation, although the current numerical program has been successfully applied in lots of the recent publications (Zhao et al. 2008, Wang et al. 2012, Liu et al. 2012), including forced convection and mixed convection. The validation is done by comparing the CFD results with experimental data obtained by the on-site measurements.

An AERASGARD CO_2 sensor shown in Fig. 2.13 with an accuracy of ±100 ppm of the measured values inside the classroom was installed in one sampling location (X = 9 m, Y = 1.8 m, Z = 0 m). In Fig. 3.3 it can be seen that the CFD simulation and measurement results in the same position (X = 9 m, Y = 1.8 m, Z = 0 m) are very similar. The maximal discrepancy between CFD values and measurement data is within 80 ppm, which can guarantee the reliability of the CFD numerical program.

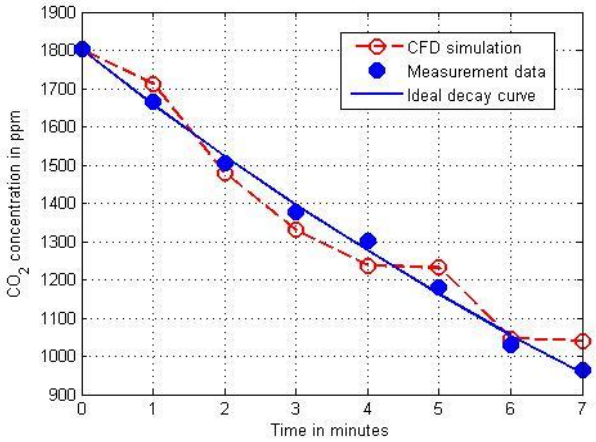

Figure 3.3: CO_2 concentration comparisons. It shows CO_2 concentrations of CFD simulation results and measurement data from CO_2 sensor installed in one sampling location (X = 9 m, Y = 1.8 m, Z = 0 m), which is the same as CFD simulation inside the classroom.

On the location of student 2.1, five thermocouples were perpendicularly distributed along the vertical lines. The error for measuring temperature by the thermocouples is ±0.2 ^{0}C. Shown in Fig. 3.4, the temperature gradient in the lower part of the classroom is much larger than that in the upper part, thus relatively large discrepancies between CFD values and measurements are observed in the lower levels. Nevertheless, the computed temperatures agree with the measured data within 1.2 ˚C, which can also convince the reliability of the subsequent CFD numerical investigations.

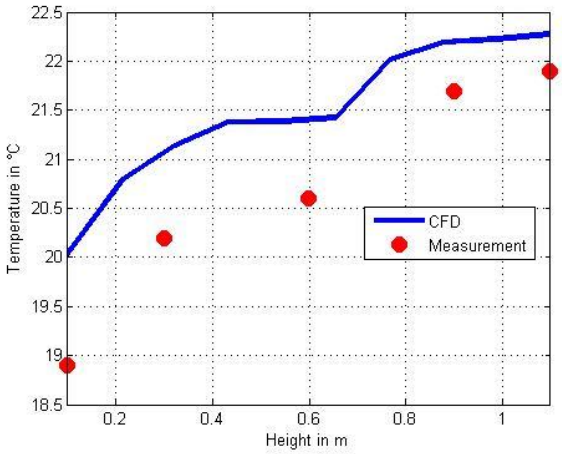

Figure 3.4: Indoor air temperature comparisons between CFD and measurements. It illuminates indoor air temperatures of CFD modelling results and measurements from thermocouples distributed along vertical lines at one sampling location, i.e., student 2.1.

3.2.3 Results and discussion

The classroom air motions established by the mechanical ventilation system aim to create a comfortable thermal environment, which could be evaluated with a suitable combination of thermal comfort parameters including metabolic rate, clothing, air velocity, ait temperature, radiant temperature, draft rate, and vertical air temperature difference, to name just a few (Khudhair et al. 2004). Among the amount of thermal comfort models available in the research fields, parameters of percentage dissatisfied (*PD*) and temperature difference between ankle and head ($\Delta T_{a,v}$) are suitable in this classroom thermal comfort criteria (Puteh et al. 2012, Bond et al. 1999, Noh et al. 2007).

On the other hand, indoor air quality (IAQ) is also an important factor for evaluating the performance of the ventilated classroom (Yu et al. 2011). Different gaseous components, such as VOCs, formaldehyde, NO_x, SO_x, Ozone, CO_2, CO and particulate matters, have been frequently adopted as indicators for IAQ (Liu et al. 2012). The concentrations of VOCs and formaldehyde are mainly influenced by the building materials, and the regulations of the building material emission rates will not be considered in the present work. Particularly, indoor concentrations of these gaseous contaminants except CO_2 have been measured to be low in classrooms, whereas the classroom CO_2 concentration is generally measured higher due to the air-tightness materials and low ventilation rates of low energy buildings (Karimipanah et al. 2007, Noh et al. 2007, Yu et al. 2011, Chua et al. 2013, Hughes et al. 2012, Ascione et al. 2013). That is to say, volumes of fresh air required to dilute such high concentration CO_2 could be enough to simultaneously dilute such low concentration VOCs and formaldehyde coexisted within the classroom. Therefore, indoor CO_2 concentration will be used as an indicator of IAQ in the present investigation.

3.2.3.1 Steady classroom airflow and thermal stratification comfort

As this mechanical ventilation unit is preliminarily put into use, fresh air from the diffusers is usually maintained at M_{fresh} = 660 m^3/h and T_{supply} = 19 °C supplied into the enclosure, to meet the air volume requirement of each occupant 20 m^3/h in Germany, although this ventilation rate level is a little low, which is considering based on the balance between the energy saving and thermal comfort. Subsequently, steady airflow and thermal dispersion will be established with such displacement ventilation forms.

As shown in Fig. 3.5(a), the first row students' feet near the inlets are directly subjected to room air of relatively low temperature (around 20 °C), being a bit lower than that of regions where other students seated. As the fresh air spreads forward, classroom heating objectives

(occupants and equipment) will gradually enhance its temperature level. Around the floor region of the third row, air temperatures are observed higher than 21.0 °C; as air arrives to the region of the sixth row, its temperature approaches 22.0 °C. Observing from Fig. 3.5(b), horizontal plane elevated 1.1 m from the floor, air temperatures in the majority of students occupation area are higher than 22.0 °C. This demonstrates that the displacement ventilation flow pattern would result in the vertical thermal stratification.

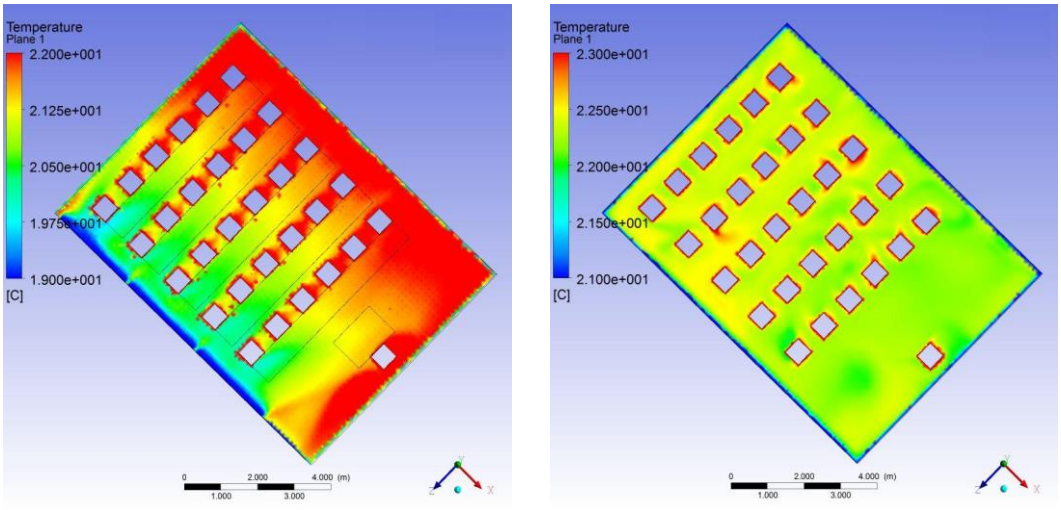

(a) Isothermal distributions at 0.10 m (b) Isothermal distributions at 1.10 m

Figure 3.5: Spatial distributions of air temperatures in winter. They are across horizontal sections respectively at elevating height of 0.10 m (a) and 1.10 m (b), both immediately from the floor.

Some selected observations are illustrated in Fig. 3.6, which contains the vertical air temperature distributions at the places of 6 students and the teacher. Classroom air temperature level around the students of Line 2 and Rows 1-6 varies from 20.0 °C to 22.6 °C, whereas it does from 21.5 °C to 22.5 °C around the teacher. Particularly, vertical temperature difference of the Student 2.1 is higher than 2.0 °C, but less than 3.0 °C, such that it could not lead to the significant local thermal discomfort (Noh et al. 2007). Usually, vertical air temperature difference between head and ankles ($\Delta T_{a,v}$) can be put into the formulation of percentage dissatisfied (Yuan et al. 1998, Chen et al. 2009),

$$PD = \frac{100\%}{1+\exp\left(5.76-0.856\cdot\Delta T_{a,v}\right)} \tag{3.9}$$

where temperature difference $\Delta T_{a,v} = T_{head} - T_{ankle}$ can be determined from the aforementioned results. The above formulation is only suitable for $\Delta T_{a,v} < 8.0\ ^0$C due to it is derived from the original data using logistic regression analysis (Chen et al. 2009). Additionally, the height difference between head and ankle for sitting students is 1.0 m (1.1 m – 0.1 m), while it increases up to 1.6 m (1.7 m – 0.1 m) for the standing teacher.

General correlations between *PD* and vertical air temperature difference are plotted in Fig. 3.7, where one can observe that *PD* will exponentially increase with the vertical temperature difference $\Delta T_{a,v}$. As expected, occupants will have better human thermal comfort with lower values of vertical temperature difference. In fact, continuously decreasing vertical temperature difference will reduce the thermal stratification sensitivity of occupants, which has been represented by the values of *PD*. Some sampling locations and data are summarized in Table 3.1, including the temperatures of ankle and head positions, head to ankle temperature difference as well as percentage dissatisfied. One can easily observe that the vertical temperature difference at student 2.1 (the worst case) still does not exceed the limit value (3 °C). This is mainly due to daylight solar radiation has been employed to heat the classroom floor (modelled as a floor heating source), which can build up an almost uniform thermal distribution and enhance their classroom thermal comfort.

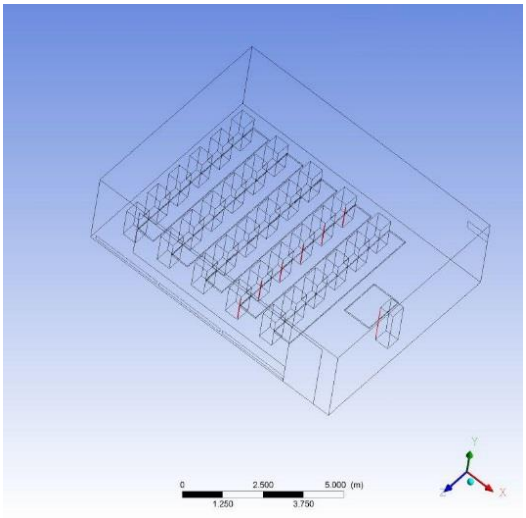

(a) General locations of vertical temperature observations (Line 2, Rows 1-6, Teacher)

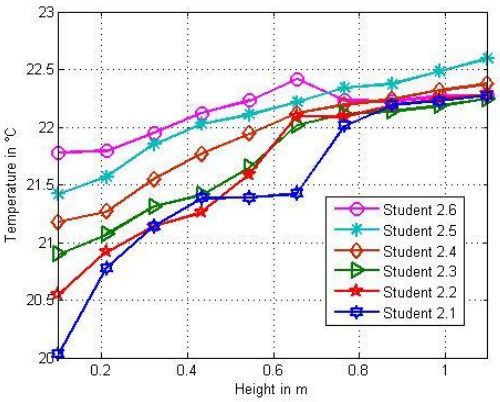

(b) Temperature distributions for students

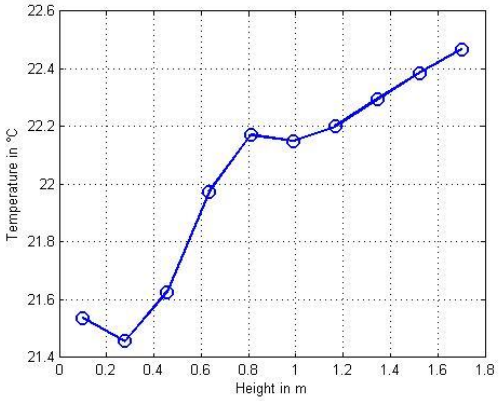

(c) Temperature distributions for Teacher

Figure 3.6: Vertical distributions of air temperature in winter. It shows vertical distribution ((b), ranging from 0.10 m to 1.10 m) of air temperature profile in the positions of students seated of Line 2 and Rows 1-6, and those in the standing teacher ((c), ranging from 0.10 m to 1.70 m). Detailed locations are illustrated in (a) as red lines.

Table 3.1: Vertical temperature levels and Percentage Dissatisfied (winter). They include that sampling locations, ankle temperature, head temperature, and vertical difference temperature level between head and ankle as well as *PD* at those sampling locations around the Teacher and Students 2.1 to 2.6.

Location	**Ankle**	**Head**	**Vertical difference**	***PD***
	°C	**°C**	**°C**	**%**
Teacher	21.5	22.5	0.9	0.7
Student2.1	20.0	22.3	2.2	2.1
Student2.2	20.5	22.3	1.7	1.4
Student2.3	20.9	22.2	1.3	1.0
Student2.4	21.2	22.4	1.2	0.9
Student2.5	21.4	22.6	1.2	0.8
Student2.6	21.8	22.3	0.5	0.5

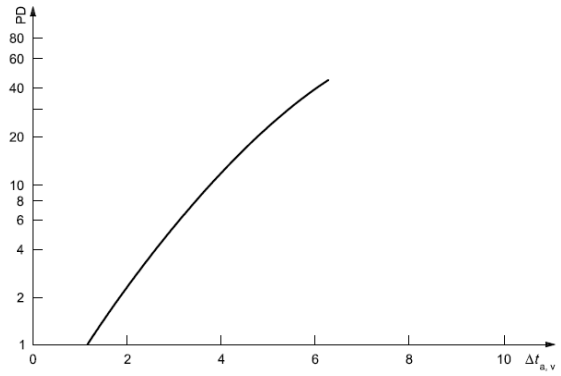

Figure 3.7: Comfort parameter *PD* as function of vertical air temperature difference.

Area averaged temperatures at some elevated horizontal planes, from 0.1 m to 2.9 m, are illustrated in Fig. 3.8(a). With such displacement ventilation, the vertical thermal stratification mainly occurs at the altitude below 1.3 m, which moderately influences the thermal comfort of occupants. This also explains why most of students in the classroom have relatively low values of *PD*.

In order to clearly visualize the characteristics of classroom thermal stratification, the normalized standard deviations of the horizontal plane temperatures are plotted in Fig. 3.8(b), obtained by the normalization with the classroom volume averaged air temperature (22.3 °C). As shown in Fig. 3.8(b), the highest deviation (approximately 1%) is achieved at the elevation of 0.1 m, where classroom diffusers deliver fresh air across the lower region with cool air sinking down to the floor. With the increasing elevation of horizontal planes, the standard deviation decreases sharply toward to 0.2 as the vertical elevation achieves at 0.5 m, 1.3 m or 1.5 m immediately above the floor, where average temperature is very close to the classroom volume averaged temperature 22.3 °C. Except these critical planes elevated at 0.5 m, 1.3 m and 1.5 m, air temperatures are relatively lower or higher than the volume averaged temperature level. Moreover, immediately above the critical plane elevated at 0.5 m, local air temperature levels are almost higher than classroom volume averaged temperature level. Buoyant thermal flows gradually accumulate in the upper regions of this classroom, which favourably produces the thermal buffers to reduce the heat transfer rates between surroundings and building ceilings. This observation has been collaborated by the past researches of displacement ventilation (Yuan et al. 1999).

Furthermore, as the temperature level in the classroom should be monitored by a single thermocouple or a thermal sensor for the future energy cost evaluation of the whole low

energy school building (Wang et al. 2014). With the knowledge of classroom air motions and thermal transport, the thermal sensor should be directly put inside the bottom half region of the classroom (vertically elevated at 0.5 m) shifting aside from diffusers towards the outlet, to represent the average temperature level of the whole classroom (Wang et al. 2014).

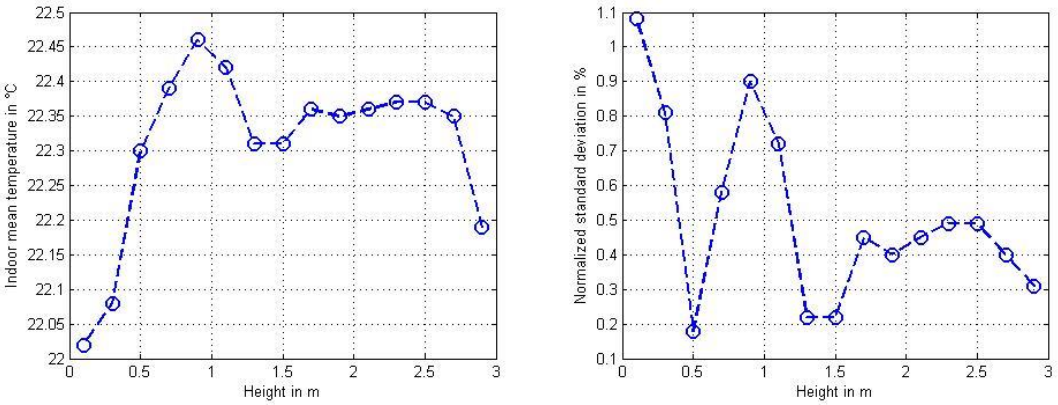

(a) Horizontal plane mean temperatures (b) Normalized standard deviation

Figure 3.8: Horizontal plane averaged temperatures and normalized STD in winter. Normalized standard deviations of the horizontal plane temperature are as functions of their vertical elevations in the classroom with stable displacement ventilation rate of 660 m^3/h and supplying air temperature 19 °C.

Thermal comfort of classroom occupants is essentially influenced by the airflow velocities. Mean velocity of airflow drafted toward people normally should not exceed 0.25 m/s, otherwise draft dissatisfaction will arise (ISO EN 7730 2005). Characteristic velocity vectors in a vertical cross plane (Z = 6.6 m) located between the diffusers and the closest row students are shown in Fig. 3.9. As the supplying fresh air drifts toward the nearby students, with the effect of jet decaying, its axial flow rate decreases from 0.30 m/s to 0.23 m/s; whereas, plane averaged air flow intensity in this cross plane is only 0.055 m/s, far lower than 0.25 m/s. Therefore, from the point view of airflow intensity, displacement ventilation inside the classroom does not cause the problem of draft dissatisfaction.

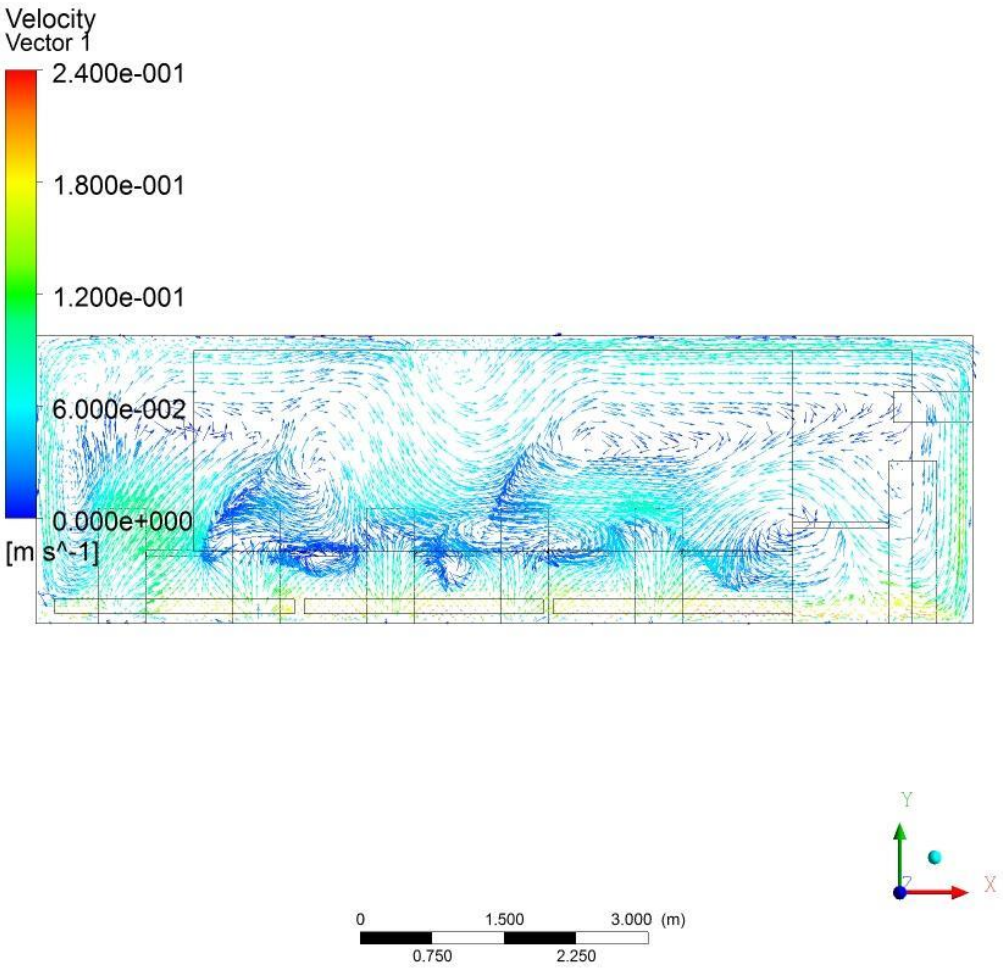

Figure 3.9: Velocity vector flow fields in winter. They are along the vertical plane (Z = 6.60 m) locates between the diffusers and the nearby row students).

Observing from Fig. 3.9, complicated airflow vortex structures do exist in the classroom. Physically, air flow streams are subjected to diverse flow forces, including the mechanical ventilation and thermal plume forces. Here, supplying jet flows will firstly sink toward floor with negative buoyancy effect, while air flows around the human body will rise upward due to positive buoyancy effect. These flow streams interact with each other and result in such complicated flow circulations shown in Fig. 3.9. Micro-circulation of airflow around the human body will hinder the pollutants removed from the breathe regions (discussed later), which easily results in poor air quality for occupants. However, the air flow structures in the regions between the first line students and the teacher are observed not to contain any micro-circulations. That is to say, the distance between each line of students should be enlarged to reduce such interferences, to create favourable air environment for the occupants.

3.2.3.2 Effects of ventilation flow rates and supplying air temperatures

Classroom airflow patterns and heat transfer structures could be heavily affected by the supplying velocities or the mechanical ventilation flow rates. Now, the aforementioned controlling parameters and boundary conditions are maintained excluding the supplying ventilation flow rates are gradually promoted from 10 m^3/h to 880 m^3/h. The volume averaged classroom temperatures and vertical thermal gradients between the head and ankle on the locations of student 2.1 and 2.2 are illustrated in Fig. 3.10, as functions of classroom ventilation rates.

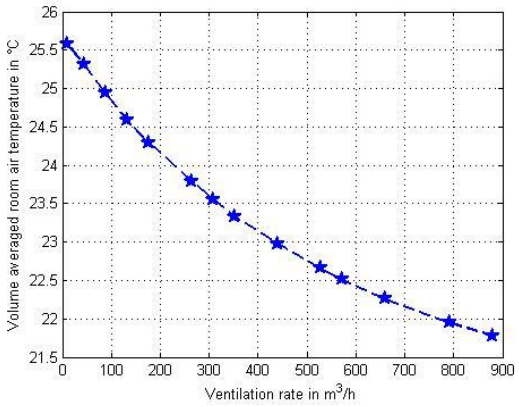

(a) Volume averaged classroom temperatures

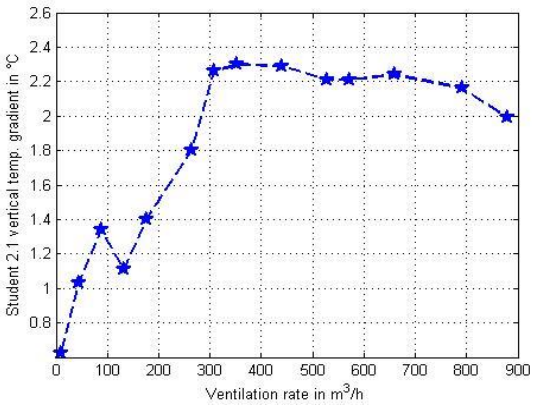

(b) Vertical thermal gradient for student 2.1

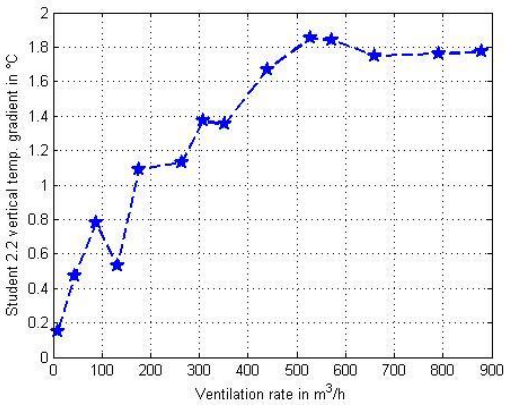

(c) Vertical thermal gradient for student 2.2

Figure 3.10: Variations of room averaged temperature and vertical thermal gradients. They are at some selected points as the functions of ventilation flow rate.

Observing from Fig. 3.10(a), almost exponentially decaying function between the ventilation flow rates and the classroom volume averaged temperatures could be set up. Classroom air could be easily cooled with increasing volumes of air delivered from the air conditioning unit.

However, as shown in Figs. 3.10(b) and 3.10(c), the local thermal gradients along the latitudinal direction do not coincide with the decaying trend, whereas they tend to achieve peak values around at M_{fresh} = 360 m^3/h and 530 m^3/h, respectively, and maintain few oscillatory after the delivering fresh air volume exceeding the threshold of required ventilation rates (660 m^3/h). Subsequently, the effects of supplying fresh air temperature on the classroom air motions have been investigated. Here, the supplying fresh air temperature could change from 17.0 °C to 27.0 °C, whereas the supplying air volume is maintained at M_{fresh} = 660 m^3/h. Observing from Fig. 3.11, temperature level of the exhausting air linearly increases with that of supplying air. In addition, with the increasing of the supplying fresh air temperature, the temperature difference between the supplying air and exhaust air will shrink from about 4 °C to 0.5 °C.

Closely scrutinizing the thermal flow charts inserted in the frame of Fig. 3.11, with the promotion of supplying air temperatures, marked thermal stratifications shift downward from central region to the lower region adjacent to the floor, which could lightly decrease the values of *PD* and intensify the thermal buffers within the upper region of the classroom.

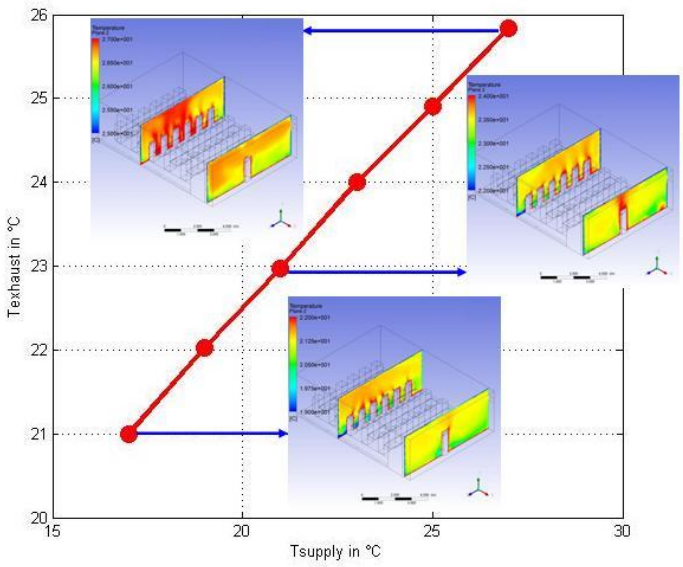

Figure 3.11: Variations of classroom exhaust air temperatures in winter. They are as function of the fresh supplying air temperatures with some representative parameters, M_{fresh} = 660 m^3/h and T_{fresh} = -4.5 °C.

3.2.3.3 Effect of displacement ventilation on transient CO_2 dispersions

The fundamental roles of building ventilation are to remove indoor pollutants and dilute the stale air within the rooms. As mentioned earlier, indoor CO_2 concentration will be used

as an indicator of IAQ in the present investigation. Each occupant in the classroom generates about 2.0×10^{-2} m^3/h of pure CO_2 due to respiration, and their total contributions will significantly increase overall CO_2 concentration levels within such classroom of low air infiltration ($ACH_{K\text{-}P} = 0.01h^{-1}$). One can easily estimate that room averaged CO_2 concentration will exponentially increase up to 1000 ppm after 15 minutes, if there are no purification and dilution through entraining ambient fresh air.

Actually, the distribution of CO_2 is influenced by many issues. First, it depends on the disposal of CO_2 such as the position of occupants etc. Second, it is also determined by the status of the opening e.g. the windows and inlets as well as outlets. Third, it lies on the heat emission of the dummies etc. (Steiger et al. 2008)

With the same initial volume averaged CO_2 concentration 1350 ppm, two different levels of mechanical ventilation rates (M_{fresh}) are respectively implemented, 660 m^3/h and 88 m^3/h, while T_{supply} is kept constant (19.0 °C); other momentum and thermal boundary conditions implemented in the above thermal flow simulations are maintained. As illustrated in Fig. 3.12, temporal evolutions of indoor mean CO_2 concentration and its normalized standard deviation are plotted as functions of time lapse, respectively shown in Figs. 3.12(a) and 4.12(b).

Observing from Fig. 3.12(a), for the case of high ventilation rate (blue line), indoor mean CO_2 concentration level decays rapidly due to the volume of fresh air entrained into the room is far larger than the CO_2 production from the crowded occupants. But, after 5 minutes, decaying rate of this curve tends to be flat due to the entraining fresh air gradually dilutes the room in a whole level.

On the other hand, the curve represented by the case of low ventilation rate always shows that the pollutant concentration linearly increases with time. This is due to the fact that CO_2 production rate of occupants far exceeds that fresh air dilution rate of low ventilation rate. In contrast, mechanical ventilation of high level ventilation rate can quickly dilute the room air (within 15 minutes) into less polluted level, i.e., volume averaged CO_2 concentration being less than 1250 ppm.

Therefore, promotion of mechanical ventilation rate can directly contribute to the quick dilution of indoor air pollutants, and too low ventilation rate could not effectively inhibit the increase of indoor CO_2 concentration levels. In addition, it also illuminates that the practical mechanical ventilation rate 660 m^3/h of the volume control system in this passive school building could be enough for maintaining high indoor air quality.

Mechanically supplying air not only quickly dilutes indoor air, but also causes the non-uniform distributions of pollutants. Non-uniformity of CO_2 dispersions can be essentially represented by the values of standard deviations of pollutant concentration shown in Fig. 3.12(b).

In terms of high ventilation rate, dilution of indoor CO_2 could be implemented within several minutes, but the non-uniformity of indoor pollutant distributions increases greatly, achieving maximum of 17.2% just after 25 minutes. Thereafter fresh air is continuously entrained into the room, both pollutant concentration levels and its spatial non-uniformity decrease. For the case of low ventilation rate, the pollutant levels always increase with time and the non-uniformity of pollutant distribution increases slightly, being up to maximum of 6.3% after 8 minutes. Physically, the fresh air delivered by relatively low ventilation rate will gradually penetrate into the room mixtures, which will not drastically and suddenly change the original distributions of pollutants.

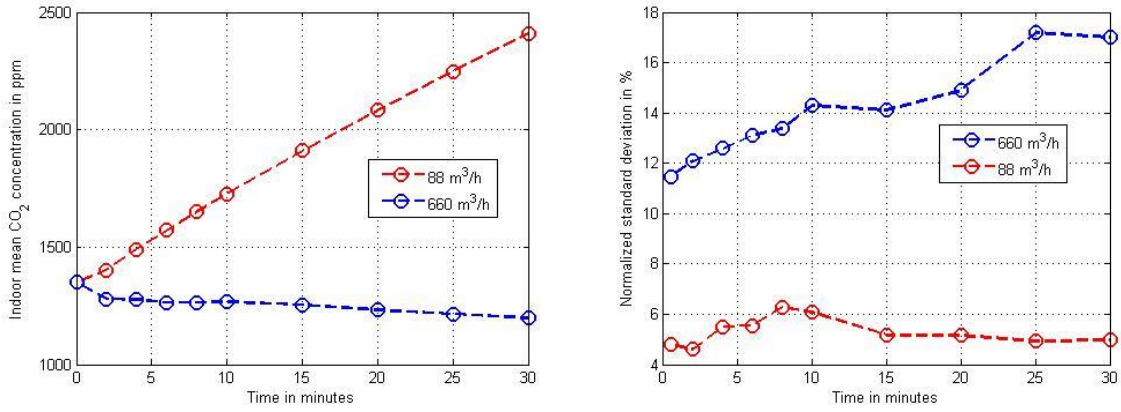

(a) Indoor mean CO_2 concentration (b) Normalized standard deviation

Figure 3.12: Indoor mean CO_2 concentration and its normalized STD in winter. (a) shows temporary evolutions of indoor mean CO_2 concentration and (b) is its normalized standard deviation inside the classroom with two different levels of mechanical ventilation rates and the same initial pollutant concentrations, i.e., 660 m^3/h and 1350 ppm (blue line), and 88 m^3/h and 1350 ppm (red line).

In addition to the supplying flow momentum, the displacement ventilation flow pattern could result in a sensible species boundary layer in the lower region of this classroom. Observing from Fig. 3.13, spatial distributions of pollutants are divided by the pollution layers, where the CO_2 concentration difference between upper and lower layers is greater than 200 ppm. This can also explain its peak values of standard deviations shown in Fig. 3.12. Remarkable species stratification is not observed in the displacement ventilation classroom shown in Fig. 3.13. This is mainly due to the floor heating source by the solar radiation could

alleviate the non-uniformity of classroom air temperatures, whereas put little effect on the dilution of classroom CO_2 concentration. As indicated by the black arrows in Fig. 3.13, the appropriate installing location for a species concentration sensor should be in the upper region of this classroom, where local species concentration can favourably represent the volume-averaged concentration level of the whole classroom. With such installations, general pollutant emissions across this school building could be monitored in the long-term running time (Wang et al. 2014). Such long-term on-site measurements on this whole building scale should be conducted in the future. For example, this important results have been already successfully employed for our new project – Diedorf school building project with plus-energy standard.

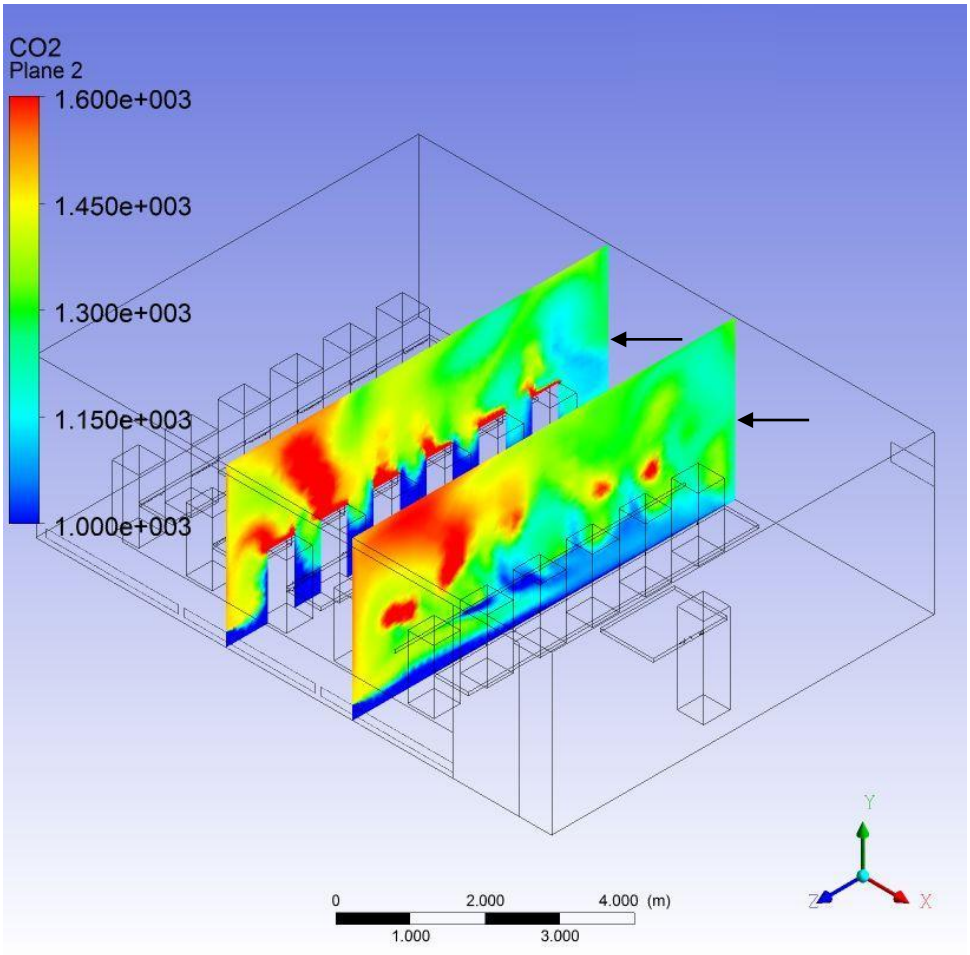

Figure 3.13: Spatial distributions of CO_2 concentration at time instant 25 minutes. This is the worst case situation with M_{fresh} = 660 m^3/h, T_{supply} = 19 °C and initial classroom CO_2 level of 1350 ppm.

3.2.3.4 Effect of heat recovery efficiency and energy conservation ratio

The exhaust air is firstly delivered passing the heat recovery unit to pre-heat the entrained outdoor fresh air, and the heat recovery efficiency of the heat recovery facility could put the

effect on the operation of the air handle unit. Diverse situations of energy conservation ratio and heat recovery efficiency have been correlated in terms of the temperature difference between surrounding fresh air and supplying air, shown in Fig. 3.14,

$$\ln(\varphi/\eta) = - 0.021\times(T_{supply} - T_{fresh}) + 0.610 \quad (3.10)$$

As expected, energy conservation of the air handle unit could be enhanced both with increasing heat recovery efficiency of the heat recovery facility and with shrinking temperature difference between the supplying air and fresh air. That is to say, the heat recovery facility could become less effective when the supplying air gradually approaches the ambient one. Accordingly, the energy conservation of the air conditioning unit becomes less important if the ambient air could be directly delivered into the classroom.

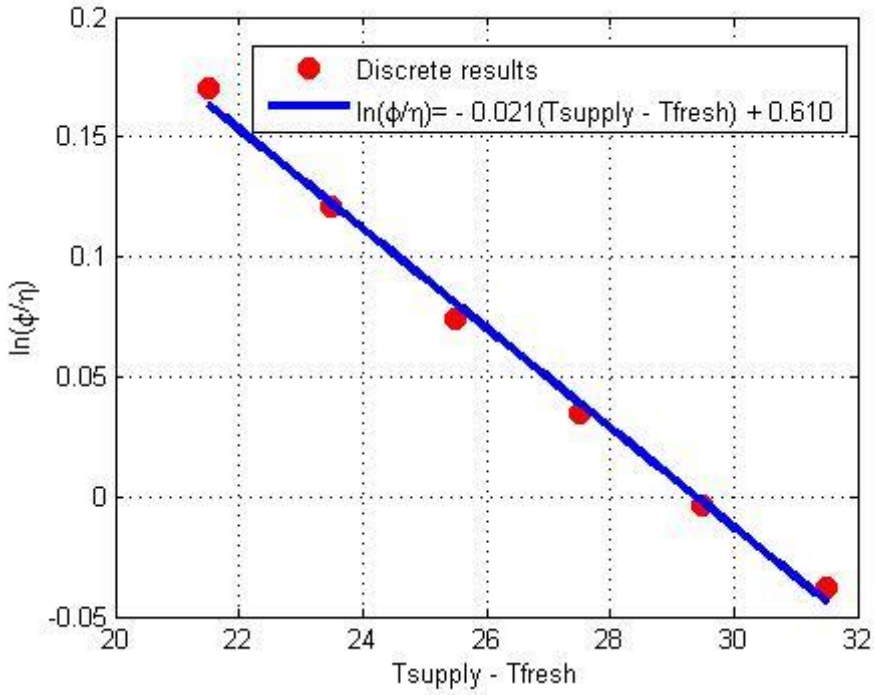

Figure 3.14: Correlations of heat recovery efficiency and energy conservation ratio. It is as a function of temperature difference between fresh air and supplying air.

3.2.4 Summary and conclusions

In winter days, classroom displacement ventilation, air handle unit and heat recovery facility are jointly put into operation with full closed windows and airtight building envelopes, which aim to reduce the building heat transfer losses and enhance the building energy efficiency. Classroom thermal comfort and indoor air quality in the new-built Passive House

school building as well as school building energy conservation performance have been numerically and experimentally investigated in the present work, together with the analytical modelling of heat recovery and energy conservation. Some representative on-site measurements have been implemented to favourably validate the present CFD methodology and numerical codes, although some observed discrepancies existed between CFD results and measurements.

(1) Displacement ventilation thermal stratification is demonstrated by the spatial thermal distributions and their normalized standard deviations. Sharp thermal gradients are observed below 0.5 m, whereas roughly uniform isotherms and thermal buffers present in the upper regions in the classroom. Sensible draft dissatisfaction does not appear inside this classroom, although it has been reported in earlier researches of displacement ventilation inside office or residential buildings.

(2) Airflow patterns and thermal transport structures in the classroom are heavily affected by the ventilation flow rates and supplying air temperatures. Volume averaged temperature level of the classroom linearly decays with the ventilation flow rate, whereas local thermal gradients are the complex functions of classroom ventilation flow rates. The increasing temperature of supplying fresh air not only linearly promotes the temperature of exhaust air, but also pushes thermal stratifications shifting downward from central area to the floor level.

(3) Temporal evolutions of classroom mean CO_2 concentration indicate that promotion of classroom mechanical ventilation rate can directly contribute to the quick dilution of classroom air pollutants. Standard deviations of transient classroom pollutant concentrations clearly illuminate that non-uniformity of indoor pollutant distributions increases with the mechanical ventilation rate.

(4) Energy conservation ratio of the air conditioning system and the heat recovery efficiency of the heat recovery facility have been correlated in terms of the temperature difference between surrounding fresh air and supplying air, which shows that energy conservation of the air conditioning unit could be enhanced with the increasing heat recovery efficiency of the heat recovery facility and the shrinking temperature difference between the supplying air and fresh air.

This research could benefit for the classroom environment guide and the low energy school building ventilation design for the winter case situation. It illuminated that enhancement of classroom air quality and reduction of school building energy consumption could be simultaneously achieved with the appropriate operation of heat recovery air conditioning unit and ventilation system in winter.

3.3 Summer case

3.3.1 Heat recovery unit and preliminary exchange analysis

As mentioned earlier, the ventilation of this school building is facilitated by a heat recovery unit, which is integrated with the mechanical ventilation system. For the summer case, with the illustrated ventilation flows shown in Fig. 3.15, where exterior surrounding fresh air of T_{fresh} is firstly passed through the hot side of the heat recovery unit, after releasing its heat to the cold side of that unit, its temperature decreased to T_{in} and then it is entrained into the air conditioning unit for further cooling and cleaning, finally delivered into the school rooms with temperature T_{supply}. On the other side, stale air of relatively low temperature $T_{exhaust}$ in the classrooms is firstly bypassing the cold side of the heat recovery unit, after heating by the ambient air and its temperature increased to T_{out}, and then it is exhausted to the outdoor ambient environment. Therefore, energy balance of the heat recovery facility ventilating the fresh air and exhaust air could be described in the following relation,

$$M_{fresh} \times \rho_{fresh} \times C_{fresh} \times (T_{fresh} - T_{in}) = M_{exhaust} \times \rho_{exhaust} \times C_{exhaust} \times (T_{out} - T_{exhaust}) \quad (3.11)$$

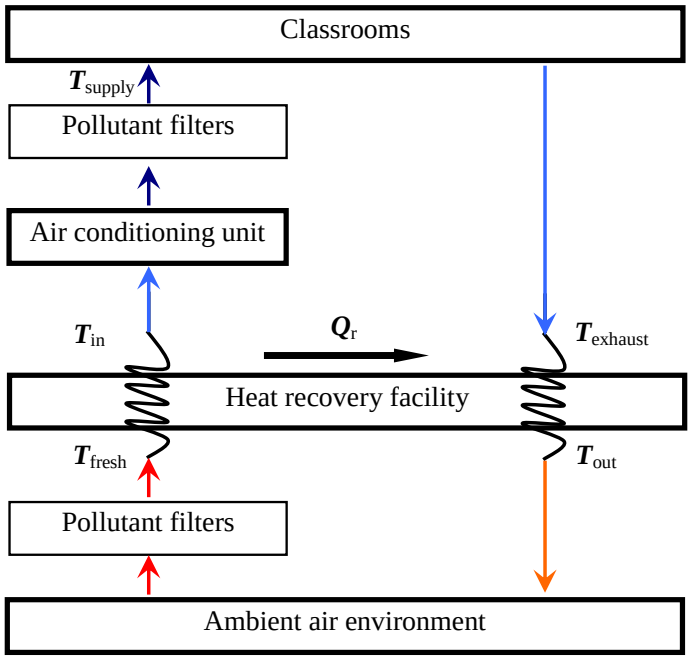

Figure 3.15: Heat recovery unit and thermal energy flowing charts for summer case.

In addition, the volumes of air flow rates across this school building should be maintained balance, i.e.,

$$M_{fresh} = M_{exhaust} \quad (3.12)$$

Assuming constant heat capacity and density for air in the range of the studied temperatures, energy balance equation can be further written as,

$$T_{fresh} - T_{in} = T_{out} - T_{exhaust} \tag{3.13}$$

As expected, the temperature difference of this heat exchanger would be asymptotically approaching to $T_{fresh} - T_{exhaust}$ for the ideal situation. As such, the efficiency of the heat recovery facility ($0 < \eta < 1$) can be defined as,

$$\eta = \frac{T_{fresh} - T_{in}}{T_{fresh} - T_{exhaust}} \times 100\% = \frac{T_{out} - T_{exhaust}}{T_{fresh} - T_{exhaust}} \times 100\% \tag{3.14}$$

One could observe that temperatures of entraining fresh air and exhausting stale air could respectively approach those of room air and outdoor air temperatures, if the heat recovery efficiency could be unit ($\eta = 1$).

As mentioned before, the stale air exhausted from the classrooms is $T_{exhaust}$. The supplying fresh air from the diffusers is maintained at T_{supply}, which could be determined by the operations of the air conditioning unit. As the heat recovery displacement ventilation system is operated, the efficiency of the air conditioning unit could be enhanced by the shrinking temperature difference between supplying air and entrained fresh air, i.e., $T_{fresh} - T_{supply}$ being replaced by $T_{in} - T_{supply}$. Theoretically, the cooling load $M_{fresh} \times C_{fresh} \times \rho_{fresh} \times (T_{fresh} - T_{supply})$ could be conserved due to the heat recovery process, such that the system cooling load reduces to $M_{fresh} \times C_{fresh} \times \rho_{fresh} \times (T_{in} - T_{supply})$. With energy conservation, the cooling load reduction equals the heat recovery thermal energy Q_r, i.e., being written as,

$$M_{\text{fresh}} \times \rho_{\text{fresh}} \times C_{\text{fresh}} \times (T_{\text{fresh}} - T_{\text{supply}}) = M_{\text{fresh}} \times \rho_{\text{fresh}} \times C_{\text{fresh}} \times (T_{\text{in}} - T_{\text{supply}}) + Q_{\text{r}} \tag{3.15}$$

Combining with aforementioned formulations and assumptions, the energy conservation ratio of the air conditioning unit could be defined by,

$$\varphi = \frac{Q_r}{M_{fresh} \rho_{fresh} C_{fresh} (T_{fresh} - T_{\text{supply}})} = \frac{T_{fresh} - T_{in}}{T_{fresh} - T_{\text{supply}}} = \frac{T_{out} - T_{exhaust}}{T_{fresh} - T_{\text{supply}}} \tag{3.16}$$

The energy conservation ratio could be equivalent to unity as the heat recovery unit could replace the air conditioning unit. In fact, the air conditioning unit could not be replaced as it provides cooling for the whole ventilation system. In addition, the heat recovery volume of cooling load only occupies relatively smaller ratio of the whole cooling load for summer case, such that $\varphi << 1$. Combining both definitions of η and φ, one can observe,

$$\varphi \times (T_{\text{fresh}} - T_{\text{supply}}) = \eta \times (T_{\text{fresh}} - T_{\text{exhaust}}) \tag{3.17}$$

In the typical Munich region summer day, ambient environment averaged highest temperature is approximately 30 °C (T_{fresh}) (Jacob et al. 2008), while the supplying and exhausting air temperatures T_{supply} and $T_{exhaust}$ actually are the nominal temperatures of the supplying ports and exhausting ports, respectively. In the present investigation, like the above winter case, exhausting air temperatures could be also determined by the full CFD modelling of classroom airflows upon the supplying air temperatures are given as a priori.

3.3.2 Results and discussion

3.3.2.1 Steady classroom airflow and thermal stratification comfort

As this mechanical ventilation unit is originally put into use, fresh air from the diffusers is usually maintained at M_{fresh} = 660 m^3/h and T_{supply} = 17 °C supplied into the enclosure in summer, to meet the air volume requirement of each occupant 20 m^3/h in Germany. Subsequently, steady airflow and thermal dispersion will be established with such displacement ventilation system for the summer case. Solar radiation from the windows of such school buildings is almost avoided with the shading system installed outward from the windows for the classroom in order to shrink much more heat gains to warm the classroom in summer.

Observing from Fig. 3.16(a), the first row students' feet near the inlets are directly subjected to the conditioned air of very low temperature (around 18 °C) and relatively high density, being far lower than that of regions where other students are seated. As the fresh air spreads forward, classroom heating objectives will gradually enhance its temperature level. Around the floor region of the third row, air temperatures are observed higher than 21 °C; as air arrives to the region of the sixth row, its temperature approaches 24 °C. Observing from Fig. 3.16(b), horizontal plane elevated 1.10 m from the floor, air temperatures in the majority of students occupation area are higher than 24 °C. This demonstrates that the displacement ventilation flow pattern will result in the vertical thermal stratification.

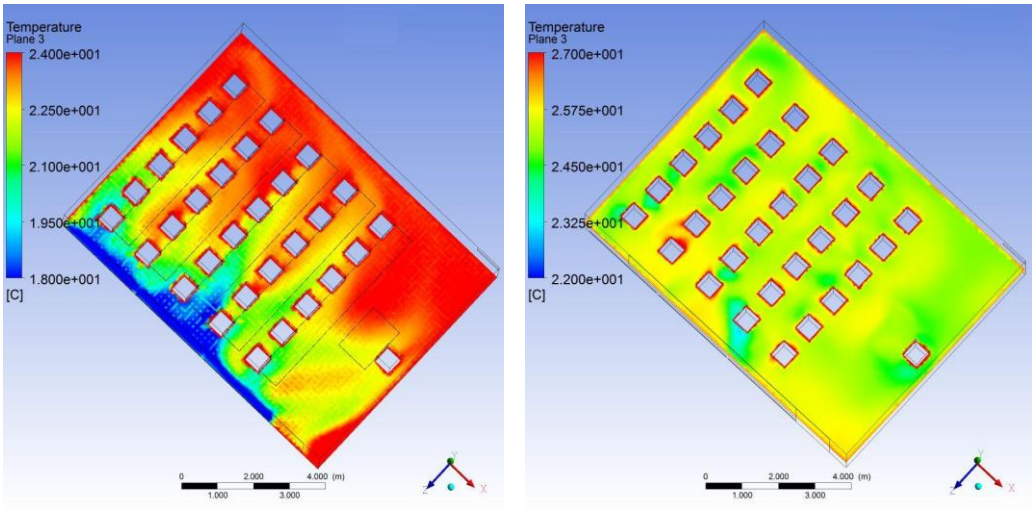

(a) Isothermal distributions at 0.10 m (b) Isothermal distributions at 1.10 m

Figure 3.16: Spatial distributions of air temperatures in summer. They are across horizontal sections respectively at elevating height of 0.10 m (a) and 1.10 m (b), both immediately from the floor.

Some same selected observations as the winter case are illustrated in Fig. 3.17, which includes the vertical air temperature distributions around 6 students and the teacher. For the students of Line 2 and Rows 1-6, air temperatures around them range from 18.7 °C to 28.2 °C, whereas those around the teacher range from 22.8 °C to 26.4 °C. Particularly, for the Student 2.1, vertical temperature difference of his/her is higher than 5 °C, exceeding the maximum temperature difference between foot ankle and head 3 °C, which will directly lead to the local thermal discomfort (Noh et al. 2007).

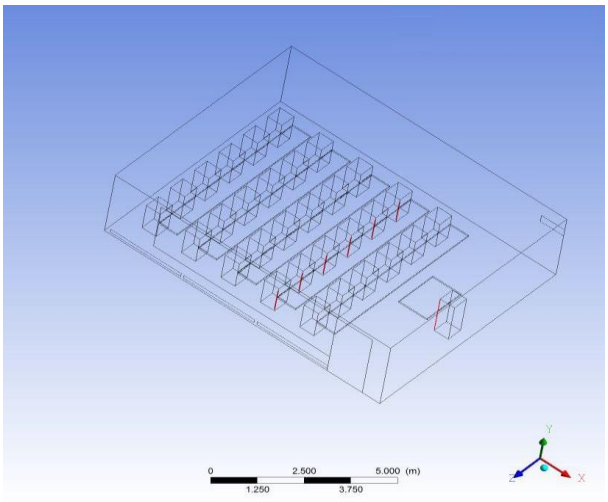

(a) General locations of vertical temperature observations (Line 2, Rows 1-6, Teacher)

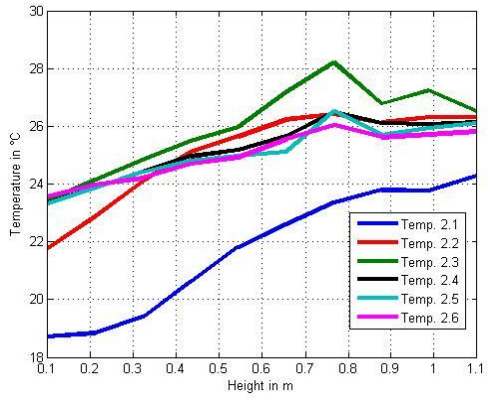

(b) Temperature distributions for students

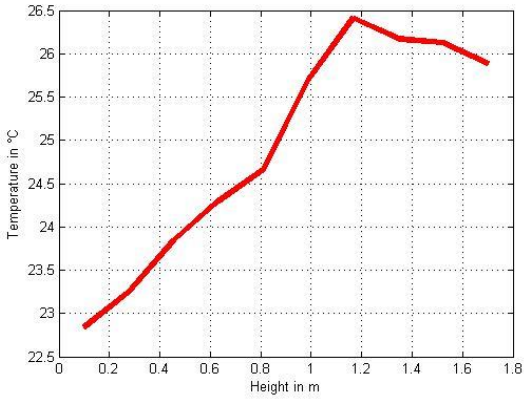

(c) Temperature distributions for Teacher

Figure 3.17: Vertical distributions of air temperature in summer. They include vertical distribution ((b), ranging from 0.10 m to 1.10 m) of air temperature profile in the positions of students seated of Line 2 and Rows 1-6, and those in the standing teacher ((c), ranging from 0.10 m to 1.70 m). Detailed locations are illustrated in (a) as red lines.

As expected, occupants will have better human thermal comfort with lower values of vertical temperature difference. Actually, continuously decreasing vertical temperature difference will reduce the thermal stratification sensitivity of occupants, which has been represented by the values of *PD*.

Some same sampling locations and data as the winter case are also summarized in Table 3.2, including the temperatures of ankle and head positions, head to ankle temperature difference as well as percentage dissatisfied.

Vertical temperature differences at students 2.1 and 2.2 significantly exceed the permitted value (3 °C), such that their *PD* values are higher than other locations. Therefore students should take seats a bit far from the fresh air inlets, to enhance their thermal comfort. With this rule, the first row students near the inlets should move to the positions of between the second and third row a little such as 0.2 m, meanwhile, the rest of students should be distributed uniformly in the rest of space of the classroom. They actually do not feel thermal discomfort after the moving. Or the inlet supplying air temperature should be higher a little e.g. 18 °C or 19 °C so as to enhance their thermal comfort. In fact, they indeed feel favourable thermal comfort after the inlet temperature is changed into 19 °C, which is now setpoint through the optimization for the control system.

Area averaged temperatures at some elevated horizontal planes, from 0.10 m to 2.90 m, are illustrated in Fig. 3.18(a). With such displacement ventilation, the vertical thermal stratification mainly occurs at the altitude below 1.50 m, which heavily influences the thermal

comfort of occupants. This also explains why the students' rows close the supplying ports have relatively high values of *PD*. Further modifications and optimizations of this displacement ventilation system should be implemented.

Table 3.2: Vertical temperature levels and Percentage Dissatisfied (summer). They include that sampling locations, ankle temperature, head temperature and vertical difference temperature level between head and ankle as well as *PD* at those sampling locations around the Teacher and Students.

Location	**Ankle**	**Head**	**Vertical difference**	***PD***
	°C	**°C**	**°C**	**%**
Teacher	22.8	25.8	03.0	04.0
Student 2.1	18.7	24.3	05.6	27.5
Student 2.2	21.8	26.3	04.5	12.9
Student 2.3	23.4	26.5	03.1	04.3
Student 2.4	23.4	26.1	02.7	03.1
Student 2.5	23.3	26.1	02.8	03.3
Student 2.6	23.6	25.8	02.2	02.0

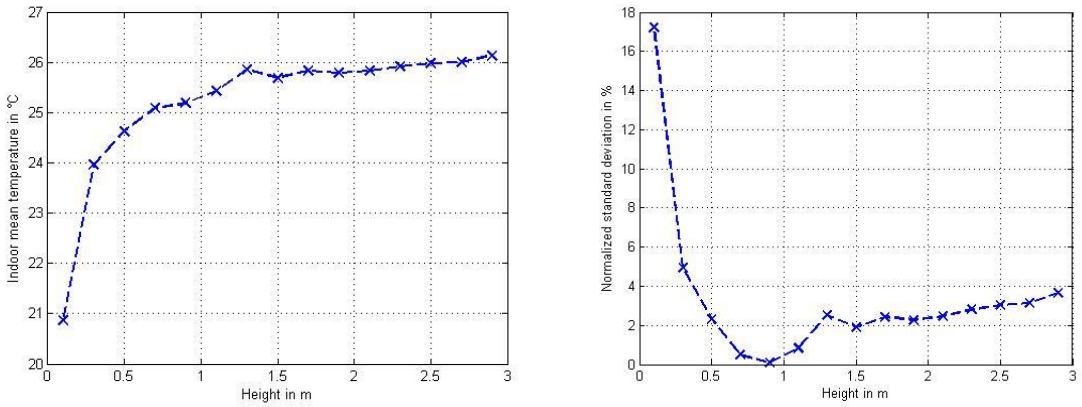

(a) Cross horizontal plane mean temperatures (b) Normalized standard deviation

Figure 3.18: Horizontal plane mean temperatures and normalized STD in summer. Normalized standard deviations are as functions of their vertical elevations in classroom with stable displacement ventilation rate of 660 m^3/h and supplying air temperature 17 °C.

In order to clearly disclose the thermal stratification characteristics by the plane averaged temperatures and volume average temperature, as plotted in Fig. 3.18(b), the normalized standard deviations of the horizontal cross section plane averaged temperatures are obtained by the normalization with the enclosure volume averaged air temperature (25.2 °C).

Observing from Fig. 3.18(b), the highest deviation (approximately 17%) is achieved at the elevation of 0.10 m, where classroom diffusers deliver cold and fresh air across the lower region with cold air sinking down to the floor. With the increasing elevation of horizontal

planes, the standard deviation decreases sharply toward to zero as the vertical elevation achieves at 0.90 m immediately above the floor, where average temperature is very close to the classroom volume averaged temperature 25.2 °C. Below this critical plane elevated at 0.90 m, air temperatures are lower than volume averaged temperature; whereas, above that critical plane, air temperatures exceed the volume averaged one, and their deviations increase a little, asymptotically approaching 4%. This is due to the fact that upper regions of this classroom tend to be of uniform isotherms, which favourably produces the thermal buffers to reduce the heat transfer rates between surroundings and building ceilings. This observation has been collaborated by the past researches of displacement ventilation (Yuan et al. 1999).

Furthermore, as the classroom air temperatures should be monitored by a single thermocouple or a thermal sensor for the future energy cost evaluation of the whole low energy school building, it should be directly put inside the bottom half region of the classroom (vertically elevated at 0.90 m) shifting aside from diffusers towards the outlet, to represent the average temperature level of the whole classroom (Wang et al. 2014).

In addition, thermal comfort of occupants will be influenced by the airflow velocities. Mean velocity of airflow drafted toward people normally should not exceed 0.25 m/s; otherwise draft dissatisfaction will arise. Characteristic velocity vectors in a vertical cross plane (Z = 6.60 m) located between the diffusers and the closest row students are shown in Fig. 3.19. As the supplying fresh air drifts toward the nearby students, with the effect of jet decaying, its axial flow rate decreases from 0.30 m/s to 0.22 m/s; whereas, plane averaged air flow intensity in this cross plane is only 0.08 m/s, far lower than 0.25 m/s. Therefore, from the airflow intensity point view, displacement ventilation inside the classroom does not cause the problem of draft dissatisfaction.

Observing from Fig. 3.19, complicated airflow vortex structures truly exist in the classroom, especially between the first line students and second line students. Physically, these air flow streams are subjected to diverse flow forces, including the mechanical ventilation and thermal plume forces. Here, supplying jet flows will firstly sink toward floor with negative buoyancy effect, while air flows around the human body will rise upward due to positive buoyancy effect. These flow streams interact with each other and result in such complicated flow circulations shown in Fig. 3.19. Micro-circulation of airflow around the human body will hinder the pollutants removed from the breathe regions (discussed later), which easily results in poor air quality for occupants. However, the air flow structures in the regions be-

tween the first line students and the teacher are observed not to contain any micro-circulations. That is to say, the distance between each line of students should be enlarged to reduce such interferences, to create favourable breathe environment for any occupants.

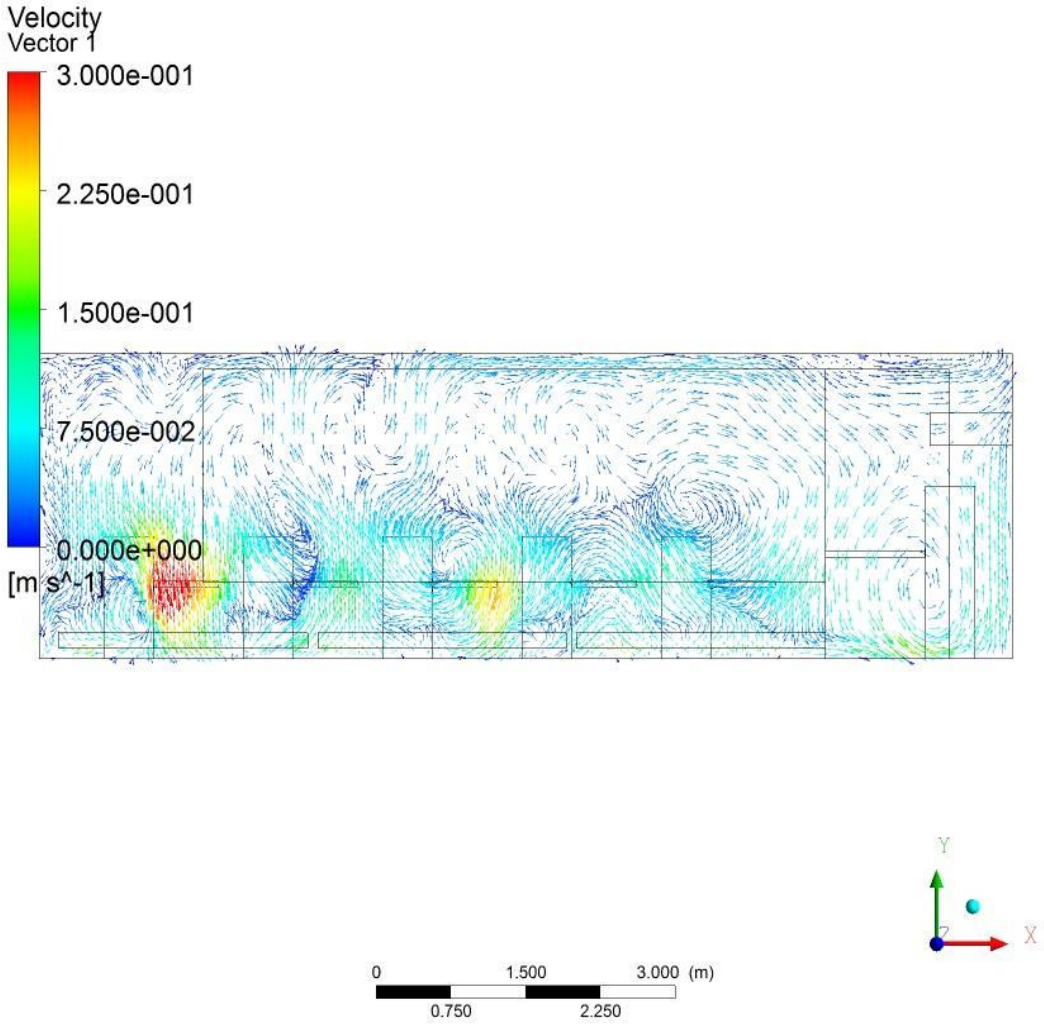

Figure 3.19: Velocity vector flow fields in summer. They are along the vertical plane (Z = 6.60 m) locates between the diffusers and the nearby row students).

3.3.2.2 Effects of ventilation flow rates and supplying air temperatures

Actually, the airflow patterns and heat transfer structures in the classroom could be heavily affected by the supplying velocities or the mechanical ventilation flow rates. Now, the aforementioned controlling parameters and boundary conditions are maintained excluding the supplying ventilation flow rates gradually promote from 10 m^3/h to 880 m^3/h. The volume averaged classroom temperatures and vertical thermal gradients between the head and ankle on the locations of student 2.1 and the teacher have been illustrated in Fig. 3.20, as functions of classroom ventilation rates.

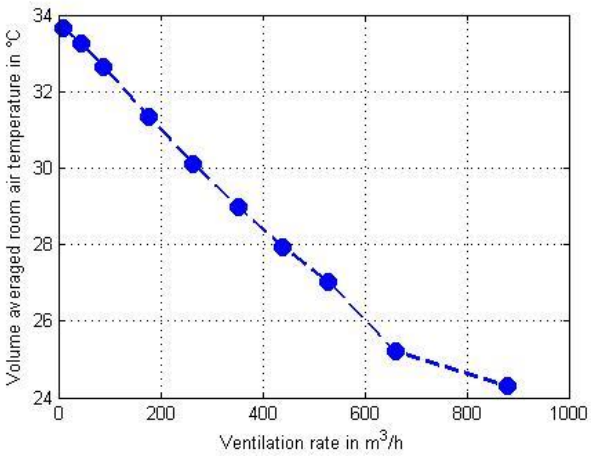

(a) Volume averaged classroom temperatures

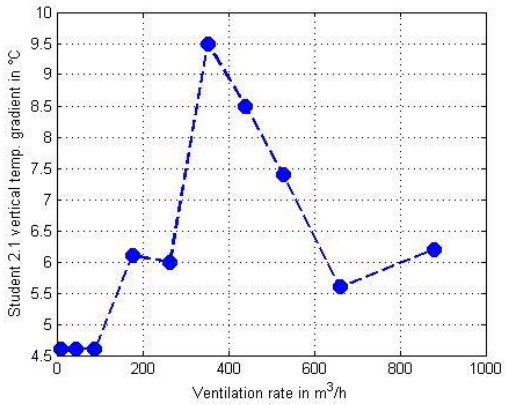

(b) Vertical thermal gradient for student 2.1

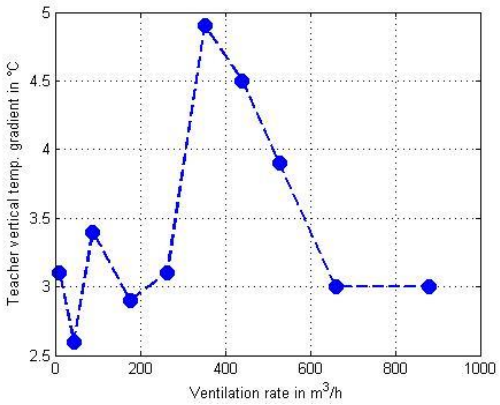

(c) Vertical thermal gradient for Teacher

Figure 3.20: Variations of mean temperature and thermal gradients in summer. Indoor temperature will be very high up to about 34 °C if without mechanical ventilation. Selected points are shown as functions of ventilation flow rate. For student 2.1 and teacher, both of them have very bad thermal comfort at 360 m^3/h.

Observing from Fig. 3.20(a), almost linearly decaying function between the ventilation flow rates and the classroom volume averaged temperatures could be established. Classroom air could be easily cooled with increasing volumes of air delivered from the air conditioning unit.

However, as shown in Figs. 3.20(b) and 3.20(c), the local latitude thermal gradients do not coincide with the decaying trend, and they tend to achieve peak values around at M_{fresh} = 360 m^3/h and decrease sharply until the delivering fresh air volume could satisfy the threshold of required ventilation rates (660 m^3/h).

Subsequently, the supplying fresh air temperatures could be varied, from 15 °C to 25 °C, while the supplying air volume is maintained at M_{fresh} = 660 m^3/h. Observing from Fig. 3.21,

exhaust air temperatures could linearly increase with the supplying air temperature. In addition, with the increasing of the supplying fresh air temperature, the temperature difference between the supplying air and exhaust air will decrease from about 10 °C to 5 °C.

Closely scrutinizing the thermal flow charts inserted in the frame of Fig. 3.21, with the promotion of supplying air temperatures, remarkable thermal stratifications shift downward from central area to the floor level, which could increase the values of *PD* a little and intensify the thermal buffers in the upper region of the classroom.

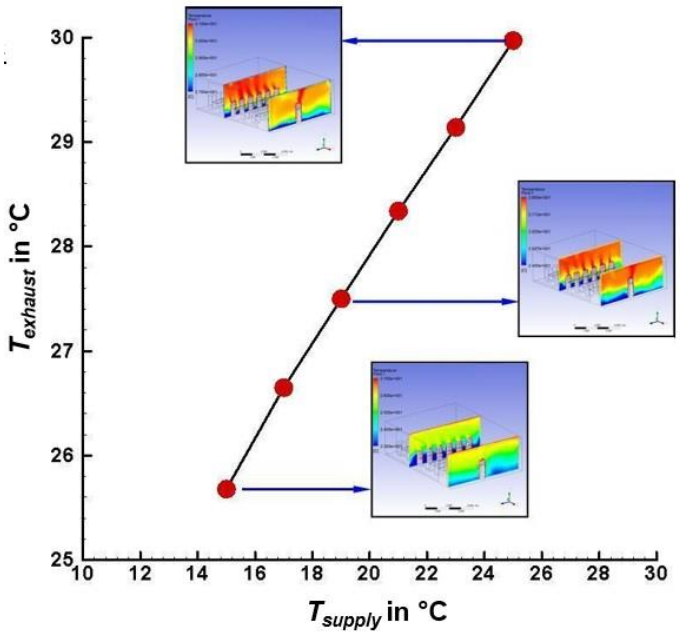

Figure 3.21: Variation of classroom exhaust air temperatures in summer. $T_{exhaust}$ as function of the fresh supplying air temperatures with representative parameters, M_{fresh} = 660 m^3/h and T_{fresh} = 30 °C.

3.3.2.3 Effect of displacement ventilation on transient CO_2 dispersions

Removal of indoor pollutants and dilute the stale air are the essential roles of building ventilation. As mentioned before, generally, indoor CO_2 concentration will be used as an indicator of IAQ in the present investigation. Each occupant in the classroom generates about 2.0×10^{-2} m^3/h of pure CO_2 due to respiration, and their total contributions will significantly increase overall CO_2 concentration levels in such classroom of low air infiltration.

With the same initial volume averaged CO_2 concentration 1350 ppm, two different levels of mechanical ventilation rates (M_{fresh}) are respectively implemented, 660 m^3/h and 88 m^3/h, while T_{supply} is kept constant (17 °C) and other momentum and thermal boundary conditions implemented in the above steady thermal flow simulations are maintained. As illustrated in

Fig. 3.22, temporary evolutions of indoor mean CO_2 concentration and its normalized standard deviation are plotted as the functions of time, respectively shown in Figs. 3.22(a) and 3.22(b). Observing from Fig. 3.22(a), for the case of high ventilation rate, indoor mean CO_2 level decays rapidly due to the quantity of fresh air entrained into the room is far higher than the CO_2 production from the crowded occupants. But, after 15 minutes, decaying rate of this curve tends to be flat due to the entraining fresh air gradually dilutes the room in a whole level. On the other hand, the curve represented by the case of low ventilation rate always shows the pollutant concentration almost linearly increases with time. Actually, this is due to the CO_2 production rate of occupants far exceeds that fresh air dilution rate of low ventilation rate. In contrast, mechanical ventilation of high level ventilation rate can quickly dilute the room air (within 10 minutes) into less polluted level (less than 900 ppm). Therefore, promotion of mechanical ventilation rate can directly contribute to the quick dilution of indoor air pollutants, and too low ventilation rate could not effectively inhibit the increase of indoor CO_2 concentration levels.

Mechanically supplying air not only quickly dilutes indoor air, but also causes the non-uniform distributions of pollutants. Non-uniformity of CO_2 dispersions can be essentially represented by the values of standard deviations of pollutant concentration shown in Fig. 3.22(b). For the case of high ventilation rate, dilution of indoor CO_2 could be implemented within several minutes, but the non-uniformity of indoor pollutant distributions increases greatly, achieving maximum of 59% just after 15 minutes. Thereafter fresh air is continuously entrained into the room, both pollutant concentration levels and its spatial non-uniformity decrease. For the case of low ventilation rate, the pollutant levels always increase with time and the non-uniformity of pollutant distribution increases slightly, being up to 18% after 30 minutes. Physically, the fresh air delivered by low ventilation rate will gradually penetrate into the room mixtures, which will not drastically and suddenly change the original distributions of pollutants.

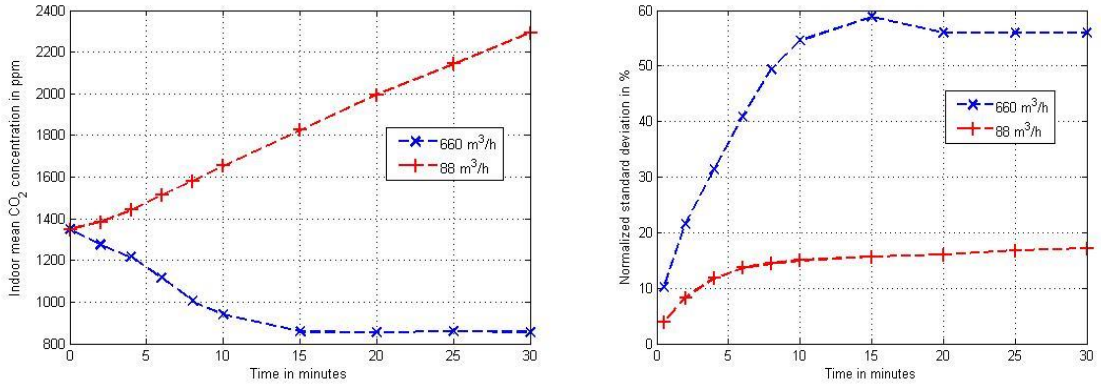

(a) Volume mean concentration of indoor CO_2 (b) Normalized standard deviation

Figure 3.22: Indoor mean CO_2 concentration and its normalized STD in summer. (a) shows temporary evolutions of indoor mean CO_2 concentration and (b) is its normalized standard deviation inside the classroom with two different levels of mechanical ventilation rates and the same initial pollutant concentrations, i.e., 660 m^3/h and 1350 ppm (blue line), and 88 m^3/h and 1350 ppm (red line).

In addition to the supplying flow momentum, the displacement ventilation flow pattern could result in a sensible species boundary layer in the lower region of this classroom. Observing from Fig. 3.23, spatial distributions of pollutants are significantly divided by the pollution layer, where the CO_2 concentration difference between upper and lower bands is greater than 300 ppm. This can also explain its peak values of standard deviations shown in Fig. 3.22.

Species stratification is also observed in the displacement ventilation classroom shown in Fig. 3.23. With such stratification, pollutants almost could not take long residence in the occupant regions (vertical altitude less than 2.0 m), whereas they will gradually accumulate in the upper regions toward the ceiling, where local CO_2 concentration is far higher than 1000 ppm near the ceiling. Therefore, the appropriate installation location for a CO_2 sensor should be in the upper region of this classroom (as indicated by the black arrows in Fig. 3.23) (Wang et al. 2014), where local species concentration can represent the volume-averaged concentration level, which is the same conclusion as the winter case. It could illustrate that the temperature difference does not have the large influence on the CO_2 distributions normally. With such installations, the whole pollutant emissions across this low energy building could be monitored in the long running time.

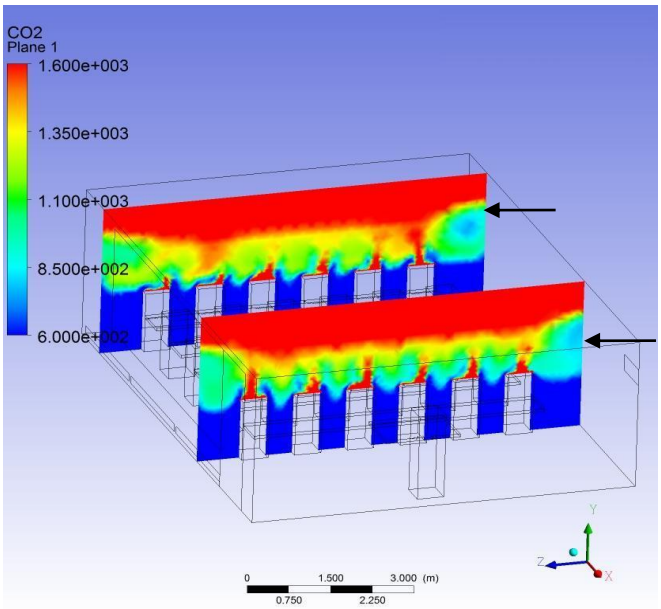

Figure 3.23: Spatial distributions of CO_2 concentration at time instant 15 minutes. This moment is the largest normalized standard deviation situation with M_{fresh} = 660 m^3/h and T_{supply} = 17 °C.

3.3.2.4 Effect of heat recovery efficiency and energy conservation ratio

The exhaust air will be firstly delivered passing the heat recovery unit to pre-cool the entrained outdoor fresh air, and the heat recovery efficiency of the heat recovery facility could put the effect on the operation of the air conditioning unit. Diverse situations of energy conservation ratio and heat recovery efficiency have been correlated in terms of the temperature difference between surrounding fresh air and supplying air, shown in Fig. 3.24,

$$\ln(\varphi/\eta) = 0.102\times(T_{fresh} - T_{supply}) - 2.695 \quad (3.18)$$

As expected, energy conservation of the air conditioning unit could be enhanced with the heat recovery facility and the enlarged temperature difference between the supplying air and fresh air. However, it should be noted that the aforementioned correlation is only suitable for cooling operation and the temperature difference T_{fresh} - T_{supply} should be no less than 6 °C (illustrated in Fig. 3.24). That is to say, the heat recovery facility could become less effective when the supplying air gradually approaches the ambient one. Accordingly, the energy conservation of the air cooling unit becomes less important if the ambient air could be promptly delivered into the classroom.

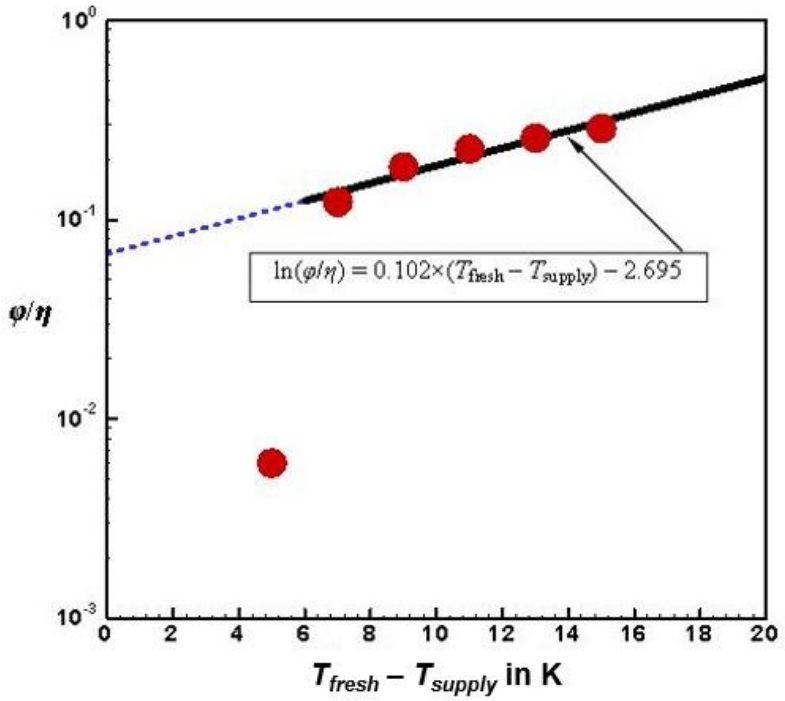

Figure 3.24: Correlations of η and φ for summer case. It is as functions of temperature difference between fresh air and supplying air.

3.3.2.5 Summary and conclusions

Displacement ventilation unit and heat recovery facility are put into operation with full closed windows and airtight building envelopes in summer, aiming to reduce the building heat transfer losses and enhance the building energy efficiency. Classroom thermal comfort and indoor air quality in the new Passive House School Building have been numerically investigated, together with the analytical modelling of heat recovery and energy conservation relations.

(1) Displacement ventilation thermal stratification has been demonstrated by the spatial thermal distributions and their normalized standard deviations. Sharp thermal gradients are observed below 0.90 m, whereas uniform isotherms present in the upper regions, where favourably produces the thermal buffers to reduce the heat transfer rates between surroundings and building ceilings. In addition, displacement ventilation inside this classroom does not cause the problem of draft dissatisfaction.

(2) The airflow patterns and heat transfer structures in the classroom are heavily affected by the ventilation flow rates and supplying air temperatures. Classroom volume averaged temperature linearly decays with the ventilation flow rate, while the local thermal gradients

are the complex function of the ventilation flow rates. The increasing temperature of supplying fresh air not only linearly promotes the exhaust air temperature, but also pushes thermal stratifications shifting downward from central area to the floor level.

(3) Temporary evolutions of indoor mean CO_2 concentration indicate that promotion of mechanical ventilation rate can directly contribute to the quick dilution of indoor air pollutants. Standard deviations of temporary pollutant concentrations clearly illuminate that non-uniformity of indoor pollutant distributions increases with the mechanical ventilation rate. Sensible species boundary layer and species stratification have been observed in the process of displacement ventilation in this classroom. With such stratification, pollutants will gradually accumulate in the upper area adjacent to the classroom ceiling.

(4) The heat recovery facility interacts with the operation of the air conditioning unit. Energy conservation ratio of the air conditioning unit and the heat recovery efficiency have been correlated in terms of the temperature difference between surrounding fresh air and supplying air, which shows that energy conservation of the air conditioning unit could be enhanced with the heat recovery facility and the enlarged temperature difference between the supplying air and fresh air.

This research could benefit for the classroom environment guide and the low energy ventilation design for the summer case, particularly school building with Passive House standard.

3.4 Case of transitional seasons

Natural ventilation is an effective method to simultaneously improve indoor air quality and reduce energy consumption in buildings (Allocca et al. 2003, Gratia et al. 2007, Karava et al. 2007, Haase et al. 2009, Zhong et al. 2012), especially when indoor temperature is close to ambient temperature e.g. the transitional seasons in Germany. Heat loss due to opened window and ventilation effectiveness ratio are analytically modelled. Following that, the effects of thermal buoyancy on the steady classroom airflow and thermal stratification comfort as well as the contaminant dispersion are discussed. Classroom displacement ventilation and its thermal stratification as well as indoor air quality indicated by the CO_2 concentration have been investigated concerning the effects of supplying air temperature and delivering ventilation flow velocity. Representative thermal comfort parameters, percentage dissatisfied and temperature difference between ankle and head have been evaluated. Subsequent

energy consumption efficiency analysis illuminates that classroom energy demands for natural ventilation could be decreased with the promotion of the ventilation effectiveness ratio for heat distribution when the natural ventilation rate maintains a constant, and with the shrinking of the ventilation effectiveness ratio for heat distribution when the supplying air temperature is not variable. Detailed correlations of heat loss resulted from opened window and ventilation effectiveness of natural ventilation inside the classroom have been presented.

3.4.1 Heat loss and ventilation effectiveness as well as preliminary analysis

For the total natural displacement ventilated classroom shown in Fig. 3.1, the heat loss (heat removal) q_{heat} due to opened window is determined by the relation,

$$q_{heat} = Q_{supply} \times \rho_{supply} \times C_{supply} \times (\overline{T}_{in} - T_{supply}) \tag{3.19}$$

where, Q_{supply} represents the supplying fresh airflow rates (m^3/s) by the natural ventilation. Its specific thermo-physics have been, respectively, determined by the supplying air density ρ_{supply} (kg/m^3) and the specific heat capacity of air C_{supply} (J/kg·K). The difference between indoor volume averaged air temperature and exterior surrounding air temperature is ($\overline{T}_{in}$ – T_{supply}) (K).

There are two significant ventilation parameters to assess the effectiveness of the ventilation (Rydberg et al. 1947, Sandberg 1981 and 1983, Awbi 1998, Karimipanah et al. 2002, Zhai 2006, Jin et al. 2012, Wu et al. 2013).

One is ventilation effectiveness ratio for heat distribution (ε_t). This is similar to heat exchanger efficiency and can be defined as,

$$\varepsilon_t = \frac{T_{exhaust} - T_{supply}}{\overline{T}_{in} - T_{supply}} \tag{3.20}$$

Where, $T_{exhaust}$ is the stale air temperature exhausted from the classrooms (K).

Another parameter is ventilation effectiveness ratio for contaminant removal (ε_C). It is a measure of how effective the ventilation system is in eliminating internally produced contaminant. It can be defined by the following relation,

$$\varepsilon_C = \frac{C_{exhaust} - C_{supply}}{\overline{C} - C_{supply}} \tag{3.21}$$

Where, $C_{exhaust}$ and C_{supply} represent the exhaust contaminant concentration (ppm) and the supplying contaminant concentration (ppm) respectively, $\overline{C}$ represents the volume averaged indoor contaminant concentration (ppm). The aforementioned two parameters depend on the pattern of indoor airflow distribution, room characteristics, and heat and contaminant sources etc. (Wang et al. 2014)

Substituting Eq. (3.20) into Eq. (3.19), the following relationship can be obtained,

$$q_{heat} = Q_{supply} \times \rho_{supply} \times C_{supply} \times (T_{exhaust} - T_{supply}) / \varepsilon_t \tag{3.22}$$

In the transitional seasons of Germany, ambient air environment averaged temperature is approximately from 10 °C to 20 °C (T_{supply}) (Jacob et al. 2008), while the exhausting air temperatures $T_{exhaust}$ actually is the nominal temperature of the exhausting ports. In the present investigation, exhausting air temperatures could be determined by the full CFD modelling of classroom airflows upon the supplying air temperatures are given as a priori. It is tried for test of grid independence solutions with a set of 383302, 463360, 511511, and 623220 nodes inside the enclosure. Volume averaged air temperature is almost unchanged (20.4 °C) after 511511 nodes were implemented, for the typical steady flow situation with fresh air natural ventilation rate maintained at 3.7 1/h based on our aforementioned measurements. Therefore, grid system of 511511 nodes will be adopted in the subsequent researches. The new modelling classroom with natural ventilation is shown in Fig. 3.25, which is including a small window with 1.25 m x 2.10 m as a fresh air inlet and a large window sizing of 5.00 m x 2.10 m, as the aforementioned earlier in Section 3.1.

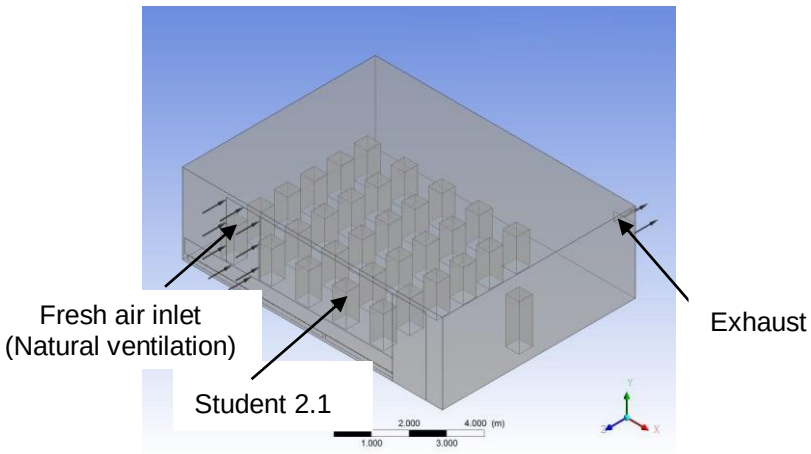

Figure 3.25: Geometry of the modelled classroom with natural ventilation. It is extracted from the Passive School Building.

3.4.2 Results and discussion

Firstly, the effect of thermal buoyancy on the steady classroom airflow and thermal stratification comfort as well as the contaminant dispersion is discussed. Following that, attention is focused herein on variation of the following parameters with thermal plume effect: supply air temperature and supply air velocity. Subsequently, the effect of those variable parameters on the ventilation effectiveness ratio is investigated. Finally, detailed correlations of heat loss due to displacement natural ventilation and ventilation effectiveness ratio for heat distribution have been presented.

3.4.2.1 Effect of classroom thermal buoyancy

As this displacement natural ventilation is preliminarily put into use, fresh air from the small window flows into the classroom, and it is maintained at natural ventilation rate N_{supply} = 3.7 1/h and T_{supply} = 16 °C supplied into the enclosure. Subsequently, steady classroom airflow and thermal dispersion will be established with such displacement ventilation forms.

As shown in Fig. 3.26(a), the teacher and the fourth row students' feet near the floor are directly subjecting to indoor air of relatively low temperature (around 18 °C); however, indoor air temperatures elevated approximately above the 1 m from the floor are close to 21 °C. It demonstrates that the displacement natural ventilation flow pattern with thermal buoyancy will result in the remarkable vertical thermal stratification, build up almost uniform thermal distribution and enhance the classroom thermal comfort.

Observing from Fig. 3.26(b), due to no thermal buoyancy inside the classroom, the wind from the exterior surrounding air dominates over the ventilation flow pattern. The indoor-produced heat is passively transported by the external forced air flow, and the wind forces dissipate lots of heat energy inside the classroom through the exhaust. The thermal distribution randomizes and air temperatures in the majority of the occupation area are only between 18 °C and 19 °C. It discloses clearly that thermal buoyancy heavily influences the thermal comfort of occupants.

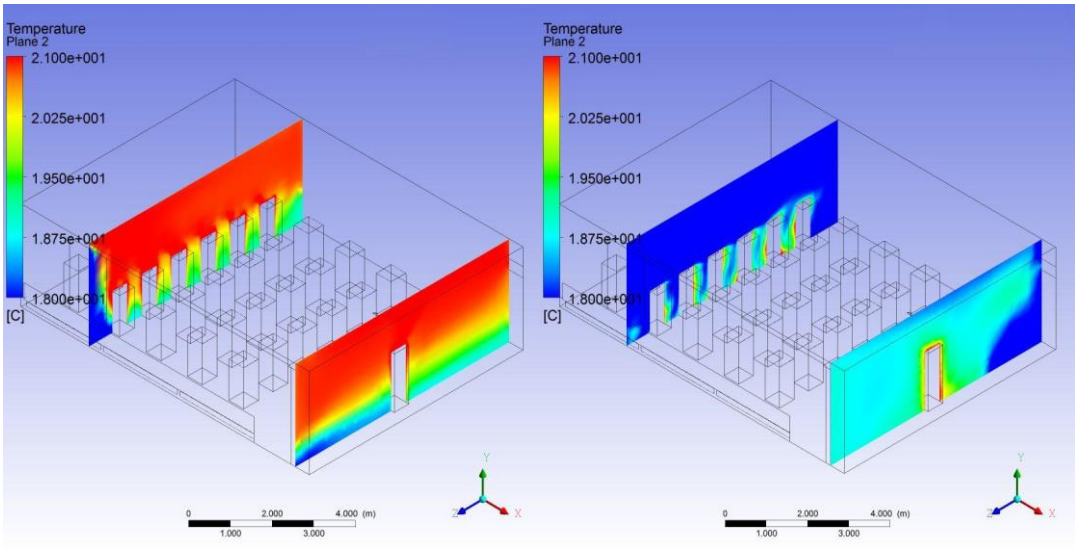

(a) Isothermal distribution with buoyancy (b) Isothermal distribution without buoyancy

Figure 3.26: Spatial distributions of air temperatures (transitions). They are across vertical sections respectively at X = 2.3 m (worst case: near the opened window) and 9.3 m with thermal buoyancy (a) and without thermal buoyancy (b), with the natural ventilation rate = 3.7 1/h, T_{supply} = 16 °C and initial classroom indoor air temperature of 20 °C.

Removal of indoor pollutants and to dilute the stale air are the essential roles of building ventilation. Generally, indoor CO_2 concentration will be used as an indicator of IAQ in the present investigation. Each occupant in the classroom generates about 2.0×10^{-2} m^3/h of pure CO_2 due to respiration.

With the same initial volume averaged CO_2 concentration 1803 ppm based on our earlier experiments, the same level of natural ventilation rate (N_{supply} = 3.7 1/h) is implemented, while T_{supply} is kept constant (16 °C) and other momentum and thermal boundary conditions implemented in the above steady thermal flow simulations are maintained. As illustrated in Fig. 3.27(a), for the case of with thermal buoyancy, the displacement ventilation flow pattern could result in a sensible species boundary layer in the lower region of this room. Spatial distributions of pollutants are divided by the pollution layer, where the CO_2 concentration difference between upper and lower bands is close to 200 ppm. Remarkable species stratification is observed in the displacement natural ventilation classroom shown in Fig. 3.27(a).

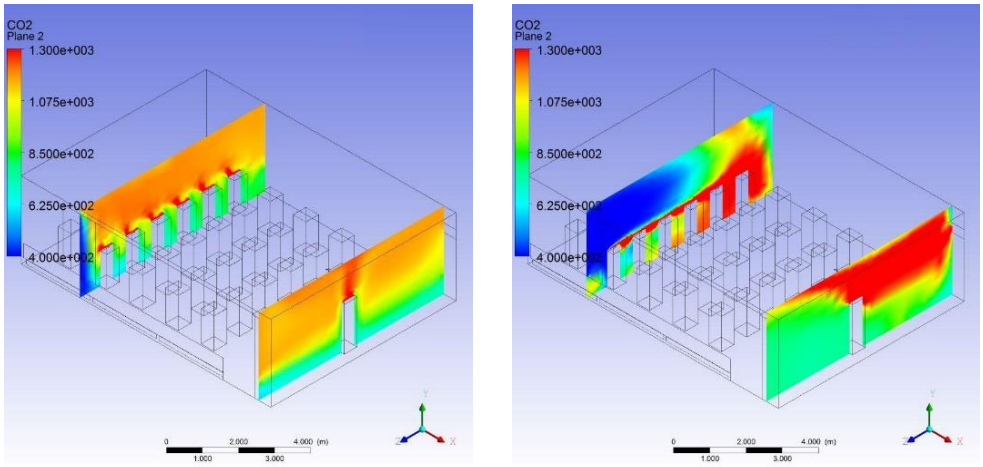

(a) Iso-concentration distribution with buoyancy (b) Iso-concentration distribution without buoyancy

Figure 3.27: Spatial distributions of CO_2 concentrations (transitions). They are across vertical sections respectively at X = 2.3 m (worst case: near the opened window) and 9.3 m with thermal buoyancy (a) and without thermal buoyancy (b), with the natural ventilation rate = 3.7 1/h, T_{supply} = 16 °C and initial classroom indoor air temperature of 20 °C as well as initial classroom indoor CO_2 concentration of 1803 ppm.

Observing from Fig. 3.27(b), since there is no thermal buoyancy effect inside the classroom, the wind from the outdoor air dominates over the ventilation flow pattern. This results in non-regular species distribution and non-remarkable species stratification. Spatial distributions of classroom pollutants are divided by the pollution layer, where the CO_2 concentration difference between inside and outside bands is greater than 450 ppm. The aforementioned cases illustrate that the thermal buoyancy has a strong effect on the spatial distribution of the contaminants. Thermal plume not only affects the air flow pattern, but also tends to decrease indoor pollutant concentration.

3.4.2.2 Effects of classroom supply air temperatures

The airflow patterns and heat transfer structures as well as contaminant concentrations in the classroom could be affected by the supplying air temperatures. Now, the aforementioned controlling parameters and boundary conditions are still adopted excluding the supplying air temperatures gradually promote from 10 °C to 20 °C, while the supplying air volume is maintained at N_{supply} = 3.7 1/h.

The classroom volume averaged air temperatures and vertical thermal gradients between the head and ankle on the locations of student 4.1 and 4.2 have been illustrated in Fig. 3.28, as functions of supplying air temperatures. Observing from Fig. 3.28(a), almost linearly increasing function between the ventilation airflow supplying temperatures and the classroom

volume averaged temperatures could be set up. Classroom air could be easily warmed with increasing temperatures of air delivered from the exterior surrounding. Moreover, as shown in Figs. 3.28(b) and 3.28(c), the local latitude thermal gradients coincide with the above increasing trend, i.e. the higher classroom volume averaged temperatures, the smaller local latitude thermal gradients.

As expected, occupants will have better human thermal comfort with lower values of vertical temperature difference. In fact, continuously decreasing vertical temperature difference will reduce the thermal stratification sensitivity of occupants, which has been represented by the values of *PD*. One can easily observe that the vertical temperature differences at student 4.1 in Fig. 3.28(b) for the supplying air temperatures of 10 °C and 12 °C exceed the permitted value (3 °C), such that the *PD* values of these two supplying air temperatures are higher than other supplying air temperature levels. Therefore, natural ventilation should be implemented when the supplying air temperature is higher than 12 °C, to enhance human thermal comfort.

Subsequently, seen from Fig. 3.29, exhausting air temperatures could also linearly increase with the supplying air temperature. Closely scrutinizing the thermal flow charts inserted in the frame of Fig. 3.29, with the promotion of supplying air temperatures, remarkable thermal stratifications shift downward from central region to the lower region adjacent to the floor, which could intensify the thermal buffers in the upper region of the classroom and also explain why it can decrease the values of *PD* a little.

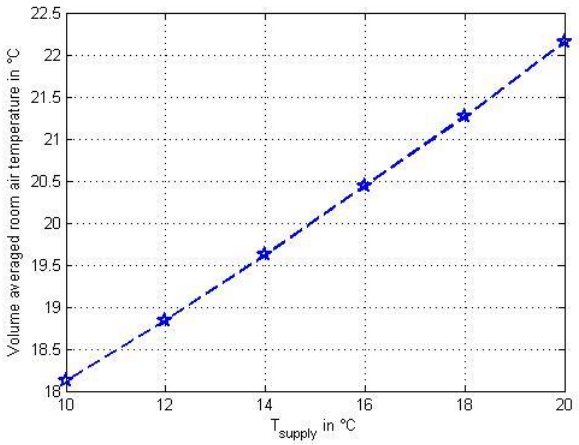

(a) Volume averaged classroom temperatures

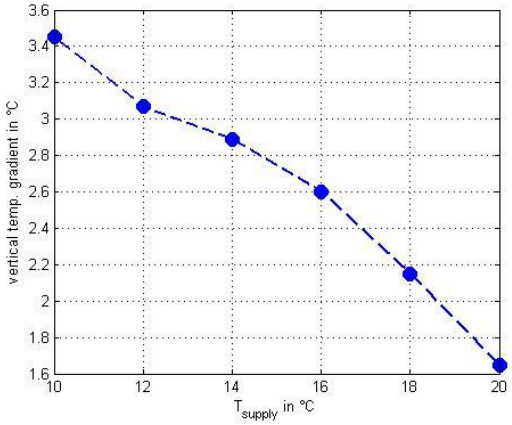

(b) Vertical thermal gradient for student 4.1

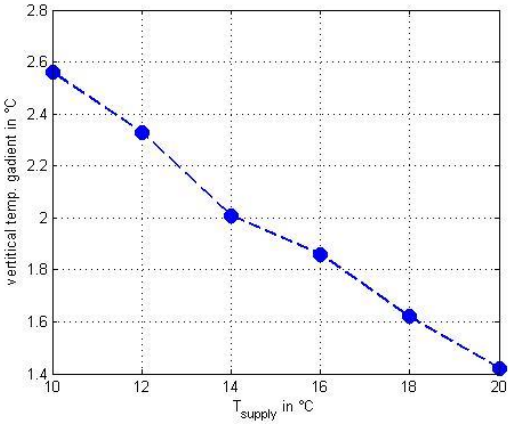

(c) Vertical thermal gradient for student 4.2

Figure 3.28: Variations of mean temperature and thermal gradients (transitions). Both of them are at some selected points as functions of the fresh supply air temperature. It shows that the higher volume averaged temperatures, the smaller local thermal gradients.

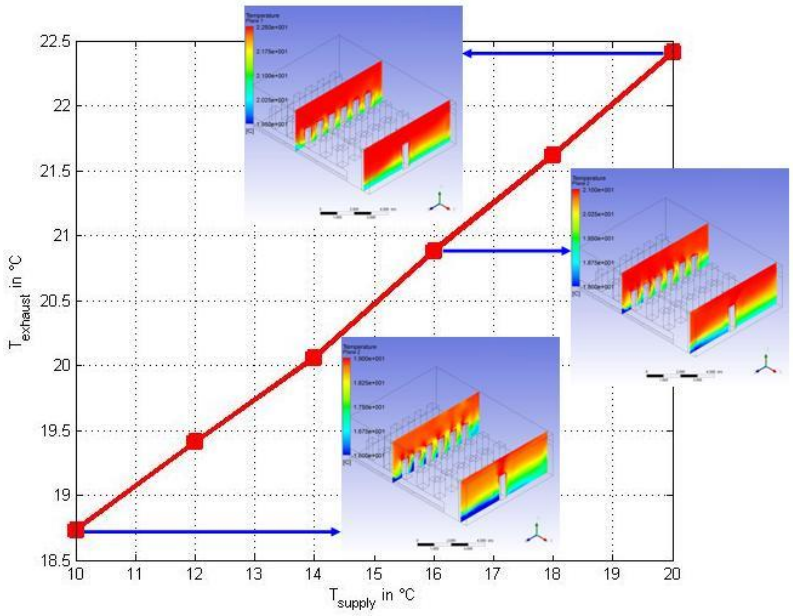

Figure 3.29: Variation of classroom exhaust air temperatures (transitions). It is as function of the fresh supply air temperatures with the natural ventilation rate = 3.7 1/h and initial classroom indoor air temperature of 20 °C.

With the same initial volume averaged CO_2 concentration of 1803 ppm, the same level of natural ventilation rate (N_{supply} = 3.7 1/h) is imposed on this classroom flow, while the supplying fresh air temperature is assumed to be varied, from 10 °C to 20 °C, and other momentum and thermal boundary conditions implemented in the above steady thermal flow simulations are maintained.

As illustrated in Fig. 3.30, almost exponentially decreasing function between the ventilation airflow supplying temperatures and the classroom volume averaged CO_2 concentrations could be established, although the decreasing scope of CO_2 concentrations is not large. Closely observing the species flow charts inserted in the frame of Fig. 3.30, with the rise of supplying air temperatures, non-remarkable species stratifications shift downward from central region to the lower region adjoining to the floor, which could favourably improve indoor air quality.

In order to assess the effect of the supply air temperature on the effectiveness of the displacement natural ventilation, the parameters of the ventilation effectiveness ratio for heat distribution (ε_t) and the ventilation effectiveness ratio for contaminant removal (ε_C) were also investigated as shown in Fig. 3.31. As represented in Fig. 3.31, nearly exponentially increasing functions between the supply air temperatures and the ventilation effectiveness ratio for thermal distribution and contaminant removal could be determined. This also explains why increasing supply air temperature could decrease the values of *PD* a little and meanwhile improve indoor air quality with the promotion of supplying air temperatures as the aforesaid investigations.

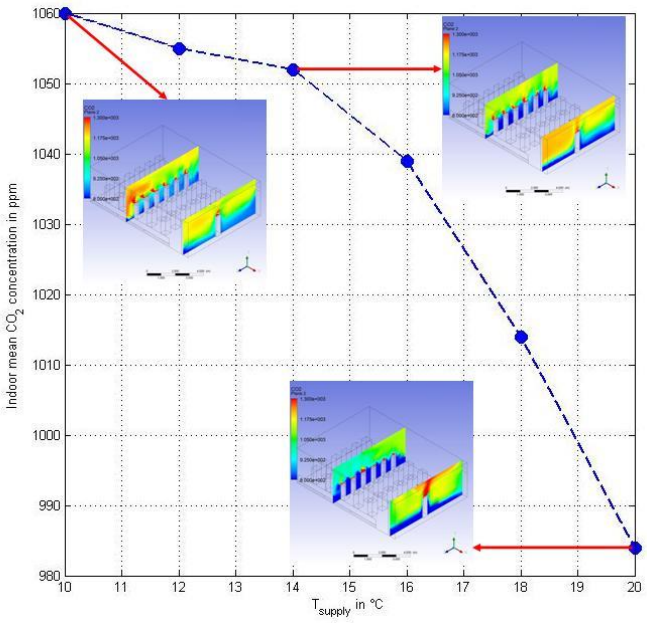

Figure 3.30: Variation of classroom volume averaged CO_2 concentration with T_{supply}. It is as function of the fresh supplying air temperatures with the natural ventilation rate = 3.7 1/h and initial classroom indoor air temperature of 20 °C as well as initial indoor CO_2 concentration of 1803 ppm.

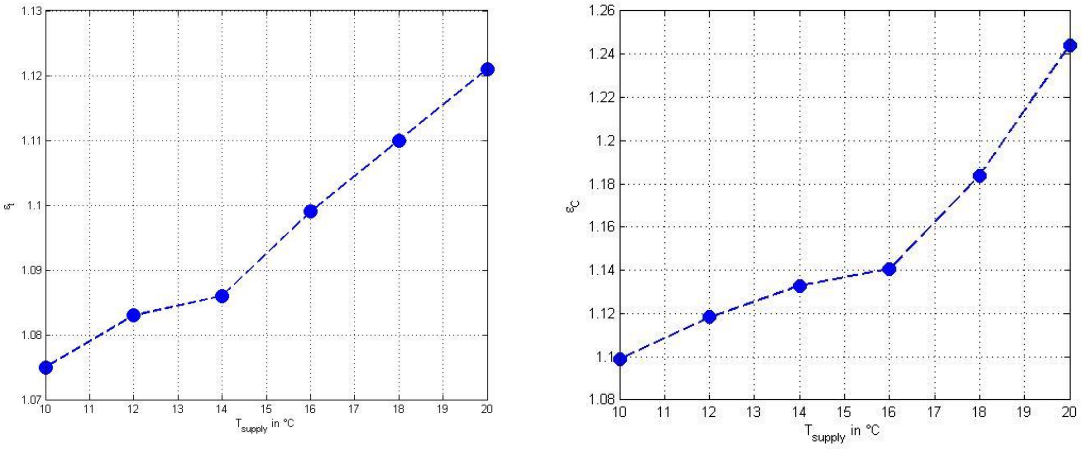

(a) Ventilation effectiveness for heat distribution (b) Ventilation effectiveness for pollutant removal

Figure 3.31: Variations of ventilation effectiveness ratio with T_{supply}. They are for heat distribution (a) and ventilation effectiveness ratio for contaminant removal (b) as functions of the fresh supply air temperature.

3.4.2.3 Effects of classroom supply air velocity

The airflow patterns and heat transfer structures as well as the pollutant dispersions inside the classroom could also be heavily affected by the supplying air velocities or the natural ventilation flow rates. Now, the aforementioned controlling parameters and boundary conditions are maintained unchangeable excluding the supplying air velocities V_{supply} gradually increase from 0.001 m/s to 1 m/s, while the supplying air temperature is kept at T_{supply} = 16 °C.

The volume averaged classroom temperatures and vertical thermal gradients between the head and ankle on the locations of student 4.1 and 4.2 have been illustrated in Fig. 3.32, as functions of supplying air velocities.

Observing from Fig. 3.32(a), an almost exponentially decreasing function between the ventilation airflow velocities and the classroom volume averaged temperatures could be set up. Classroom air could be easily cooled with increasing velocities of air delivered from the outdoor surrounding.

Moreover, as shown in Figs. 3.32(b) and 3.32(c), the local latitude thermal gradients do not coincide with the decaying trend, whereas they tend to achieve peak values around at V_{supply} = 0.1 m/s and 0.2 m/s, respectively, and almost decrease sharply after reaching maximal values.

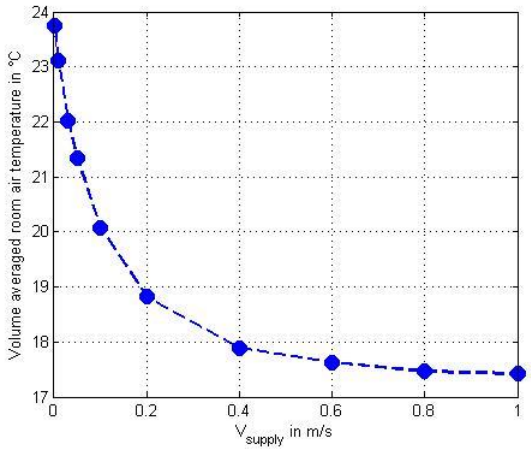

(a) Volume averaged classroom temperatures

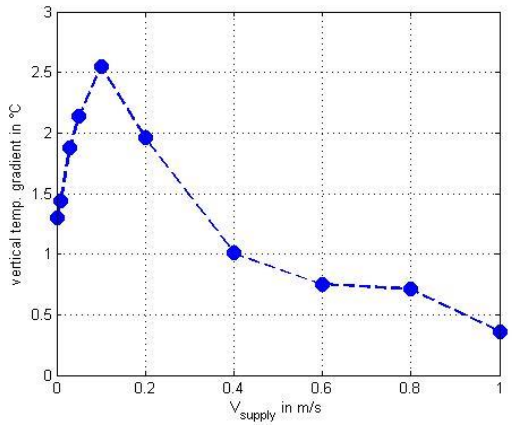

(b) Vertical thermal gradient for student 4.1

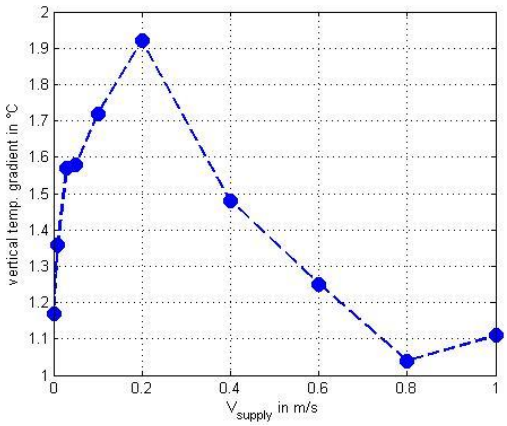

(c) Vertical thermal gradient for student 4.2

Figure 3.32: Variations of mean temperature and thermal gradients with V_{supply}. All those values at some selected points are as functions of the fresh supplying air velocity.

Following that, observing from Fig. 3.33, exhausting air temperatures could also exponentially decrease with the supplying air velocities. Closely scrutinizing the thermal flow charts inserted in the frame of Fig. 3.33, with the promotion of supplying air velocities, visible thermal stratifications shift upward from the lower region adjacent to the floor to the central region, which could alleviate the thermal buffers in the upper region of the classroom and also explain why it can increase the values of *PD* a little until V_{supply} = 0.1 m/s. However, for V_{supply} = 1 m/s, the thermal distribution randomizes completely. This is mainly due to the fact that the wind force dominates over the thermal buoyancy at this moment. It results in that there is no remarkable thermal stratification inside the classroom. This also coincides with the aforementioned investigations of non-thermal buoyancy effect.

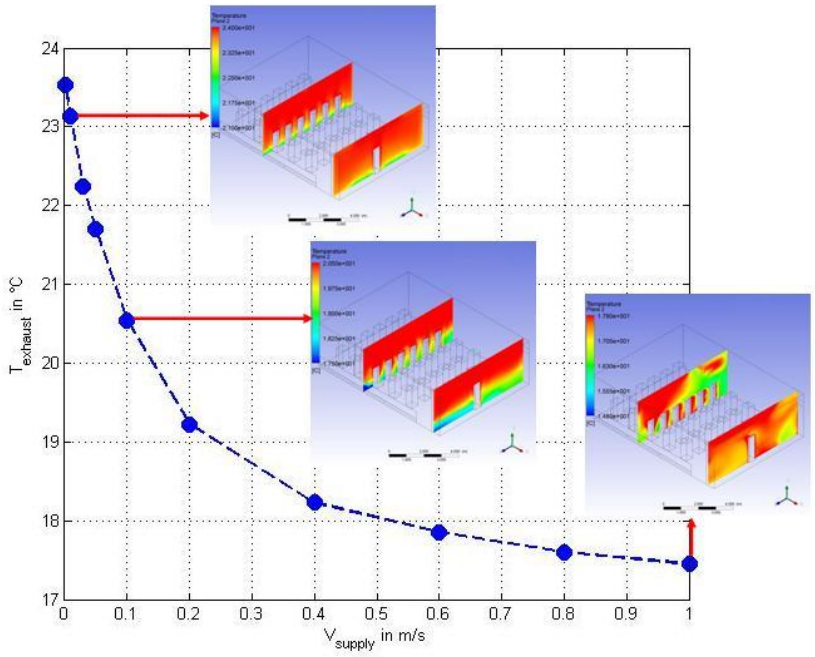

Figure 3.33: Variation of exhaust air temperatures with V_{supply}. They are as function of the fresh supplying air velocity with T_{supply} = 16 °C and initial classroom indoor air temperature of 20 °C.

With the same initial volume averaged CO_2 concentration 1803 ppm, the same level of the supplying air temperature (T_{supply} = 16 °C) is implemented, while the supplying fresh air velocities could be varied, from 0.05 m/s to 0.4 m/s, and other momentum and thermal boundary conditions implemented in the above steady thermal flow simulations are maintained. As illustrated in Fig. 3.34, almost exponentially decreasing function between the ventilation airflow supplying velocities and the classroom volume averaged CO_2 concentrations could be established.

Closely observing the species dispersion plots inserted in the frame of Fig. 3.34, with the rise of supplying air velocities, remarkable species stratifications shift upward from the lower region adjoining to the floor to the central region, which could improve indoor air quality. However, for V_{supply} = 0.3 m/s, the species distribution randomizes a little. The major reason is that the wind force dominates over the thermal buoyancy at this moment. It results in that there is non-remarkable species stratification inside the classroom. This coincides with the aforementioned studies of without thermal buoyancy case likewise.

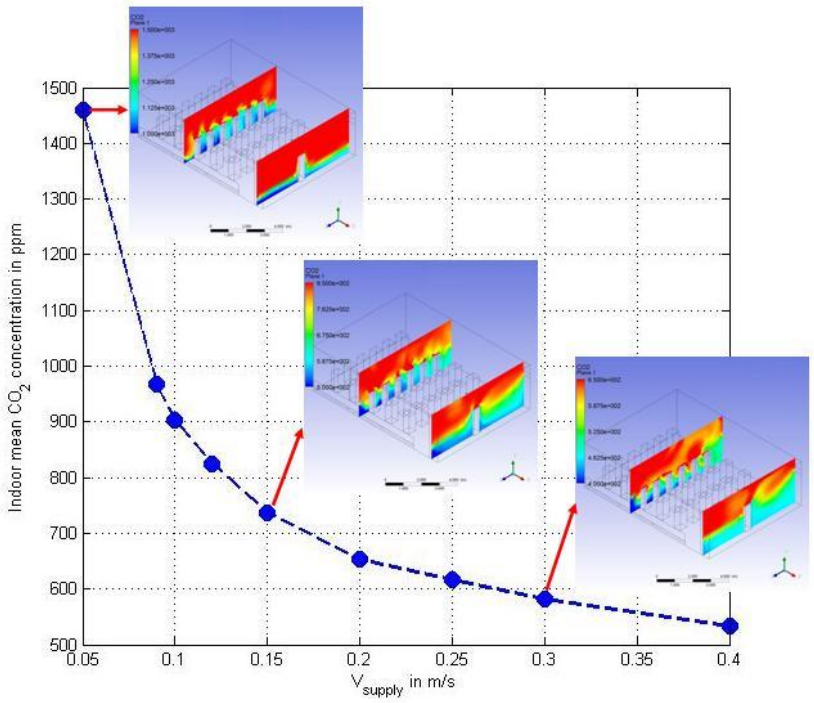

Figure 3.34: Variations of volume averaged CO_2 concentration with V_{supply}. Variations of averaged CO_2 concentration are as function of fresh supplying air velocity with T_{supply} = 16 °C and the initial classroom indoor air temperature of 20 °C as well as initial indoor CO_2 concentration of 1803 ppm.

In order to evaluate the effect of the supplying air velocity on the effectiveness of the displacement natural ventilation, the parameters of the ventilation effectiveness ratio for heat distribution (ε_t) and the ventilation effectiveness ratio for contaminant removal (ε_C) also are investigated as shown in Fig. 3.35.

As represented in Fig. 3.35(a), nearly exponentially increasing functions between the supplying air velocities and the ventilation effectiveness ratio for heat distribution and could be determined. This also explains why it could increase the values of *PD* a little with the promotion of supplying air velocities as the aforesaid investigations. Observing from Fig. 3.35(b), however, the ventilation effectiveness ratios for contaminant removal are the complex functions of the supplying air velocities, which tends to achieve the peak value at V_{supply} = 0.1 m/s.

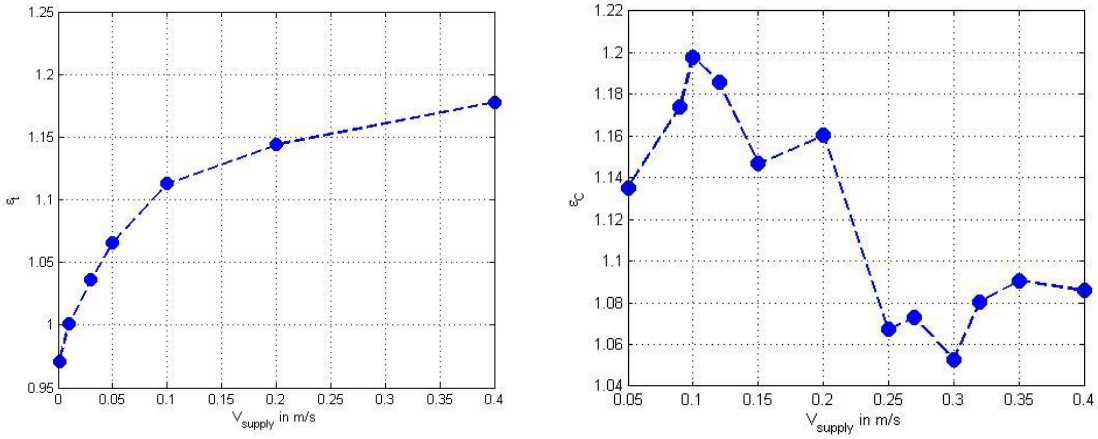

(a) Ventilation effectiveness for heat distribution (b) Ventilation effectiveness for pollutant removal

Figure 3.35: Variations of ventilation effectiveness ratio with V_{supply}. All those are for heat distribution (a) and ventilation effectiveness ratio for contaminant removal (b) as functions of the fresh supplying air velocity.

3.4.2.4 Effect of ventilation rate on heat distribution and energy analysis

Based on the aforementioned preliminary analysis in Section 3.4.1, the ventilation effectiveness ratio for heat distribution could put the effect on the heat loss (q_{heat}) due to the natural ventilation. Table 3.3 shows the results with invariable natural ventilation rate N_{supply} = 3.7 1/h, including the ventilation effectiveness ratio for heat distribution and the heat loss due to the natural ventilation. One can easily observe that if the ventilation effectiveness ratio for heat distribution is increased from 1.075 to 1.121, q_{heat} could be reduced by approximately 73.5% ((2152.97 W - 570.06 W)/2152.97 W = 0.735). For the case of invariable supplying air temperature T_{supply} = 16 °C, as illustrated in Table 3.4, q_{heat} could increase by about 90.6% ((2409.98 W – 226.97 W)/2409.98 W = 0.906), comparing the ventilation effectiveness ratio for heat distribution 1.178 with 1.001.

Table 3.3: Ventilation Effectiveness Ratio and Heat Loss (N_{supply} constant). Heat loss is due to the natural ventilation with the natural ventilation rate as a constant 3.7 1/h.

Ventilation Effectiveness Ratio	1.075	1.083	1.099	1.110	1.121
Heat Loss (W)	2152.97	1813.58	1177.24	864.37	570.06

Table 3.4: Ventilation Effectiveness Ratio and Heat Loss (T_{supply} constant). Heat loss is due to the natural ventilation with the supplying air temperature as a constant 16 °C.

Ventilation Effectiveness Ratio	1.001	1.036	1.066	1.113	1.178
Heat Loss (W)	226.97	576.67	852.74	1300.62	2409.98

Multiple situations of heat loss due to the natural ventilation have been correlated in terms of the ventilation effectiveness ratio for heat distribution, shown in Fig. 3.36,

$$\ln(q_{heat}) = -25.52\,\varepsilon_t + 35.04 \quad (\text{constant } N_{supply} = 3.7\ 1/h) \tag{3.23}$$

and

$$\ln(q_{heat}) = 13.06\,\varepsilon_t - 7.446 \quad (\text{constant } T_{supply} = 16\ °C) \tag{3.24}$$

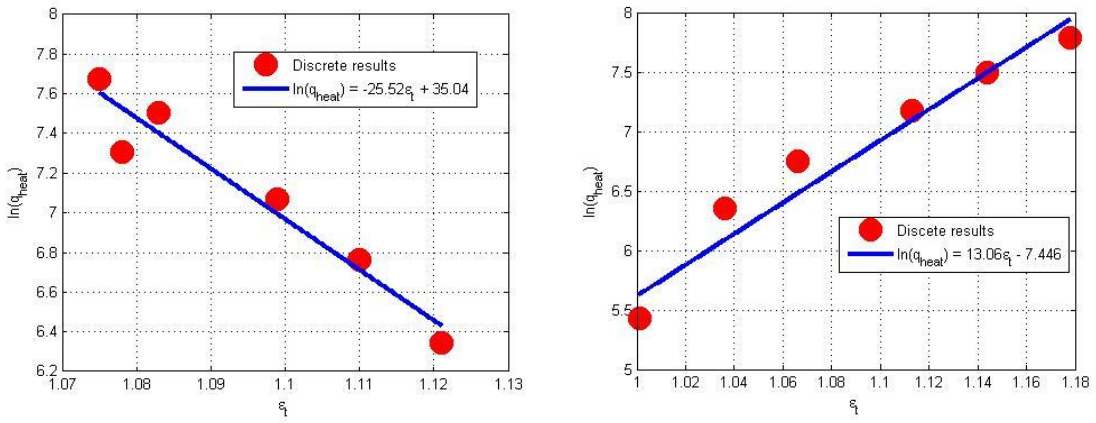

(a) Natural ventilation rate is a constant (b) Supplying air temperature is a constant

Figure 3.36: Correlations of the heat loss and ventilation ratio. Heat loss due to the natural ventilation is as functions of the ventilation effectiveness ratio for heat distribution with the natural ventilation rate as a constant 3.7 1/h (a) and with the supplying air temperature as a constant 16 °C (b), with the initial classroom indoor air temperature of 20 °C.

As expected, energy conservation of the natural ventilation could be enhanced with the ventilation effectiveness for heat distribution if natural ventilation rate maintains constant, and the shrinking ventilation effectiveness for heat distribution when the supplying air temperature keeps invariable. That is to say, the heat loss due to natural ventilation could become smaller when the temperature difference between the supplying air and indoor mean temperature decreases, and with a constant natural ventilation rate. On the other hand, the heat loss due to natural ventilation could become larger when the supply air velocity increases and the supply air temperature maintains invariable.

3.4.2.5 Summary and conclusions

In transitional seasons, classroom displacement natural ventilation is put into operation when indoor temperature is close to ambient temperature, which aims to reduce the building heat transfer losses and enhance the building energy efficiency. Classroom thermal comfort and indoor air quality in the new-built low energy school building have been numerically and experimentally investigated in the present work, together with the analysis of heat loss and ventilation effectiveness.

(1) The thermal buoyancy has a strong effect on the spatial distribution of the classroom air temperatures and gaseous contaminants. Thermal plume not only affects the air flow pattern, but also tends to enhance thermal stratification and decrease indoor pollutant concentration. In addition, the thermal buoyancy heavily influences the thermal comfort of occupants. Uniform isotherms due to the thermal buoyancy present in the upper regions, where favourably produces the thermal buffers to reduce the heat transfer rates between the surroundings of ceilings and building ceilings.

(2) Airflow patterns and heat transfer structures as well as contaminant concentrations in the classroom are heavily affected by the supplying fresh air temperatures and ventilation flow velocities. Classroom volume averaged temperature linearly increases with the supply air temperature, while the local thermal gradients are the decreasing functions of the supply air temperatures. The increasing temperature of supplying fresh air not only linearly promotes the exhaust air temperature, but also pushes thermal stratifications shifting downward from central area to the floor level, and almost exponentially decreases the classroom volume averaged CO_2 concentrations. On the other hand, classroom volume averaged temperature exponentially decays with the supply air velocity, while the local thermal gradients are the complex functions of the supply air velocities. The increasing velocity of supply fresh air not only exponentially reduces the exhaust air temperature, but also pushes thermal stratifications shifting upward from the floor level to central area until the wind force dominates over the thermal buoyancy, and exponentially decreases the classroom volume averaged CO_2 concentrations.

(3) Almost exponentially increasing functions between the supply air temperatures or velocities and the ventilation effectiveness ratios for heat distribution and contaminant removal could be set up, while the ventilation effectiveness ratios for contaminant removal are the complex functions of the supply air velocities.

(4) Heat loss due to the natural ventilation has been correlated in terms of the ventilation effectiveness ratio for heat distribution, which shows that energy conservation of the natural

ventilation could be enhanced with the ventilation effectiveness ratio for heat distribution if natural ventilation rate maintains constant, and the shrinking ventilation effectiveness ratio for heat distribution when the supply air temperature keeps invariant: e.g. when the ventilation effectiveness ratio for heat distribution is increased from 1.075 to 1.121 with invariable natural ventilation rate, q_{heat} must be decreased by approximately 73.5% (Table 3.3). For the case of invariable supply air temperature, q_{heat} can be larger by about 90.6%, compared the ventilation effectiveness ratio for heat distribution 1.178 with 1.001 (Table 3.4).

In the transitional seasons, natural ventilation could replace mechanical ventilation, and it could also provide high thermal comfort in the aforementioned classroom if outdoor temperature maintains approximately between 16 °C and 20 °C and outdoor air velocity is lower than 0.1 m/s.

4 HVAC system energy analysis, evaluation and optimization

4.1 Introduction

In this chapter, the physical model of the investigated reference classroom 2.28, which is the same as chapter 3, has been introduced. A set of representative on-site measurement data has been then implemented to favourably validate present Building Energy Simulation (BES) methodology and numerical codes. Following that, BES simulation parameters and conditions including building location, weather data, ventilation, heating and cooling, heat recovery facility, internal gains, occupancy, sun-shading system and school time schedule etc. have been presented. Subsequently, energy performance for a single reference classroom from six different design points of view based on practical operational situations in the school building has been investigated. Energy demands such as heating/cooling demands of the single test classroom have been analysed and evaluated concerning the effects of different indoor set-point temperatures in winter/summer, pre-ventilation in winter, the air exchange rates of night ventilation in summer, sun-shading system and the efficiency of the heat recovery facility etc. Human thermal comfort has been also investigated according to all those of six different design points. In particular, the evaluation of the thermal comfort zone has been experimentally presented and analysed based on measurement data. Finally, energy performance for the whole building, which is separated into 35 different zones, has been investigated based on three building scenarios.

4.2 Mathematical modelling and numerical program

The energy performance of reference classrooms and the entire building, including energy balance, energy consumption/demand and escaping heat etc., could be simulated using the technique of Building Energy Simulation (BES). Detailed numerical methods will be introduced, before the numerical procedure and code could be validated against a set of experimental data.

4.2.1 Numerical methods and modelling

The Building Energy Simulation (BES) software package TRNSYS/TRNBuild is used to simulate energy demand, coupled multi-zone building thermal performance, occupant behaviour, control strategies of HVAC systems and alternative energy systems (wind, solar, photovoltaic, and hydrogen systems) etc., which is a transient system simulation program with a modular structure based on the network model (TRNSYS 2006). It can predict the important parameters of building energy consumption and thermal environment e.g. air temperature, enclosure surface temperature, energy demand etc. (Gowreesunker et al. 2013, Leenknegt et al. 2013, Terziotti et al. 2012). The software has a primary visual interface, i.e., TRNSYS Simulation Studio and a modular structure, such that complicated systems could be separated into some smaller components (types) and newly created or defined components by users, which could be simply integrated (TRNSYS 2006, Ampatzi et al. 2012). Type 56 is a non-geometrical and energy balance model, which employs one air node per zone to denote thermal capacitances of air-volume, furniture and internal other objects (TRNSYS 2006, Ampatzi et al. 2012). The fundamental assumption of energy balance model is that air in each thermal zone can be modelled as well stirred with uniform temperature throughout (Crawley et al. 2001). TRNBuild is both the visual interface of the multi-zone building modelling (Type 56) and a pre-processor of an important file, which can deal with the input and output data requested for its description (Seem 1987, Ampatzi et al. 2012). In TRNBuild, the multi-zone building is separated into zones, and each of the zones is composed of enclosure surfaces. Each surface is not defined by horizontal or vertical coordinates but represented as internal, external, adjacent or boundary category and could be assigned an orientation, area, materials, and etc. (TRNSYS 2006, Ampatzi et al. 2012).

The thermal model described by the set of mathematical equations, including convective heat flux to the air node, radiative heat flows related to the walls and windows, and the heat conduction at wall surface equations, which can be found in the recent publications (Terziotti et al. 2012, Ampatzi et al. 2012, Firlag et al. 2013, Gowreesunker et al. 2013, Leenknegt et al. 2013) and may be respectively expressed as,

$$\dot{Q}_i = \dot{Q}_{surf,i} + \dot{Q}_{\inf,i} + \dot{Q}_{vent,i} + \dot{Q}_{g,c,i} + \dot{Q}_{cp\lg,i} \tag{4.1}$$

where $\dot{Q}_i$ is the total convective heat flux to the air node *i* (kJ/h); $\dot{Q}_{surf,i} = U_{w,i} A_{w,i} (T_{wall,i} - T_{air})$, i.e., convective heat flow from all inside surfaces (kJ/h); $\dot{Q}_{\inf,i} = \dot{V} \rho c_p (T_{outside} - T_{air})$, i.e., infiltration losses (air flow only from outside) (kJ/h);

$\dot{Q}_{vent,i} = \dot{V}\rho c_p(T_{vent} - T_{air})$, i.e., ventilation losses (air flow from a user-defined source, e.g. an HVAC system) (kJ/h); $\dot{Q}_{g,c,i}$ is the internal convective gains by people, equipment, illumination, and radiators etc. (kJ/h); $\dot{Q}_{cp\lg,i} = \dot{V}\rho c_p(T_{zone,i} - T_{air})$, i.e., the gains due to air flow from zone *i* or boundary condition (kJ/h).

$$\dot{Q}_{r,w_i} = \dot{Q}_{g,r,i,w_i} + \dot{Q}_{sol,w_i} + \dot{Q}_{long,w_i} + \dot{Q}_{wall-gain} \tag{4.2}$$

where $\dot{Q}_{r,w_i}$ is the radiative gains for the wall surface temperature node *i* (kJ/h), $\dot{Q}_{g,r,i,w_i}$ is the radiative zone internal gains received by wall (kJ/h), $\dot{Q}_{sol,w_i}$ is the solar gains through zone windows receives by walls (kJ/h), $\dot{Q}_{long,w_i}$ is the long wave radiation exchange between this wall and all other walls and windows (kJ/h), and $\dot{Q}_{wall-gain}$ is the user-specified heat flow to the wall or window surface (kJ/h).

$$\dot{q}_{s,i} = \sum_{k=0}^{n_{b_s}} b_s^k T_{s,o}^k - \sum_{k=0}^{n_{c_s}} c_s^k T_{s,i}^k - \sum_{k=1}^{n_{d_s}} d_s^k \dot{q}_{s,i}^k \tag{4.3}$$

$$\dot{q}_{s,o} = \sum_{k=0}^{n_{a_s}} a_s^k T_{s,o}^k - \sum_{k=0}^{n_{b_s}} b_s^k T_{s,i}^k - \sum_{k=1}^{n_{d_s}} d_s^k \dot{q}_{s,o}^k \tag{4.4}$$

where $\dot{q}_{s,i}$ is the conduction heat flux from the wall at the inside surface (kJ/h), $\dot{q}_{s,o}$ is the conduction heat flux into the wall at the outside surface (kJ/h), $T_{s,i}$ is inside surface temperature (K), $T_{s,o}$ is outside surface temperature (K), the coefficients of the time series a_s, b_s, c_s, and d_s are determined within the TRNSYS program using the z-transfer function routines of references (Mitalas et al. 1971, TRNSYS 2006). These time series equations in terms of surface temperatures and heat fluxes are evaluated at equal time intervals. The superscript *k* refers to the term in the time series. The current time is *k* = 0, the previous time is for *k* =1, etc. The time-base on which these calculations are based is specified by the user within the TRNSYS description (TRNSYS 2006).

4.2.2 Validation of BES simulations against with on-site measurements

It is necessary to validate the BES program before it has been extensively adopted as a tool of the study, although the current numerical program has been successfully applied in

lots of the recent publications (Firlag et al. 2013, Gowreesunker et al. 2013, Leenknegt et al. 2013). The validation was done by comparing the TRNSYS results with experimental data by the on-site measurements.

4.2.2.1 Boundary conditions for validation

The weather data employed Medview2 Software/Database of ZAE Bayern for monitoring the school building from June 9th to June 11th (3840 h…3896 h), 2012 including the outdoor temperature, outdoor relative humidity and global horizontal solar radiation etc. The reference classroom 2.28 capacitance was set by 2301.4 kJ/K based on the empirical value for the room with lots of furniture (TRNSYS 2006). The infiltration rate is 0.01 1/h, which has been measured and known by blower door tests. The air change rate of night natural ventilation in primary rooms is 1.30 1/h, which has been determined based on measurements. The heating, cooling and mechanical ventilation are not employed, meanwhile, there is no internal gains in classroom due to night ventilation in summer. The air flow temperature of night ventilation is outdoor air temperature. The classroom initial indoor air temperature is 25.35 °C based on the record of the Medview2 database. The simulation time step is 1 minute, which is the same as the time step of the weather data from the database.

4.2.2.2 Comparison between BES simulation and measurement results

In Fig. 4.1 it can be seen that the measurement and BES simulation results – shown for the night ventilation case – are very close. Both of the results are in very good agree with each other. The maximal discrepancy between BES values and measurement data is just within 0.5 °C, which can guarantee the reliability of the subsequent BES numerical investigations. The mainly reasons resulting in the difference between BES simulation and measurement results are as follows: 1) the measurement error of temperature sensor inside the room, and the concrete installing position influence of temperature sensor inside the classroom, which is not like air node in TRNSYS that can stand for uniform temperature throughout. 2) The accuracy of night ventilation rate measurement and calculation under actual operative condition. 3) The setting/calculation of indoor air and furniture capacitance values.

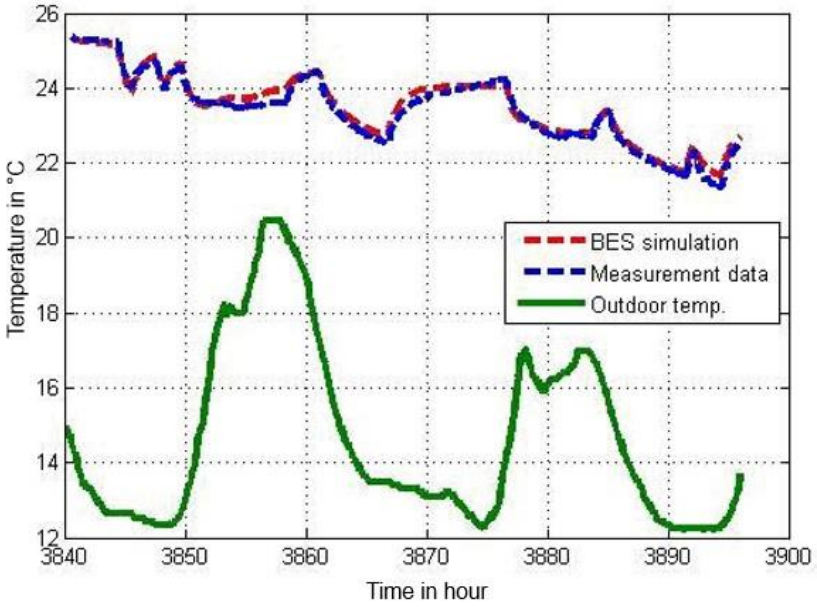

Figure 4.1: Indoor air temperature comparisons between BES and measurements. It demonstrates indoor air temperatures of BES simulation results (red broken line) and measurement data (blue broken line) in the classroom 2.28 under night ventilation with 1.30 1/h as well as measured outdoor temperature (green line) (horizontal coordinate represents the time of June 9th to June 11th (3840 h…3896 h), 2012).

4.2.3 Simulation parameters and conditions

4.2.3.1 Location

The new school building with Passive House standard of the FOS/BOS Erding situates in the region of Munich (Lat.: 48°18'40", Long.: 11° 53' 49", Southern Germany, see Fig. A.1 location plan in Appendix A). The building rotation is -15° to west.

4.2.3.2 Weather data

As aforementioned earlier, the weather data from the Medview2-Database base on measurements from the local weather stations on the roof of this school building used for calibration/validation. In addition, TRNSYS also supplied corresponding city's weather data in Meteonorm in TMY2 (Typical Meteorological Year) format (TRNSYS, 2006) utilized for simulations of a standard year. In this study, the weather data of Munich airport from Meteonorm in TMY2 format was as the preference due to the position where is the nearest away from the school building.

4.2.3.3 Regular day ventilation

As mentioned Section 3.2.3.1 said already, fresh air rate from the diffusers in each primary classroom, which is supplied by the mechanical ventilation unit, usually meets the minimal average air volume requirement of each occupant 20 m^3/h in German school buildings. Besides that, the ventilation rate is maintained 0 m^3/h when the room is not occupied in the daytime e.g. breaks between the courses etc. Furthermore, pre-ventilation has been put into operation for one hour before the class in the winter morning during the optimization process of the school building. In summer, night ventilation could actually replace the function of pre-ventilation.

4.2.3.4 Night ventilation for passive cooling

The night ventilation rate for primary rooms in summer is usually maintained at 1.30 1/h as mentioned earlier in Section 4.2.2.1 based on the volume of whole building and the capacity of the ventilators in atrium roof, and night ventilation can employ the cold night outdoor air to cool down the massive construction of a building and store the cooling energy within the concrete ceiling etc. inside the primary rooms. Following that, the cooled fabric can then reduce the indoor temperature and improve thermal comfort by reducing both the indoor air and wall temperature rises in the daytime of the following day (Blondeau et al. 1997). Besides, in fact, the concrete operation time schedule of night ventilation depends on the actual climatic and weather situation, especially on outdoor temperature in the daytime and at night. The night ventilation in the school building is usually running from May to September.

4.2.3.5 Heating and cooling

Normally, the set-point temperature of air cooling for mechanical ventilation system in summer is from 19 °C to 21 °C after the optimization for the control system (Wang et al. 2014), and the set-point temperature of air heating for mechanical ventilation system in winter is 19 °C. In addition, the set-point temperature of wall heating (if needed) is 21.5 °C in the daytime in winter. In order to determine the total active cooling demand in the classroom/building, 26 °C is usually set in the simulation as the set-point temperature of active cooling, although night ventilation instead of active cooling as the cooling method in summer in real operating situation of the school building. Furthermore, as mentioned earlier, the preheating/pre-cooling system can provide the aforementioned set-points entering the room

for the air heating/cooling (day ventilation) after the heat/cooling recovery unit. The air supply heating and wall heating are supplied by the return of a geothermal district heating. The air supply cooling is provided by the groundwater cooling system.

4.2.3.6 Heat/cooling recovery facility

As mentioned in chapter 2, a rotary heat exchanger (AL-KO Therm GMBH) has been employed in the mechanical ventilation system. Through the rough calculations of the data from the monitoring database during more than 3 years, the average heat recovery rate in winter has been normally maintained at 0.8 for simulations. In fact, the real measured average value is 0.76. However, the operation of the cooling recovery is much less than the heat recovery due to the local weather conditions in summer. Since there are only a few days with high outdoor temperatures of larger than 30 °C (Jacob et al. 2008), and the temperature difference between inside and outside in the daytime locally is not very large etc.

4.2.3.7 Internal gains and occupancy

Usually, internal gains mainly include the gains from the occupancy, which is the important part for the school, the gains from artificial lighting and electrical appliances e.g. computer and printer etc. Based on EN ISO 7730 (ISO EN 7730 2005), a seated student can produce about 60 W sensible heat gains, which will be employed in the following simulation investigation part.

Normally, for a regular classroom there are 32 students and one teacher at maximal level, however, on average there are 26 students and one teacher. The office includes one or two teachers or staff usually. For the following simulation part, 750 occupants (750 x 60 W = 45000 W) on average in the morning within the complete school building have been modelled as occupant load.

4.2.3.8 Sun-shading system

This passive school building is equipped with exterior shading systems, which are implemented in all facades with external venetian blinds and on the atrium roof with awnings. The suggested on/off control strategy by the TRNSYS manual for the shading system introduces empirical values (TRNSYS 2006), which includes that the shading system is activated when the incident radiation for horizontal orientation is higher or equal to 300 W/m^2; on the contrary, the shading system is deactivated when the indoor incident radiation for horizontal orientation is lower or equal to 100 W/m^2. In addition, the shading factor is set by 0.7.

4.2.3.9 Artificial lighting

The control strategy of on/off lighting is based on empirical suggested values (TRNSYS 2006). The artificial lighting is on when the indoor incident radiation for horizontal orientation is lower or equal to 120 W/m^2 when occupied; however, the artificial lighting is off when the indoor incident radiation for horizontal orientation is higher or equal to 200 W/m^2.

4.2.3.10 School time schedule

The time schedule of class in the school is fixed for each semester. The occupied time of classrooms is from 8 am to 9.5 am, 9.75 am to 11.25 am, 11.5 am to 1 pm in the morning and 1.75 pm to 4 pm in the afternoon from Monday to Friday. The aforementioned time interval between each other is the unoccupied time for the classroom e.g. breaks and lunch time etc. In addition, it takes into account national celebrations, vacations and weekends.

4.2.3.11 Single zone model for reference classrooms

The single reference classroom 2.28 is employed as the research platform for the following simulation investigation. All detailed simulation parameters are shown in Appendix B.1. The main parameters include that the heat capacitance of the room is 2301.4 kJ/K, and the net volume is 239.73 m^3. Six different design points are selected for the different simulation cases, which will be presented in the following.

4.2.3.12 Multi-zone separation for the complete building model

The building including southern and northern buildings as well as the atrium (see Fig. A.1 location plan in Appendix A) was separated into 35 zones (including 3 air zones, which are situated under the basement floor), which have been shown in Appendix A: Fig. A.2 to A.5 (3 air zones have not been shown there or see Fig. 2.8), based on the experiences of dividing multi-zones in buildings and their similar characteristics of rooms, e.g., the usage of rooms (separated by classrooms, offices and atrium) and different mechanical ventilation rates (separated by primary rooms, secondary rooms and atrium), as well as relative references. (TRNSYS 2006, McDowell 2003). The main simulation parameters and conditions of all 35 zones, as mentioned earlier, are illuminated in Table 4.1. Note that “morning” in Table 4.1 means occupancy time or ventilation time, whose value is just 0 or 1, e.g. for occupancy 43+125*morning, it means that there are 168 occupants for zone 2 in the morning; 43 occupants in the afternoon. The total net volume for 35 zones is 26865.7 m^3. For occupant heat loads, it is 45000 W (750 occupants: heat gain per occupant with 60 W on average) in the morning and 11280 W (188 occupants) in the afternoon. The kitchen and

café have been simulated as the passive thermal zones without occupants and without considering mechanical ventilation.

Table 4.1: Representative parameters of the multi-zone building model

Type	Net volume m^3	Occupancy [-]	Ventilation rate 1/h	Comments
Zone 1	8135.6	0	0.38+1.1*morning	atrium zone
Zone 2	2398.5	43+125*morning	0.33+1.08*morning	10 classrooms
Zone 3	912.5	3+8*morning	0	secondary rooms
Zone 4	720.1	0	1.8	toilets
Zone 5	480.6	8+23*morning	0.33+1.08*morning	2 classrooms
Zone 6	239.1	4+13*morning	0.33+1.08*morning	1 classroom
Zone 7	92.7	1+1*morning	0	secondary room
Zone 8	719.7	12+38*morning	0.33+1.08*morning	3 classrooms
Zone 9	92.7	1+1*morning	0	secondary room
Zone 10	960	17+49*morning	0.33+1.08*morning	4 classrooms
Zone 11	719.8	12+38*morning	0.33+1.08*morning	3 classrooms
Zone 12	101.2	1+1*morning	0	secondary room
Zone 13	357.3	3+12*morning	0.84	offices
Zone 14	722.1	7+15*morning	0.6	offices
Zone 15	202	1+3*morning	0	2 secondary rooms
Zone 16	90.1	0	0	2 secondary rooms
Zone 17	243	0	0	2 ventilation rooms
Zone 18	168.2	0	0	kitchen
Zone 19	150.5	0	0	cafe
Zone 20	96.3	0	0	copy room
Zone 21	1970.9	0	0.38+1.1*morning	atrium zone
Zone 22	1199.7	20+66*morning	0.33+1.08*morning	5 classrooms
Zone 23	466.8	0	0.43	technical room
Zone 24	478.3	12+38*morning	0.5+1.6*morning	IT classrooms
Zone 25	101.2	1+1*morning	0	secondary room
Zone 26	96.3	0	0	server room
Zone 27	1199.2	20+63*morning	0.33+1.08*morning	5 classrooms
Zone 28	268.4	1+1*morning	0	secondary rooms
Zone 29	140.4	1+1*morning	0.4	offices
Zone 30	478.8	8+26*morning	0.33+1.08*morning	2 classrooms
Zone 31	478.8	8+26*morning	0.33+1.08*morning	2 classrooms
Zone 32	239.7	4+13*morning	0.33+1.08*morning	Ref. classroom 2.28
Zone 33	1964.2	0	0	air zone
Zone 34	33.3	0	0	air zone
Zone 35	147.8	0	0	air zone

4.3 Results and discussion for the single classroom

4.3.1 Energy performance for the single reference classroom

In order to investigate and evaluate energy performance of the single reference classroom, it is very necessary to make a reference setting list for simulation parameters (see Appendix B.1: Reference List for single classroom). There are six design points as different simulation cases, shown in Table 4.2, which represent six practical operative situations in the school building i.e. peak loads, average loads and minimal loads for the south and north buildings respectively. For this study, it is applied the annual weather conditions of Munich airport in Meteonorm in TMY2 format supplied by TRNSYS (temporal resolution of data acquisition is 0.1 hours). The relative humidity of the indoor air is set to 50%.

Table 4.2: Design point settings for different simulation cases for single classroom

	Occupancy No.	**Building Direction**
Design Point 1	33	South
Design Point 2	27	South
Design Point 3	15	South
Design Point 1	33	North
Design Point 2	27	North
Design Point 3	15	North

Fig. 4.2 illuminates the annual energy balance (no considering the heating energy of heat recovery system) for the case of design point 1 in south building (simulation conditions: heating set-point 21.5 °C, air exchange rate of night ventilation: 1.3 1/h, day ventilation temperature in summer/winter: 19 °C, 70% shading). Since night ventilation instead of active cooling in summer is employed in this passive school building, the active cooling energy is thus zero, which can be clearly observed from Fig. 4.2. However, ventilation heat losses including night ventilation accounts for approximately 40.4% (2282 kWh/a of 5646.9 kWh/a for total energy losses), which can ensure favourable thermal comfort at the same time in summer. The average indoor air temperature when occupied in July is only 24.5 °C based on the simulation results (detailed thermal comfort analysis in Section 4.3.2), which lies in the range of the favourable thermal comfort (EN 15251 2007, ANSI/ASHRAE Standard 55 2004, 2010). The annual wall heating and pre-heating energy are very small, just 72.11 kWh/a and 39.39 kWh/a respectively, but, which can also afford rather favourable thermal comfort in winter. The average indoor classroom temperature when occupied in February is 22.7 °C according to the simulation results (detailed thermal comfort analysis in Section

4.3.2). Both of wall heating and pre-heating is called active heating. The part of heating energy generated by the heat recovery facility is not considered by the active heating. The heat recovery unit can heat the outdoor air temperature level for the input temperature level of the pre-heating unit. In addition, the solar gains and internal gains play a vital role in providing heat gains for the classroom especially in winter, which is also a most significant character for passive house i.e. the energy in buildings/rooms could be obtained through passive modes.

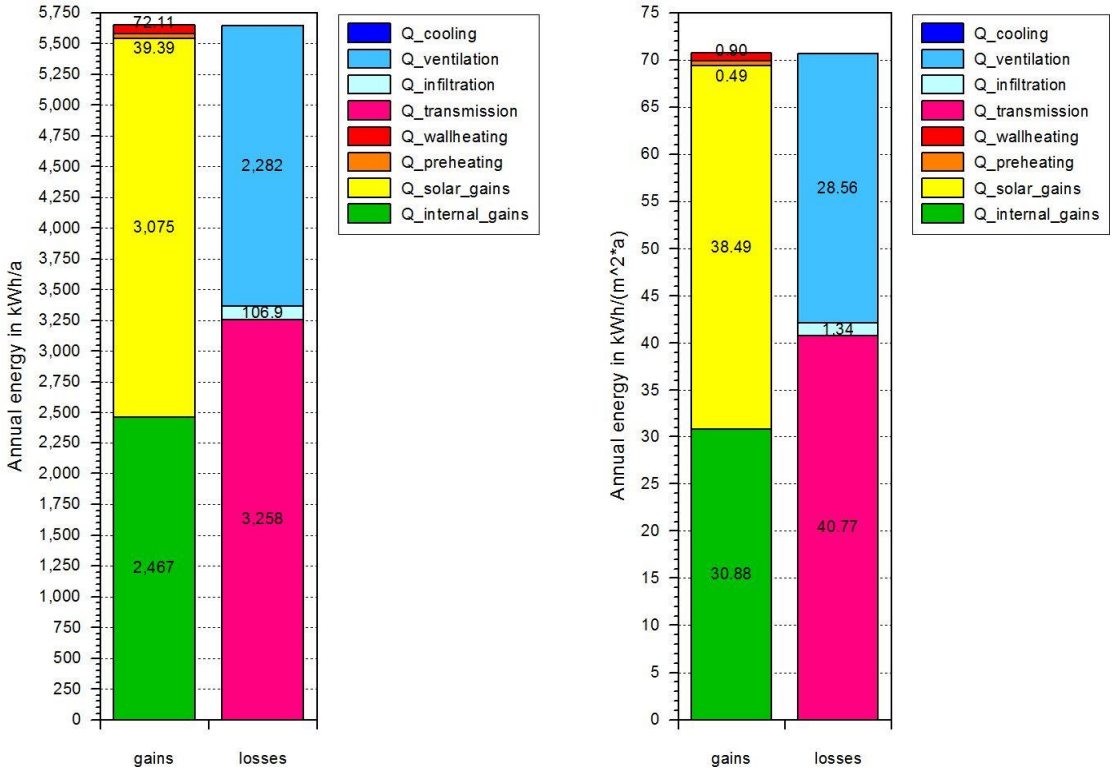

(a) Energy (b) Specific energy

Figure 4.2: Annual energy balance in the reference classroom. It includes comparison between energy gains (including wall heating, pre-heating, solar gains and internal gains) and losses (including cooling, ventilation with 19 °C inlet temperature, infiltration and transmission) for design point 1 in the south building. Heat transmission is the major heat losses. Cooling demand is zero due to night ventilation (night cooling instead of active cooling in summer).

Fig. 4.3 illustrates the annual energy balance (considering the heating energy supplied by heat recovery system with 80% heat recovery rate) for the same case of design point 1 in south building. Seen from Fig. 4.3., heat recovery facility undertakes most part of the work for heating the room, which accounts for extremely large percentage approximately 93.7% (1648 kWh/a of 1759.5 kWh/a) in the whole heating energy.

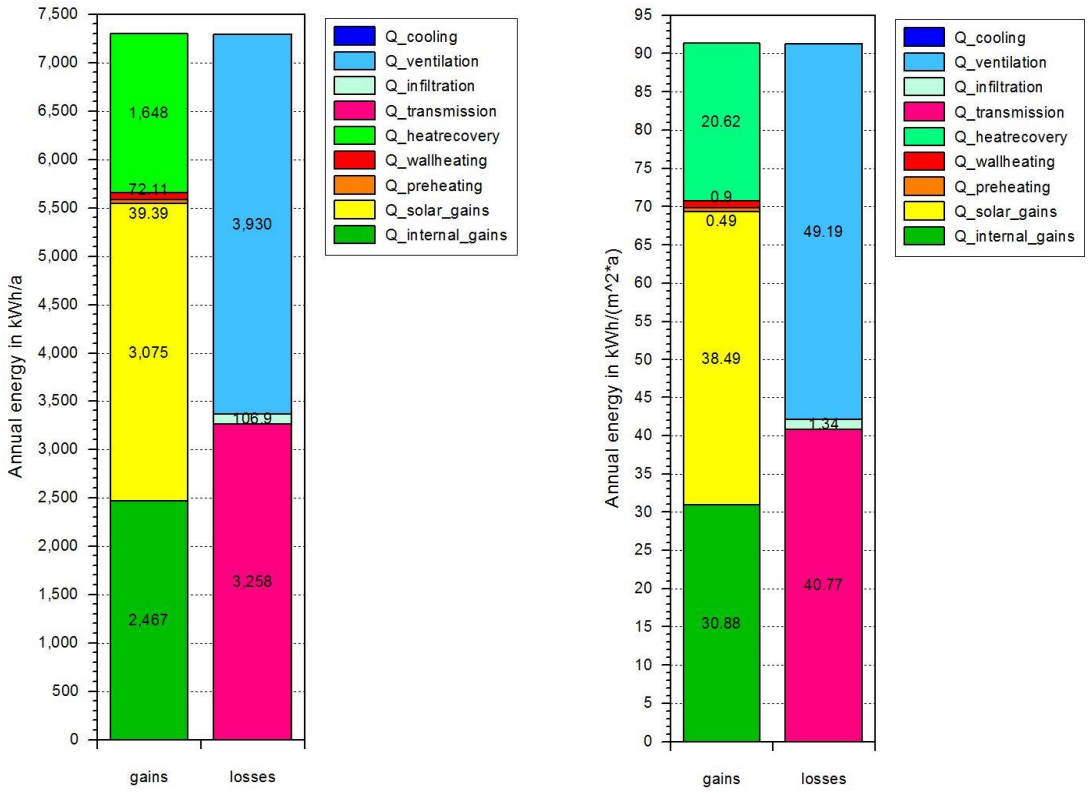

(a) Energy (b) Specific energy

Figure 4.3: Annual energy balance in reference room and heat recovery system. It shows the comparison between energy gains (including heat recovery heating, wall heating, pre-heating, solar gains and internal gains) and losses (including cooling, ventilation, infiltration and transmission) for design point 1 in the south building. The heat recovery facility undertakes most part of the energy for heating the room.

Heat recovery facility and pre-heating unit are put into use during winter time, on the contrary, cooling recovery and pre-cooling systems are put into operation for summer. It is therefore necessary to investigate the annual energy balance considering the classroom and cooling energy of cooling recovery and pre-cooling systems. Fig. 4.4 shows the annual energy balance (considering the cooling energy supplied by cooling recovery system) for the case of design point 2 in north building (simulation conditions: heating set-point 21.5 °C, active cooling set-point 26 °C, no night ventilation, day ventilation temperature: 19 °C, 70% shading). Since active cooling with set-point 26 °C instead of night ventilation in summer is set here for reasons of simulation investigation, the ventilation energy is thus decreasing a lot although different design points, which can be obviously observed from Fig. 4.4 compared to Fig. 4.2. However, in summer, it is not obvious that cooling recovery facility and pre-cooling unit undertake to cool the room compared with heat recovery facility in winter, which is rather similar to real operation situation in the school building. This is mainly because the cooling recovery operation is very occasional in relation to heat recovery in winter

due to the local weather condition in summer e.g. only a few days with high outdoor temperatures of larger than 30 °C (Jacob et al. 2008), and the temperature difference between inside and outside in the daytime locally is not very large. The active cooling with 26 °C set-point therefore accounts for more than half percentage of cooling energy approximately 56.7% (366.4 kWh/a/(280.3+366.4) kWh/a) to cool the thermal zone into 26 °C.

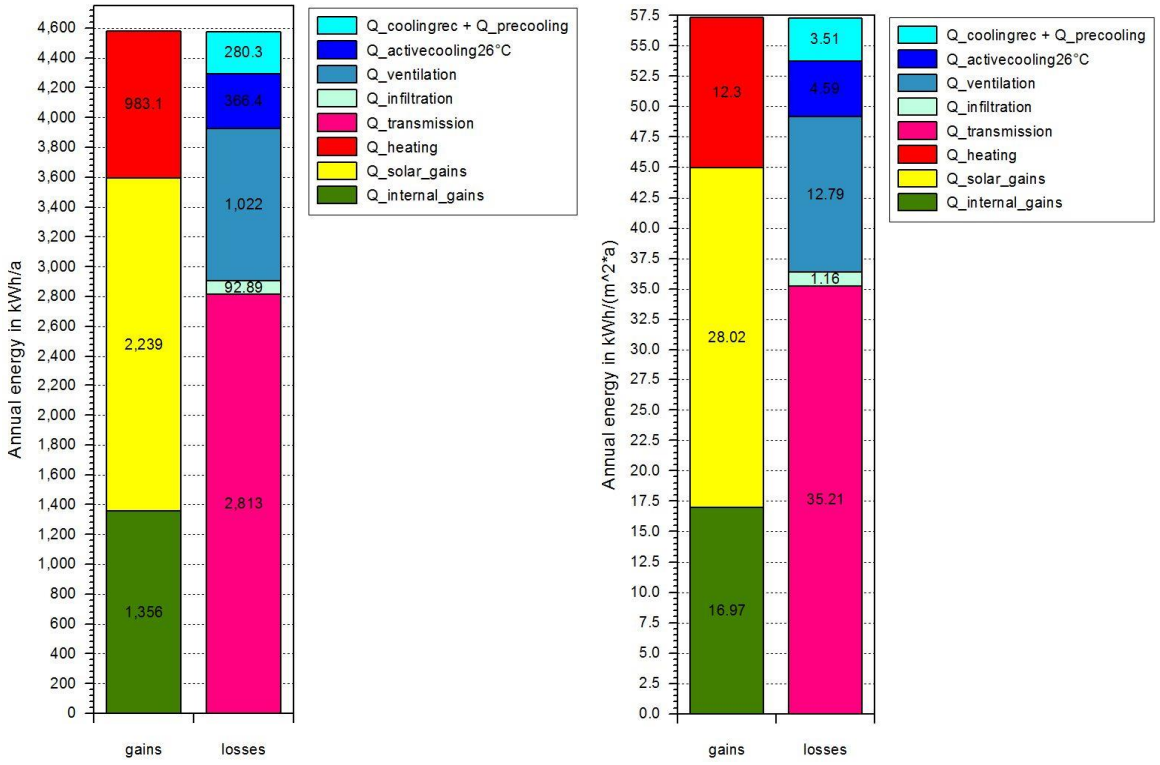

(a) Energy (b) Specific energy

Figure 4.4: Annual energy balance in classroom and cooling recovery system. It shows the comparison between energy gains (including heating, solar gains and internal gains) and losses (including cooling recovery plus pre-cooling, active cooling, ventilation, infiltration and transmission) for design point 2 in the north building. The cooling recovery facility and pre-cooling unit undertake only a part of the cooling demand. Active cooling instead of night cooling accounts for 56.7% of total cooling demand.

In fact, the different heating energy in winter including heat recovery ($Q_{\_heatrecovery}$), pre-heating ($Q_{\_preheating}$) and wall heating ($Q_{\_wallheating}$) have been also investigated separately for reasons of comparison. Fig. 4.5 shows the different heating demands for the six different simulation cases (simulation conditions: heating set-point 21.5 °C, air exchange rate of night ventilation: 1.3 1/h, day ventilation temperature in summer: 19 °C, heat recovery rate: 0.8, day ventilation temperature in winter = ambient temperature (calculating $Q_{\_heatrecovery}$) or min.

(19 °C, heat recovery temperature) (calculating $Q_{\_preheating}$) or 19 °C (calculating $Q_{\_wallheating}$), 70% shading).

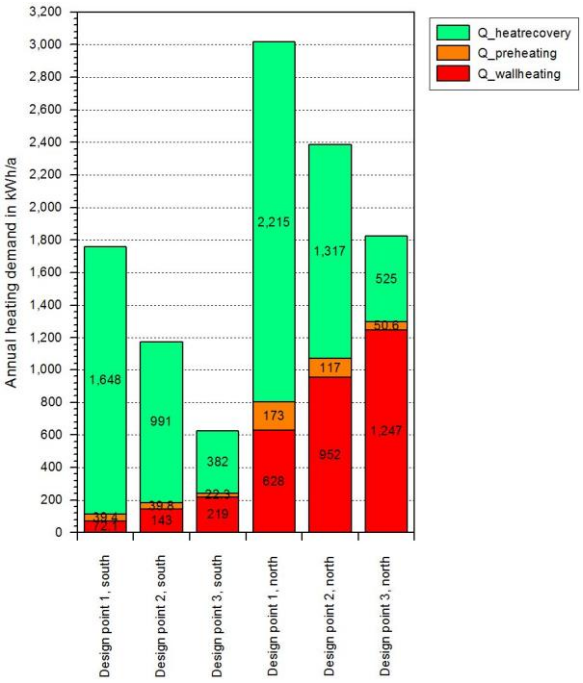

Figure 4.5: Annual heating demands for 6 design points. It includes heat recovery heating ($Q_{\_heatrecovery}$), pre-heating ($Q_{\_preheating}$) and wall heating ($Q_{\_wallheating}$) in the classroom for 6 design points. Total heating and heat recovery heating demands decrease with the decreasing of the occupancy number. However, the active heating demand increases with the decreasing number of occupants.

Observed from Fig. 4.5, $Q_{\_wallheating}$ and active heating demand ($Q_{\_wallheating}$ plus $Q_{\_preheating}$) obviously increase with the decreasing number of occupants from design point 1 (occupancy number: 33, the same as below) to 3 (15) due to the decreasing internal gains in winter, not only for the south building but also for the north building. For design point 2 and 3 of south building, active heating demands increase by 63.9% (71.3 kWh) and 116.4% (129.8 kWh) respectively compared to design point 1, to name just a few. On the contrary, $Q_{\_heatrecovery}$ apparently is reduced due to the decreasing number of occupants. The reasons are less air mass flows provided from the mechanical ventilation control system based on minimal average flow rate 20 m^3/h per occupant, and the outlet temperature of the classroom to the mechanical ventilation system. The efficiency of the heat recovery unit decreases with the number of occupants under the identical ambient temperature conditions, what causes a decrease of the heating energy supplied by the heat recovery. In addition, from the point of view of total supply heating demand, the sum of supply heating demands for design points indeed increases with the occupancy number from design point 3 (15) to 1 (33), not only for the south building but also for the north building. The reason is that the

less number of occupants correspond with less air mass flows from the mechanical ventilation.

Heating demand per unit floor area is another important index for investigating and evaluating energy performance. Fig. 4.6 illustrates the different heating demand per unit floor area (79.9 m^2) for six different simulation cases corresponding to Fig. 4.5. Closely scrutinizing the active heating demand ($Q_{\_wallheating}$ plus $Q_{\_preheating}$) of Fig. 4.6, nearly all of the active heating demands (except design point 3 of north building: 16.2 kWh/(m^2a); others: from 1.4 kWh/(m^2a) to 13.4 kWh/(m^2a)) are less than 15 kWh/(m^2a), even far less than it especially for the south building, which is Passive House standard of building energy requirements.

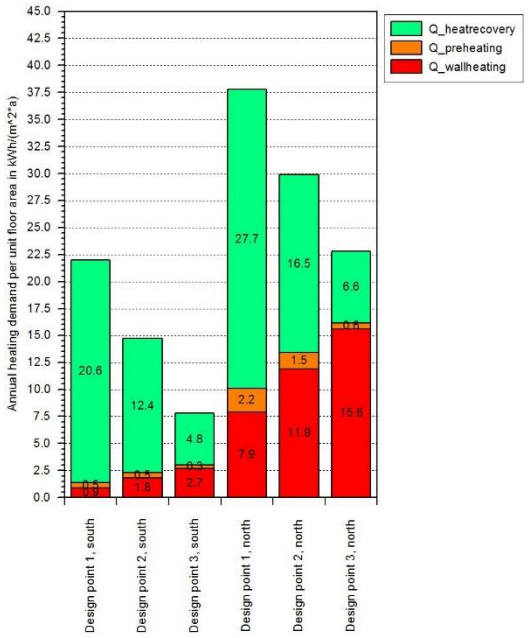

Figure 4.6: Annual heating demands per unit floor area for 6 design points. The floor area of the reference classroom is 79.9 m^2. Heating demands include heat recovery heating ($Q_{\_heatrecovery}$), preheating ($Q_{\_preheating}$) and wall heating ($Q_{\_wallheating}$) in the classroom for 6 design points. Annual specific active heating demand is expectedly low from 1.4 kWh/m^2h to 16.2 kWh/m^2a.

Meanwhile, the different cooling energy demand in summer including active cooling with 26 °C set-point and cooling recovery cooling ($Q_{\_coolingrec}$) plus pre-cooling ($Q_{\_precooling}$) have been also investigated separately for reasons of comparison. Observed from Fig. 4.7(a), cooling recovery cooling energy ($Q_{\_coolingrec}$) plus pre-cooling energy ($Q_{\_precooling}$) for the south and north buildings are rather similar to each other. It is due to the fact that cooling recovery operation in summer is not very often compared to the heat recovery operation in winter due to the local weather condition in summer. Therefore, the amount of cooling recovery

energy is very small in relation to main energy demand. The missing cooling energy is generated from air pre-cooling, whose energy is provided from the groundwater cooling system. As one kind of renewable energy, groundwater can reduce the school buildings energy costs and minimize the energy consumption. The detailed building cooling demand is described in chapter 4.4.

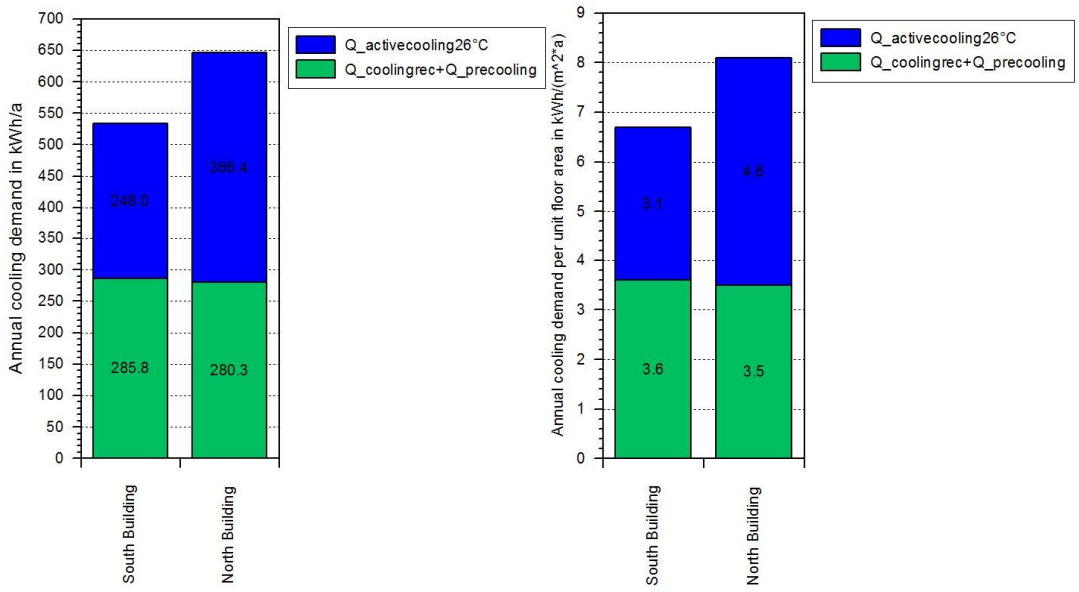

(a) Cooling demand (b) Specific cooling demand

Figure 4.7: Annual cooling demands and cooling demands per unit floor area. The floor area of the reference classroom is 79.9 m^2. Cooling demands include active cooling with 26 °C set-point and cooling recovery cooling energy ($Q_{\_coolingrec}$) plus pre-cooling ($Q_{\_precooling}$) in the classroom for design point 2 including south and north buildings. Annual specific cooling demand is expectedly low for both buildings.

However, the active cooling demand with 26 °C set-point in the south building is lower than the north building. The main reason includes using the sun-shading system during daytime on the south facade, particularly, the shading system on the north façade will be activated only around after 7 pm (solar radiation level is up to the maximal) in the north building for summer case. In addition, for annual active cooling demand per unit floor area (Fig. 4.7(b)), both of them i.e. south and north building are less than 5 kWh/(m^2a), even annual total space cooling demand (6.7 kWh/(m^2a): south, 8.1 kWh/(m^2a): north) is also very low.

4.3.1.1 Effect of indoor set-point temperature

Indoor set-point temperatures not only heavily influence human thermal comfort but also strongly affect the energy demand. Now, the aforementioned controlling parameters and

boundary conditions are maintained excluding the set-point indoor air temperatures, the average values of 23 °C…26 °C/19 °C…22 °C as the set-point temperatures in summer/winter were selected during class hours for reasons of comparison, without considering the effect of heat recovery facility and night ventilation. The aforementioned settings are in accordance with most suggestions for the thermally comfortably indoor air temperatures in summer/winter (ISO EN 7730 2005, ASHRAE 2009).

4.3.1.1.1 26 °C as indoor set-point temperature in summer

With the same indoor air set-point temperature 26 °C as T_{cool} in summer, different levels of indoor air set-point temperature as T_{heat} in winter were respectively implemented, from 19 °C to 22 °C. Observing from Fig 4.8, almost exponentially increasing functions between the set-point temperatures for heating and the wall heating demands could be set up, not only for the south building but also for the north building. For north building, compared with the combination (26/21.5) °C the wall heating demand must be decreased by 39.1% ((945.6 kWh/a – 575.8 kWh/a)/945.6 kWh/a) when using (26/19) °C and can be increased by 8.5% ((1026.1 kWh/a – 945.6 kWh/a)/945.6 kWh/a) with (26/22) °C per year, to name just a few. The above results also illuminate that the energy consumption heavily depends on indoor air set-point temperatures.

In addition, the wall heating demands in north building are far more than that in south building due to less solar gains in winter compared to south building. For example, for the combination (26/21.5) °C, the wall heating demand in north building must be increased by 85.3% ((945.6 kWh/a – 139.0 kWh/a)/945.6 kWh/a) compared to the south building. What is more, the wall heating demand in south building is almost zero, i.e. 9.7 kWh/a, all over the year for the combination (26/19) °C. The main reason is because the day ventilation temperature in each classroom is 19 °C in winter, which means this ventilation system can heat up the thermal zone, meanwhile there are 27 occupants inside the classroom as internal gains. In other words, day ventilation in winter is enough to assist heating the room up to 19 °C as the set-point value.

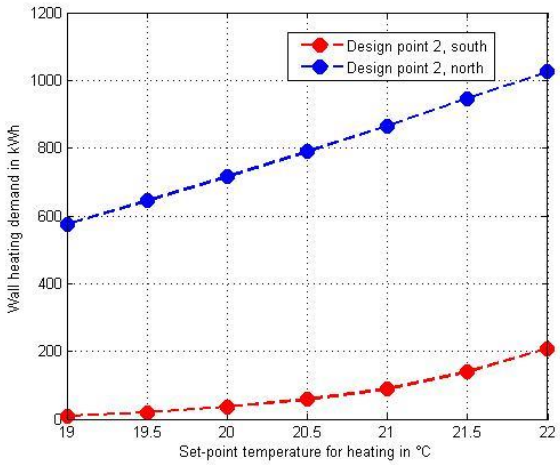

Figure 4.8: Annual wall heating demand of reference classroom. It is as functions of set-point temperatures T_{heat} for design point 2 in south (red line) and north (blue line) buildings. Wall heating demand in south building is far less than in north in winter.

4.3.1.1.2 21.5 °C as the indoor set-point temperature in winter

With the same indoor air set-point temperature 21.5 °C as T_{heat} in winter, different levels of indoor air set-point temperature as T_{cool} in summer were respectively implemented, from 23 °C to 26 °C. Seen from Fig. 4.9, almost exponentially decaying functions between the set-point temperatures for the cooling and active cooling demands could be set up, not only for the south building but also for the north building. Compared to the combination (25/21.5 °C) the active cooling demand in south building must be decreased by 31.8% ((363.6 kWh/a – 248.0 kWh/a)/363.6 kWh/a) when using (26/21.5 °C) and can be increased by 44.6% ((656.9 kWh/a – 363.6 kWh/a)/656.9 kWh/a) with (23/21.5 °C) per year.

Besides that, there is an interesting phenomenon as the active cooling demands in the north building are larger than that in the south building. The main reason includes sun-shading systems, which could be activated by the same control strategy (total solar radiation ≥ 300 W/m^2) for both buildings under different solar radiation levels in summer, in particular, the shading system will be activated just around 7 pm (solar radiation reaches > 300 W/m^2 on north façade) in the north building for summer case. In addition, the reason also includes the different heat transmission effects between inside and outside in two building directions.

Fig. 4.9 also illuminates that the set-point combination (26/21.5 °C) could be selected as an appropriate indoor air temperature set-point, which could not only meet the requirement of thermal human comfort (ISO EN 7730 2005, ASHRAE 2009), but also could guarantee energy conservation effect, i.e., it can save approximately 408.9 kWh/a (656.9 kWh/a –

248.0 kWh/a: south building) or 388 kWh/a (754.4 kWh/a – 366.4 kWh/a: north building) only for one single typical classroom compared to the combination 23/21.5 °C.

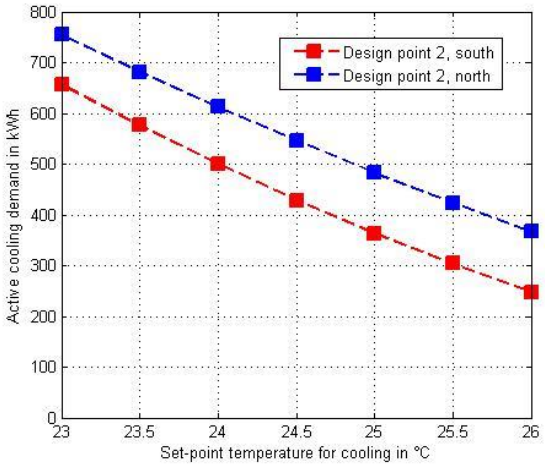

Figure 4.9: Annual active cooling demand of reference classroom. It is as functions of set-point temperatures T_{cool} for design point 2 in south (red line) and north (blue line) buildings. Active cooling demand in south building is less than in north in summer.

4.3.1.2 Effect of ventilation on energy demand

The ventilation system aims to create a comfortable thermal environment and to improve indoor air quality; however, ventilation is one of main sources of heating loss in buildings (Fouih et al. 2012), which will also enhance energy demands and consumption. In this study, effects of all kinds of ventilation types including regular day ventilation, pre-ventilation and night ventilation on energy demands were considered and investigated.

With regard to the regular day ventilation, all the aforementioned parts have already been investigated, which will be not repeated in this section.

4.3.1.2.1 Effect of pre-ventilation on heating demand

It is rather significant to implement the pre-ventilation in order to supply a healthy and comfortable indoor air environment before the classrooms and toilets in the school building are occupied every morning compared to regular day ventilation. Now, the aforementioned controlling parameters and boundary conditions are maintained excluding pre-ventilation with 19 °C from 6.5 am to 7.5 am in winter. However, in summer, there is the night ventilation before occupied, which can also ensure healthy and comfortable indoor air environment.

Observing from Fig. 4.10, $Q_{\_wallheating}$ and active heating demand ($Q_{\_wallheating}$ plus $Q_{\_preheating}$) for the case of with pre-ventilation obviously decreases a little compared to without pre-

ventilation due to the operation of pre-ventilation in winter, which can assist active heating to heat the classroom. This is caused by the operation of the heat recovery instead of wall heating during the period of pre-ventilation, not only for the south building but also for the north building. The active heating demand for with pre-ventilation in south and north building decreases 16.5% (30.2 kWh/a) and 6.1% (65 kWh/a), respectively, compared to no pre-ventilation, to name just a few.

On the contrary, $Q_{\_heatrecovery}$ apparently increases compared to the case of without pre-ventilation. It is mainly because the case of with pre-ventilation will partly enhance the operation of heat recovery facility, which can result in increasing $Q_{\_heatrecovery}$ a little. In addition, from the total supply heating demand point of view, the sum of supply heating demand for the case of with pre-ventilation indeed increases a little compared to the case of no pre-ventilation.

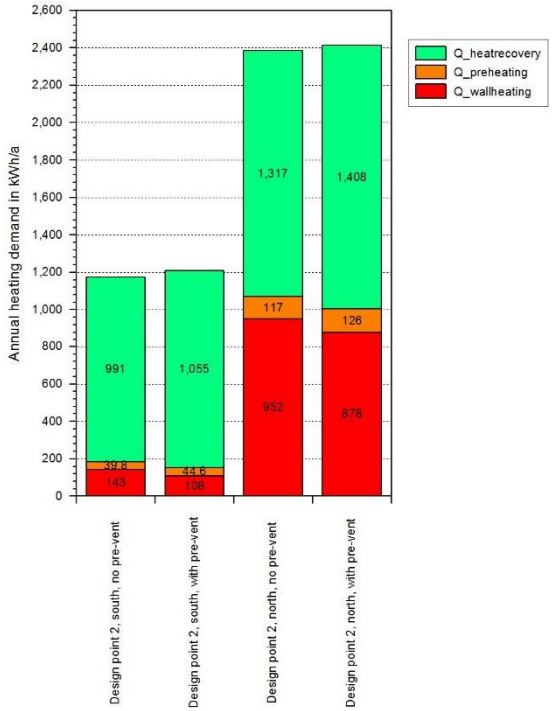

Figure 4.10: Annual heating demand with and no pre-ventilation. It includes heat recovery heating ($Q_{\_heatrecovery}$), pre-heating ($Q_{\_preheating}$) and wall heating ($Q_{\_wallheating}$) in the classroom with and without pre-ventilation for design point 2 including south and north buildings. Total heating and heat recovery demands increase a little, however, active heating demands decrease a little.

Fig. 4.11 illustrates the different heating demands per unit floor area (79.9 m^2) for the different simulation cases corresponding to Fig. 4.10. Closely scrutinizing the active heating demand ($Q_{\_wallheating}$ plus $Q_{\_preheating}$) of Fig. 4.11, the active heating demand ranges from 2 kWh/(m^2a) to 13.4 kWh/(m^2a) i.e. actually less than 15 kWh/(m^2a). Even far less than it especially for the south building, which is obviously fulfilling the Passive House standard of

building energy requirements for the school building, not only for the case of no pre-ventilation but also for the case of with pre-ventilation.

Fig. 4.12 shows the measurement data of CO_2 concentration for the reference classroom 2.28 under pre-ventilation from 6.5 am to 7.5 am on January 30th, 2013. It can be seen that indoor air quality indicated by the CO_2 concentration could be quickly improved i.e. indoor CO_2 concentration reduced from almost 1000 ppm to around 500 ppm, which is close to outside conditions (fresh air), after one hour pre-ventilation. Following that, it would provide a high level indoor air quality for the present students and teacher, who took the first class at 8 am.

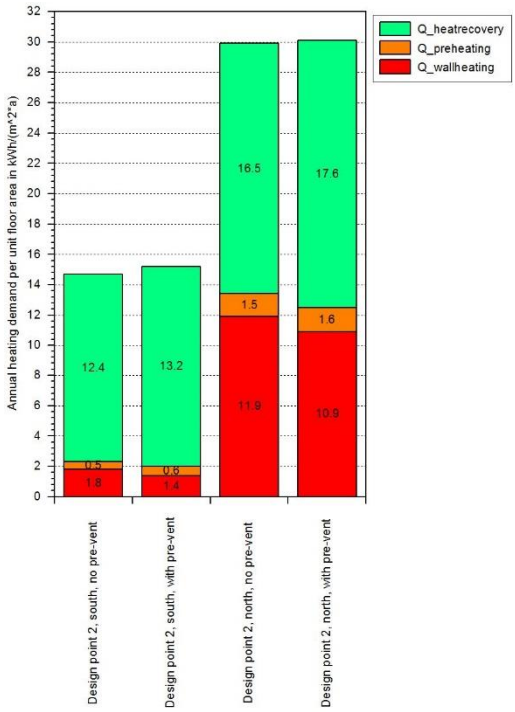

Figure 4.11: Annual heating demand per unit floor area with and no pre-ventilation. The floor area of the reference classroom is 79.9 m^2. Heating demand includes heat recovery heating ($Q_{\_heatrecovery}$), pre-heating ($Q_{\_preheating}$) and wall heating ($Q_{\_wallheating}$) in the classroom with and without pre-ventilation for design point 2 including south and north buildings. Annual specific active heating demands decrease 0.3 kWh/m^{2}a and 0.9 kWh/m^{2}a for south and north buildings respectively.

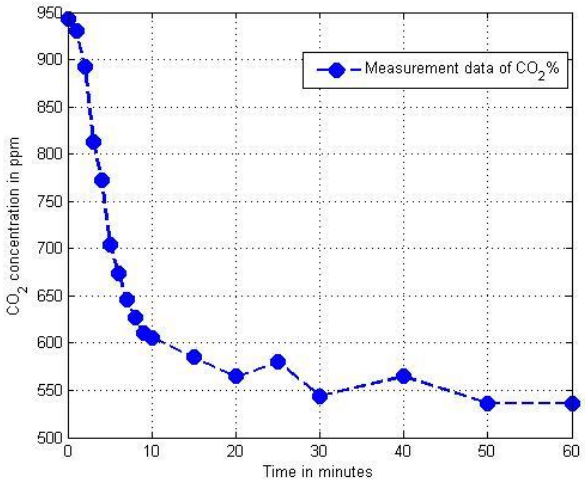

Figure 4.12: Measurement data of CO_2 concentration for classroom 2.28 (south). The measurement data are recorded from 6.5 to 7.5 am, January 30th, 2013 under pre-ventilation. Seen from this figure, indoor air quality will be close to outside conditions after pre-ventilation.

4.3.1.2.2 Effect of night ventilation rate

Energy requirement and indoor air temperature (human thermal comfort) at the next day could be heavily affected by the night ventilation rates. Now, the aforementioned controlling parameters and boundary conditions are maintained excluding the night ventilation rates, which are gradually increased from 1 1/h to 3 1/h. The annual ventilation demands and the occupied indoor air temperature in July (the hottest month for the school building occupied) are illustrated in Fig. 4.13.

Seen from Fig. 4.13, almost exponentially increasing function between the night ventilation rate and annual ventilation demand could be established. As the increasing of night ventilation rate, annual ventilation demand can be enhanced by about 14.3% ((2224 kWh – 1905 kWh)/ 2224 kWh) comparing 3 1/h with 1 1/h. Meanwhile, almost exponentially decaying function between the night ventilation rate and indoor average air temperature of July when occupied could be also set up. The indoor air of the classroom could be easily cooled down the next day with increasing value of the night ventilation rate in summer.

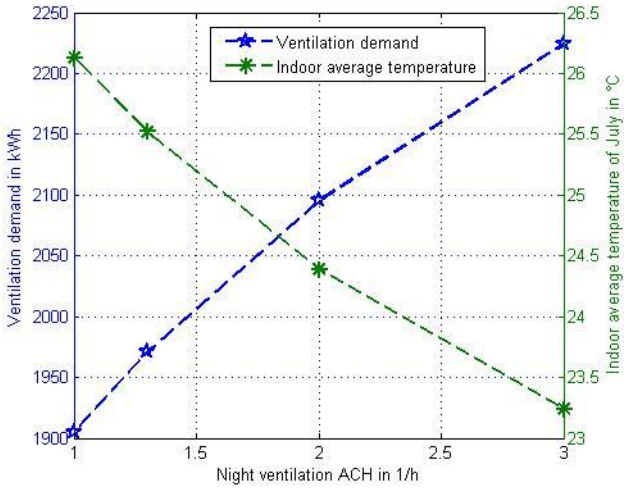

Figure 4.13: Annual ventilation demands and indoor average air temperature. It shows annual ventilation demands (blue line) and indoor average air temperature (green line) of July when occupied in reference classroom as functions of night ventilation rates for design point 1 south building. Increasing night ventilation ACH will increase the ventilation demand and decrease indoor mean temperature for the following day.

4.3.1.3 Effect of the sun-shading system

Sun-shading systems can provide thermal and visual comfort in buildings. Meanwhile, it should prevent unwanted solar gains in summer and permit high solar gains in winter (Kuhn 2001). Therefore, this school building also makes full use of the advantages of the sun-shading system. All the shading systems are normally activated in summer, on the contrary, they are not activated in winter for the sake of permitting solar gains entering inside the classrooms in winter. That is to say, energy demands could be also heavily affected by the shading system especially for its direction of the building e.g. the effect on the south building is normally larger than on the north building. It is thus necessary to investigate the effect of the shading system on the building energy performance. Now, the aforementioned controlling parameters and boundary conditions are maintained excluding the settings of the sun-shading systems, which are gradually changed from no shading to 70% shading factor in summer and with 70% shading factor all over the year.

The annual energy $Q_{\_cooling}$, $Q_{\_wallheating}$ and $Q_{\_solar\_gains}$ for the cases of no shading, with 70% shading in summer and with 70% shading all over the year in south building are illustrated in Fig. 4.14.

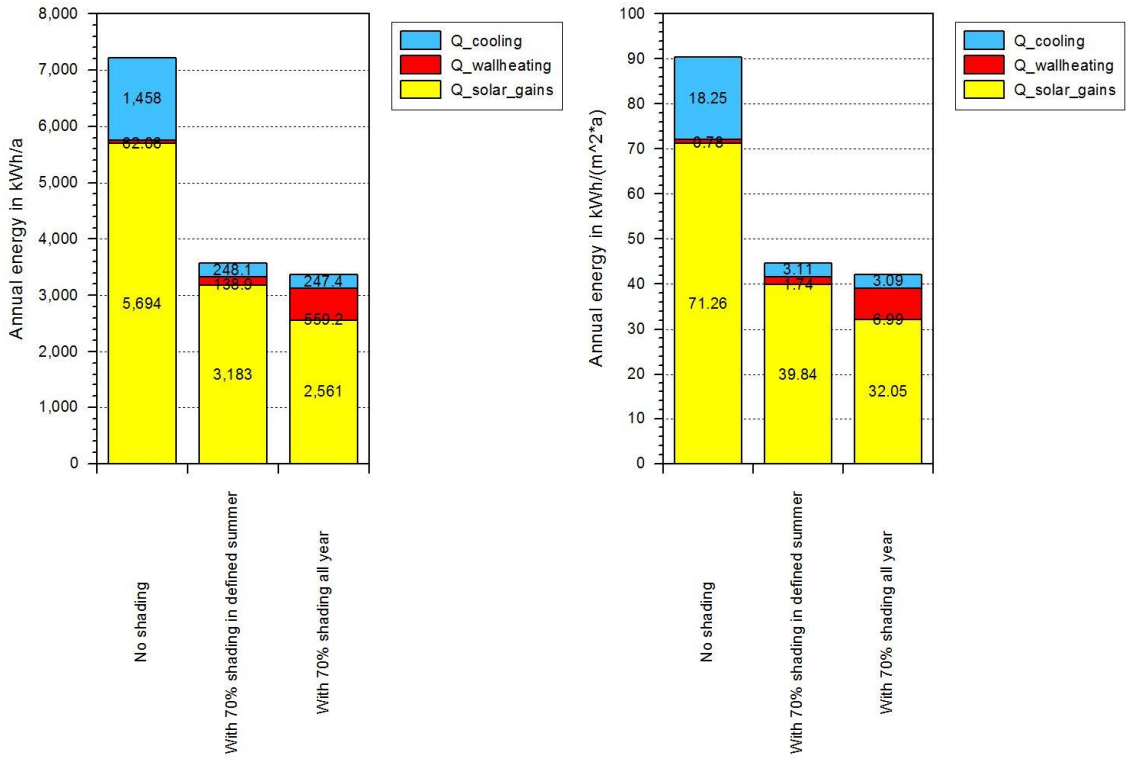

(a) Energy demand (b) Specific energy demand

Figure 4.14: Annual energy demand for different shading strategies (south). It shows $Q_{\_cooling}$, $Q_{\_wallheating}$ and $Q_{\_solar\_gains}$ for the cases of no shading, with 70% shading factor in summer and with 70% shading factor all over the year in reference classroom for design point 2 in south building. The best control strategy for sun-shading system in south building is 70% shading during non-heating seasons, which has expectedly low wall heating and cooling demands.

Observed from Fig. 4.14, compared to the case of with 70% shading in summer, the active cooling demand must be increased by 83.0% ((1458 kWh – 248.1 kWh)/1458 kWh) when no using shading system, although the heating demand could be decreased by 55.3% ((138.9 kWh – 62.06 kWh)/138.9 kWh); and the active cooling demand could be decreased by 0.3% ((248.1 kWh – 247.4 kWh)/248.1 kWh) with 70% shading all over the year, but the heating demand must be increased by 75.2% ((559.2 kWh – 138.9 kWh)/559.2 kWh). Therefore, the control strategy of with 70% shading in summer is the best one considering the balance of the active cooling and heating demands as well as thermal comfort compared to the other control strategies for south building.

Fig. 4.15 shows the annual energy $Q_{\_cooling}$, $Q_{\_wallheating}$ and $Q_{\_solar\_gains}$ for the cases of no shading, with 70% shading in summer and with 70% shading all over the year in the north building. In Fig. 4.15 it can be seen that the annual energy of $Q_{\_cooling}$, $Q_{\_wallheating}$ and $Q_{\_solar\_gains}$ for all of the cases including no shading, with 70% shading in summer and with 70%

shading all over the year in north building are almost similar. It can be therefore concluded that the effect of sun-shading systems on energy is nearly identical to each other in north building.

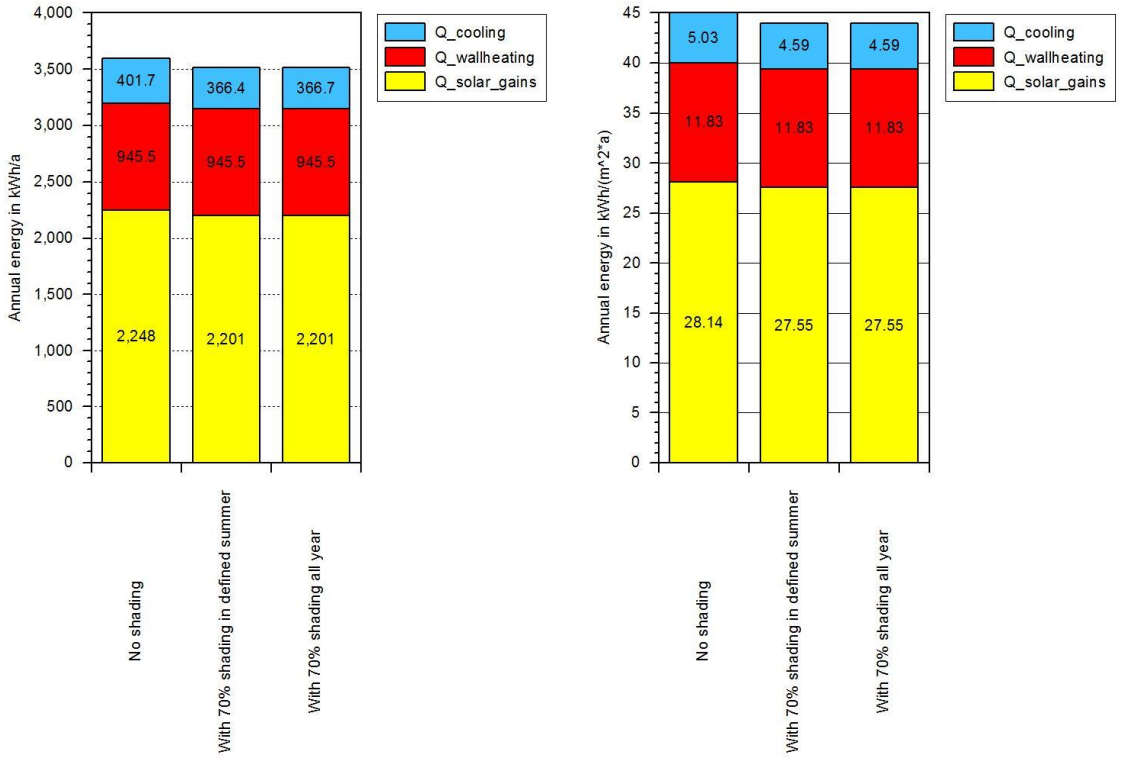

(a) Energy demand (b) Specific energy demand

Figure 4.15: Annual energy demand for different shading strategies (north). It shows $Q_{\_cooling}$, $Q_{\_wallheating}$ and $Q_{\_solar\_gains}$ for the cases of no shading, with 70% shading in summer and with 70% shading all over the year in reference classroom for design point 2 in north building. There is only slight effect of sun-shading system on energy-saving in the north building.

4.3.1.4 Effect of the efficiency of the heat recovery ventilation facility

Heat recovery ventilation facility can provide fresh air and improve climate control, while also provide saving heat energy by decreasing significantly heating loads due to recovering heat from exhaust air, particularly in airtight and well insulated buildings (Fouih et al. 2012) e.g. the school building of the FOS/BOS Erding with Passive House standard. Heating requirements could be also heavily affected by the efficiency of the heat recovery facility. Now, the aforementioned controlling parameters and boundary conditions are maintained excluding the efficiency of the heat recovery facility, which are gradually promoted from 0 to 1.0.

As the mechanical ventilation unit with heat recovery system is preliminary put into use, for the winter case, annual active heating demands are illustrated in Fig. 4.16, as functions

of heat recovery rates. Seen from Fig. 4.16, the decaying function between the heat recovery rate and active heating demands could be set up. For the active heating demand of heat recovery rate as 0.9, heating demand can shrink by approximately 89.9% ((2516 kWh/a–255.4 kWh/a)/2516 kWh/a) compared to without heating recovery facility i.e. the heat recovery rate as 0. For the aforementioned results, it could be demonstrated that for the heat recovery rates of from 0.76 to 0.9, which are the practical operating ranges of the heat recovery unit in this passive school building, it has thus expectedly small active heating demand.

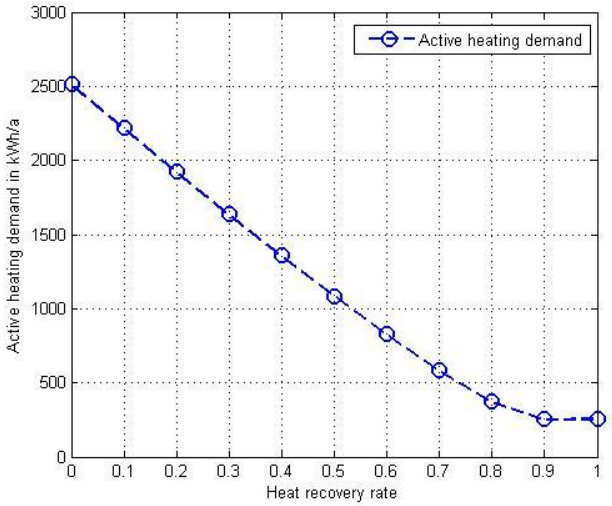

Figure 4.16: Active heating demand in winter with heat recovery rate. It illuminates active heating demand for reference classroom in winter as the function of heat recovery rates for design point 1 in south building. Total annual active heating demand for the practical operating range of 0.76 to 0.9 is reduced by 80.9% to 89.9% compared to without heat recovery.

In addition, according to the definition equation of Q_{vent} in Section 4.2.1 and the definition Eq. (4.5) of air conditioning energy Q_{ac} (i.e. $Q_{pre\text{-}heating}$), the following relationship (4.6) can be obtained,

$$Q_{ac} = \dot{V}\rho c_p (T_r - T_{vent}) \tag{4.5}$$

$$Q_{ac} = Q_{vent} \frac{T_r - T_{vent}}{T_{vent} - T_{air}} \tag{4.6}$$

Where, T_r represents the air temperature of exhaust from the heat recovery unit and entraining into the air conditioning unit. In winter, T_{vent} is set as 19 °C delivered into each classroom based on the Section 4.2.3.5. One method to calculate the air conditioning energy is only supplied here. Meanwhile, it can be concluded from the Eq. (4.6) that Q_{ac} is a

linear function of Q_{vent}. However, it is very necessary to calculate the time average by integrating of T_r and T_{air} if one wants to obtain Q_{ac} for a given period of time.

As mentioned before (Section 4.3.1), for the summer case, the effect of cooling recovery in summer is not very obvious compared to winter case based on the energy conservation. This is mainly because of the local weather condition in summer e.g. only a few days with high outdoor temperatures of larger than 30 °C (Jacob et al. 2008), and the temperature difference between inside and outside in the daytime locally is not large etc.

4.3.2 Thermal comfort

Classroom environment and thermal comfort play an important role in teaching and learning, as they help students to engage in activities that promote their performances, such as an understanding of concepts, problem solving abilities and attitudes towards learning etc. (Puteh et al. 2012). It is therefore significant to investigate whether the classroom environment can meet the requirement of thermally human comfort (ISO EN 7730 2005, ASHRAE 2009) in this school building with Passive House standard, especially the indoor air temperature range of recommended thermal comfort i.e. between 20 °C and 26 °C (CEN EN 15251 2007, ANSI/ASHRAE Standard 55 2004, 2010).

Now, the indoor temperatures during the coldest and hottest months i.e. February and July respectively in the reference classroom with six design points as different simulation cases, which are the real operation conditions in the school building, have been investigated and evaluated through analysing how many hours lie in the different temperature ranges when occupied. Fig. 4.17 and Fig. 4.18 illuminate the winter case (in February: the heating set-point is 21.5 °C) and summer case (in July: with the night ventilation of air exchange rate 1.3 1/h) respectively. Observing from Fig. 4.17, the indoor air temperatures of entire six design points can meet the set-point 21.5 °C (equal to or higher than 21.5 °C), which lie within the thermal comfort range, when occupied. The aforementioned results illustrate that the classroom in the school building with Passive House standard under the controlled heating system can provide high human thermal comfort under different conditions (e.g. occupancy amounts, building direction etc.) in winter, even the coldest month February (Jacob et al. 2008).

Closely scrutinizing Fig. 4.17, the classroom temperatures in south building are always higher than in north building due to the different effects of solar gains on two building orientations. In addition, the average indoor temperatures decrease with the occupancy amounts

from 33 (design point 1) to 15 (design point 3) not only for the south building but also for the north building.

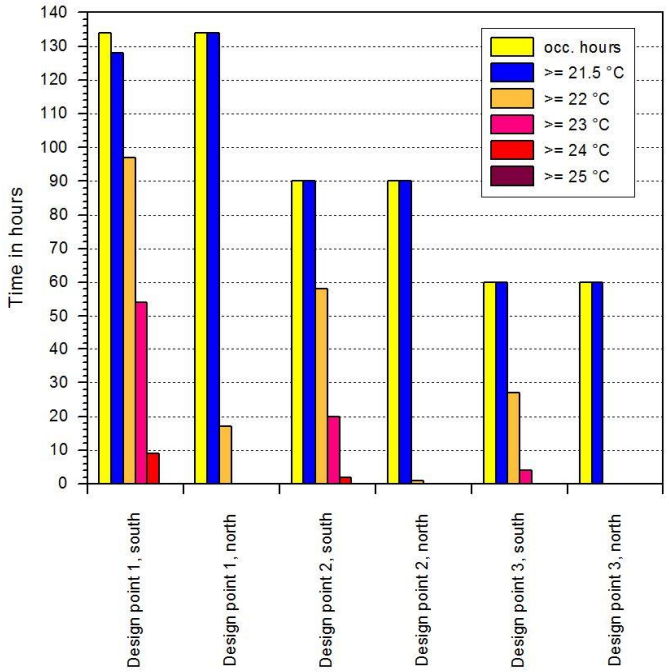

Figure 4.17: Hour-amounts of different temperatures when occupied in February. The heating temperature set-point is 21.5 °C. It shows the hour-amounts under the different temperature ranges when occupied in February for reference classroom with six different design points. For all six different conditions, it could obtain high thermal comfort under heating set-point 21.5 °C.

Seen from Fig. 4.18, the indoor air temperatures of all six design points could almost fulfil within the range of thermal comfort (20 °C to 26 °C) when occupied in summer, except design point 1 north building only a few hours with indoor temperature higher than 26 °C. It can be thus concluded that night ventilation under the ventilation control system in summer can provide favourable human thermal comfort under different conditions (e.g. occupancy amounts, building direction etc.), even the hottest month July. Besides that, there is an interesting phenomenon that the classroom temperatures in north building are larger than that in south building due to different shading activation situation, which also explains why the north building needs a little more cooling energy (Fig. 4.9) in summer based on the aforementioned results although active cooling instead of night ventilation cooling for that case. Furthermore, it is identical to the winter case that the average indoor temperatures decrease with the occupancy amounts from 33 (design point 1) to 15 (design point 3) not only for the south building but also for the north building.

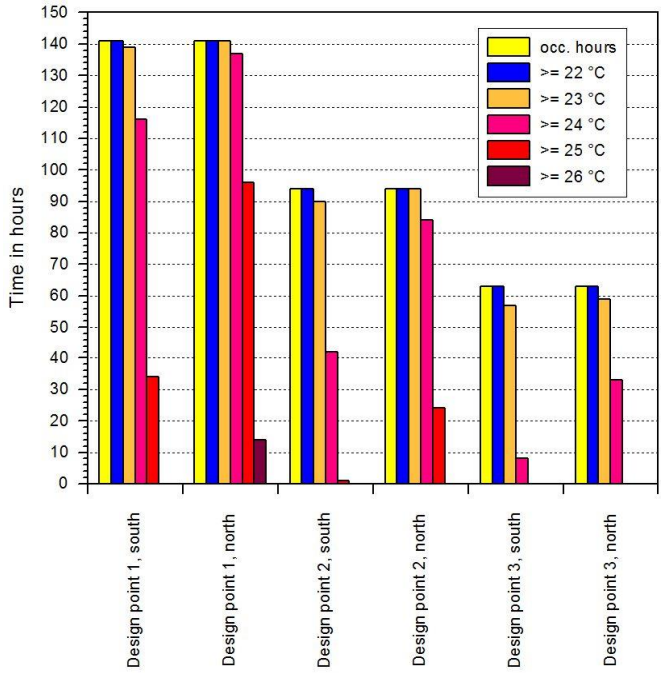

Figure 4.18: Hour-amounts of different temperatures when occupied in July. It shows hour-amounts under the different temperature ranges when occupied in July (with night ventilation under 1.3 1/h ventilation rate) for reference classroom with six different design points. For almost all six different conditions, it could obtain high thermal comfort under night ventilation.

In fact, the comfort zone depends on the applicable metabolic rate and clothing insulation (Frank 1975, Pistohl 2009), different metabolic rate and clothing insulation will result in comfort zone range changing a little. Comfort zone has been also experimentally investigated based on our measurement data. Fig. 4.19 and 4.20 show the comfort zone when occupied in winter and in summer, respectively, based on our measurement data from December 1st, 2012 to February 28th, 2013 and from June 1st, 2013 to August 31st, 2013, respectively.

Observing from Fig. 4.19, completely all measurement data lie within comfortable zone, which illustrates that the classroom in this school building with Passive House standard under heating and mechanical ventilation control systems could provide high human thermal comfort in winter and validate aforementioned BES results. The reason for the temperatures of lower than 20 °C is occupant behaviour e.g. opening the windows and changing of occupant number etc.

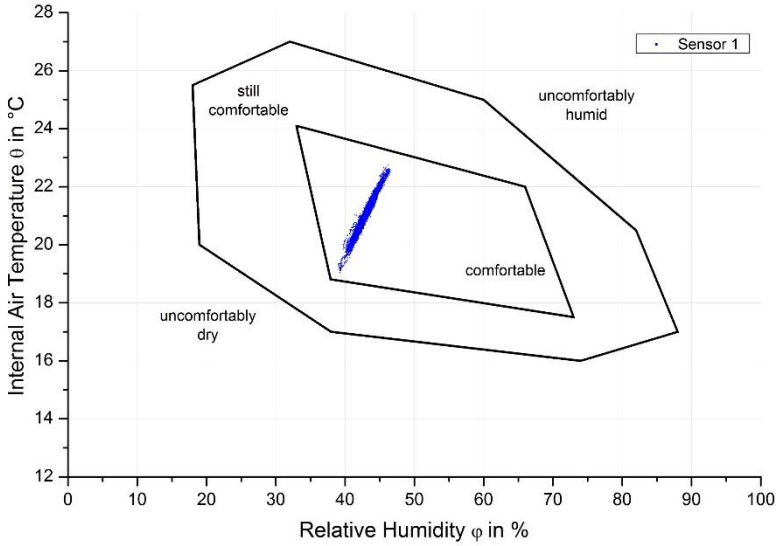

Figure 4.19: Comfort zone in winter. It shows the comfort zone of reference classroom 2.28 (south) when occupied in winter (from December 1st, 2012 to February 28th, 2013). Measurement data from the monitoring database (Sensor 1: Indoor air temperature and RH sensor in classroom 2.28). All measurement data lie within the comfort zone in winter.

Seen from Fig. 4.20, almost whole measurement data lie within comfortable and still comfortable zone, although a few data exceeds the still comfortable zone, whose temperature level is however near to or higher than 26 °C. The reason for the temperatures of higher than 26 °C is also occupant behaviour e.g. opening the windows and changing of occupant number etc.

It demonstrates that the classroom in this school building with Passive House standard under night ventilation control system could provide favourable human thermal comfort in summer and validate aforementioned BES results because of the fact that there is good correspondence between BES results and measurement data. In particular, the classroom with night ventilation instead of active cooling could provide favourable thermal comfort i.e. only very few hours higher than 26 °C in summer.

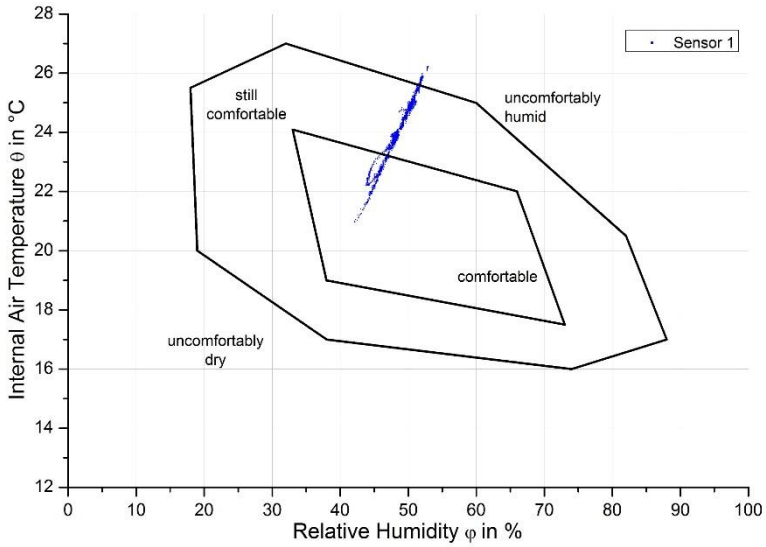

Figure 4.20: Comfort zone in summer. It shows the comfort zone of reference classroom 3.3 (north: due to no classes for reference classroom 2.28 of south building in June) when occupied in summer (from June 1st, 2013 to August 31st, 2013). Measurement data from the monitoring database (Sensor 1: Indoor air temperature and RH sensor in classroom 3.3). Nearly all measurement data lie within the comfort zone in summer.

4.4 Energy performance for the whole building

The whole building annual performance should be more significantly investigated compared to the single room from the energy point of view. That is mainly because it is more necessary to analyse whether this school building energy requirements could meet Passive House standard or not. In addition, it is also significant that the effects of all those above parameters on the building energy demands should be investigated and evaluated in order to compare with the single room case (Hernandez 2008).

Like the section of single room, in order to investigate energy performance of the whole building, it is also very necessary to make a reference setting list for simulation parameters (see Table 4.1 and Appendix B.2: Reference List for whole building). There are three building scenarios as different simulation cases, shown in Table 4.3, which represent three operative situations in this school building for the sake of calculating all kinds of total energy demands in buildings e.g. active cooling demand, wall heating demand etc., and energy analysis and evaluation based on different energy balances. For instance, the case of scenario 1 can determine the total active cooling energy requirement for the complete building, although it is not the real operative condition of the school building.

Table 4.3: Scenario settings for different simulation cases for whole building

	Summer	Winter
Scenario 1	With 26 °C active cooling No night ventilation	With 21.5 °C wall heating No heat recovery
Scenario 2	With 26 °C active cooling No night ventilation	With 21.5 °C wall heating With heat recovery
Scenario 3	With night ventilation	With 21.5 °C wall heating With heat recovery

4.4.1 Building scenario 1

As mentioned before, all controlling parameters and boundary conditions of 35 zones are set based on building scenario 1 without considering the effects of heat recovery facility and night ventilation and Appendix B.2.

Fig. 4.21 illuminates the annual energy balance without considering the energy of pre-heating system and heat recovery for the case of building scenario 1 (general simulation conditions: heating set-point 21.5 °C, cooling set-point 26 °C, day ventilation temperature 19 °C, with pre-ventilation in winter and 70% shading factor in summer).

Observed from Fig. 4.21, heat transmission energy accounts for approximately 84.6% (269463 kWh/a/(12844 + 24880 + 11480 + 269463) kWh/a) for total energy losses, which is just almost equal to the sum of solar and internal gains. The above results illustrate that heat transmission is most primary energy consumption source in buildings. The annual wall heating energy requirement for the whole building only heats the rooms into heating set-point temperature of 21.5 °C under the inlet ventilation temperature of 19 °C.

Fig. 4.22 shows the annual energy of $Q_{\_cooling}$, $Q_{\_wallheating}$ and $Q_{\_ventilation}$ for the cases of no pre-ventilation and with pre-ventilation in whole building based on building scenario 1. Seen from Fig. 4.22, the active cooling demand, which just cool the classroom into cooling set-point temperature of 26 °C under the inlet ventilation temperature of 19 °C, maintains the similar between with and without pre-ventilation due to only implementing pre-ventilation in winter. $Q_{\_ventilation}$ enhances approximately 2.19 MWh with implementing pre-ventilation compared to without pre-ventilation. Meanwhile, wall heating demand also correspondingly increases 1.86 MWh compared using pre-ventilation with no pre-ventilation in order to heat the thermal zones in winter.

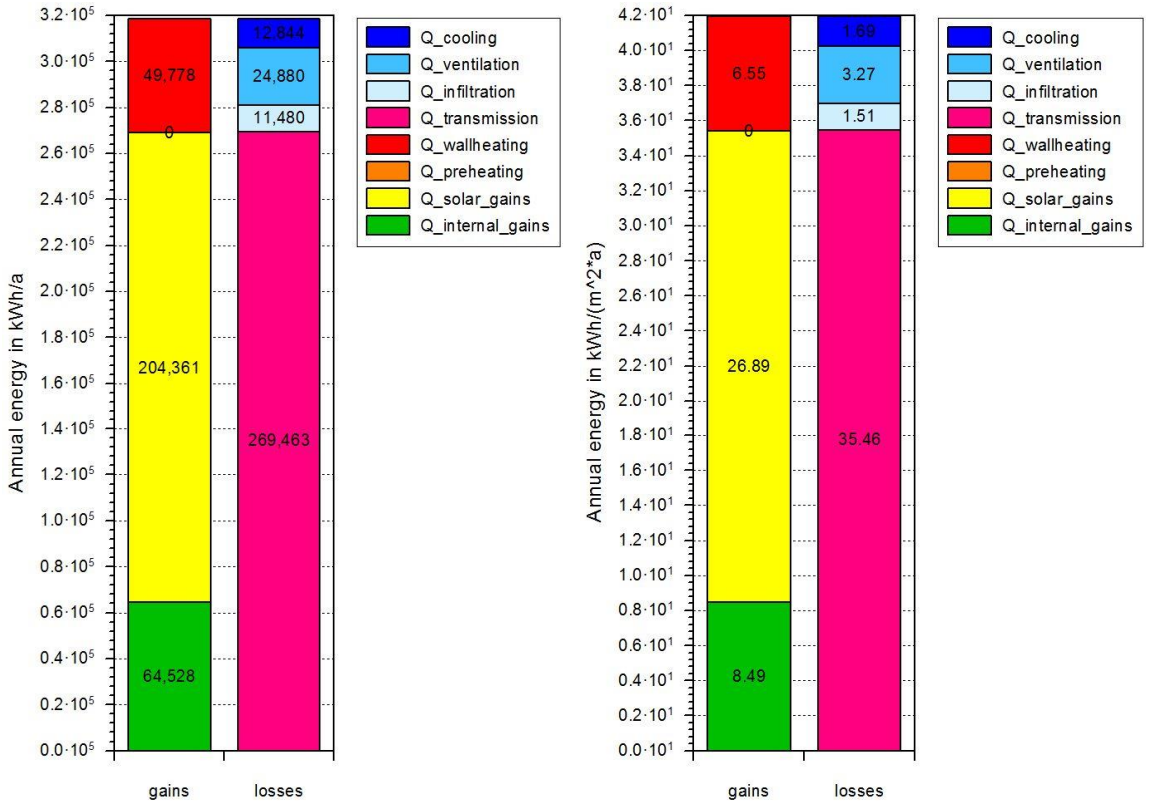

(a) Energy (b) Specific energy

Figure 4.21: Annual energy balance for building scenario 1. Annual energy balance for the school building: comparison between energy gains (including wall heating, pre-heating, solar gains and internal gains) and losses (including cooling with 26 °C set-point, ventilation, infiltration and transmission) for building scenario 1. Heat transmission causes the major energy loss, the cooling demand is expectedly small.

Fig. 4.23 illustrates the different energy demands per unit floor area (energy reference area (Energiebezugsfläche): in all 7600 m^2) corresponding to Fig. 4.22. Closely scrutinizing Fig. 4.23, the wall heating demand with pre-ventilation is only 6.55 kWh/(m^2a) far less than 15 kWh/(m^2a), which is Passive House standard of building energy requirements.

As mentioned earlier, it is also necessary to investigate the annual energy balance of the whole building considering cooling energy of cooling recovery and pre-cooling systems. Fig. 4.24 shows the annual energy balance (considering the cooling energy supplied by cooling recovery and pre-cooling systems) for the case of building scenario 1 (general simulation conditions: heating set-point 21.5 °C, cooling set-point 26 °C, no night ventilation, day ventilation temperature: 19 °C, with pre-ventilation in winter, 70% shading). The active cooling with set-point 26 °C instead of night ventilation in summer is set here for reasons of simulation investigation to determine the total active cooling energy.

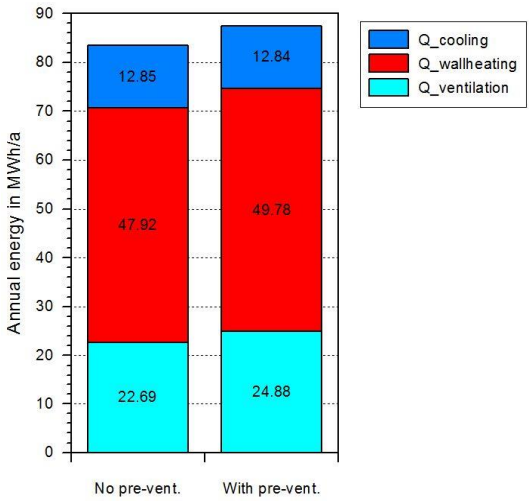

Figure 4.22: Annual energy demands for building scenario 1. It shows the annual energy demands including active cooling ($Q_{\_cooling}$), wall heating ($Q_{\_wallheating}$), and ventilation energy demand ($Q_{\_ventilation}$) in the whole building for building scenario 1.

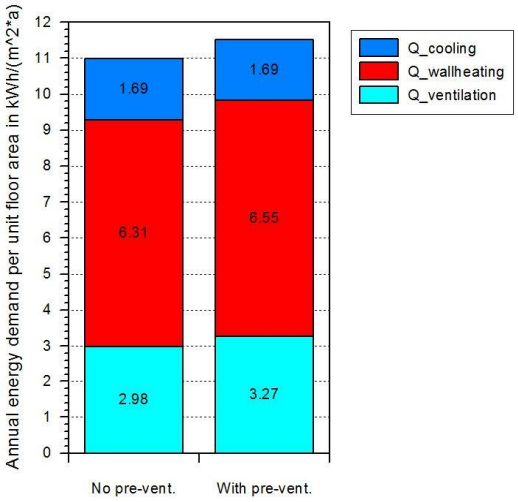

Figure 4.23: Annual energy demands per unit floor area for building scenario 1. The energy reference floor area of the whole building is 7600 m^2. It shows annual energy demands per unit floor area including active cooling ($Q_{\_cooling}$), wall heating ($Q_{\_wallheating}$), and ventilation energy demand ($Q_{\_ventilation}$) in whole building for building scenario 1. For both control strategies, expectedly low specific energy demands are shown.

Like the aforementioned single classroom section, in summer, it is not obvious that cooling recovery facility and pre-cooling unit, particularly cooling recovery facility only occupies very small part, undertake to cool the rooms compared with heat recovery facility in winter, which is very similar to real operation situation in the school building. This is mainly because the cooling recovery operation is not very often compared to the heat recovery in winter due

to the local weather condition in summer e.g. only a few days with high outdoor temperatures of larger than 30 °C (Jacob et al. 2008), and the temperature difference between inside and outside in the daytime locally is not large etc. The active cooling therefore accounts for more than half percentage of supply cooling energy approximately 63.0% (12844 kWh/(7556+12844) kWh) to cool the building into 26 °C.

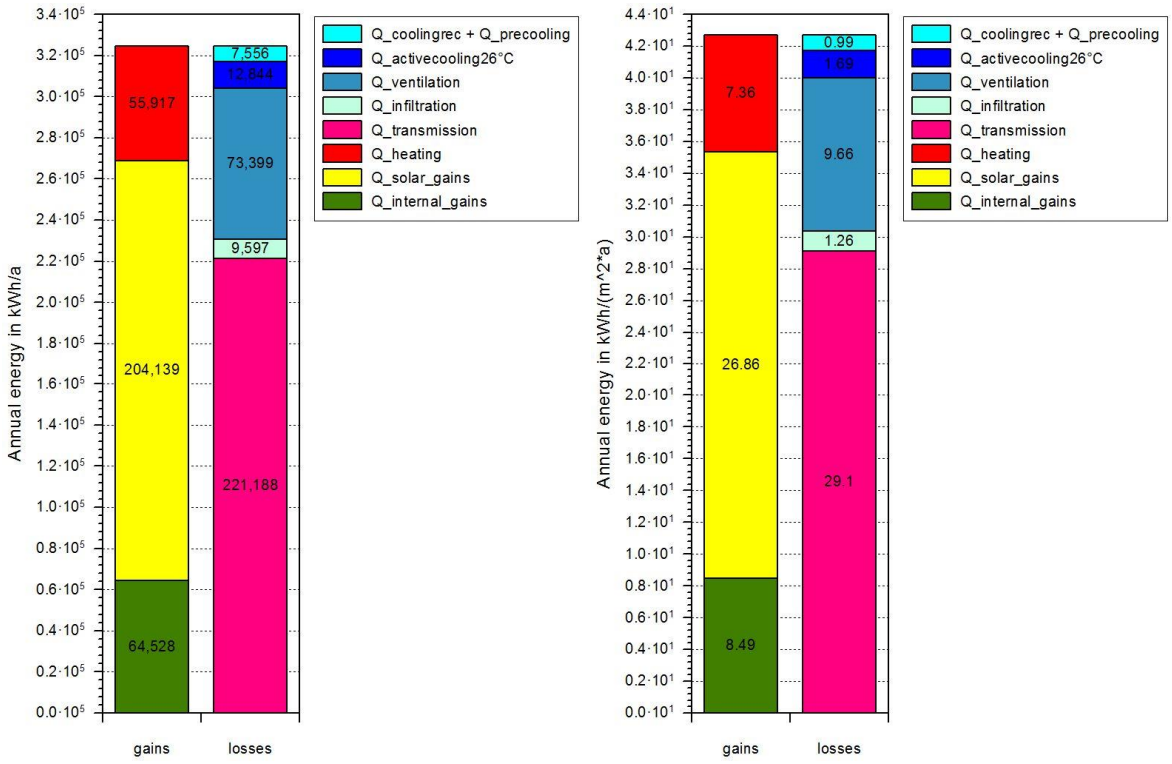

(a) Energy (b) Specific energy

Figure 4.24: Energy balance of building, cooling recovery and pre-cooling system. It shows the annual energy balance in whole building including cooling recovery and pre-cooling system: comparison between energy gains (including heating, solar gains and internal gains) and losses (including cooling recovery plus pre-cooling, active cooling, ventilation, infiltration and transmission) for building scenario 1. The total cooling demand is expectedly low.

4.4.2 Building scenario 2

Now, all controlling parameters and boundary conditions of 35 zones are set based on scenario 2 (considering the effects of heat recovery facility and without night ventilation) and Appendix B.2.

Fig. 4.25 illuminates the annual energy balance (considering the energy of pre-heating system) for the case of building scenario 2 (general simulation conditions: heating set-point

21.5 °C, cooling set-point 26 °C, day ventilation temperature 19 °C, with pre-ventilation in winter and 70% shading in summer).

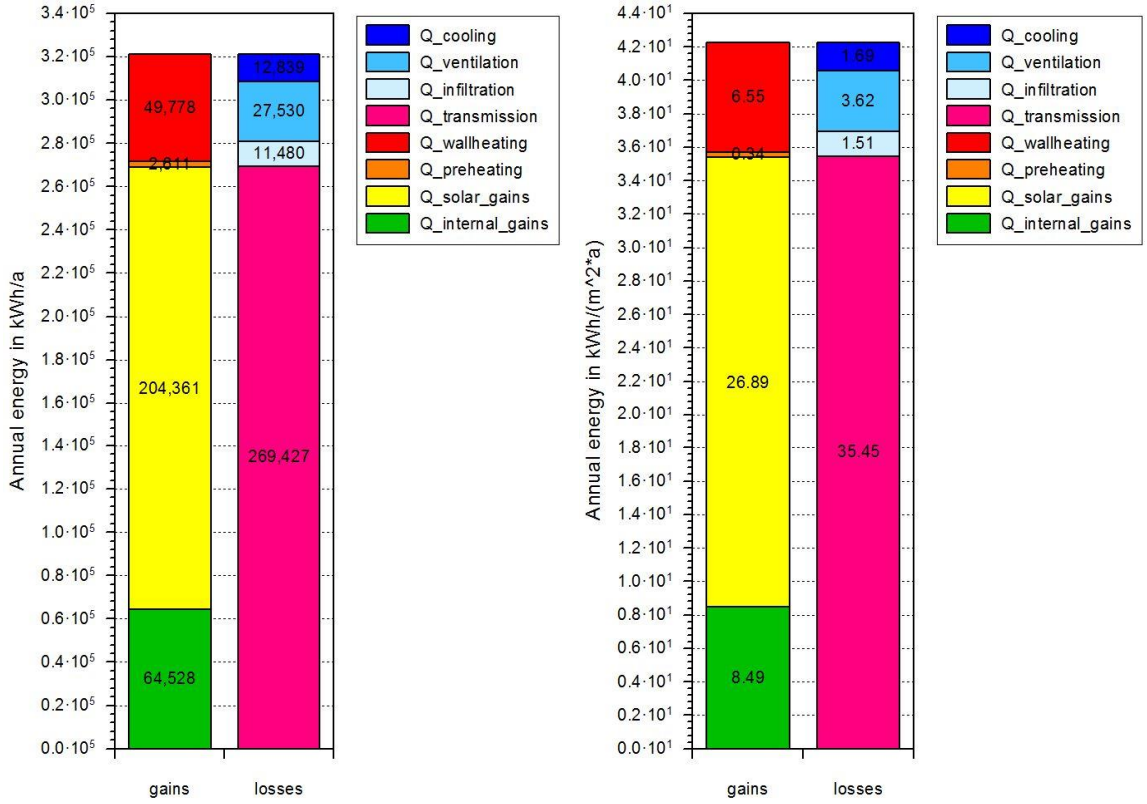

(a) Energy (b) Specific energy

Figure 4.25: Annual energy balance for building scenario 2. It shows the annual energy balance in this school building: comparison between energy gains (including wall heating, pre-heating, solar gains and internal gains) and losses (including cooling, ventilation, infiltration and transmission) for building scenario 2. The air pre-heating demand and the cooling demand are expectedly low.

Observed from Fig. 4.25, heat transmission energy accounts for approximately 83.9% (269427 kWh/a/(12839 + 27530 + 11480 + 269427) kWh/a) for total energy losses. The annual air pre-heating energy requirement for the whole building is expectedly small only 2611 kWh/a compared to the annual wall heating demand.

Fig. 4.26 illustrates the annual energy balance (considering the heating energy supplied by heat recovery system with heat recovery rate 80%) for the case of building scenario 2. Seen from Fig. 4.26, wall heating undertakes significant part of the work for heating the building, which accounts for very large percentage approximately 56.9% (49778 kWh/(49778 + 2611 + 35167) kWh) in the total heating energy. In addition, heat recovery facility also plays an important role in affording necessary heating energy for the building in winter, which accounts for approximately 40.2% (35167 kWh/(49778 + 2611 + 35167) kWh) in the whole heating energy.

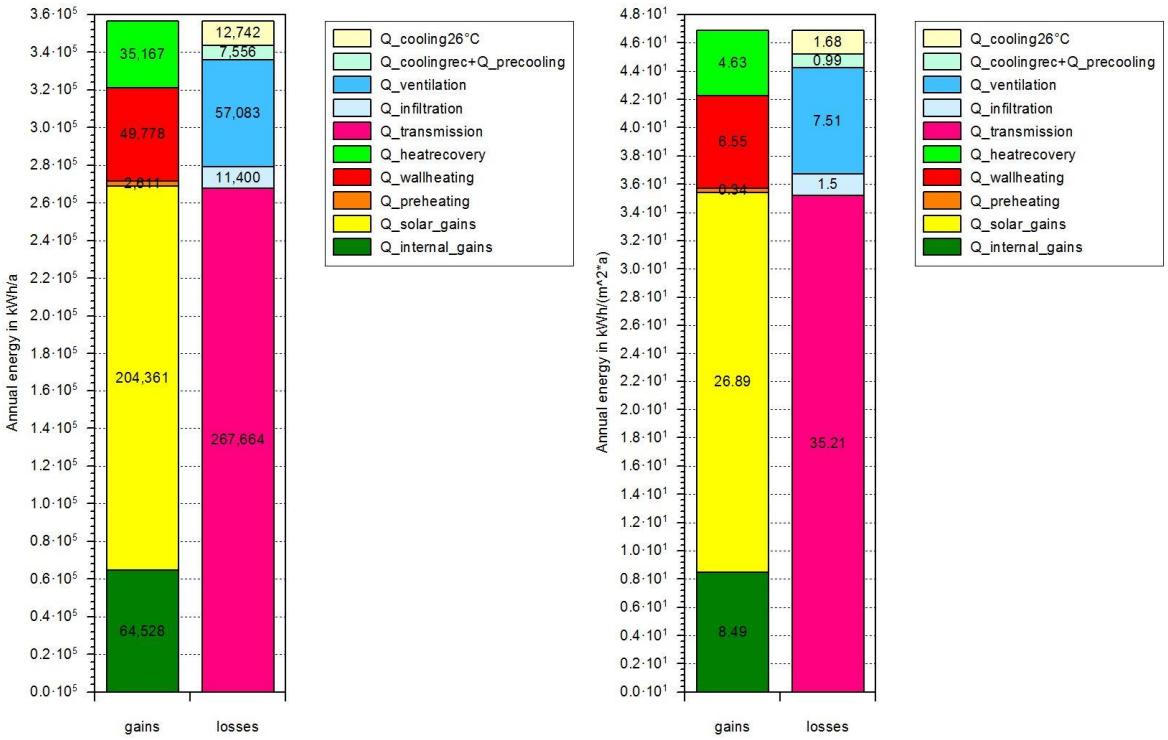

(a) Energy (b) Specific energy

Figure 4.26: Annual energy balance of building plus heat recovery system (No.2). Annual energy balance for the school building and heat recovery system: comparison between energy gains (including wall heating, pre-heating, heat recovery heating, solar gains and internal gains) and losses (including cooling, ventilation, infiltration and transmission) for building scenario 2. Compared to total heating demand, total cooling demand is expectedly low.

Fig. 4.27(a) and (b) show the annual heating demands and annual heating demands per unit floor area of $Q_{\_wallheating}$, $Q_{\_preheating}$ and $Q_{\_heatrecovery}$ in whole building based on building scenario 2 respectively.

Closely scrutinizing Fig. 4.27(b), the following is interesting to note: both of the wall heating demand (6.55 kWh/(m^{2}a)) and active heating demand (i.e. wall heating plus pre-heating demands: 6.89 kWh/(m^{2}a)), even total annual heating demand (11.52 kWh/(m^{2}a)), are far less than 15 kWh/(m^{2}a), which is Passive House standard of building energy requirements. The aforementioned results can be again concluded that this school building under building HVAC control systems can favourably meet the Passive House standard from the annual heating-demand point of view for the case of building scenario 2.

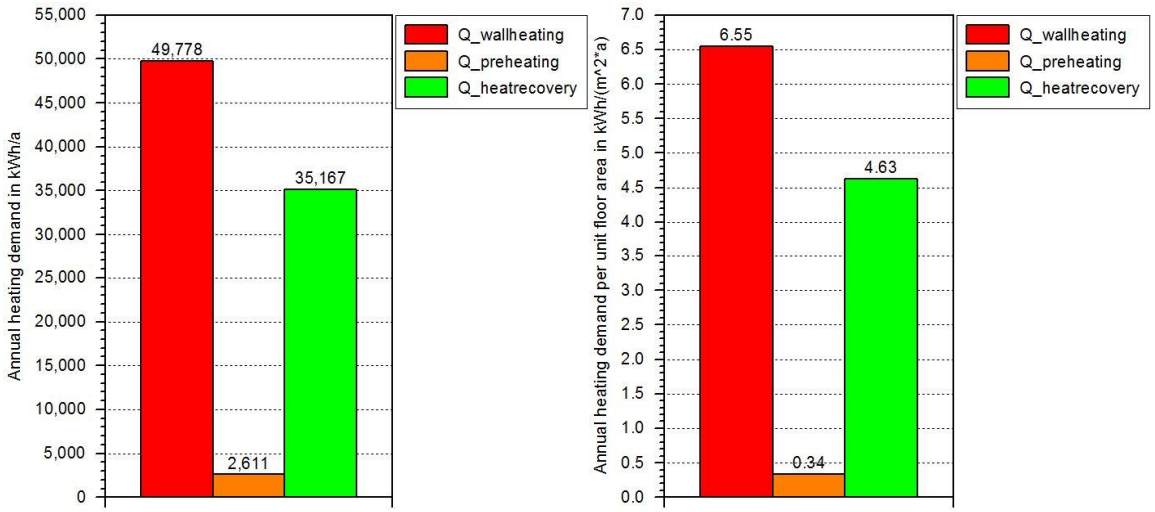

(a) Heating demand (b) Specific heating demand

Figure 4.27: Annual heating energy demands for building scenario 2. It shows the annual heating energy demands (a) and the annual heating demand per unit floor area (b) including wall heating ($Q_{\_wallheating}$), pre-heating ($Q_{\_preheating}$), and heat recovery energy ($Q_{\_heatrecovery}$) in whole building for building scenario 2. Active heating demand, even total heating demand, is less than 15 kWh/(m^2a), which is the Passive House standard.

4.4.3 Building scenario 3

As mentioned earlier, all controlling parameters and boundary conditions of 35 zones are set based on building scenario 3 considering the effects of heat recovery facility and night ventilation and Appendix B.2.

Fig. 4.28 illuminates the annual energy balance (only considering the energy of pre-heating system, not considering heat recovery facility) for the case of building scenario 3 (general simulation conditions: heating set-point 21.5 °C, day ventilation temperature 19 °C, with night ventilation in summer and pre-ventilation in winter and 70% shading in summer). Observed from Fig. 4.28, like the aforementioned building scenarios, heat transmission energy also accounts for significant percentage approximately 79.4% (256131 kWh/a/(288 + 55027 + 10969 + 256131) kWh/a) for total energy losses.

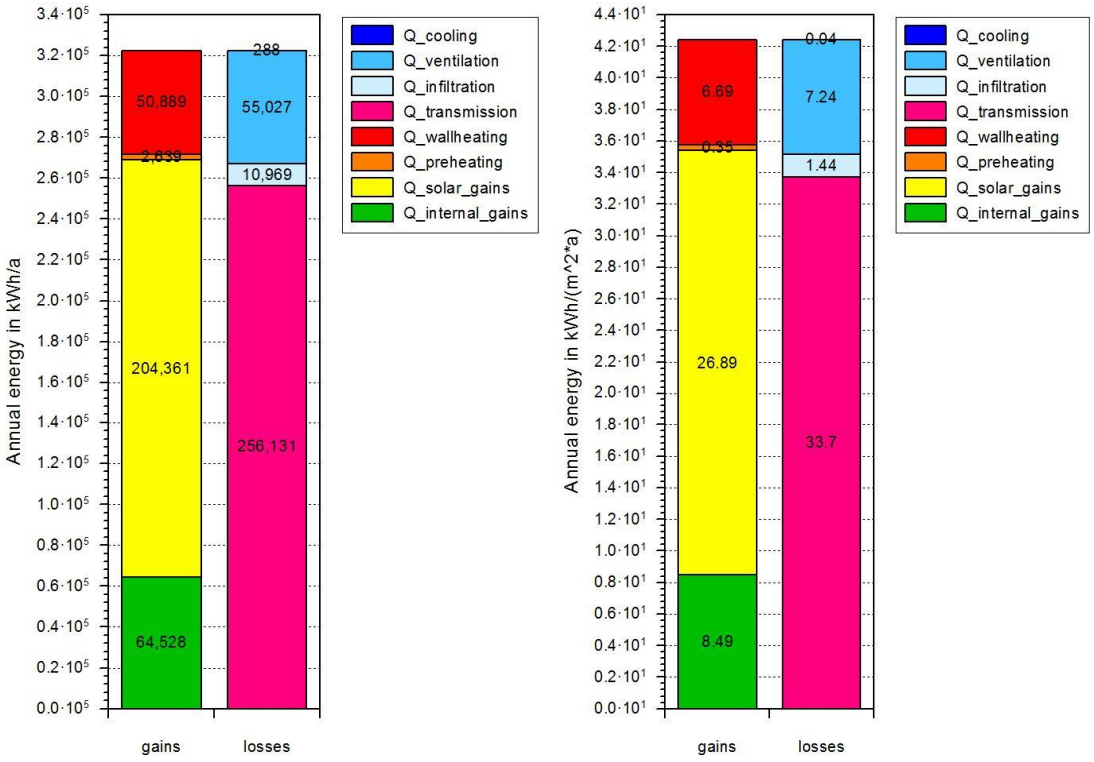

(a) Energy (b) Specific energy

Figure 4.28: Annual energy balance for building scenario 3. Annual energy balance for the school building: comparison between energy gains (including wall heating, pre-heating, solar gains and internal gains) and losses (including cooling, ventilation, infiltration and transmission) for building scenario 3. Active cooling demand is necessary only for the server room.

Fig. 4.29 illustrates the annual energy balance considering the heating energy supplied by heat recovery system with heat recovery rate 80% for the case of building scenario 3. Seen from Fig. 4.29, wall heating undertakes most part of the work for heating the building, which accounts for rather large percentage approximately 57.2% (50889 kWh/a/(50889 + 35361 + 2639) kWh/a) in the whole heating energy. In addition, heat recovery facility also plays a vital role in affording necessary heat energy for the building in winter, which accounts for approximately 39.8% (35361 kWh/a/(50889 + 35361 + 2639) kWh/a) in the whole heating energy. Furthermore, the active heating (wall heating plus pre-heating) demand increases only 1139 kWh/a compared to building scenario 2 (Fig. 4.26). It is due to that indoor temperature is less than 26 °C in summer i.e. night ventilation could provide higher thermal comfort compared to with 26 °C active cooling's control strategy, whose indoor temperature in summer is a little higher or just equal to 26 °C based on the simulation results. In other words, total ventilation energy demand for building scenario 3 due to with

night ventilation increases 32.4% (27389 kWh) compared to building scenario 2 (Fig. 4.26). What's more, $Q_{\_cooling}$ is very small only for the server room.

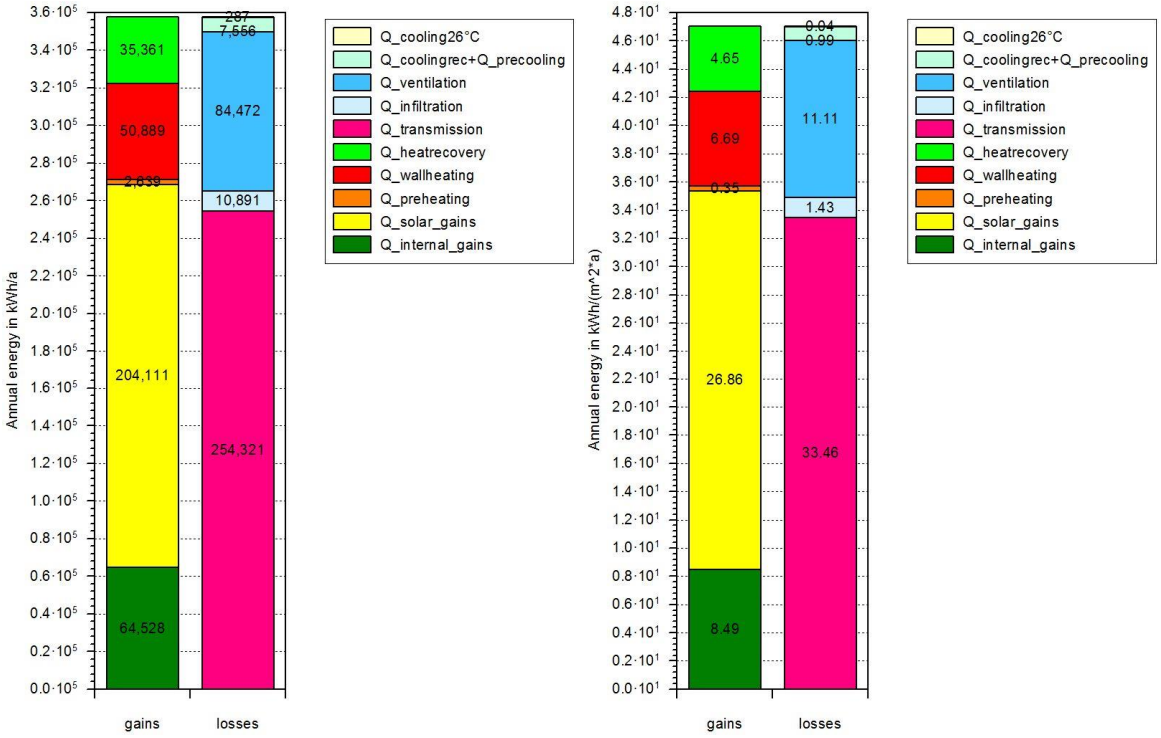

(a) Energy (b) Specific energy

Figure 4.29: Annual energy balance of building plus heat recovery system (No.3). It shows the annual energy balance for the school building with heat recovery system: comparison between energy gains (including wall heating, pre-heating, heat recovery heating, solar gains and internal gains) and losses (including cooling, ventilation, infiltration and transmission) for building scenario 3. Active cooling is necessary only for the server room. Active cooling and air pre-cooling demands are provided from the groundwater cooling system.

Fig. 4.30(a) and (b) show the annual heating demands and annual heating demands per unit floor area of $Q_{\_wallheating}$, $Q_{\_preheating}$ and $Q_{\_heatrecovery}$ in whole building based on building scenario 3 respectively. Closely scrutinizing Fig. 4.30(b), the following is interesting to note: both of the wall heating (6.69 kWh/(m^2a)) and active heating (i.e. wall heating plus pre-heating: 7.04 kWh/(m^2a)) demands, even total annual heating demand (11.69 kWh/(m^2a)), are far less than 15 kWh/(m^2a), which is Passive House standard of building energy requirements. The above results can be again concluded this school building under building HVAC control systems can obviously meet Passive House standard from the annual heating-demand point of view in building scenario 3 operation mode.

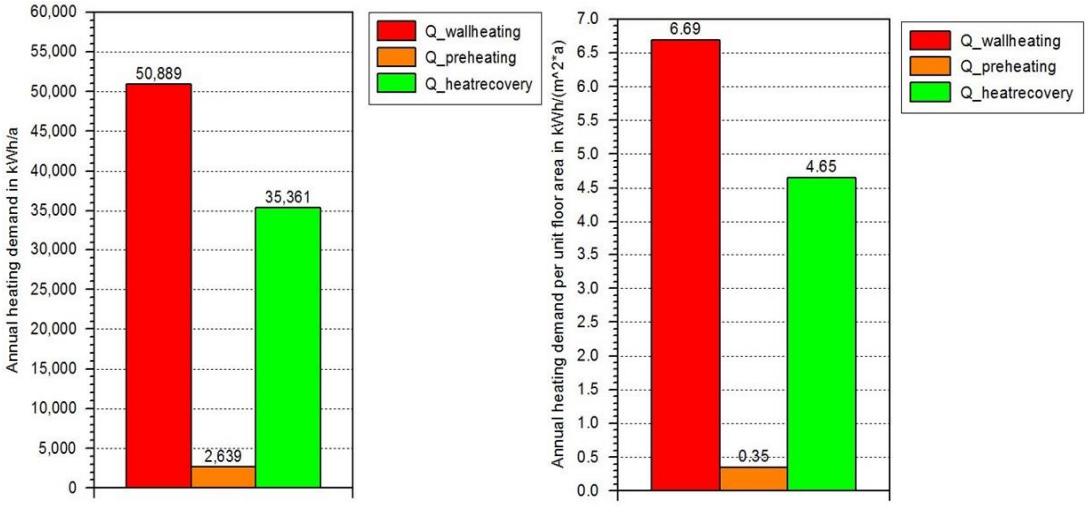

(a) Heating demand (b) Specific heating demand

Figure 4.30: Annual heating energy demands for building scenario 3. Annual heating energy demands (a) and annual heating demand per unit floor area (b) including wall heating ($Q_{\_wallheating}$), preheating ($Q_{\_preheating}$), and heat recovery energy ($Q_{\_heatrecovery}$) in whole building for building scenario 3. Active heating demand, even total heating demand, is less than 15 kWh/m^{2}a, which is the Passive House standard.

4.5 Summary and conclusions

In this section, energy performance of single reference classroom and whole building have been numerically and experimentally investigated in the present study, together with the evaluation of classroom thermal comfort in this school building with Passive House standard. The representative on-site measurements have been implemented to favourably validate the present BES methodology and numerical codes, although some observed discrepancies existed between BES results and measurement data.

(1) Annual active heating for the whole building could favourably meet the Passive House standard – less than 15 kWh/(m^{2}a) - for energy requirements under all different operative conditions e.g. with or no pre-ventilation etc. In addition, from the total supply heating demand point of view, the sum of supply heating demand for each design point indeed increases with the occupancy number from design point 3 (15) to 1 (33), not only for the south building but also for the north building.

(2) The solar and internal gains play a vital role in affording necessary heat energy for the building/classroom in winter in order to compensate against the most primary

energy loss source in buildings: heat transmission, which is a most significant character for passive house at the same time i.e. the energy in buildings/room could be obtained through passive modes.

(3) Heat recovery facility undertakes most part of the work for heating the room/building, which accounts for extremely large percentage in the whole supply heating energy. Almost linearly decaying function between the heat recovery rate and active heating demands could be set up. For the heat recovery rates of from 0.76 to 0.9, which are the practical operating ranges of the heat recovery unit in this passive school building, there is expectedly small active heating (wall heating plus pre-heating) demand. However, the amount of energy from cooling recovery operation is very small due to the local weather condition in summer e.g. only a few days with high outdoor temperatures of larger than 30 °C.

(4) Almost exponentially increasing functions between the set-point temperatures for heating and the wall heating demands could be set up, not only for the south building but also for the north building. On the contrary, almost exponentially decaying functions between the set-point temperatures for cooling and the active cooling demands could be set up, not only for the south building but also for the north building. Energy consumption including heating and cooling heavily depends on the room set-point.

(5) Night ventilation instead of active cooling in summer could shrink the maximum daytime indoor temperature in buildings, particularly, which is suitable for the unoccupied public school building at night. Night ventilation could not only provide more appropriate living conditions for the following day but also save lots of energy costs for cooling at day. In addition, the climatic conditions in Munich region is exceedingly suitable for night ventilation cooling due to intensely large temperature difference (more than 10 °C) between day and night in summer.

(6) Pre-ventilation before the classes in the winter morning could not only improve indoor air quality, i.e. indoor conditions are close to outside, but also assist to heat the classrooms. In addition, the best control strategy for sun-shading system is 70% shading during non-heating seasons, which shows expectedly low wall heating and cooling demands for the south building.

(7) The classroom in this school building with Passive House standard under building HVAC control systems could provide high human thermal comfort - the classroom air temperatures of entire six design points could lie within the thermal comfort range (20 °C to 26 °C) when occupied - under different conditions (e.g. occupancy amounts, building direction etc.) not only in winter but also in summer, even the

coldest/hottest month February/July. In addition, nearly all measurement data also lie within the comfort zone when occupied in winter and summer.

5 Conclusions

The recently-built school building with Passive House standard of the FOS/BOS Erding has adopted a novel heat recovery ventilation system. In order to appropriately model the single reference classroom and the whole building equipped with all different kinds of controlled systems including heating (wall heating, air pre-heating and heat recovery), cooling (air pre-cooling and night cooling), ventilation, artificial lighting and sun-shading systems etc., the air exchange rates including the infiltration rate and natural ventilation rate and the thermal time constants were measured.

In winter/summer days, classroom displacement mechanical ventilation, air conditioning system (including air pre-heating and air pre-cooling) and heat recovery facility are jointly put into operation with fully closed windows and airtight building envelopes, which aims to reduce the building heat losses and enhance the building energy efficiency. Indoor environment including thermal comfort and indoor air quality of one representative classroom have been numerically and experimentally as well as theoretically investigated in the present work, together with the analytical modelling of heat recovery and energy conservation. Some representative on-site measurements have been implemented to favourably validate the present CFD methodology and numerical codes, although some observed discrepancies existed between CFD results and measurements. For winter/summer case with mechanical ventilation:

(1) The thermal stratification of the displacement ventilation is illustrated by the 3D spatial thermal distributions and their normalized standard deviations. Roughly uniform isotherms and thermal buffers present in the upper regions in the classroom, where reduce favourably the heat transfer rates between surroundings and building ceilings. In addition, sensible draft dissatisfaction does not exist inside this classroom, although it has been reported in earlier researches of displacement ventilation inside the office or residential buildings.

(2) Thermal transport structures and airflow patterns inside the classroom are strongly affected by the ventilation air flow rates and supplying air temperatures. The volume averaged temperature level decreases linearly with the ventilation air flow rate, whereas local thermal gradients are complex functions of the ventilation air flow rates. An increasing temperature

of supplying fresh air not only enhances linearly the temperature of the exhaust air, but also pushes thermal stratifications shifting downward from central area to the floor level.

(3) Temporal evolutions of classroom average CO_2 concentration demonstrate that increasing of mechanical ventilation rate could directly contribute to the quick dilution of classroom air pollutants. Normalized standard deviations of transient classroom pollutant concentrations obviously illuminate that non-uniformity of indoor pollutant distributions increases with the mechanical ventilation rate. Sensible species boundary layer and species stratification have been observed in the process of displacement ventilation in this classroom. With such stratification, pollutants will gradually accumulate in the upper area adjacent to the classroom ceiling.

(4) The heat recovery facility interacts with the operation of the air conditioning unit. Energy conservation ratio of the air conditioning unit and the heat recovery efficiency of the heat recovery facility have been correlated in terms of the temperature difference between surrounding fresh air and supplying air, which shows quantitative low energy conservation of the air conditioning unit could be enhanced with the increasing heat recovery efficiency of the heat recovery facility and the shrinking/increasing temperature difference between the supplying air and fresh air in winter/summer.

(5) The 3D distributions of the indoor temperature and CO_2 concentration could provide valuable insight about the best locations of sensors to representatively measure the temperature and CO_2 concentration inside the classroom.

For transitional seasons with natural ventilation:

(1) Classroom thermal buoyancy puts remarkable effects on the spatial distribution of the classroom air temperature and gaseous contaminants. Thermal plume not only affects the air flow pattern, but also tends to enhance thermal stratification and decrease indoor pollutant concentration. In addition, thermal buoyancy heavily influences thermal comfort of occupants. Uniform isotherms due to the thermal buoyancy present in the upper region, where favourably produces the thermal buffers to reduce the heat transfer rates between the surrounding and building ceiling.

(2) Airflow patterns and heat transfer structures as well as contaminant concentrations in the classroom are heavily influenced by the entrained fresh air temperature and ventilation flow velocity. Classroom volume averaged temperature linearly increases with the supplying air temperature, while the local thermal gradient is the decreasing function of the supplying air temperature. The increasing temperature of supplying fresh air not only linearly promotes the exhaust air temperature, but also pushes thermal stratifications shifting downward from

central area to the floor level, and almost exponentially decreases the classroom volume averaged CO_2 concentrations. On the other hand, classroom volume averaged temperature exponentially decays with the supplying air velocity, while the local thermal gradient is a complex function of the supplying air velocity. The increasing velocity of entraining fresh air not only exponentially reduces the exhaust air temperature, but also pushes thermal stratification shifting upward from the floor level to the central area until the wind force dominates over the thermal buoyancy, and exponentially decreases the classroom volume averaged CO_2 concentration.

(3) Almost exponentially increasing function between the entraining air temperature or velocity and the ventilation effectiveness ratio for heat distribution and contaminant removal could be set up, while the ventilation effectiveness ratio for the contaminant removal is a complex function of the supplying air velocity.

(4) Mathematical influence and numerical analysis of ventilation effectiveness ratio for heat distribution on ventilation heat losses could be quantified. Heat loss due to natural ventilation has been correlated in terms of the ventilation effectiveness ratio for heat distribution, which shows that energy conservation of the natural ventilation could be enhanced with the ventilation effectiveness ratio for heat distribution if natural ventilation rate maintains constant, and the ventilation effectiveness ratio for heat distribution decreases when the supplying air temperature keeps invariant.

This research could benefit for the building operators and construction builders to separately control the classroom environment and design the low energy school building ventilation network, particularly when the school building should be built according with the Passive House standard in moderate climatic conditions. It also illuminated that enhancement of classroom air quality and human thermal comfort and reduction of school building energy consumption could be simultaneously achieved with the appropriate operation of heat recovery air conditioning unit and school building ventilation systems in winter/summer. However, in transitional seasons, natural ventilation could replace mechanical ventilation, and it could also provide high thermal comfort in the aforementioned classroom if outdoor temperature maintains approximately between 16 °C and 20 °C and outdoor air velocity is lower than 0.1 m/s.

The single reference classroom and the global school building energy performance investigation through annual energy balance analysis and reference design point and sce-

nario comparisons has been performed respectively. The representative on-site measurements have been implemented to favourably validate the present BES methodology and numerical codes, although some observed discrepancies existed between BES results and measurement data.

Very low heating and cooling demands and high indoor thermal comfort could be realized at the same time. The annual active heating (including wall heating and air pre-heating) and the annual active cooling demands are very few, particularly annual heating demand per unit floor area could fulfil the most important assessing criterion of Passive House – far less than 15 kWh/(m^2a) - for energy requirements under different operative conditions. Meanwhile, those heating/cooling demands could also provide favourable human thermal comfort in winter/summer, even in the coldest/hottest month February/July.

The solar gains and internal gains play a crucial role in affording heat gains for the passive school building, which could compensate in winter against the most primary energy loss source in buildings: heat transmission, which is a most significant character for passive house, i.e., the energy in buildings could be obtained through passive modes.

In addition, the wall heating demand obviously increases with the decreasing of the occupancy number from classroom design point 1 (33) to 3 (15) due to the decreasing of internal gains in winter, not only for southern building but also for northern building. On the contrary, the heating demand of the heat recovery and air pre-heating demand apparently reduce with the decreasing of the occupancy number.

Indoor set-point temperatures, pre-ventilation in winter, night ventilation flow rate in summer and sun-shading system not only heavily influence thermal comfort but also strongly affect the energy demand.

Heat recovery facility undertakes the major work for room heating, which accounts for extremely large percentage in the whole supplying heating energy. Almost linearly decaying function between the heat recovery rate and active heating (wall heating plus air pre-heating) demands could be established. For the heat recovery rates of from 0.76 to 0.9, which are the practical operating ranges of the heat recovery unit in this passive school building, there is expectedly small active heating demand. However, cooling recovery operation in summer is very occasional compared to the heat recovery operation in winter due to the local weather condition in summer.

A pre-ventilation before the classes in the winter morning could not only improve indoor air quality, whose indoor conditions are close to outside, but also decrease active heating demand due to that pre-ventilation assists to heat the classrooms. Meanwhile, this passive

school building employs the air pre-cooling from the groundwater cooling system and the return of a geothermal district heating for active heating including wall heating and air supply heating, which could conserve lots of cooling and heating energy. In addition, the best control strategy for shading is 70% shading during non-heating seasons, which shows very low wall heating and cooling demands for the south building.

Night ventilation instead of active cooling in summer could provide favourable human thermal comfort for the following day inside the classroom based on simulation results and measurement data for the comfort zone, which could reduce avalanche energy costs for cooling at the same time.

The optimized control systems for HVAC (including wall heating, heating/cooling recovery, mechanical ventilation, pre-ventilation and air pre-heating/cooling etc.) and sun-shading show a very energy efficient performance. This research could benefit for the low energy school building HVAC control system design, which includes the temperature set-point settings for the air pre-heating, air pre-cooling, wall heating and active cooling considering occupancy number, the supply air flow rate settings for the mechanical ventilation system based on indoor different levels of CO_2 concentrations, and the control strategies for the sun-shading system, night cooling system and pre-ventilation.

References

M. Abadie, K. Limam, F. Allard. Indoor particle pollution: effect of wall textures on particle deposition. Building and Environment 26 (2001) 821-827.

M. Abadie, K. Limam, J. Bouilly, D. Genin. Particle pollution in the French high-speed train (TGV) smoker cars: measurement and prediction of passengers' exposure. Atmospheric Environment 38 (2004) 2017-2027.

C. Allocca, Q. Chen, L. Glicksman. Design analysis of singel-sided natural ventilation. Energy and Buildings 35 (2003) 785-795.

E. Ampatzi, I. Knight. Modeling the effect of realistic domestic energy demand profiles and internal gains on the predicted performance of solar thermal systems. Energy and Buildings 55 (2012) 285-298.

ANSI/ASHRAE Standard 52.2, Air filter, ASHRAE Inc., Atlanta, 1999.

ANSI/ASHRAE Standard 55, Thermal Environmental Conditions for Human Occupancy, ASHRAE Inc., Atlanta, 2004.

ANSI/ASHRAE Standard 55, Thermal Environmental Conditions for Human Occupancy, ASHRAE Inc., Atlanta, 2010.

ANSI/ASHRAE Standard 62, Ventilation for acceptable indoor air quality, ASHRAE Inc., Atlanta, 2010.

ANSI S12.60-2002, Acoustical Performance Criteria, Design Requirements, and Guidelines for Schools. American National Standards Institute, New York, US, 2002.

ANSYS CFX Introduction, Release 14.0, 2012. ANSYS Inc., Canonsburg, USA.

F. Ascione, L. Bellia, A. Capozzoli. A coupled numerical approach on museum air conditioning: Energy and fluid-dynamic analysis. Applied Energy 103 (2013) 416-427.

M. R. Ashmore, C. Dimitroulopoulou. Personal exposure of children to air pollution. Atmospheric Environment 43 (2009) 128-141.

ASHRAE Handbook Fundamentals, 2009. ASHRAE Inc., Atlanta.

A. Audenaert, S. H. De Cleyn, B. Vankerckhove. Economic analysis of passive houses and low-energy houses compared with standard houses. Energy Policy 36 (2008) 47-55.

A. Auliciems, R. de Dear. Air conditioning in Australia, human thermal factors. Architecture Science Review 29 (1986).

Y. Avsar, M. T. Gonullu. Determination of safe distance between roadway and school buildings to get acceptable school outdoor noise level by using noise barriers. Building and Environment 40 (2005) 1255-1260.

H. B. Awbi. Energy efficient room air distribution. Renewable Energy 1998; 15:293-299.

V. Badescu, B. Sicre. Renewable energy for passive house heating Part I. Building description. Energy and Buildings 35 (2003) 1077-1084.

V. Badescu, B. Sicre. Renewable energy for passive house heating Part II. Model. Energy and Buildings 35 (2003) 1085-1096.

C. Beecken, S. Schulze. Energieeffizienz von Wohngebäuden: Energieverbräuche und Investitionskosten energetischer Gebäudestandards. Bauphysik 33 (2011) 338-344.

B. Berglund, I. Johansson, T. Lindvall. A longitudinal study of air contaminants in a newly built preschool. Environment International 8 (1982) 111-115.

R. Berry, V. Brown, S. Coward, D. Crump etc., Indoor air quality in homes, the building research establishment indoor environment study. BRE Reports BR299 and BR300. CRC Ltd., Watford, UK, 1996.

E. Beusker, C. Stoy, S. N. Pollalis. Estimation model and benchmarks for heating energy consumption of schools and sport facilities in Germany. Building and Environment 49 (2012) 324-335.

P. Blondeau, M. Sperandio and F. Allard. Night ventilation for building cooling in summer. Solar Energy 61 (1997) 327-335.

M. A. Bond, S. D. Probert. Energy thrift and thermal comfort in public houses. Applied Energy 62 (1999) 1-65.

G. S. Brager, R. de Dear. Climate, comfort, natural ventilation: A new adaptive comfort standard for ASHRAE Standard 55. Windsor, UK, 2001.

V. Brown, D. Crump, H. Mann. The effect of measures to alleviate the symptoms of asthma on concentrations of VOCs and formaldehyde in UK homes. Proceedings of Indoor Air, Nagoya, Japan. 4 (1996) 69-74.

CEN EN 15251, Indoor Environmental Input Parameters for Design and Assessment for Energy Performance of Buildings Addressing Indoor Air Quality, Thermal Environment, Lighting and Acoustics, European Committee for Standardization, Brussels, Belgium, 2007.

A. Chel, G.N. Tiwari. Thermal performance and embodied energy analysis of a passive house – case study of vault roof mud-house in India. Applied Energy 86 (2009) 1956-1969.

Q. Chen. Ventilation performance prediction for buildings: a method overview and recent applications, Building and Environment 44 (2009) 848-858.

Q. Chen Z. Zhai. The use of CFD tools for indoor environmental design. Advanced Building Simulation. Spon Press, New York, (2004) 119-140.

P. N. Cheremisinoff, R. A. Young. Pollution engineering practice handbook, 1975.

W. K. Chow. Wind-induced indoor-air flow in a high-rise building adjacent to a vertical wall. Applied Energy 77 (2004) 225-234.

A. A. Chowdhury, M. G. Rasul, M. M. K. Khan. Thermal-comfort analysis and simulation for various low energy cooling technologies applied to an office building in a subtropical climate. Applied Energy 85 (2008) 449-462.

K. J. Chua, S. K. Chou, W. M. Yang, J. Yan. Achieving better energy-efficient air conditioning – A review of technologies and strategies. Applied Energy 104 (2013) 87-104.

D. Chwieduk. Towards sustainable-energy buildings. Applied Energy 76 (2003) 211-217.

D. B. Crawley, L. K. Lawrie, F. C. Winkelmann etc. EnergyPlus: creating a new-generation building energy simulation program. Energy and Buildings 33 (2001) 319-331.

R. J. de Dear, G. S. Brager, D. Cooper. Developing an adaptive model of thermal comfort and preference. Final Report ASHRAE RP-884, ASHRAE Inc., Atlanta, 1997.

R. J. de Dear, G. S. Brager. Developing an adaptive model of thermal comfort and preference. ASHRAE Transaction 104 (1998) 145-167.

H. Djamila, K. Sivakumar, M. C. Chi. A conceptual review on residential thermal comfort in the humid tropics. International Journal of Engineering Innovation & Research 1 (2012) 539-544.

A. Dodoo, L. Gustavsson, R. Sathre. Building energy-efficiency standards in a life cycle primary energy perspective. Energy and Buildings 43 (2011) 1589-1597.

T. Drinkuth. *Kommunikation für die Energiesanierung: Das dena-Gütesiegel Effizienzhaus*. Berlin: Deutsche Energie-Agentur, 2010.

U. Eicker. Cooling strategies, summer comfort and energy performance of a rehabilitated passive standard office building. Applied Energy 87 (2010) 2031-2039.

P. O. Fanger. *Thermal Comfort*. Danish Technical Press, 1970.

Fanger 1970, ANSI/ASHRAE Standard 55 2004, 2010.

W. Feist. Passivhaus Projektierungs Paket 2002, Anforderungen an qualitätsgeprüfte Passivhäuser, Passivhaus Institut, Darmstadt, 2002.

W. Feist, J. Schnieders, V. Dorer, A. Haas. Re-inventing air heating: convenient and comfortable within the frame of the passive house concept. Energy and Buildings 37 (2005) 1186-1203.

J. M. Field. Effect of personal and situational variables upon noise annoyance in residential areas. Journal of the Acoustical Society of America 93 (1993) 2753-2763.

S. Firlag, S. Murray. Impact of airflows, internal heat and moisture gains on accuracy of modelling energy consumption and indoor parameters in passive building. Energy and Buildings 64 (2013) 372-383.

S. Fitzgerald, A. Woods, Natural ventilation of a room with vents at multiple levels, Building and Environment 39 (2004) 505-521.

A. Flaga-Maryanczyk, J. Schnotale, J. Radon, K. Was. Experimental measurements and CFD simulation of a ground source heat exchanger operating at a cold climate for a Passive House ventilation system. Energy and Buildings 68 (2014) 562-570.

Y. E. Fouih, P. Stabat, P. Riviere, P. Hoang, V. Archambault. Adequacy of air-to-air heat recovery ventilation system applied in low energy buildings. Energy and Buildings 54 (2012) 29-39.

W. Frank. *Raumklima und thermische Behaglichkeit*. Berlin, München, Düsseldorf: Wilhelm Ernst und Sohn KG Verl., 1975.

S. F. Fux, A. Ashouri, M. J. Benz, L. Guzzella. EKF based self-adaptive thermal model for a passive house. Energy and Buildings 68 (2014) 811-817.

L. Georges, M. Berner, H. M. Mathisen. Air heating of passive houses in cold climates: Investigation using detailed dynamic simulations. Building and Environment 74 (2014) 1-12.

L. Georges, C. Massart, G. Van Moeseke, A. De Herde. Environmental and economic performance of systems for energy-efficient dwellings: Case of passive and low-energy single-family houses. Energy Policy 40 (2012) 452-464.

B. L. Gowreesunker S. A. Tassou, M. Kolokotroni. Coupled TRNSYS-CFD simulations evaluating the performance of PCM plate heat exchangers in an airport terminal building displacement conditioning system. Building and Environment 65 (2013) 132-145.

E. Gratia, A.D. Herde, Guideline for improving natural daytime ventilation in an office building with a double-skin façade, Solar Energy 81 (2007) 435-448.

M. Gustafsson, G. Dermentzis, J. A. Myhren, C. Bales, F. Ochs, S. Holmberg, W. Feist. Energy performance comparison of three innovative HVAC systems for renovation through dynamic simulation. Energy and Buildings 82 (2014) 512-519.

M. Haase, A. Amato, An investigation of the potential for natural ventilation and building orientation to achieve thermal comfort in warm and humid climates, Solar Energy 83 (2009) 389-399.

E. Halawa, J. van Hoof. The adaptive approach to thermal comfort: A critical overview. Energy and Buildings 51 (2012) 101-110.

P. Hernandez, K. Burke, J. O. Lewis. Development of energy performance benchmarks and building energy ratings for non-domestic buildings: An example for Irish primary schools. Energy and Buildings 40 (2008) 249-254.

http://www.thiesclima.com/ClimasensorD_precipitation_e.html

B. R. Hughes, J. K. Calautit, S. A. Ghani. The development of commercial wind towers for natural ventilation: A review. Applied Energy 92 (2012) 606-627.

M. A. Humphreys. Comfortable indoor temperatures related to the outdoor air temperature. Building Service Engineering 44 (1976) 5-27.

Indoor environmental Quality: Building Ventilation. National Institute for Occupational Safety and Health, 2008.

ISO EN 7730, Ergonomics of the thermal environment- analytical determination and interpretation of thermal comfort using calculation of the PMV and PPD indices and local comfort criteria, International Standards Organisation, Geneva, 2005.

ISO EN 7730, Moderate thermal environments – Determination of the PMV and PPD indices and specification of the conditions for thermal comfort, International Standards Organisation, Geneva, 2005.

ISO EN 9972, Thermal performance of buildings – Determination of air permeability of buildings – Fan pressurization method, International Standards Organization, Geneva, 2006.

D. Jacob, H. Göttel, S. Kotlarski, P. Lorenz, K. Sieck. *Klimaauswirklungen und Anpassung in Deutschland*. Umwelt Bundes Amt Für Mensch und Umwelt, Hamburg, 2008.

Y. Jiang, Q. Chen, Buoyancy-driven single-sided natural ventilation in buildings with large opening, International Journal of Heat and Mass Transfer 46 (2003) 973-988.

M. Jin, F. Memarzadeh, K. Lee, Q. Chen. Experimental study of ventilation performance in laboratories with chemical spills. Building and Environment 57 (2012) 327-335.

Johannes Volland. *Energieeinsparverordnung (EnEV)*. Hüthig Jehle Rehm, 2014.

I. Johansson. Determination of organic compounds in indoor air with potential reference to air quality. Atmospheric Environment 12 (1978) 1371-1377.

L. Johansson, L. Westerlund. Energy savings in indoor swimming-pools: comparison between different heat-recovery systems. Applied Energy 70 (2001) 281-303.

P. Karava, T. Stathopoulos, A.K. Athienitis, Wind-induced natural ventilation analysis, Solar Energy 81 (2007) 20-30.

T. Karimipanah, H.B. Awbi, M. Sandberg and C. Blomqvist. Investigation of air quality, comfort parameters and effectiveness for two floor level air supply systems in classrooms. Building and Environment 42 (2007) 647-655.

D. Katunsky, A. Korjenic, J. Katunska, M. Lopusniak, S. Korjenic, S. Doroudiani. Analysis of thermal energy demand and saving in industrial buildings: A case study in Slovakia. Building and Environment 67 (2013) 138-146.

J. Khodakarami, I. Knight. Required and current thermal conditions for occupants in Iranian hospitals. HVAC&R Research 14 (2008) 175-194.

A. Khudhair, Farid M. A review on energy conservation in building applications with thermal storage by latent heat using phase change materials. Energy Conversation Management 46 (2004) 263-275.

V. Koci, Z. Bazantova, R. Cerny. Computational analysis of thermal performance of a passive family house built of hollow clay bricks. Energy and Buildings 76 (2014) 211-218.

kplan AG und IB Baumann: *Bestandsplanung der FOS/BOS Erding – Gebäudeplanung und Auszüge aus der TGA-Planung*. Abensberg, 2011.

J. M. Kuckelkorn. Optimizing operations and energetic evaluation of non-residential buildings. 2010 Annual Report of ZAE Bayern, 2010, 86-87.

T. E. Kuhn, C. Buehler, W. J. Platzer. Evaluation of overheating protection with sun-shading systems. Solar Energy 69 (2001) 59-74.

M. K. Kuzman, P. Groselj, N. Ayrilmis, M. Zbasnik-Senegacnik. Comparison of passive house construction types using analytic hierarchy process. Energy and Buildings 64 (2013) 258-263.

P. La Roche. *Carbon-neutral architectural design*. Taylor & Francis CRC Press, Boca Raton, 2011.

B. E. Launder, D. B. Spalding. The numerical calculation of turbulent flows. Computer Methods in Applied Mechanics and Engineering 3 (1974) 269-289.

S. Leenknegt, R. Wagemakers, W. Bosschaerts, D. Saelens. Numerical study of convection during night cooling and the implications for convection modelling in Building Energy simulation models. Energy and Buildings 64 (2013) 41-52.

F. P. Leusden, H. Freymark. *Darstellungen der Raumbehaglichkeit für den einfachen praktischen Gebrauch*. GI 72, 1951.

R. W. Lewis, P. Nithiarasu, K. N. Seetharamu. Fundamentals of the finite element method for heat and fluid flow. Wiley, England, 2004.

Y. Li, Buoyancy-driven natural ventilation in a thermally stratified one-zone building, Building and Environment 35 (2000) 207-214.

Y. Li, A. Delsante, Natural ventilation induced by combined wind and thermal forces, Building and Environment 36 (2001) 59-71.

Z. Lin, T. T. Chow, K. F. Fong, C. F. Tsang, Q. Wang. Comparison of performances of displacement and mixing ventilations Part 2: indoor air quality. International Journal of Refrigeration 28 (2005) 288-305.

P. Linden, P. Cooper, Multiple sources of buoyancy in a naturally ventilated enclosure, Journal of Fluid Mechanics 311 (1996) 177-192.

P. Linden, G. Lane, D. Smeed, Empting filling boxes: the fluid mechanics of natural ventilation, Journal of Fluid Mechanics 212 (1990) 309-335.

D. Liu, F.Y. Zhao, G.F. Tang. Active low-grade energy recovery potential for building energy conservation. Renewable and Sustainable Energy Reviews 14 (2010) 2736-2747.

D. Liu, F.Y. Zhao, H.Q. Wang, E. Rank. Turbulent transport of airborne pollutants in a residential room with a novel air conditioning unit. International Journal of Refrigeration 35 (2012) 1455-1472.

A. Mahdavi, E. Doppelbauer. A performance comparison of passive and low-energy buildings. Energy and Buildings 42 (2010) 1314-1319.

T. P. McDowell, J. W. Thornton, S. Emmerich, G. Walton. Integration of airflow and energy simulation using CONTAM and TRNSYS. ASHRAE Transactions 109 (2003) 1-14.

G. P. Mitalas, J. G. Arseneault. Fortran IV program to calculate z-transfer functions for the calculation of transient heat transfer through walls and roofs. Division of National Research Council of Canada, Ottawa, 1971.

C. A. Mydlarz, R. Conetta, D. Connolly, T. J. Cox, J. E. Dockrell, B. M. Shield. Comparison of environmental and acoustic factors in occupied school classrooms for 11-16 year old students. Building and Environment 60 (2013) 265-271.

J. F. Nicol, M. A. Humphreys. Adaptive thermal comfort and sustainable thermal standards for buildings. Energy and Buildings 34 (6) (2002) 563-572.

J. F. Nicol, S. Roaf. Pioneering new indoor temperature standard: the Pakistan project. Energy and Buildings 23 (1996) 169-174.

K. C. Noh, J. S. Jang, M. D. Oh. Thermal comfort and indoor air quality in the lecture room with 4-way cassette air-conditioner and mixing ventilation system. Building and Environment 42 (2007) 689-698.

W. Passchier-Vermeer, W. F. Passchier. Noise exposure and public health. Environmental Health Perspectives 108 Suppl. (2000) 123-131.

S. V. Patankar. *Numerical Heat Transfer and Fluid Flow*. Taylor & Francis, Washington D.C., 1980.

L. Perez-Lombard, J. Ortiz, C. Pout. A review on buildings energy consumption information. Energy and Buildings 40 (2008) 394-398.

A. Persily. Evaluating building IAQ and ventilation with indoor carbon dioxide. ASHRAE Trans. 103(2) (1997) 193-204.

W. Pistohl. *Handbuch der Gebäudetechnik; Band 2: Heizung, Lüftung, Beleuchtung, Energiesparen.* 7. neu bearbeitete und erweiterte Auflage. Köln: Werner Verlag, 2009.

M. Puteh, M.H. Ibrahim, M. Adnan, C.N. Cheahmad, N.M. Noh. Thermal comfort in classroom: constraints and issues. Procedia – Social and Behavioural Sciences 46 (2012) 1834-1838.

I. Ridley, J. Bere, A. Clarke, Y. Schwartz, A. Farr. The side by side in use monitored performance of two passive and low carbon Welsh houses. Energy and Buildings 82 (2014) 13-26.

P. Rohdin, A. Molin, B. Moshfegh. Experiences from nine passive houses in Sweden – Indoor thermal environment and energy use. Building and Environment 71 (2014) 176-185.

L. M. Ronsse, L. M. Wang. Effects of noise from building mechanical systems on elementary school student achievement. ASHRAE Transactions 116 (2010) 347-354.

S. Rosen, P. Olin. Hearing loss and coronary heart disease. Archives of Otolaryngology 82 (1965) 236.

J. Rydberg, E. Kulmar. Ventilationens effektivitet vid olika placering av inblasnings- och utsugningsoppningarna (in Swedish). Sartryck ur tidskrift VVS 3; 1947.

W. Saman, M. Oliphant, L. Mudge, E. Halawa. Study of effect of temperature settings on accurate cooling energy requirements and comparison with monitored data. Final report submitted to residential buildings sustainability, Canberra, 2008.

M. Sandberg. What is ventilation efficiency? Building and Environment 16 (1981) 123-135.

M. Sandberg, M. Sjoeberg. The use of moments for assessing air quality in ventilated rooms. Building and Environment 18 (1983) 181-197.

Schmidt, W. Charles. Noise that annoys: Regulating unwanted sound. Environmental Health Perspectives 113 (2005) A42-A44.

J. Schnieders, A. Hermelink. CEPHEUS results: measurements and occupants' satisfaction provide evidence for Passive Houses being an option for sustainable building. Energy Policy 34 (2006) 151-171.

J. E. Seem. Modelling of heat transfer in buildings, PhD Thesis. Solar Energy Laboratory, University of Wisconsin Madison, 1987.

L. Shao, S. B. Riffat. Accuracy of CFD for predicting pressure losses in HVAC duct fittings. Applied Energy 51 (1995) 233-248.

M. H. Sherman. The use of blower-door data. Indoor Air 5 (1995) 215-224.

M. H. Sherman. Estimation from leakage and climate indicators. Energy and Buildings 10 (1987) 81-86.

K. Spasokukotskiy. Modellgestützte Messung thermodynamischer Größen zur Verbesserung der Behaglichkeit und zur Energieeinsparung in Gebäuden. Berlin, Mensch-&-Buch-Verl., 2005.

J. Srebric, Q. Chen. An example of verification, validation, and reporting of indoor environment CFD analyses (RP-1133). ASHRAE Transactions 108(2) (2002) 185-194.

Staples, L. Susan. Human response to environmental noise: Psychological research and public policy. American Psychologist 51 (1996) 143-150.

S. Steiger, R. T. Hellwig, E. Junker. Distribution of carbon dioxide in a naturally ventilated room with high internal heat load. Nordic Symposium on Building Physics 2008, Copenhagen Denmark, 2008.

E. Sterling, E. Mcintyre, C. W. Collett, J. Meredith, T. D. Sterling. Field measurements for air quality in office buildings: a three-phased approach to diagnosing building performance problems. Sampling and Calibration for Atmospheric measurements (ASTM Special Technical Publication 957), Philadelphia, PA, USA, 1987 46-65.

R. Stonier. CO_2: powerful IAQ diagnostic tool. Heat, Piping and Air Conditioning 67(3) (1995).

L. T. Terziotti, M. L. Sweet, J. T. Mcleskey Jr. Modeling seasonal solar thermal energy storage in a large urban residential building using TRNSYS 16. Energy and Buildings 45 (2012) 28-31.

TRNSYS 16 Manual, 2006. Solar Energy Lab, University of Wisconsin-Madison, Madison, USA.

M. Von Pettenkofer. *Ueber den Luftwechsel in Wohngebaeuden* (in German). Cotta, Munich, 1858.

H.Q. Wang, C.H. Huang, D. Liu, F.Y. Zhao, et al. Fume transports in a high rise industrial welding hall with displacement ventilation system and individual ventilation units. Building and Environment 52 (2012) 119-128.

Y. Wang, F. Y. Zhao, J. Kuckelkorn, D. Liu, L. Q. Liu, X. C. Pan. Cooling energy efficiency and classroom air environment of a school building operated by the heat recovery air conditioning unit. Energy 64 (2014) 991-1001.

Y. Wang, F. Y. Zhao, J. Kuckelkorn etc. School building energy performance and classroom air environment implemented with the heat recovery heat pump and displacement ventilation system. Applied Energy 114 (2014) 58-68.

Y. Wang, F. Y. Zhao, J. Kuckelkorn, D. Liu, J. Liu, J. L. Zhang. Classroom energy efficiency and air environment with displacement natural ventilation in a passive public school building. Energy and Buildings 70 (2014) 258-270.

Y. Wang, F. Y. Zhao, J. Kuckelkorn, X. H. Li, H. Q. Wang. Indoor air environment and night cooling energy efficiency of a southern German passive public school building operated by the heat recovery air conditioning unit. Energy and Buildings 81 (2014) 9-17.

Y. Wang, J. Kuckelkorn, F. Y. Zhao, etc. Evaluation on classroom thermal comfort and energy performance of passive school building by optimizing HVAC control systems. Building and Environment 89 (2015) 86-106.

Y. Wang, Y. Shao, etc. Demand controlled ventilation strategies for high indoor air quality and low heating energy demand. Proceedings of Instrumentation and Measurement Technology Conference 2012, 870-875.

W. Wild. Nachhaltiger Schulhausneubau der Fachoberschule/Berufsoberschule Erding in Passivhausbauweise – Projektumsetzung und Nutzerbeteiligung: Erfahrungen der Bauleitung. Schulbauten für die Zukunft – wirtschaftlich, energieeffizient, nachhaltig und pädagogisch Konferenz 2011, München.

Williams, L. Kemp, L. Rick. Environmental Health Secrets. Philadelphia: Elsevier Health Science, 2000.

X. Wu, B. W. Olesen, L. Fang, J. Zhao. A nodal model to predict vertical temperature distribution in a room with floor heating and displacement ventilation. Building and Environment 59 (2013) 626-634.

X. J. Ye, Z. P. Zhou, Z. W. Lian, H. M. Liu, C. Z. Li, Y. M. Liu. Field study of a thermal environment and adaptive model in shanghai. Indoor Air 16 (2006) 320-326.

C. W. F. Yu, J. T. Kim. Building environment assessment schemes for rating of IAQ in sustainable buildings. Indoor and Built Environment 20 (2011) 5-15.

X. Yuan, Q. Chen, L. R. Glicksman. A critical review of displacement ventilation. ASHRAE Transactions 104 (1998) 78-90.

X. Yuan, Q. Chen, L.R. Glicksman, Y. Hu, and X. Yang. Measurement and computations of room airflow with displacement ventilation. ASHRAE Transactions 105 (1999) 340-352.

Z. Q. Zhai. Application of computational fluid dynamics in building design: aspects and trends. Indoor and Built Environment 15 (2006) 305-313.

H. Zhang, E. Arens, C. Huizenga, T. Han. Thermal sensation and comfort models for non-uniform and transient environments: Part 1: local sensation of individual body parts, 2009.

H. Zhang, E. Arens, C. Huizenga, T. Han. Thermal sensation and comfort models for non-uniform and transient environments: Part 2: local comfort of individual body parts, 2009.

H. Zhang, E. Arens, C. Huizenga, T. Han. Thermal sensation and comfort models for non-uniform and transient environments: Part 3: whole body sensation, 2009.

F.Y. Zhao, D. Liu, G.F. Tang. Multiple steady fluid flows in a slot-ventilated enclosure. International Journal of Heat and Fluid Flow 29 (2008) 1295-1308.

F. Y. Zhao, E. Rank, D. Liu, H. Q. Wang, Y. L. Ding. Dual steady transports of heat and moisture in a vent enclosure with all round states of ambient air. International Journal of Heat and Mass Transfer 55 (2012) 6979-6993.

K. Zhong, X. Yang, W. Feng, Y. Kang, Pollutant dilution in displacement natural ventilation rooms with inner sources, Building and Environment 56 (2012) 108-117

Appendix A

Location Plan, Floor Plans and Separated Building Zones

In the following, location plan of the school building and four floors plans (i.e. the basement, ground floor, first floor and second floor) including separated zones with different colors, which have been employed in BES simulation part, are shown in detail respectively.

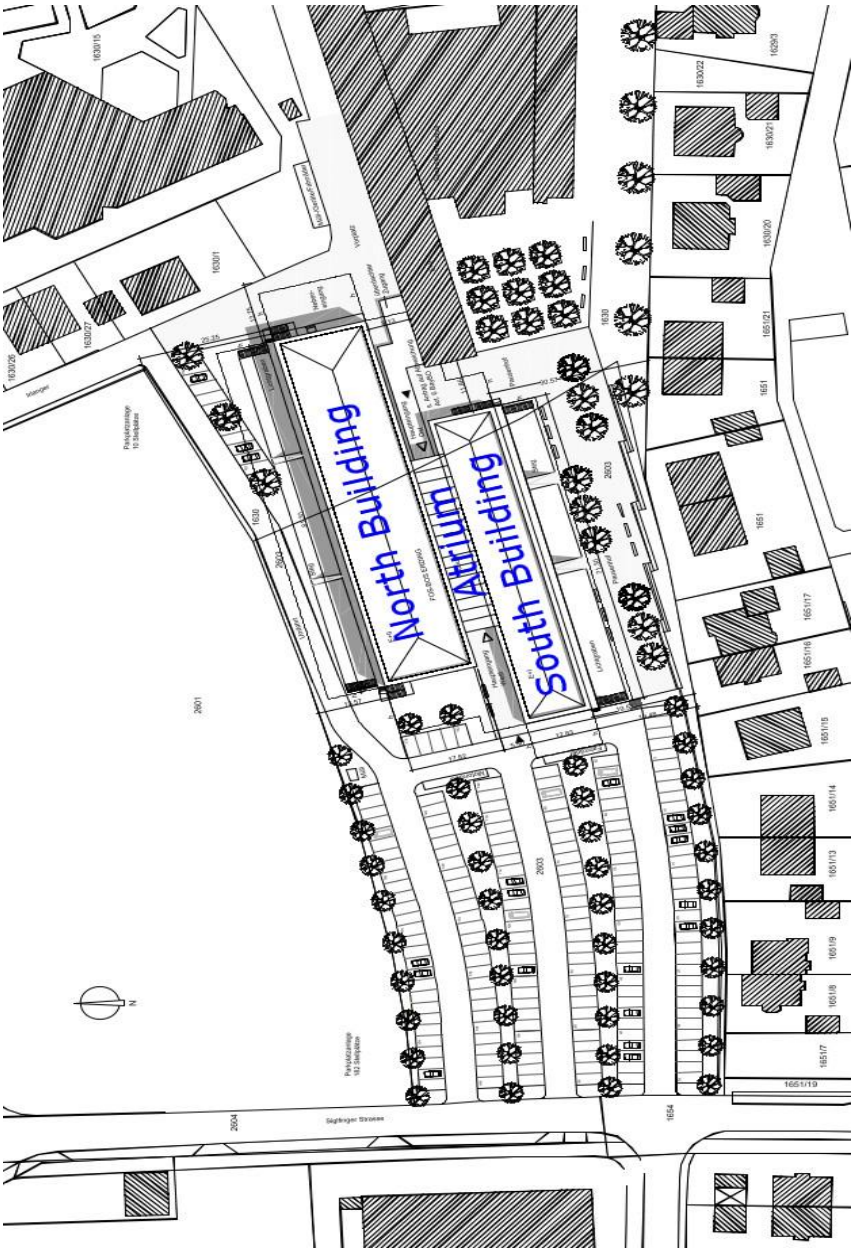

Fig. A.1: Location plan of the FOS/BOS Erding (excerpt from (kplan 2011)).

Fig. A.2: Floor plan of building basement including separated zones with different colors (background plan from (kplan 2011), black zones mean no considering in simulation, the same as below).

Fig. A.3: Floor plan of the building ground floor including separated zones with different colors (background plan from (kplan 2011)).

Fig. A.4: Floor plan of the building first floor including separated zones with different colors (background plan from (kplan 2011)).

Fig. A.5: Floor plan of the building second floor including separated zones with different colors (background plan from (kplan 2011)).

Appendix B

Reference Setting List for BES Simulation Parameters

B.1 Single Classroom 2.28

FOS BOS Erding				
BES simulation parameters for reference classroom 2.28 (Zone 32)		**Settings for reference simulation**		
		TRNSYS	**Unit**	**Comments**
Simulation				
Software		**TRNSYS 16.1**		
Time step		**0.1**	h	
Tolerance integration		**0.001**		
Tolerance convergence		**0.001**		
Room capacitance		**2301.4**	kJ/K	
Location and conditions				
Position lat.		**48.311**	°	
Position shift		**-3.2**	°	
Building rotation		**345**	°	
Climate data				
Weather data file		**Meteornorm Muenchen-Airp-108700.tm2**		
Geometry				
Thermal zones				
	Total thermal volume	**303.52**	m^3	
Net zones				
	Net volume	**239.73**	m^3	
Walls and layers				
External walls				
	U-value	**0.128**	W/m^2K	
	Concrete thickness	**260**	mm	
	Concrete conductivity	**7.56**	kJ/(hmK)	
	Concrete c_p	**0.8**	J/(gK)	
	Concrete density	**2400**	kg/m^3	
	Insulation thickness	**240**	mm	
	Insulation conductivity	**0.1152**	kJ/(hmK)	
	Insulation c_p	**0.8**	J/(gK)	
	Insulation density	**40**	kg/m^3	
Internal walls North & West & East				

	U-value	**4.357**	W/m²K	
	Concrete thickness	**125**	mm	
	Concrete conductivity	**7.56**	kJ/(hmK)	
	Concrete c_p	**0.8**	J/(gK)	
	Concrete density	**2400**	kg/m^3	
Floor				
	U-value	**3.587**	W/m²K	
	Concrete thickness	**1**	mm	
	Concrete conductivty	**7.56**	kJ/(hmK)	
	Concrete c_p	**0.8**	J/(gK)	
	Concrete density	**2400**	kg/m^3	
	Estrich thickness	**65**	mm	
	Estrich conductivity	**2.16**	kJ/(hmK)	
	Estrich c_p	**1**	J/(gK)	
	Estrich density	**800**	kg/m^3	
Ceiling/Roof				
	U-value	**0.094**	W/m²K	
	Concrete thickness	**300**	mm	
	Concrete conductivty	**7.56**	kJ/(hmK)	
	Concrete c_p	**0.8**	J/(gK)	
	Concrete density	**2400**	kg/m^3	
	Insulation thickness	**360**	mm	
	Insulation conductivity	**0.126**	kJ/(hmK)	
	Insulation c_p	**0.8**	J/(gK)	
	Insulation density	**40**	kg/m^3	
Windows	Type	**12007**		
	U-value	**0.87**	W/m²K	Total 4+1 manual windows + 1 door-window + 1 motor-window
	U-value for glass	**0.7**	W/m²K	
	Frame ratio	**0.1896**		
	U-value for frame	**1.6**	W/m²K	
	g-value for glass	**0.501**		
<u>TRNSYS Sim. Reference Settings</u>				
Infiltration				
	Infiltration rate	**0.01**	1/h	

Ventilation				
	Ventilation rate	**2.75/2.25/1.25**	1/h	
Pre-Ventilation				
	Ventilation rate	**1.2**	1/h	
Night ventilation				
	Ventilation rate	**1.3**	1/h	
	6.5 am … 23	**0**		
	23 … 6.5 am	**1**		
	Running function schedule	**(May1st to Sep. 30th)*LT(23,$T_{concrete}$)**		Run when $T_{concrete}$>23°C in sum.
	Temperature	**$T_{ambient}$**	°C	
Heat recovery				
	Efficiency	**0.8**		
	Schedule	**winter**		
Air cooling				
	$T_{air\ inlet\_day}$	**19**	°C	
	T_{room_day} (active cooling)	**26**	°C	Active cooling off when night ventilation runs
	Schedule	**summer**		
Air heating				
	T air inlet	**19**	°C	
	Schedule	**winter**		
Wall heating				
	T_{room_day}	**21.5**	°C	
	Max. heat load	**999999**	kW	
	Radiative part	**40**	%	
	Schedule	**winter*GT(22,$T_{concrete}$)**		Run when $T_{concrete}$<22°C in winter
Shading				South direction
	On	**300**	W/m²	
	Off	**100**	W/m²	
	Shading factor	**0.7**		
	Time schedule	**LT(22, $T_{concrte}$)**		Run when $T_{concrete}$>22°C
Internal gains				
	Person accounts	**33/27/15**		Design Point 1/2/3
	Gains	**60**	W/Person	After ISO 7730
	Specific gains	**2.8**	W/m²	
	occupancy dentisy	**0.39**	occupants/m²	

	Schedule	**Only occupied**		
Artificial lighting				
	On	**120**	W/m²	
	Off	**200**	W/m²	
	Related floor area	**79.9**	m²	
	Total heat gain	**0**	W/m²	
	Schedule	**Only occupied**		
Other schedules also for building				
	Day occupancy schedule for students			
Morning	0…8 am	**0**		Morning starts
	8…9.5 am	**1**		
	9.5…9.75 am	**0**		
	9.75…11.25 am	**1**		
	11.25…11.5 am	**0**		
	11.5 am…13	**1**		
Afternoon	13…13.75	**0**		Afternoon starts
	13.75…16	**1**		
	16…24	**0**		
	Night ventilation schedule			Only in summer
	6.5 am … 23	**0**		
	23 … 6.5 am	**1**		
	Pre-Ventilation schedule			Only in winter
	6.5 am … 7.5 am	**1**		
	7.5 am … 6.5 am	**0**		
	Workdays			
	0…120 h	**1**		
	120…168 h	**0**		
	Winter			
	0…2160 h	**1**		
	6553…8760 h	**1**		
	Summer			
	2161…6552 h	**1**		
	Holidays			
	0…168	**1**		
	1513…1680	**1**		
	2544…2880	**1**		

	5040…6120	**1**		
	7224…7440	**1**		
	8568…8760	**1**		
	Month			
	Jan.	**1…744**	h	
	Feb.	**745…1416**	h	
	Mar.	**1417…2160**	h	
	Apr.	**2161…2880**	h	
	May	**2881…3624**	h	
	Jun.	**3625…4344**	h	
	Jul.	**4345…5088**	h	
	Aug.	**5089…5832**	h	
	Sep.	**5833…6552**	h	
	Oct.	**6553…7296**	h	
	Nov.	**7297…8016**	h	
	Dec.	**8017…8760**	h	

B.2 School Building of the FOS/BOS Erding

FOS BOS Erding			
BES simulation parameters for whole building	**Settings for reference simulation**		
	TRNSYS	**Unit**	**Comments**
General simulation parameters			
Software	**TRNSYS 16.1**		
Timestep	**0.1**	h	
Tolerance integration	**0.001**		
Tolerance convergence	**0.001**		
Location and conditions			
Position lat.	***48.311***	°	
Position shift	**-3.2**	°	
Building rotation	**345**	°	
Climate data			
Weather data file	**Meteornorm Muenchen-Airp-108700.tm2**		
Room capacitance	**9.6*volume**	kJ/K	
Infiltration rate	**0.01**	1/h	
Pre-ventilation rate	**1.2**	1/h	

Night ventilation				
	Ventilation rate	**1.3**	1/h	
	Running schedule	**May1st to Sep. 30th**		
	Temperature	**$T_{ambient}$**	°C	
Heat recovery				
	Efficiency	**0.8**		
	Schedule	**winter**		
Air cooling				
	Tempeature	**19**	°C	For classrooms and primary rooms
	Schedule	**summer**		
	T_{room_day} (active cooling)	**26**	°C	Active cooling off when night ventilation runs
Air heating				
	Temperature	**19**	°C	For classrooms and primary rooms
	Schedule	**winter**		
Wall heating				
	T_{room_day}	**21.5**	°C	
	Max. heat load	**999999**	kW	
	Radiative part	**40**	%	
	Schedule	**winter**		
Shading				
	On	**300**	W/m²	
	Off	**100**	W/m²	
	Shading factor	**0.7**		
	Time schedule	**summer**		
Zone 1 and 21				Atrium zones
Ventilation				
	Ventilation rate	**0.38+1.1*morning**	1/h	
Night ventilation				
Heat recovery				RLT 1 and 2
Air cooling				
	$T_{air\ cooling}$	$\sum_1^n(\dot{v}_i T_i) / \sum_1^n(\dot{v}_i)$	°C	$\dot{v}_i$: volume rate of classroom *i*, T_i : tem. of classroom *i*.
Air heating				

	$T_{air\ heating}$	$\sum_1^n(\dot{v}_i T_i) / \sum_1^n(\dot{v}_i)$	°C	
Wall heating				
Internal gains				
	Person accounts	**0**		
Zone 2, 5, 6, 8, 10, 11, 22, 27, 30, 31, 32				Classrooms
Ventilation				
	Ventilation rate	**0.33+1.08*morning**	1/h	
Night ventilation				
Heat recovery				RLT 1 and 2
Air cooling				
Air heating				
Wall heating				
Internal gains				
	Person accounts			See Table 4.1
Zone 3, 7, 9, 12, 15, 16, 25, 28				Secondary rooms
Ventilation				
	Ventilation rate	**0**	1/h	
Wall heating				
Internal gains				
	Person accounts			See Table 4.1
Zone 4				WC
Ventilation				
	Ventilation rate	**1.8**	1/h	
	Temperature	$\mathbf{T_{heatrec.}}$	°C	For RLT3 heat recovery
Heat recovery				
Internal gains				
	Person accounts		**0**	
Zone 13, 14, 29				Primary rooms
Ventilation				
	Ventilation rate		1/h	See Table 4.1
Night ventilation				
Air cooling				
Air heating				
Wall heating				
Shading				North
Internal gains				

	Person accounts			See Table 4.1
Zone 17, 18, 19				Passive zones
Ventilation				
	Ventilation rate	**0**	1/h	
Shading				South
Internal gains				
	Person accounts	**0**		
Zone 20				Copy room
Ventilation				
	Ventilation rate	**0**	1/h	
Internal gains				
	Person accounts	**0**		
	Printer accounts	**2**		300 W/printer
Zone 23				Technical room
Ventilation				
	Ventilation rate	**0.43**	1/h	
	Temperature	$\mathbf{T_{heatrec.}}$	°C	For RLT3 heat recovery unit
Heat recovery				
Internal gains				
	Person accounts	**0**		
Zone 24				3 IT classrooms
Ventilation				
	Ventilation rate	**0.5+1.6*morning**	1/h	
Night ventilation				
Heat recovery				
Air cooling				
Air heating				
Wall heating				
Shading				North
Internal gains				
	Person accounts	**12+38*morning**		
	PC accounts	**12+38*morning**		230W/PC
Zone 26				Server room
Ventilation				
	Ventilation rate	**0**	1/h	
Active cooling				

	T_{room_day}	**26**	°C	All year
Internal gains				
	Person accounts	**0**		
Zone 33, 34, 35				Air zones
Ventilation				
	Ventilation rate	**0**	1/h	
Internal gains				
	Person accounts	**0**		